Water treatment using electrohydraulic discharge system

By

Emile Salomon Massima Mouele

BSc Honours (Chemistry) University of the Western Cape

A thesis submitted in fulfilment of the requirements for the degree of Magister Scientiae

Department of Chemistry

University of the Western Cape

Supervisor: Prof L F. Petrik

Co-supervisor: Dr O. Fatoba

November 2014

ABSTRACT

In South Africa, water pollution problems have continued to increase due to increasing anthropogenic activities. The increasing number of organic contaminants in various water sources can be attributed to industrial development, population growth and agricultural run-off. These activities have impacted negatively on the availability and accessibility to sustainable clean water resources, exposing citizens to water borne diseases such as cholera, diarrhoea and typhoid fever; commonly reported among children. Advanced oxidation technologies such as dielectric barrier electrohydraulic discharge (EHD), also referred to as dielectric barrier discharge (DBD), have the ability to decompose persistent organics and eliminate microbes. DBD offers advantages such as efficiency, energy saving, rapid processing, use of few or no chemicals, and non-destructive impact on the ecosystem. The system is also capable of generating ozone, hydrogen peroxide, singlet oxygen, superoxide radicals, hydroxyl radicals and other active species. The combination of these reactive species has been reported to degrade biological and chemical pollutants rapidly and efficiently.

In this study, the DBD system was optimized by investigating the effect of physico-chemical, electrical parameters and reactor configurations on Methylene Blue (MB) decolouration efficiency. The physico-chemical parameters included MB concentration, solution pH and conductivity, solution volume, NaCl electrolyte concentration in the electrode compartment and air flow rate. As for electrical parameters, the effects of voltage, electrode type and size on MB decolouration efficiency were studied. The effect of the aforementioned parameters on MB decolouration efficiency was assessed by varying one parameter at a time.

The following physico-chemical parameters: time (from 0 - 60 minutes), pH (2.5 - 10.5), solution conductivity (5 - 20 mS/cm), MB concentration (0.5 – 10 mg/L), solution volume (500 – 2000 mL), NaCl electrode electrolyte concentration (10 – 50 g/L) and air flow rate (2 – 4 L/min) were varied in their respective ranges under the applied experimental conditions: reactor air gap 2 mm, solution volume 1500 mL, NaCl electrolyte concentration of 50 g/L in the electrode compartment, voltage 25 V (7.8 kV), airflow rate 3 L/min, 0.5 mm silver electrode and a running time of 60 minutes. As for electrical parameters, voltage (from 20 - 25 V), electrode type (copper, silver and stainless steel) and electrode diameter (0.5 – 1.5 mm) were also altered individually at the applied experimental conditions. The reactor air gap was varied from 2 to 6 mm. At the same experimental conditions, the free reactive species generated mainly H_2O_2 and O_3, were detected and quantified using the Eisenberg and indigo methods, respectively.

The optimum physico-chemical parameters were found to be MB concentration 5 mg/L, concentration of NaCl electrolyte used in the central compartment of the DBD reactor 50 g/L, solution pH 2.5, solution conductivity 10 mS/cm, air flow rate 3 L/min, solution volume 1500 mL and an optimum contact time of 30 minutes. The optimum electrical parameters were found to be: applied voltage 25 V and 1.5 mm silver electrode. The following parameters MB concentration, solution conductivity and pH, applied voltage and reactor configuration significantly affected MB decolouration efficiency compared to parameters such as solution volume, the inlet air flow rate, electrode type and size and NaCl electrolyte concentration in the electrode compartment, which were less effective in enhancing MB decolouration. Moreover, for all DBD experiments performed at the applied experimental conditions, complete decolouration of MB was achieved in the first 30 minutes. However, trends between the optimized parameters and MB decolouration efficiency were mostly observed after 10 minutes. The optimized DBD system reduced the treatment time from 30 to 20 minutes without any chemical additives. Moreover, at 5 mg/L MB under the applied optimum conditions, it was proved that besides 99% of MB decolouration reached after 60 minutes, 53% of total organic carbon (TOC) removal was also achieved. The chemical oxygen demand (COD) characterizing MB toxicity was less than 5 mg/L before as well as after the DBD experiment.

After 10 minutes of experiment under the following conditions: Applied voltage 25 V, MB concentration 5 mg/L, solution pH (in between 6.04 and 6.64), solution volume 1500 mL, air flow rate 3 L/min, 0.5 mm silver electrode and a contact time of 60 minutes, about 3.73 x 10^{-5} mol/L H_2O_2 was produced which decreased to 2.93 x 10^{-5} mol/L 10 minutes later, while O_3 concentration was initially very low and could not be detected. However, 0.5 mol/L of O_3 was detected after 20 minutes of operating time, thereafter, H_2O_2 concentration decreased continuously with time while that of O_3 fluctuated as the treatment time increased. Likewise, the energy density for the production of free reactive species reached 0.87 g/ kWh in the first 10 minutes due to the presence of chromophoric functional groups such as $=N+(CH_3)_2$ in MB structure that had to be destroyed. Thereafter, the energy consumption decreased progressively to zero with an increase in treatment time due to the destruction of $=N^+(CH_3)_2$ groups in MB structure with time. The correlation between the rise in the of H_2O_2 concentration and energy density after 10 minutes was probably due to dissociation of OH-OH bonds in H_2O_2 by UV light to yield OH radicals which unselectively may have attacked MB dye. Thus, MB decomposition in the current DBD reactor was mostly initiated by H_2O_2 and O_3. The irradiation of H_2O_2 by UV light generated in the DBD system was found to

accelerate dye decomposition in the first 30 minutes of the experiment. The UV-vis analysis of treated MB samples confirmed that the complete decolouration of MB achieved in the first 30 minutes was due to the destruction of the chromophoric [=N+(CH_3)$_2$] group in Methylene blue structure, while the FT-IR confirmed the presence of traces of various functional groups such as C=C, C=O, C=N, NH, NH_3, NO_2, etc. characteristics of carboxylic acids, amines, amides, nitrogen based compounds (salts), aliphatic and unsaturated by-products remaining in the bulk solution after treatment. The salts analysis after treatment showed that 16 mg/L of nitrates and nitrites and 1.1 mg/L of sulphates mainly originating from air and MB decomposition were present in the treated samples.

The EHD/DBD system used in this study offers an approach to partially treat water/wastewaters and its optimization was able to significantly enhance the decomposition of the target MB dye as indicated by the reduction of total organic carbon (TOC) from 8.3 mg/L to 3.9 mg/L. Compared to previous research, this study successfully optimised a complete double cylindrical dielectric barrier discharge (DBD) reactor at ambient condition without any chemical additives.

DECLARATION

I hereby declare that “Water treatment using electrohydraulic discharge system” is my own work, that it has not been submitted for any degree or examination in any other university, and that all the sources I have used or quoted have been specified and approved by complete references.

Emile Salomon Massima Mouele May 2014

Signed……

ACKNOWLEDGEMENTS

I would like first to thank God for giving me life, to believe and trust in him in good and hard times. Thank you father God for your love and support. You are my shield, with you I am secured and I have no fear. Thank you Lord for keeping me motivated and energised during my Master degree programme.

Special thanks go to my supervisor, Prof Leslie Petrik, for the chance she gave me to be part of the Environmental and Nanoscience research group (ENS) at UWC. Thank you Prof for all the workshops, trainings and mostly for your guidance, patience and inspiration.

I particularly thank my co-supervisor, Dr. O. Fatoba for all his advice and contributions towards my project.

Many thanks go to Dr Omotola. O. Babajide, Dr Sunday O. Ayanda and to my friend, Mr Jimoh. O. Tijani, for their support.

Lots of thanks to Mama Averil Abbott, Mama Vanessa Kellerman and to all colleagues and friends at ENS. Also I would like to thank Mr Petrus and Timo for the power supply, Ms Sylvia from glass Tech Company at Johannesburg and Mr Andre de Beer at UCT for supplying the glass tubes and manufacturing reactor tubes used in this study.

Individual thanks are directed to the Water Research commission (WRC), NRF, etc. for financial supports. I personally thank the Government of Gabon for giving me an opportunity to pursue my studies in South Africa.

Finally, warm thanks go to my dearly loved family members including my mother, Odette Boukangou; my grandmother, Mathilde Kanga, my uncles, Nicolas Boukangou and Barnabe Boukangou, etc. for all the support and love that boost my inspiration.

LIST OF ABBREVIATIONS

EHD	Electrohydraulic discharge
DBD	Dielectric barrier discharge
MB	Methylene blue
TOC	Total organic carbon
CFU	Colony forming unit
EDs	Endocrine disruptors
EE2 17 R	Ethinyl estradiol
AOPs	Advanced oxidation processes
CEHD	Corona electrohydraulic discharge
FT-IR	Fourier transform infrared spectroscopy
CP	Chemical product
HTMs	Trihalomethanes
AOTs	Advanced oxidation techniques
PhFO	Photo- Fenton/Ozone
PhCO	Photo- cathalysis/ozone
RSA	Republic of South Africa
Glass tech	Glass technology
DO	Dissolved oxygen
4-CP	4- chlorophenol
VB	Valance band
CB	Conductive band
E, E& Eng.	Electrical and Electronic Engineering
DC	Direct current
AC	Alternative current
ANTPs	Atmospheric non-thermal plasma
APPJ	Atmospheric pressure plasma jet
MHCD	Micro hollow cathode discharge
NTP	Non-thermal plasma
GC-TCD	Gas chromatography coupled with thermal conductive detector
DNPH	Dinitrophenyhydrazine
COD	Chemical oxygen demand
PCEHD	Pulsed corona electrohydraulic discharge

PSEHD	Pulsed spark electrohydraulic discharge
PAEHD	Pulsed arc electrohydraulic discharge
PPEHD	Pulsed power electrohydraulic discharge
SEM	Scanning electron microscopy
ATR	Attenuated total reflectance
PT	Proficiency testing
ICP	Induced coupled plasma
TIC	Total inorganic carbon
HOMO	Highest occupied molecular orbital
PFN	Pulsed forming network
LC- MS	Liquid chromatography coupled with mass spectrometry
GC-MS	Gas chromatography coupled with mass spectrometry
WHO	World Health Organization

TABLE OF CONTENTS

LIST OF TABLES

LIST OF FIGURES

CHAPTER ONE

1. INTRODUCTION

1.1 BACKGROUND

Water becomes a waste when it has been undesirably polluted by both organic and inorganic contaminants, bacteria and microorganisms, industrial effluent or any component that might modify its initial quality (Ibrahim, 2012). The study carried out by Ellis in 2004 (Ellis, 2004) showed that wastewater consists of various components such as proteins, carbohydrates, fats, oils and trace amounts of priority pollutants, surfactants and emerging contaminants. Wastewater originates from many sources which include municipal and industrial sources (Ibrahim, 2012). Municipal wastewater is generated as a result of liquid waste discharged by domestic residences, households and septic tank leakages.

The study conducted by Ibrahim, (2012) revealed that municipal wastewater usually contains various contaminants including colony forming units (CFU)/mL of coliform organisms, faecal streptococci, protozoan cysts, and virus particles. Studies have also shown that pharmaceuticals are also contained in municipal wastewater (Marc et al., 2005). Among the various types of pharmaceuticals detected in municipal wastewater, the presence of antibiotics, pharmaceuticals acting as endocrine disruptors (EDs) and antineoplastic agents are of great concern due to the impacts of these chemicals on the environment and ecosystems. For instance, endocrine disrupting pharmaceuticals such as 17R-ethinyl estradiol (EE2) has been found to be responsible for the feminizing and masculinising effects detected in animals living in ecosystems where EE2 is found (Pickering et al., 2003). The EE2 is considered as a harmful contaminant due to its high in-vivo potency, persistence in the environment and its capacity to bioaccumulate (Thorpe et al., 2003). Moreover, Thorpe and co-workers confirmed that antineoplastics used for chemotherapy are observed to be highly toxic agents and can dramatically impact aquatic organisms. Industrial wastewater mainly results from the effluent produced from any industrial activity such as food processing, dyeing factories, iron and steel industry, mines and quarries, and so on. Industrial wastewater generated from metal processing industry, mines or chemical industries might be rich in heavy metals, organic and inorganic compounds as well as chlorinated by-products.

On the other hand, wastewater generated from agricultural activities have a high concentration of organics resulting from animal and vegetable sources, micro-organisms, and various organic chemicals used for the control of pests and diseases. In textile industries, several organic synthetic dyes which are used for material colourization are major contributors to the organic pollutants in industrial wastewater. The release of coloured wastewater which may be very rich in organic pollutants into the environment might not only damage the aesthetics of nature, but can also be toxic to aquatic life (Martynas et al., 2013). The main concern about synthetic dyes is that these compounds are difficult to degrade in wastewater treatment plants when physical, chemical or/and biological treatment is applied. Even though these treatments have been employed recently to remove dyes from wastewaters, biological processes are widely used because of their cost effectiveness. Since most dyes are non-biodegradable, chemical and physical processes such as flocculation, coagulation, membrane processes, and ion exchange, adsorption and chemical oxidations are used to treat waters (Vujevic et al., 2004).

The decomposition of dyes is a great challenge not only because of the complexity of their structures such as monoazo, diazo, polyazo, disperse and reactive dyes, but also most of these compounds are stable and are designed to resist degradation when exposed to light, chemical, biological and microbial attacks (Yijun and Muqing, 2013). Irrespective of the source of wastewater, it is a fact that wastewater contains several organic and inorganic contaminants that need to be removed in order to avoid its indiscriminate disposal and to reduce its adverse effects on human and the environment. The protection of the environment and the sustainability of human health have recently become the major priorities of most countries in the world. In order to keep ecosystems safe, the removal of contaminants from wastewater requires suitable treatment methods; some of which have been established while some need to be further developed in order to combat the emerging pollutants in wastewaters.

Recently, advanced oxidation processes (AOPs) including direct ozonation, UV photolysis, high voltage electrical discharges, etc. have been used to decolourize and degrade organic dyes completely (Vujevic et al., 2004). Some of the above mentioned processes have also been used as pre-treatment in order to minimise the concentrations of toxins such as pesticides, surfactants, colouring matters, pharmaceuticals and endocrine disrupting chemicals that impede biological wastewater treatment methods. The current study focuses specifically on the dielectric barrier electrohydraulic discharge (DBD) system. Although various studies revealed that this process has been used as pre/post

treatment method or in combination with other techniques for water/wastewaters treatment, however there is little information on the use of DBD system as a single technology for wastewater treatment that has been reported. Thus optimization of the DBD system at ambient conditions could result in a promising advanced oxidation technology for complete treatment of water/wastewaters.

1.2 PROBLEM STATEMENT

In the past few decades, environmental pollution affecting the quality of ecosystems has become recurrent and more life-threatening. Ecosystem includes all living things such as animals, plants, humans with their activities and their environment. The ecosystem components exhibit an interconnected and interdependent network through soil, air and water. The modification of one component results in the change of the whole system. Environmental pollution is principally due to human activities and largely due to the rise of industrial activities associated with population growth (Al-Momani et al., 2007; Mulbry et al., 2008). Nowadays the major pollution problems are related to the discharge of industrial wastewaters into superficial and underground water bodies. In order to reduce the problem of pollution, a number of physical, chemical and biological approaches or the combination of these approaches has been established for wastewater treatment.

Recently, AOPs have been developed to eliminate recalcitrant/persistent pollutants and non-biodegradable organics in water. Among these, direct ozonation, UV photolysis, high voltage electrical discharges, etc., have been widely used. However, the cost and inefficiency of these methods usually limit their practical applicability. On the other hand, the EHD system has been found to yield chemical oxidative species thus inducing chemical oxidation of the contaminants in the polluted water. Alternatively, Rey et al., (2009) observed that chemical oxidation can be used as a pre-treatment technique to reduce the concentration of pollutants in wastewater before applying any conventional biological process. Although, the traditional treatment techniques such as filtration, adsorption, precipitation, coagulation and so forth, have been found to be effective in the treatment of wastewater, some organic contaminants still persist in wastewaters which require the development of new treatment techniques.

In comparison with the previously mentioned AOPs, the DBD system shows promise because it generates a high enormous amount of molecular, ionic free reactive species as well as UV radiations and shock waves at ambient conditions without any chemical

additives. Hence the combination of these species forms a cocktail in the bulk solution that quickly mineralizes pollutants into CO_2, water and harmless inorganic species. Thus the EHD system could be used as a single complete approach to treat water/wastewaters and its optimization should be able to remove the recalcitrant/persistent pollutants.

1.3 RESEARCH OBJECTIVES

The main purpose of this work is to optimize the dielectric barrier discharge (DBD) system using methylene blue (MB) dye as a model synthetic organic pollutant. This research aims at using the optimized DBD system for water/wastewaters treatment. Therefore the principal objectives of this study are to:

(i) Assess the progressive decolourization/degradation efficiency of Methylene blue;

(ii) Investigate the effect of physic-chemical, electrical parameters and reactor configurations on the decolourization /degradation efficiency of the pollutant;

(iii) Investigate the mechanism pathways for the production of active species.

(iv) Quantify active species present in the bulk solution;

(v) Determine MB degradation products by reactive species; and

(vi) Design and optimize the new EHD system.

1.4 HYPOTHESIS

Organic pollutants from water/wastewaters can be completely degraded and mineralised into carbon dioxide (CO_2), water (H_2O) and harmless inorganic ions using corona electrohydraulic discharge at ambient conditions.

The influence of various parameters upon DBD efficiency can be determined by varying one parameter at a time while other factors are kept constant.

The free reactive species such as H_2O_2 and O_3 generated during DBD treatment process can be detected and quantified at optimum conditions.

1.5 RESEARCH QUESTIONS

What are the effects of chemical and physical parameters on decolourization/degradation efficiency of MB?

How do electrical parameters and reactor configuration impact the degradation efficiency of MB?

What are the pathways of producing free active species in the DBD system?

How can reactive species be detected and quantified in the solution, and do their concentrations grow with time?

To what extent can dye molecules be degraded and which parameters influence degradation efficiency the most?

1.6 RESEARCH APPROACH

In this study, dielectric barrier electrohydraulic discharge system (DBD) was optimized in distinctive steps. Optimization of any system like the current DBD is a very complicated process because of the presence of multiple parameters which need to be controlled. Hence there is a necessity to provide a step by step study to clarify how these factors should best be optimized.
The aspects that were investigated include:

- The effect of dye concentration on colour removal percentage over time

- The impact of MB concentration on degradation efficiency and rate of degradation was assessed by varying dye concentration (mg/L) while the rest of the parameters were kept constant.
- Optimization of chemical and physical parameters

In this section, the chemical and physical parameters such as dye volume and NaCl electrolyte concentration (used in the electrode compartment), pH, electrical conductivity, air flow rate were investigated subsequently and their impact on MB degradation efficiency was evaluated.

- Analysis of the raw and treated wastewater

The initial and final sampled solutions were qualitatively and quantitatively analysed using analytical techniques such as UV- spectroscopy, Fourier Transformer Infrared spectroscopy (FT-IR) and total organic carbon (TOC).

- Optimization of electrical parameters and reactor configurations

The effect of voltage, current, electrode type and diameter on decolourization efficiency was studied. Additionally the impact of reactor configurations on colour percentage removal was also established.

- Detection and quantification of free reactive species

Free reactive species such as hydrogen peroxide (H_2O_2), ozone (O_3) and hydroxyl radicals ($^{\cdot}OH$) were detected and quantified using Eisenberg method and indigo methods, respectively.

- Detection and identification of intermediate products of MB degradation

The decomposition intermediate products of MB were detected by FT-IR analysis and their identification by LC-MS was performed.

1.7 SCOPE AND DELIMITATIONS OF STUDY

1.7.1 Scope

Dielectric barrier discharge (DBD) system has recently been used by Okolongo et al., (2012) at UWC for treating water/wastewater. However, its optimization has not been covered. Therefore, the current study is centred on the optimization of the DBD system for better efficiency. In this case, physicochemical parameters such as pH, electrical conductivity, air flow rate, and dye volume and electrolyte concentration were optimized. In addition, electrical parameters such as voltage, current, electrodes type and diameter as well as reactor configurations were evaluated. Furthermore, the quantification of free reactive species that was not covered in the previous work has been achieved in the current study.

1.7.2 Delimitations

Due to the broadness of the topic and the lack of access to sophisticated equipment, UV-vis radiations generated inside the DBD system were not quantified.

1.8 SUMMARY OF THE SUBSEQUENT CHAPTERS

The current study encapsulates six more chapters presented as follows:

Chapter Two: This chapter presents the literature review on the following aspects: advanced oxidation processes (AOPs), dielectric barrier electrohydraulic discharge (DBD), the optimization procedure, detection and quantification of free reactive species. Recapitulating previous studies conducted on DBD is prominent in having knowledge not only on what has been done and found on DBD system, but on challenges and limitations encountered in previous research work that need to be overcome. Past investigations on DBD are therefore the starting point of the actual study. For instance the general behaviour of chemical and physical parameters such as voltage, solution pH, air flow rate, etc. on removal of organic pollutants need to be understood in order to proceed with their optimization in this study. Aspects such as reaction mechanism pathways of the formation of active species, as well as their detection and quantification have been great challenges in the DBD systems, so a critical review on these features is imperatively required.

Chapter three: This chapter outlines the experimental approaches, analytical techniques and the sampling methods used in this research work. In section 1.4 of this chapter, it was hypothesised that EHD could be optimized at room temperature by degradation of organic pollutants, and that active species could be detected and quantified. However, a scientific approach requires that any hypothesis should have a constructive methodology as a route to results that could be later used for assumption verification. Therefore chapter three encapsulates all experimental procedures or methodologies used to optimize the current EHD system as well as the detection and quantification of free active species and products of the decomposition / reaction intermediated

Chapter four: This chapter shows results and discussion of the optimized chemical and physical parameters of the EHD system. However, due to the large number of parameters that were optimized, the outcomes of procedures highlighted in chapter three have been subdivided into sections. This was to simplify the understanding of several trends observed during experiments in order to get a clarified validation of theories mentioned in section 1.4 of the current chapter.

Chapter five: This chapter exhibits the continuation of results and discussion of optimization of electrical parameters such as voltage, current, electrode material and diameter and the EHD reactor configurations including the gap between the anode electrode and the inner tube and the air gap between the inner and outer tubes. The detection and quantification of free reactive species was also studied in this chapter. Again based on the plurality of ionic and molecular reactive species produced in the corona discharge, ozone and hydrogen peroxide were the main reactive species detected and quantified in this study. Thus chapter six displays not only approximated amounts of these oxidants at optimum running time but their fluctuation with time as well.

Chapter six: This chapter states the conclusions and recommendations of this study. Indeed this section is the final stage of the actual work in which the results obtained were assessed and compared, to validate the hypothesis declared in section 1.4 of chapter one. Furthermore, challenges on optimization of the different parameters during experiments as well as new suggestions to overcome the encountered limitations were highlighted.

CHAPTER TWO: LITERATURE REVIEW

2. INTRODUCTION

It is important to highlight that water is not only an economical factor but also a significant sanitation parameter. Healthy and prosperous life requires the use of safe water supplies which has unfortunately not been achieved equally around the globe. The growth of human activities has exposed communities to chemical, microbial and biological pollutants as well as to micro pollutants resulting from chemistry-related industry, common household or agricultural applications. Pollution control and prevention requires innovative, cost effective and resourceful methods for environmental protection and reducing effluent discharge into the environment which could affect human health, natural resources and the biosphere (Huang et al., 1993; Legrini et al., 1993). To solve pollution problems, various conventional techniques of treating contaminated waters have been developed. These include chlorination, wet oxidation and electrical discharges, etc. Conventional treatment methods have proven to exhibit a complete operational efficacy but the amount of residual toxins in waters is still problematic. Recently, a new generation of procedures for water/wastewater treatment has been established and proved to be potent not only in degradation of organic pollutants but in their total mineralization as well. These new techniques are termed advanced oxidation processes (AOPs). This chapter therefore gives a review on wastewater, the effect of electrical discharges on wastewater treatment as well as well as their uses. For example, corona electrohydraulic discharge (EHD), plasma with its physics and chemistry and various studies that have been conducted on AOPs as well as the degradation of organic pollutants from water/wastewater (such as methylene blue) using EHD as a typical advanced oxidation process are reviewed.

2.1 WASTEWATER TREATMENT

Generally, water becomes a waste when it has been undesirably polluted by organic contaminants, bacteria and microorganisms, industrial effluent or any compounds that might modify its initial quality (Ibrahim, 2012). According to Ibrahim (2012), wastewater originates from many sources including municipalities (usually called municipal wastewater). This refers to the liquid waste discharged by domestic residences and/or commercial properties. In addition wastewater can also be derived from industrial and

agricultural activities, commonly called industrial wastewater as presented in Figure 2-1(a and b).

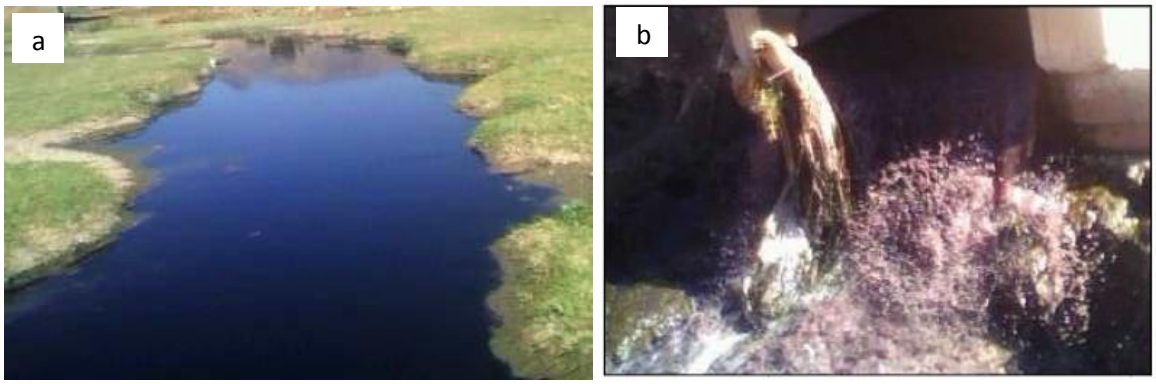

Figure 2-1: Ayka Addis textile factory wastewater discharged to the environment (a) and Ayka Addis textile factory wastewater discharge sample point (b), (Soresa, 2011).

It has been proved that wastewater contains various microbes as well as compounds such as proteins, carbohydrates, fats, oils and trace amounts of priority pollutants, surfactants and emerging contaminants (Ellis, 2004). Municipal wastewater usually contains various contaminants including colony forming units (CFU)/mL of coliform organisms, fecal streptococci, protozoan cysts, and virus particles (Ibrahim, 2012). Carpet manufacturing, dyeing, washing, textile, pulp and paper industries have been identified as the principal sources of several types of dyes. Specifically textile dying processes utilize chemicals such as acids, alkalis, surface active substances, and salts. Also, the design and use of dyes and pigments involves the generation and liberation of large amounts of organic compounds that threaten human health (Gatewood, 1995).

Moreover, the Yijun and Muqing (2013) research supported that basic dyes are another class of challenging organic contaminants that are regularly referred to as cationic dyes due to the positive charge they carry. The positive charge is often delocalized through the chromophoric system, although it is probably more localized on the nitrogen atoms. Other organic contaminants are called basic dyes because of their affinity for basic textile materials with net negative charge. These compounds are classified according to their chemical composition, their dyeing properties and are usually considered as toxic colorants. In addition, Pagga and Taeger (1994) showed that most dye contaminants in wastewater are only adsorbed on activated sludge rather than being degraded. Pagga and co-worker also stated that physical techniques such as ion exchange, adsorption, air stripping, etc., have also been found unsuccessful in degrading organic pollutants. These

techniques only transfer the pollutant from one phase to another. All contaminants should be completely removed to guarantee that treated water is free from any substance that might adversely affect human health and the environment; therefore, appropriate treatment systems need to be established. Hence, various stages in the conventional treatment of sewage have been proposed by Crites and Tchobanoglous in 1998. These include, preliminary treatment, involving the elimination of granular and inorganic solids with the size range of more than 0.1 mm, the primary treatment used to eradicate the bulk of suspended solids including both organic and inorganic matter (0.1 mm to 35 μm), the biological treatment related to the destruction of the biodegradable organic matter and nutrients and the tertiary treatment to eradicate portions of the remaining organic and inorganic solids and pathogenic microorganisms and nutrients, which is followed by chemical or physical disinfection before disposal (Ibrahim, 2012).

Effluents from agricultural activities contain a high concentration of organics resulting from animal and vegetable sources, micro-organisms, and various chemicals used for the control of pest and diseases. Factors such as land use, ground water levels and the degree of separation between storm water and sanitary wastes affect the composition of wastewater. Industrial wastewater mainly results from the effluent produced from any industrial activity, such as agriculture, food processing, dyeing factories, iron and steel industry, mines and quarries, and so on. Industrial wastewater originating from the metal processing industry, mines or chemical industries also consist of heavy metals, organic and inorganic compounds as well as chlorinated by-products. The composition of industrial effluent therefore depends on the activity involved. According to Ibrahim (2004), the composition of industrial wastewater is more complex compared to that of municipal wastewater due to the high contaminant load in the discharge of effluent water. The quality of raw wastewater/influent therefore determines the type of treatment processes used in wastewater treatment plants. Selective treatment methods are required to ensure high quality of purified water at a reasonable cost, since the earlier mentioned stages for municipal wastewater treatment could also be used for industrial wastewater treatment, but various additional physicochemical unit processes are required to ensure low or zero concentrations of specific pollutants.

2.2 WATER TREATMENT PROCESSES

The elimination or inactivation of organic pollutants is a gradual and problematic challenge for the drinking water industry. The conventional disinfection approach may not always be suitable since international regulations stipulate that new pathogens have emerged, and previously unknown disinfection by-products have been identified. Processes such as coagulation/sedimentation, granular media filtration, and chlorination have been used for years to reduce microorganisms in water and wastewater treatment. Recently, membrane filtration, ozonation, and UV irradiation have also been recognized as effective techniques for achieving microbial inactivation. According to Igawa et al. (2011), ozone is an economical, clean, simple, and efficient oxidation agent that is broadly used in industry. Likewise, ozone is commonly utilised for oxidative cleavage of a carbon-carbon double bond in organic synthesis, thus showing the significance of an addition-type oxidation of an alkene and its transformation in organic synthesis.

Historically, it was around 1906 that ozone came into use as a drinking-water disinfectant in France. From that moment, this practice has been adopted in several facilities in Europe, (Rice, 1985). First, ozone was used as a primary or sole disinfectant. Secondly, as an oxidant to regulate the flora, odour, and colour and to reduce the manganese and iron content of drinking water. So, with the improvement of the engineering sector, ozone has become widely used in flocculation of suspended particles in waters. However, ozone has attracted scientist's attention for many reasons. Firstly it was used to reduce the utilisation of free chlorine in water treatment processes. Literature reports that for years, free chlorine has been used not only as disinfectant but also as a powerful oxidant especially in North America. Nevertheless, its utilization results in the production of by-products such as trihalomethanes (THMs), which Lin and Shih (2000) and Backer et al. (2000) proved to be harmful to human health. Because of this limitation, alternatives have to be found. In recent times, chloramination (the combination of free chlorine and ammonia) has been widely used in flocculation of suspended particles in waters. Water treatment by chlorination was considered as the most popular alternative disinfection process since chloramines are free from THMs. Unfortunately, chloramines are weak oxidants, therefore stronger oxidants, such as ozone and chlorine dioxide were early established as substitutes for the chlorine treatment process. Apart from the fact that ozone was efficient compared to chlorine, ozone still shows its utility as a more powerful coagulant than chlorine, (Prendiville, 1986). Furthermore, the decomposition of ozone results in the production of

more potent radical intermediates than ozone itself. Prendiville (1986) also argued that since ozone is an unstable gas, it has to be generated where it can be used. Cold plasma discharge, usually called corona discharge, has been identified as the most suitable technique to generate ozone. In this method, ozone is formed by decomposition of diatomic oxygen O_2 according to the following equations:

O_2 (Corona Discharge) $\rightarrow$ $O^{\cdot} + O^{\cdot}$..... (2.1)

$O^{\cdot} + O_2 \rightarrow O_3$..... (2.2)

Recently, Locke et al. (2006) and Panicker (2003) reviewed the cold plasma technique used to generate ozone. This included the expansion of generators that operate in a reasonable frequency range and modifications of the tube design to give an advanced electronic system to control current. Bhattacharyya et al. (1995) proved that although it has been established that ozone is an effective oxidant towards hazardous organic pollutants, a single-phase ozonation system has limitations such as low ozone solubility, low ozone stability, and a lack of selective oxidation potential. Therefore it is crucial to mention that ozone should be combined with other agents or processes for an effective water and wastewater treatment rather than ozonation alone. These include hydrogen peroxide, UV radiations, metallic catalysts, such as reduced iron, and ultrasound. These combinations are usually referred to as Advanced Oxidation Processes (AOPs). Literature review indicates that a new generation of methods are being technologically advanced. These may reduce energy consumption, operational cost and infinitely enhance the degradation efficiency and hopefully meet future regulations associated with the microbiological quality of water (Movahedyan et al., 2009).

2.2.1 Advanced Oxidation Processes

Advanced oxidation processes (AOPs) focus on using hydroxyl radicals as primary non selective oxidants of organic pollutants. Such processes often result in a complete mineralization of organic molecules into CO_2 and water (Legrini et al., 1993). Literature shows that toxins such as pesticides, surfactants, colouring matters, pharmaceuticals and endocrine disrupting chemicals have already been treated in wastewater using Advanced Oxidation Techniques (AOTs). In addition, these methods have also been used in pre-

treatment processes aimed at reducing pollutant concentrations that impede biological wastewater treatment processes (Stasinakis, 2008). Advanced oxidation processes (AOPs) have been described as water treatment procedures that involve an input of energy (which could be chemical, electrical or radiative) into the water matrix to produce strong oxidizers. According to Carla et al. (2013), the principal function of AOPs is the in-situ production of chemical reactive species such as O_3, H_2O_2, $HO^{\bullet}$, $HO_2^{\bullet}$, and O^1 (D), etc. However, after fluorine (F_2, E^o = 3.03 V), $^{\bullet}OH$ radicals have been identified as the most effective oxidants in decomposing organic compounds into CO_2, water and inorganic salts. This is due to the $^{\bullet}OH$ high standard reduction potential (E^o = 2.8 V), compared to those of atomic oxygen (O_2, E^o = 2.42 V), ozone (E^o = 2.07 V), hydrogen peroxide (E^o =1.78 V) and Perhydroxyl radical (E^o = 1.70 V) as presented in Table 2-1.

Table 2-1: Oxidation potential of common oxidants

Oxidant	Oxidation potential (V)
Fluoride (F_2)	3.03
Hydroxyl radicals ($OH^{\bullet}$)	2.80
Atomic oxygen ($O^{\bullet}$)	2.42
Ozone (O_3)	2.07
Hydrogen peroxide (H_2O_2)	1.78
Perhydroxyl radical ($O_2H^{\bullet}$)	1.70
Permanganate (MnO_4)	1.67
Chlorine dioxide (Cl_2)	1.50
Chlorine (Cl)	1.36

Source: Carla et al. (2013); Cheng et al. (2007).

Hydroxyl radical attack occurs by abstraction of the hydrogen atoms (Equations 2.6 and 2.7), followed by electrophilic addition of $^{\bullet}OH$ (Equations 2.4 and 2.5), electron transfers (Equation 2.6) and radical-radical reactions (2.7 and 2.8) (Vujevic et al., 2013).

$HR + {}^{\bullet}OH \rightarrow R^{\bullet} + H_2O$ ..... (2.3)

$R^{\bullet} + O_2 \rightarrow RO_2^{\bullet}$ ..... (2.4)

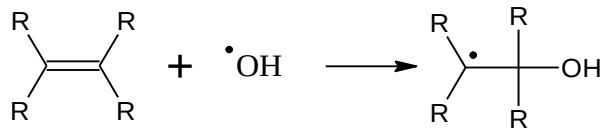

..... (2.5)

$RX + {}^{\bullet}OH \rightarrow RX^{\bullet+} + OH^{-}$ ..... (2.6)

$2OH^{\bullet} \rightarrow H_2O_2$ $k = 5.3\times109$ L mol^{-1} s^{-1} ..... (2.7)

$H_2O_2 + {}^{\bullet}OH \rightarrow HO_2^{\bullet} + H_2O$ $k = 2.7\times107$ L mol^{-1} s^{-1} ..... (2.8)

Conversely, the oxidizing species play a specific role towards organic pollutants. Active species, such as hydrogen peroxide have been proved too weak to degrade azo dyes alone at normal conditions of temperature and pressure. Furthermore, aromatic azo dyes are very stable when exposed to ozone; the reactivity of these compounds with ozone is very low compared to an olefinic or azomethine group (Galindo et al., 1999). Electrohydraulic discharge (EHD) as one of the AOPs produces a combination of all these reactive oxidizing species and has gained wide acceptance as a powerful alternative for wastewater remediation. Since AOPs have been studied for years, the most common techniques classified under AOPs definition and available in literature are listed in Table 2-2.

Table 2-2: Common advanced oxidation techniques (AOTs) available in literature

Process	Authors
O_3 / H_2O_2	(Juan et al., 2000 ; Selma, 2007)
O_3 / UV , UV / TiO_2 and UV / TiO_2 / O_3	(Farre´et al., 2005; Walid and Al-Qodah, 2006; Zou et al., 2008 ; Liuming et al., 2010)
UV / H_2O_2	(Madhu et al., 2009; Iqbal et al., 2013)
TiO_2 / UV and TiO_2 / UV/ H_2O_2	(Wu and Chern, 2006; Madhu et al., 2009)
O_3 / UV/ H_2O_2	(Selma, 2007)
TiO_2 Nanutubes / UV/ O_3 O_3 / TiO_2 / H_2O_2	(Liuming et al., 2009) (Selma, 2007)
H_2O_2 / UV /O_3 / TiO_2	(Selma, 2007)
H_2O_2 / O_3 / Fenton's reactions	(Selma, 2007 ; Wilhelmus, 2000)

UV/Ag-TiO_2/O_3	(Donghai et al., 2011)
Sonolysis	(Stasinakis, 2008)
Ozone sonolysis	(Stasinakis, 2008)
Catalytic oxidation	(Stasinakis, 2008)
Supercritical water oxidation or Wet oxidation	(Wilhelmus, 2000 ; Lukeš, 2000)
Radiolysis	(Wilhelmus, 2000; Lukeš, 2001)
Ultrasonic irradiation	(Wilhelmus, 2000 and Lukeš, 2001)

For decades most of these processes have been the subject of investigation for the degradation of organic pollutants in drinking water and wastewater treatment. In recent research studies, the Water Framework Directive of the European Commission has considered the following bio recalcitrant pesticides: alachlor, atrazine, chlorfenvinfos, diuron, isoproturon and pentachlorophenol as Priority Hazardous Substances (Wilhelmus, 2000). Literature shows that Photo-Fenton/ozone (PhFO) and TiO_2 -photo catalysis/ozone (PhCO), both combined systems, have been used as advanced oxidation processes for the degradation of these organic composites. Even though photo-Fenton reaction and TiO_2 -photo catalysis are not part of the current study, their use as common advanced oxidation processes had to be mentioned. In 2005, Farre et al. demonstrated that when PhFO and PhCO are applied respectively, the degradation process of the different pesticides occurs through oxidation of the organic molecules by means of their reaction with the generated OH radical which follows a first and zero-order kinetics. Additionally, Farre et al. (2005) investigated the total organic carbon (TOC) reduction of the different pesticides in aqueous solutions using these two advanced oxidation processes, together with the conventional ozone + UV technique. Results showed that best pesticide mineralization were obtained when PhFO was applied. The aqueous pesticide solutions became detoxified with the use of this advanced oxidation process, except in the case of alachlor and atrazine aqueous solutions after 2 and 3 hours of treatment respectively where no detoxification was achieved at the experimental conditions used in their work. Based on literature information, artificial light or solar energy has been used in different photochemical processes for the degradation of pesticides (Kochany et al., 1994; et al., 1994). Chiron et al. (2000) demonstrated that complete degradation of the pesticides is rarely achieved with such degradation processes since it requires long treatment periods. Therefore Legrini et

al. (1993) proved that an additional homogenous or heterogeneous oxidant could be used to improve the degradation power of photochemical oxidation process.

Recently, Walid and Al-Qodah (2006) combined advanced oxidation processes with biological treatment processes to remove both pesticides and then the chemical oxygen demand (COD) load from aqueous solutions. The study showed that O_3 and O_3/UV oxidation systems could remove 90 and 100%, of the pesticide deltamethrin, respectively in a period of 210 min. It was found that the combination of O_3 and UV radiation enhanced pesticide degradation and the residual pesticide reached zero in the case of Deltamethrin. Research results also revealed that at a pH value greater than 4, the combination of O_3 and UV could reduce COD up to 20%. In addition the degradation of pesticides and the removal of COD in the combined O_3/UV system followed pseudo-first-order kinetics and the parameters of this model were assessed. Walid and Al-Qodah (2006) investigated the application of the biological treatment to remove the bulk COD from different types of feed solutions. It was proved that over 95% of COD could be removed when wastewater was treated by the O_3/UV system and then fed to the bioreactor. Advanced oxidation processes (AOPs) have also been used to remove recalcitrant organic constituents from industrial and municipal wastewaters.

Moreover, recent applications to wastewater treatment as well as the advantages and drawbacks of these methods were presented (Stasinakis, 2008). Equally, some of the future challenges (decrease of operational cost, adoption of strategies for processes integration) were discussed. In addition, several organic compounds have been detected in industrial and municipal wastewater, (Stasinakis, 2008). Some of these compounds are primary constituents of organic dyes/azo dyes. On the other hand, the textile-processing industry is affecting the environment, by the release of heavily polluted wastewaters which largely contain organic azo dye compounds. Biological treatment methods have been chosen by Walid and Al-Qodah (2006) due to their reduced operational cost and they are well known as being environment-friendly. Literature highlighted that photo catalytic degradation of pollutants in the presence or absence of air is the most reasonable biological treatment strategy, (Harrelkas et al., 2008). Their study showed that in the absence of air (anaerobic), azo dyes and other types of dyes such as anthraquinone, phthalocyanine, and triphenylmethane could be decolourized. In the presence of air, aromatic amines from azo dye cleavage could be mineralized and other types of dyes could be removed by adsorption and biodegradation. However, Van der Zee and Villaverde (2005) discussed that it is

impossible that all aromatic amines can be degraded, and that the complete removal of other types of dyes is questionable.

These limitations therefore lead research to concentrate on combining biological treatment of dye-containing wastewaters with other methods such as, adsorption on solids (activated carbon, natural products such as agro wastes), coagulation - flocculation and most importantly advanced oxidation processes (AOPs). Systems such as UV-hydrogen peroxide (Daneshvar et al., 2005; Baldrian et al., 2006), ozonation (Farré et al., 2005) and O_3 / UV/ H_2O_2 (Selma, 2007), have been extensively described in literature as advanced oxidation processes and have demonstrated great detoxication efficiency. The later advanced oxidation processes are the principal driving force of dye oxidation in the present EHD system. Despite the fact that all advanced oxidation techniques have been used to treat water/wastewater, operational conditions, separation problems and mostly, the cost of some of these processes have been considered as limiting factors for these technologies. Therefore electrical discharges have emerged as novel and promising techniques for water/wastewater treatment.

2.2.1.1 ELECTRICAL DISCHARGES

The removal of pollutants from gaseous and liquid phases using electrical discharges (Sunka, 2001), has been considered as the principal AOP and various investigations have been conducted to comprehend the basic nature of these discharges. Electric discharge can be defined as the passage of a certain amount of electric energy into dielectric material which may result in excitation, dissociation and ionization of dielectric atoms and/or molecules and the process leads to the formation of a gaseous phase known as plasma. This plasma can be thermal or non-thermal depending on the energy input (Sunka, 2001). Quite a large number of electrical discharges have been reported in literature, however only four types of different electrical discharges have been extensively used in various investigations, which include lightning, arc discharges, corona and glow plasma discharge (Wilhelmus, 2000). As for corona discharge, the interaction of electrical discharge with air generates a strong electric field of about 200 KV/cm at the discharge streamer corresponding to average electron energy of about of 10 eV (Lide, 1999) which is the driving force in this process. Indeed Gupta (2007) discussed that the length of discharge streamers is enlarged with an increase of electron energy and thus, with the increase of electric field. The electron energy generated in corona discharge was later found to be

higher than the dissociation energy of water (5.16 eV), oxygen (5.17 eV) and nitrogen (9.80 eV).

This streamer discharge therefore makes corona discharge more attractive and extremely efficient compared to other advanced oxidation techniques. Also, Wilhelmus (2000) mentioned that the importance of corona discharge resides in the production of hydroxyl radicals as well as hydrogen atoms that are produced via dissociation and ionization of water molecules using the corona discharge process in water as shown in Equations 2.9 - 2.11

$H_2O + e^- \rightarrow OH + H + e^-$ dissociation..... (2.9)

$H_2O + e^- \rightarrow H_2O^+ + 2e^-$ ionization..... (2.10)

$H_2O^+ + H_2O \rightarrow H_3O^+ + OH$ dissociation..... (2.11)

Theoretically Sahni (2006) demonstrated that electrical discharges have two principal uses which include synthesis of compounds and degradation of contaminants (chemical and biological) in gas and water. Physical and chemical parameters from initiation of electrical discharges in water have been proved to be responsible for the synthesis or degradation of organic compounds.

Specialists in electrical discharges used contact glow discharge and demonstrated that complex bio-organic molecules, especially amino acids, were primarily produced by initiation of the discharge on the water surface therefore giving rise to new molecular species (Lukes et al., 2005; Grabowski, 2006). Until recently, numerous studies have been carried out and focus mainly on the utilization of electrical discharges to degrade pollutants from gaseous and aqueous streams which evolved from automobiles, chemical industries and other waste generating processes (Dang et al., 2008; Malik and Schluep, 2001). Techniques such as electrical discharges used to degrade and remove contaminants from air and water are also referred to as advanced oxidation processes (AOPs). These processes produce highly active species such as hydroxyl radicals (OH•), hydrogen peroxide (H_2O_2), atomic oxygen (O) and ozone (O_3) (Kajitvichyanukul et al., 2006). Several studies (Wilhelmus 2000) have been conducted on electrical discharges involving advanced oxidation technologies such as UV radiation and heterogeneous photo catalysis. For instance, Cooper and Ahluwalia, (2000); Savage and Oh (2001) and Griffith and

Raymond, (2002) investigated the supercritical water oxidation using electrical discharge. Also a number of combinations of hydrogen peroxide, ozone and UV light were studied (Cooper and Ahluwalia, 2000).

2.2.1.2 LIQUID PHASE ELECTRICAL DISCHARGE: ELECTROHYDRAULIC DISCHARGE

Depending on the amount of energy input and supplied voltage and current range in the system, Chang (2008) and Oi Lun Li et al, (2013) reported that electrohydraulic discharge can be divided into four different categories. These include pulsed corona electrohydraulic discharge (PCEHD) or pulsed spark electrohydraulic discharge (PSEHD) which use high voltage or low current discharges with energy per pulse of about 1 J/pulse or 10 J/pulse, respectively. However the pulsed arc electrohydraulic discharge (PAEHD) and the pulsed power electrohydraulic discharge (PPEHD) systems use higher current discharges. The PAEHD system uses energy of about 1 kJ/pulse with a few kV, whereas larger energy per pulse with higher voltages is required for the PPEHD system. Even though application of electrical discharge on the surface of water, in water and under water has been studied for many years, electrical discharge processes in liquid phase has mostly been explored in recent years for various purposes including water treatment (Chang et al., 2010), sterilization and decomposition of organic compounds (Angeloni et al., 2007; Yamatake et al., 2007).

Depending on the electrode configuration, electrohydraulic discharge involves the submersion of two electrodes in water. The high voltage and ground electrodes, when immersed into the solution, initiate a plasma channel that is characterised by both chemical and physical properties (Chang et al., 2010). Electrohydraulic discharges (above, under or directly in aqueous medium), involving the generation of plasma have been recognized to be effective at degrading and removing a number of organic pollutants such as phenols (Sun et al., 2000; Lukes et al., 2002), trichloroethylene (Sahni et al., 2002) and organic dyes (Sato et al., 2000) from water and wastewater. Yet plasma study and the effect of its properties on the decomposition of organic pollutants remains an open field for research. Since the current EHD system is based on plasma generation, therefore a full description of plasma concept has been elaborated in the following section in order to define the actual EHD system.

2.2.2 Plasma technology

Plasma is often categorised as the fourth state of matter besides solid, liquid and gas that are commonly known (Kaunas, 2012). Plasmas are generally ionized gases that consist of electrons, positive and negative ions and neutral species (Kaunas, 2012). These gases either ionise completely (100%) or are somewhat ionised (with low values between 10^{-4} – 10^{-6}). Moreover, Sturrock (1994) identified two other groups of plasmas such as low temperature plasmas (≤ 50 000 K), and high-temperature or fusion plasmas (50 000 – 10^{6}K). Nehra et al. (2008) equally classified plasmas into two categories. The first category is the one in which the active species (electrons, ions and neutrons) have the same temperature and is usually referred to as thermal equilibrium plasmas, in the case of fusion plasma ($T_e \approx T_i \approx T_n > 10^6$ K). Whereas in the second category known as non-thermal/equilibrium plasma, the aforementioned species have different temperatures in such a way that electrons are considered to have a higher temperature (10,000 – 50,000 K) than that of heavy ions and neutrals, hence ($T_e >> T_i$, with $T_i \approx T_n$). Furthermore, the authors emphasised that plasma can be classified based on pressure. Based on this, Kaunas (2012) wrote that the gas discharge plasmas can be classified into local thermodynamic equilibrium (LTE) and non-LTE plasmas. As for LTE plasma, the high pressure induces many collisions in the plasma and therefore leads to a significant energy interchange between the plasma species. On the other hand, the low gas pressure in non-LTE plasma leads to few collisions and hence different temperatures of plasma species due to poor energy exchange.

As earlier mentioned, in equilibrium plasma, electron temperature (T_e) is generally equal to ion temperature (T_i) or thermodynamic gas temperature (T_g). However, in non-equilibrium plasma, (T_e) largely exceeds (T_g) and the temperature of heavy particles. Kauna (2012) also found that in non-equilibrium plasma, the electron density (n_e) is often reasonable in the bulk region of plasma and becomes significant toward the centre of the dense volume. Based on this background information the plasma concepts are briefly summarised and presented in Table 2-3.

Table 2-3: Classification of plasma

Plasma	**State**	**Example**
	Low temperature plasma	
Thermal plasma (Quasi-equilibrium plasma)	$T_e \approx T_i \approx T_g \leq 2\times10^4 K$ $n_e \geq 10^{20}\, m$	Arc plasma, plasma torches, RF inductively coupled discharges
Non-Thermal plasma (Non-equilibrium plasma) (NTP)	$T_e >> T_i \approx T_g = 300\ldots10^3 K$ $n_e \approx 10^{10}\, m^{-3}$	Glow, corona, direct barrier discharge, atmospheric pressure plasma jets, hollow cathode discharges, electron beams, microwave and etc.

(Source: Kaunas, 2012)

A few years ago, Nehra et al. (2008) argued that low pressure discharge plasmas play a significant role in fundamental research, microelectronic industry and material technology. The use of air to generate these plasmas in numerous configurations makes these technologies extremely expensive and time consuming. Apart from this, the amount of their corresponding activated particles is small. Therefore there is an urgent need to develop new plasma sources which could maintain constant properties and operate unchangeably at atmospheric pressure. Non-thermal plasma generated at 1 atm presents operational and economic advantages which have led to the development of multiple plasma sources that have been employed in the industries. Based on these claims, great attention has been paid to ANTPs due to their substantial industrial advantages compared to low-pressure discharge. A decade ago, Mark and Schluep (2001) reported that Non-thermal atmospheric plasma (NTP) offers a number of advantages for environmental control and protection such as dry cleaning operations as well as processing of chemical waste streams.

Apart from these advantages of NTP highlighted by Mark and colleagues, Nehra et al. (2008) recalled that NTP may be obtained by a variety of electrical discharges including micro hollow cathode discharge, corona discharge, atmospheric pressure plasma jet, one atmospheric uniform glow discharge, dielectric barrier discharge (DBD), plasma needle and gliding arc discharge presenting crucial technological applications. The common

characteristics of these plasma sources based on plasma properties have been summarised by Nehra et al. (2008) and are presented in Table 2-2.

Table 2-4: Plasma properties of atmospheric discharge schemes

Parameters	**Corona Discharge**	**DBD**	**APPJ**	**Atmospheric glow MHCD**
Method and type	Sharply pointed electrode	Dielectric barrier cover on electrode	RF capacitively coupled	DC glow with micro hollow cathode electrode
Excitation	Pulsed DC	AC or RF	RF 13.5 MHz	DC
Pressure (bar)	1 bar	1 bar	760 torr	1 barr
Electron energies (eV)	5 variable	1 - 10	1 - 2	……
Electron Density (cm^3)	10^9 -10^{13}	$\approx 10^{12}$ - 10^{15}	10^{11} - 10^{12}	……..
Breakdown voltage (kV)	10 - 50	5 - 25	0.05 – 0.2	…….
Scalability & flexibility	No	yes	yes	yes
T_{max} Temp, T (K)	Room	Average gas Temp (300)	400	2000
Gas	…….	N_2 + O_2+ NO Rare gas / Rare gas halides	Helium, Argon	Rare gas, Rare gas/ rare gas halides

Source: Nehra et al. (2008).

APPJ = atmospheric pulsed plasma jet; MHCD = micro hallow cathode discharge.

Over the last few years, plasma treatment has widely attracted scientists' attention as an alternative method of cleaning water. This is due to the production of UV radiation, shock waves and mostly highly reactive species such as O_3, H_2O_2, $^{\cdot}OH$, etc. that oxidize the pollutant and mineralize it into CO_2, H_2O and simpler inorganics. Besides, electrode configurations in the aforementioned electrical discharge reactors also play a crucial role

in the treatment of polluted water. In fact most electrode arrangements in these water/wastewater technologies have failed to meet the expectations of significantly cleaning polluted water. Therefore, electrode configuration is a key parameter to differentiate electrical discharges from one another. For instance, several electrode configurations summarised by Gupta (2007) and presented in Figure 2-2 and 2-3 have been explored in corona electrohydraulic discharge reactors. In these configurations, the powered tipped anode is directly in contact with the discharged gas and the polluted liquid. This usually results in electrodes etching and corrosion. In addition, in corona discharge active species result from streamers produced at the tip of the conductive anode. This could therefore slow down/limit the production of oxidizing species responsible for the degradation of organics and microbes.

Therefore, the development of a novel reactor configuration with different electrode arrangements is of great importance to overcome water pollution dilemma. The choice of dielectric barrier discharge (DBD) over corona discharge and other types of electrical discharges lies in plasma properties proposed by Nehra et al. (2008) and presented in Table 2. In addition, the presence of one or two dielectric barriers in DBDs facilitates a fair distribution/dispersion of high energetic electrons (charges) on the surface of the whole electrode and therefore increasing micro discharge density along the anode surface. Other than the plasma generated inside the discharge zone, UV, shock waves as well as ozone is produced. In DBD, the charges are dispersed along the anode rod. This increases the yield of reactive species in the DBD reactor which improves the rate of decomposition of the pollutant. Based on these benefits of DBDs, various DBD reactor/electrode configurations have been developed. The common DBD configurations employed in literature are introduced in Figures 2-4 – 2-7, and the following paragraphs showing the structure and description of the DBD.

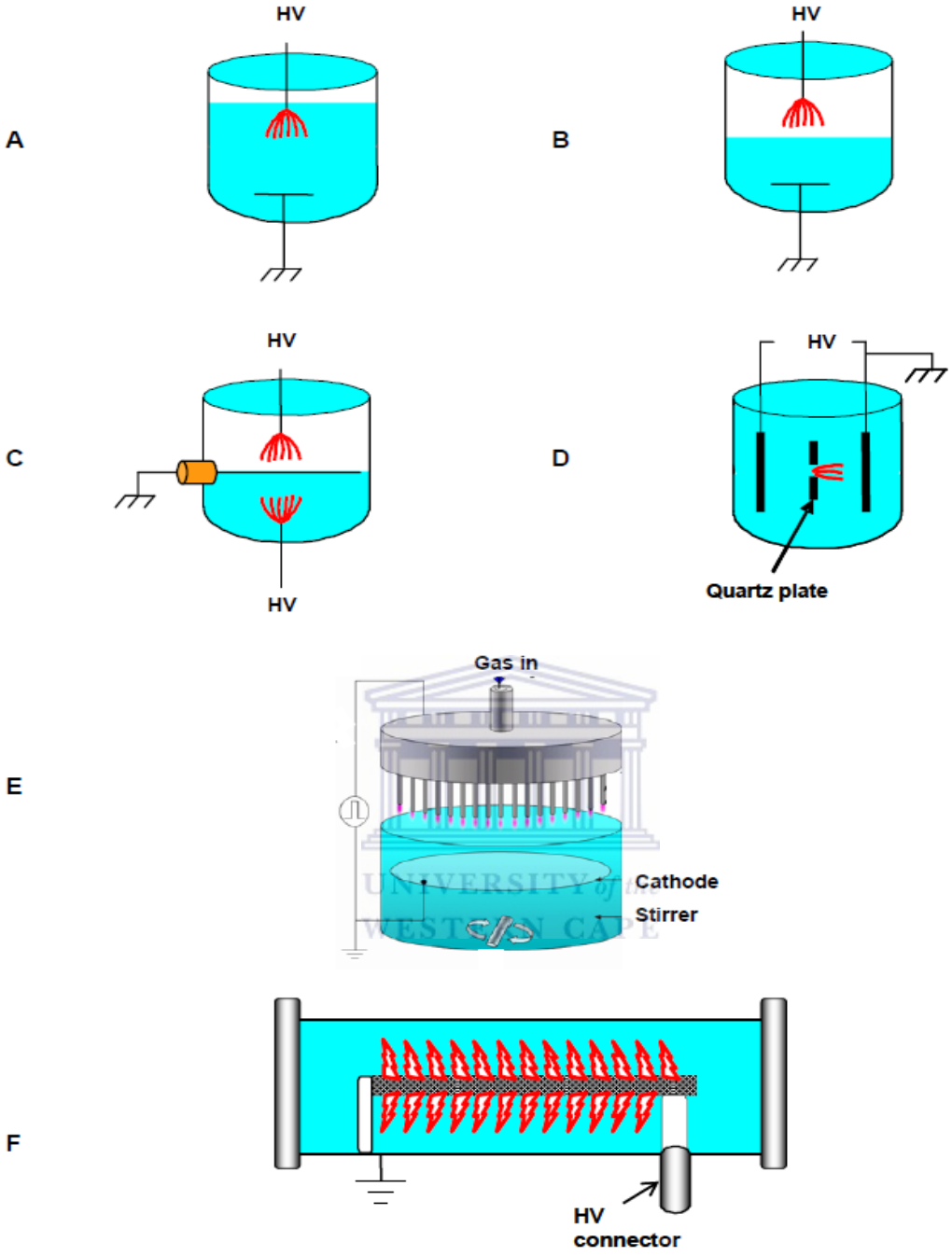

Figure 2-2: Different configurations for the initiation of streamer discharges in water[A] Point plane geometry for liquid phase corona discharges. [B] Point-plane geometry for glow discharge initiation in the gas plenum above the water. [C] Hybrid geometry for simultaneous streamer discharge initiation in the water and in the gas plenum. [D] Streamer discharge originating from a diaphragm. [E] Multi-pin reactor configuration. [F] Coaxial pulsed underwater corona reactor with anode covered by a porous ceramic layer (Gupta, 2007).

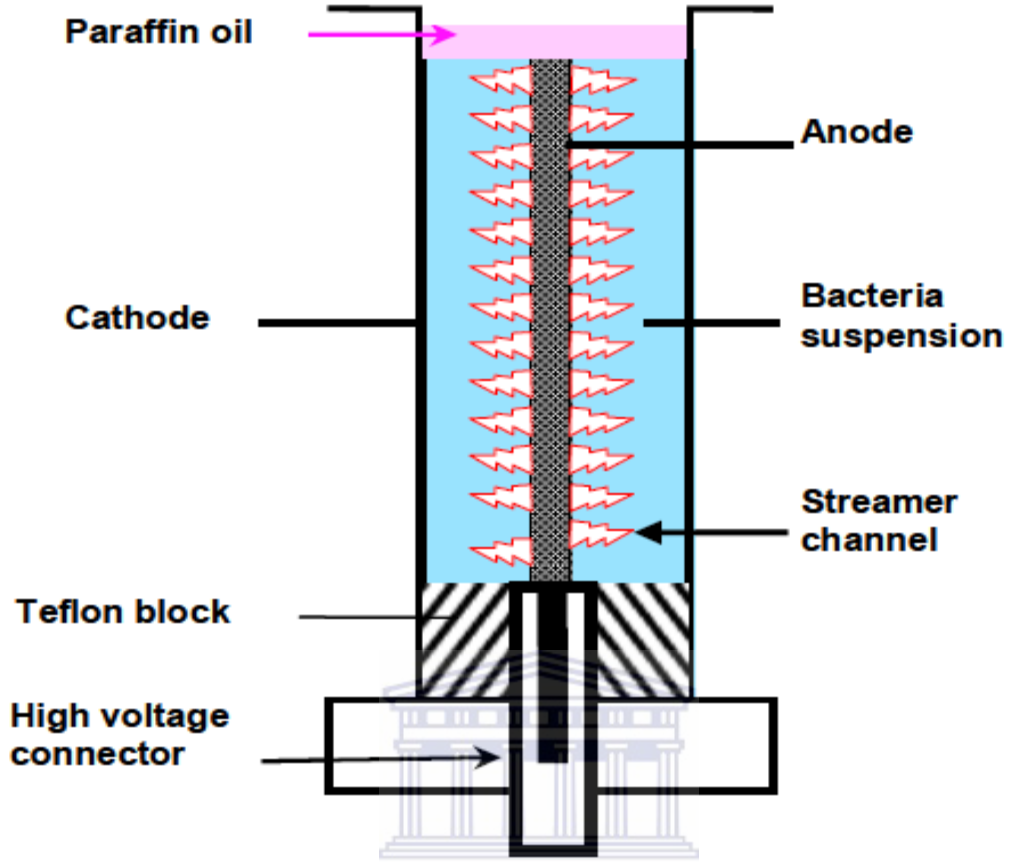

Figure 2-3: Schematic diagram of the modified corona reactor for microbiological studies (Gupta, 2007).

In Figure 2-3 the reactor was positioned vertically and the dead volume in the chamber was eliminated by a cylindrical Teflon block on the bottom and an oil paraffin layer on the top to avoid electrical breakdown in air.

2.2.3 Structure and characteristics of the dielectric barrier discharge

Mark and Schluep (2001) characterised dielectric barrier discharges (DBDs) as specific and silent AC electrical discharges providing durable thermodynamic, non-equilibrium plasma at reasonable atmospheric temperature and pressure. Based on the discharge properties and the various possibilities in configurations, different DBDs names like barrier discharge, silent discharge, ac-discharge, normal pressure glow discharge, ozonizer discharge and display discharge are often used to denote DBD (Kaunas, 2012). Their studies highlighted that DBDs are usually formed in configurations consisting of two

electrodes (anode and cathode) whereby one or both metal electrodes are normally protected with layers having a high insulating (dielectric) constant such as pyrex, quartz, ceramic, etc., that separates them from a gas layer (single dielectric). Otherwise the dielectric can also be positioned between electrodes to separate two gas layers (double dielectric). Kaunas (2012) also proved that DBD is a non-equilibrium discharge that can be operated at ambient conditions with the main goal being the long term generation of ozone. In this regard, Nehra et al. (2008) proposed that the difference between a traditional and a DBD discharge relies on the fact that in traditional discharge, electrodes are directly in contact with the discharge gas and plasmas. This consequently leads to premature electrode etching and corrosion during the discharge process. However, in DBDs the electrode (anode and cathode) is separated from the discharge gas by one or more dielectric layers and hence reducing or eliminating electrode etching and corrosion as presented in Figures 2- 4 – 2-7

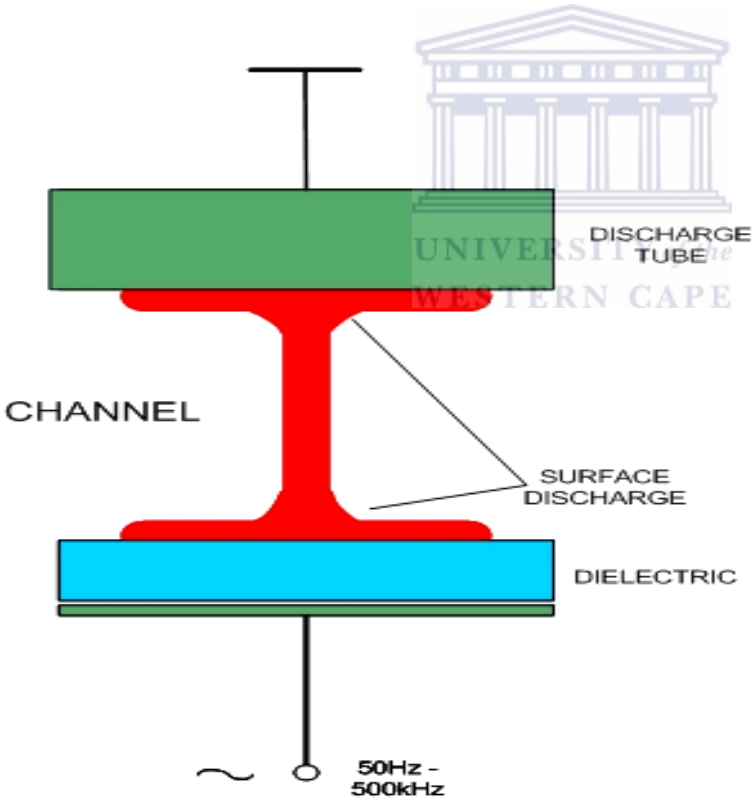

Figure 2-4: Single planar dielectric electrode configuration (Lopez, 2008):

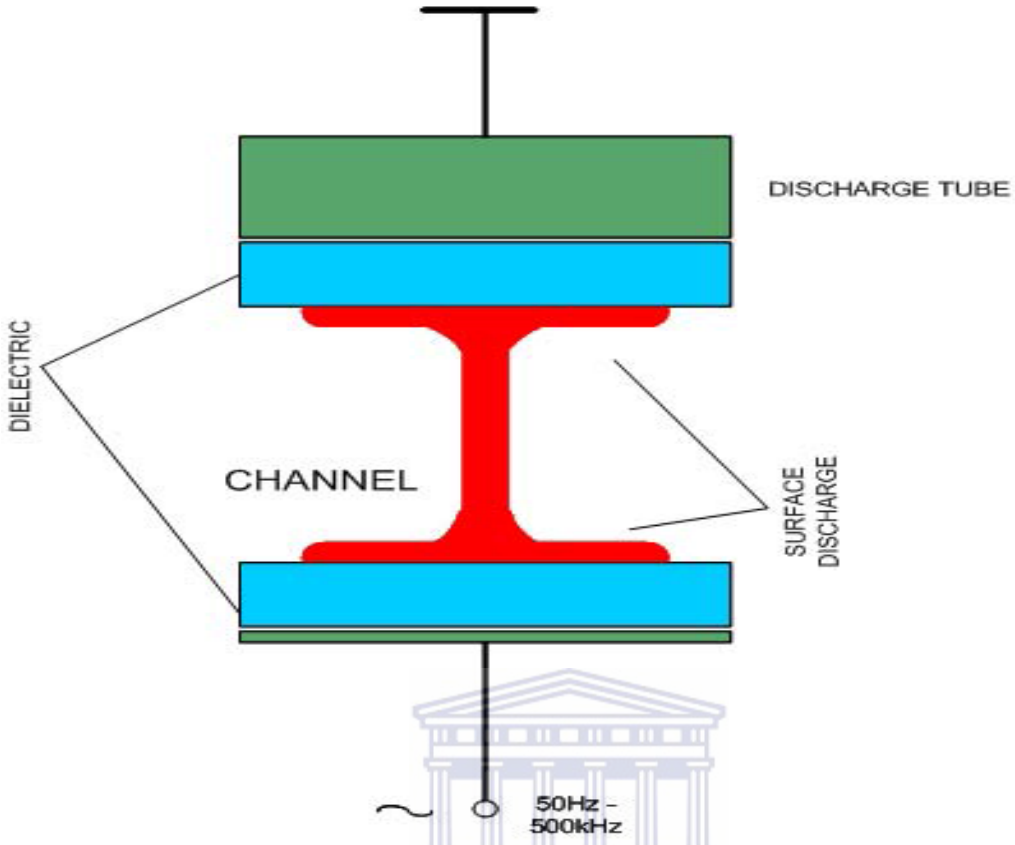

Figure 2-5: Double planar dielectric electrode configuration, (Lopez, 2008)

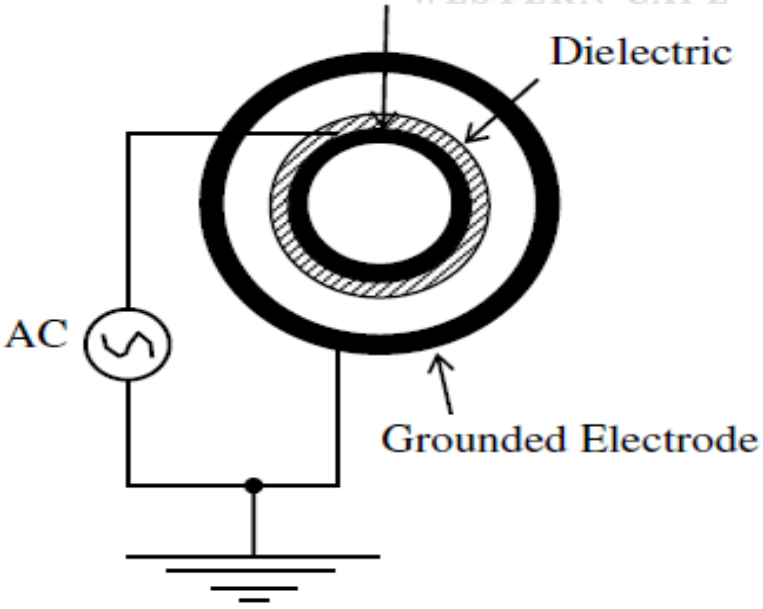

Figure 2-6:Cylindrical single dielectric electrode arrangement, (Source: Nehra et al., 2008)

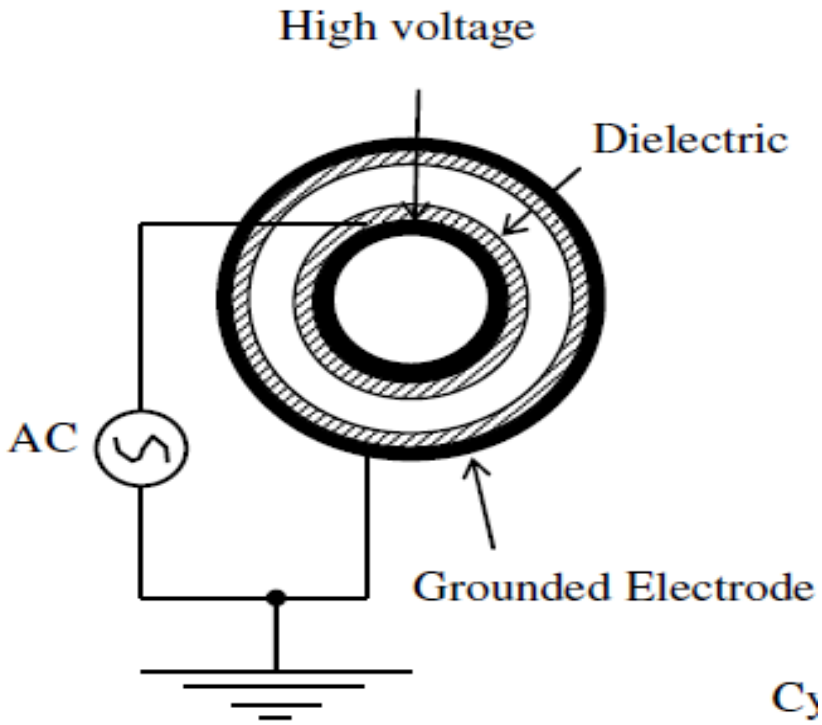

Figure 2-7: Cylindrical double dielectric electrode arrangement (Source: Nehra et al., 2008)

In addition, glass, quartz, ceramics and electroactive polymers are usually used as common dielectric materials. The distance between electrodes (gap) varies noticeably from a few millimetres to several centimetres. Also, Lopez (2008) and Kaunas (2012) recalled that the dielectric limits the amount of charges transported by a single micro discharge (micro plasma) over the entire electrode surface area. Also, Konelschatz et al. (1997) claimed that non-equilibrium plasma conditions of DBD are presented in a simpler way compared to those of other types of discharges such as electron beam, low pressure discharges and pulsed high pressure corona discharges. This aspect therefore gives DBD a possibility of being scaled up from the laboratory scale to industrial conditions. According to Lopez (2008) and Nehra et al. (2008), DBD cannot be performed using DC but can be operated at high voltage alternating current (AC) due to the capacitive coupling of dielectric which requires an alternating voltage to drive a displacement current.

A decade ago, Kogelschatz (2003) demonstrated that ionization of the discharged gas, also called breakdown, occurs in the region between the two electrodes in a DBD reactor at a sufficiently high voltage. In this process, the charges accumulated on the surface of the dielectric layer discharge somewhere else on the exterior of the insulator. Hence, plasma generation is maintained if the continuous energy source delivers a corresponding degree

of ionization preventing the recombination route that leads to the destruction of the discharge. During the discharge of the accumulated particles, an energetic photon, whose frequency and energy correspond to the type of gas used is emitted and fills the discharge gap. Kogelschatz and colleagues also showed that numerous configurations can be used to induce DBD. Some of these include parallel plates (planar) separated by a dielectric or cylindrical and coaxial plates with a dielectric tube between them. The common DBD configurations reported in literature are presented in Figure 2-8.

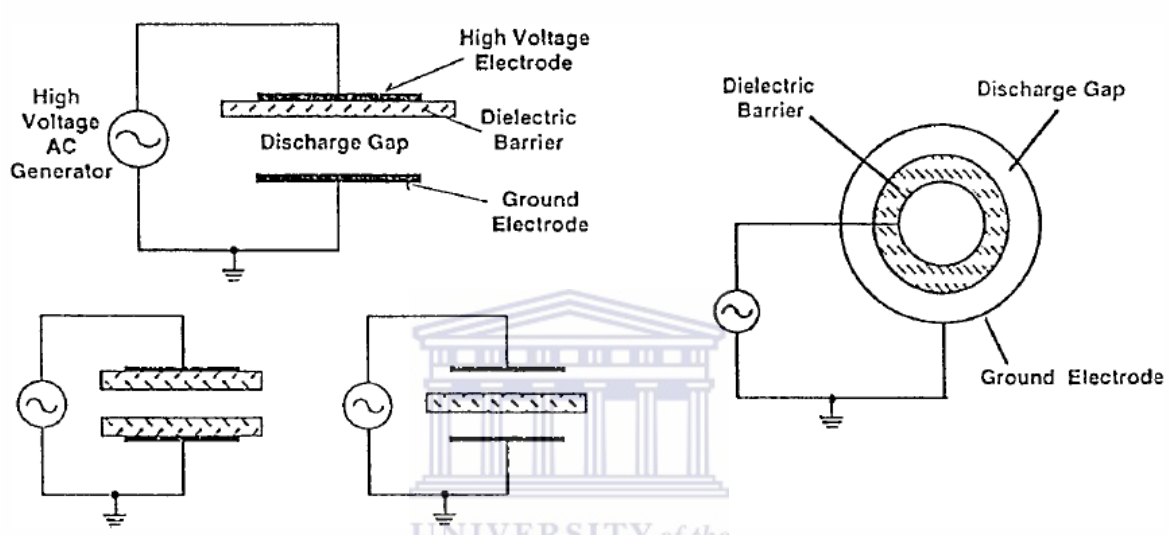

Figure 2-8: Common dielectric barrier discharge configurations with one or two dielectric barriers, (Kunas, 2014).

In addition, Mark and colleagues clarified that the creation of DBDs is characterized by the production of a huge amount of short lifetime micro discharges induced by the continuous current flow in the system. The study also proved that the dielectric barrier conformation supplies a self-ending electrical discharge regardless of the applied voltage wave shape. Their paper also highlighted that in the absence of a barrier/insulator, gas pressures of about one atmosphere and a gas discharge gap of limited millimetres, only a few localized intense arcs would develop in the gas gap between the powered metal electrodes (mark and Schluep, 2001).

However, in the presence of the dielectric layer between the conductive electrodes with an AC voltage of about 1 - 100 kV and a frequency of a few or several Hz, a significant amount of plasma is created by an important number of micro discharges in the gas discharge zone, (Nehra et al., 2008; Mark and Schluep, 2001) whereby each micro

discharge is regarded as a source of non - thermal plasma characterised by energetic electrons that produce extremely reactive free species in the plasma region. As earlier mentioned, in non-thermal plasma, species such as electrons, ions and neutrons have different temperatures and hence different kinetic energies. Thus in the case of DBD, electrons having the highest energy, initiate the formation of active species such as O_3, H_2O_2 and mostly free radicals including $O(^1D)$, $O(^3P)$, OH•, and H• from the gaseous feeds such as O_2, air, etc., which are immediately used to decompose the contaminants.

2.2.4 Degradation of organic pollutants using DBD plasma - an overview

The aforementioned advantages of DBD over the conventional plasma technologies have attracted a wide attention in various studies. Very recently, Reddy et al., (2014) used a cylindrical single dielectric barrier catalytic non-thermal plasma reactor (Figure 2-9) for mineralization of endosulfan in aqueous medium for the treatment of pesticide contaminated water.

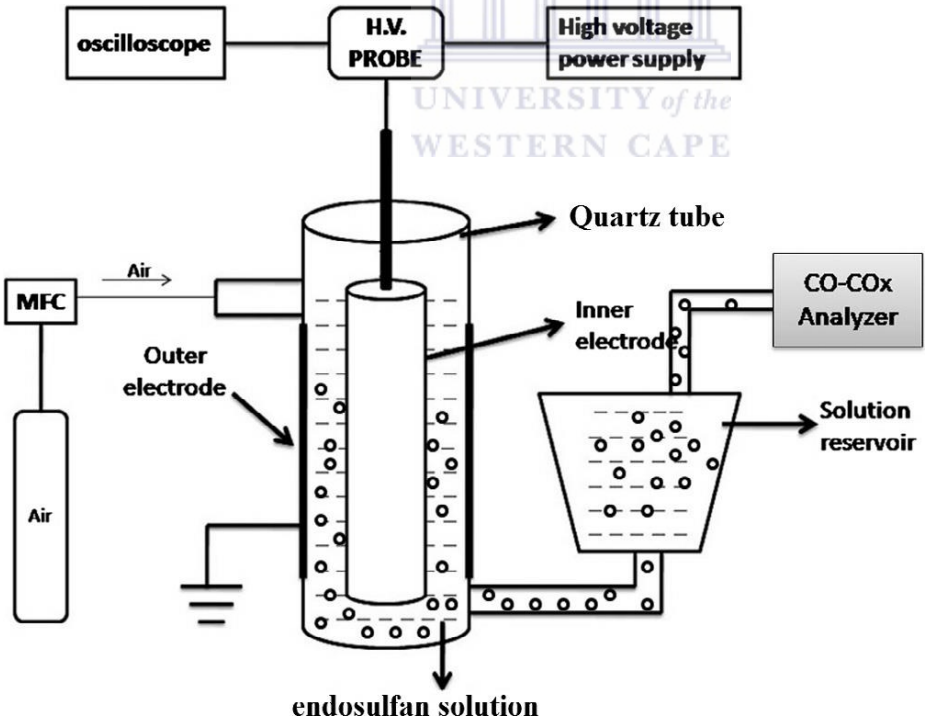

Figure 2-9: Single dielectric barrier discharge experimental setup for the treatment of endosulfan in aqueous medium (Reddy et al., 2014)

Indeed, in their study an advanced oxidation process was developed by combining non-thermal plasma with cerium oxide catalysts for the mineralization of a model pesticide endosulfan from aqueous medium. The single dielectric electrode configuration presented in Figure 2-9 shows that the endosulfan solution was mixed with air and the catalyst in the gas discharge gap and therefore exposed to micro discharge plasmas generated on the inner electrode (first dielectric quartz). Cerium oxide was used to take advantage of the UV generated by the DBD reactor. Since Emsley (2011) reported that cerium catalyst can absorb UV light, therefore the results of the study conducted by Reddy et al. (2014) showed that the synergetic effect between the catalyst and the UV light produced in the DBD reactor improved not only the conversion but also increased the mineralization efficiency of the pollutant. This was evidenced by total organic carbon and infrared spectroscopy analysis. Various similar studies on treatment of water/wastewater using single dielectric electrode configuration have been conducted. Joshi et al. (2011) reported that oxidative stress induces membrane lipid peroxidation, which leads to the production of detrimental substances causing oxidative modification in cells. Based on this claim, Joshi et al. (2011) successfully applied non-thermal plasma using a floating-electrode dielectric-barrier discharge (FE-DBD) technique for rapid inactivation of bacterial contaminants in normal atmospheric air. The study proved that reactive oxygen species (ROS) such as singlet oxygen and hydrogen peroxide-like species were the main regulator oxidative species in the oxidative stress process, these oxidising agents were also suspected to be responsible for the lipid peroxidation in *Escherichia coli.* In the same vein, Reddy et al. (2013) investigated the plasma-induced methylene blue degradation using dielectric barrier discharge. In their study, dielectric barrier discharge at the gas water interface was used as an advanced oxidation process for the oxidative degradation of dye contaminated wastewater. Mark and Schluep (2001) proved that DBD can be used to degrade volatile organic compounds (VOCs) as their emission into the atmosphere can cause adverse effects on human health such as photochemical smog formation. In that regard, Mark and Schluep (2001) used a single DBD to generate gas-phase free radicals such as O (^{1}D), O(^{3}P), $OH^{\cdot}$, etc. at low temperature (293 K) to decompose pollutants, such as benzene. The results showed that a near complete decomposition of benzene (> 99%) was reached in both wet and dry gas streams. Apart from environmental and industrial applications, DBD has also been employed in the medical sector. For example, Arjunan et al. (2012) recalled that vascularization is very important for tissue engineering and wound healing. They highlighted that non-thermal plasma principally DBD as a source of reactive oxygen

species (ROS), has been frequently used for medical applications like sterilization, malignant cell apoptosis and blood coagulation. Based on these DBD applications, Arjunan and colleagues (2012) conducted the treatment of liquids and porcine aortic endothelial cells with a non-thermal dielectric barrier discharge plasma in vitro. The successful outcomes of their study showed that endothelial cells treated with a plasma dose of 4.2 J cm^{-2} had 1.7 times more cells than untreated samples 5 days after plasma treatment. In addition, Mastanaiah et al. (2013) claimed that sterilization by plasma is faster, less toxic and multipurpose compared to traditional sterilization methods. By using low temperature, atmospheric, single dielectric barrier discharge surface plasma generator, the authors achieved great sterilization (elimination of different bacteria) in short periods of time over the conventional sterilization techniques.

Apart from the single DBD, double DBD has also been used in several different fields such as environmental, industrial and health sectors. In the double dielectric configuration, the two conductive electrodes are protected by two insulating layers (dielectrics). The discharge zone between the inner and the outer dielectric quartz is a source of highly reactive species produced via the interaction of air gas and the highly energetic electrons widely dispersed on the surface of the anode in the inner quartz tube. The resulting free radicals in the air gap are directly circulated into the polluted solution to induce oxidation process. In the same way, the single dielectric barrier discharge has been explored in various fields; several experiments have also been performed with the double dielectric barrier discharge. For instance, Rong et al. (2014) applied a cylindrical double dielectric barrier discharge (DBD) reactor (Figure 2-10) as an advanced oxidation process for the degradation of diclofenac in aqueous medium. The outcomes of their study showed that at specific conditions (power 50 W and a pH of 6.15) a 10 mg/L diclofenac was completely removed within 10 minutes. These authors also affirmed that the presence of Fe^{2+} in the liquid phase promoted the decomposition of diclofenac.

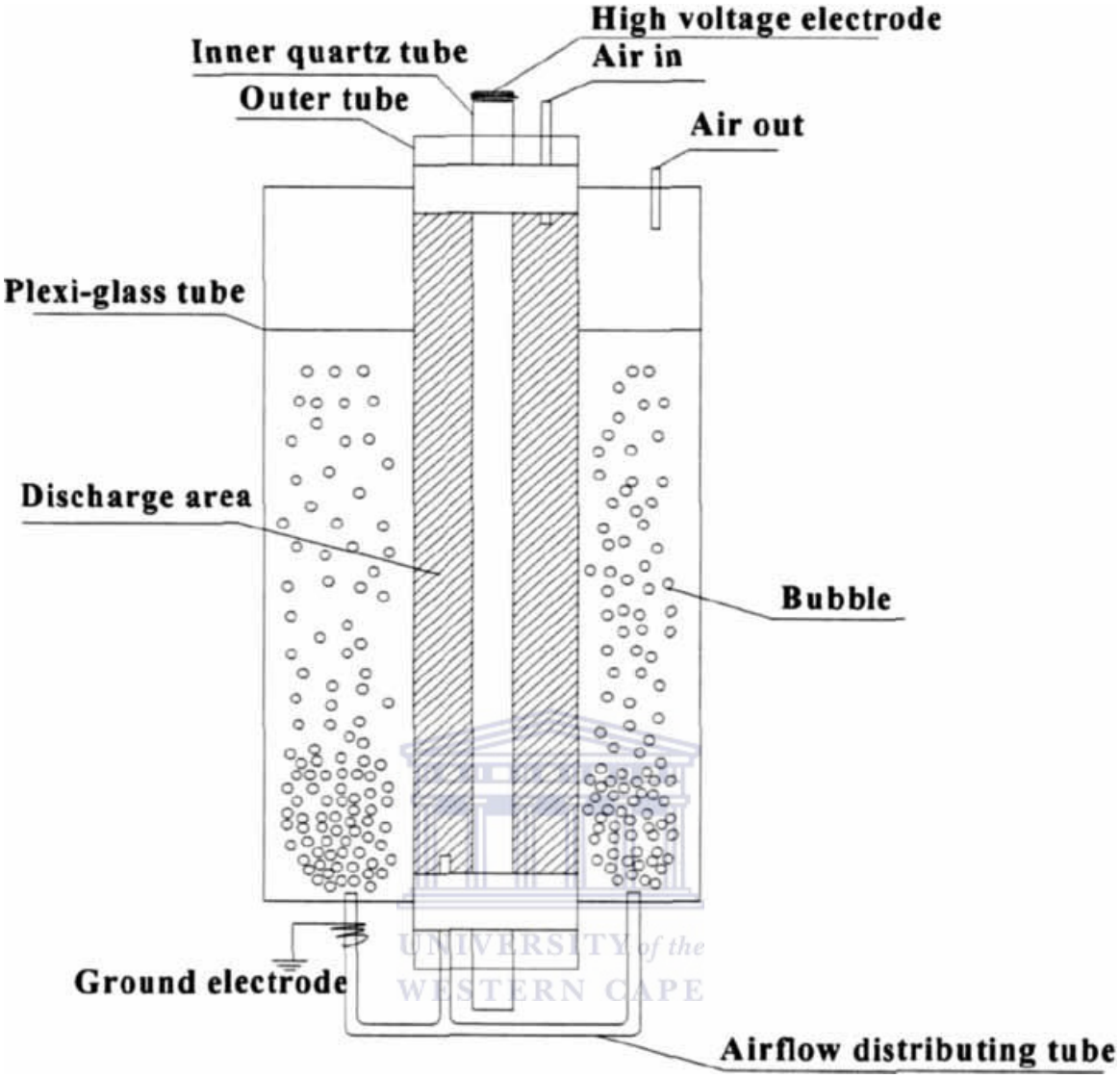

Figure 2-10: Cylindrical double DBD experimental setup (Source: Rong et al., 2014), (Discharge area = air gap).

As for medical applications, Deng et al. (2008) investigated bacterial inactivation by atmospheric pressure dielectric barrier discharge plasma jet. In their experiment, *Bacillus subtilis* and *Escherichia coli* planted in two media (agar and filter papers) were exposed to after-glow plasma generated by a double dielectric barrier discharge (DBD) plasma jet generator in open air at a temperature between about 30 to 80 ^{o}C. For the bacteria planted in agar medium, the results showed that after 5 min of treatment, the effective area of inactivation was much larger than the plasma jet and increased with the plasma treatment time. In the case of the bacteria seeded in the filter paper, the results indicated that significant inactivation was obtained when adding reactive gases such as oxygen and hydrogen peroxide vapour compared to noble gases.

As earlier mentioned in sections based on the structure and description of the DBD, electrode/reactor configuration is a very crucial parameter for treatment of effluents. The literature cited in the paragraphs above showed that the cylindrical single dielectric configuration can be employed in various applications. Likewise, the cylindrical single and double barrier has also been widely utilised in water/wastewater treatment technologies.

2.2.5 Summary of plasma properties in DBDs

Smirnov (1977) summarised plasma properties as a conductive fluid containing the same number of positive and negative charge carriers. The author further demonstrated that the fundamental property of plasma is based on the existence of the electric and magnetic field which perhaps is the driving force behind the process. Panicker (2003) submitted that different types of gas ionization occurred during plasma processes especially when air is used as a feeding gas for the production of the plasma. Thus, several ionizations were noticed among which are, particle impact ionization, photo or irradiative ionization and electric field ionization. These ionization categories are discussed below.

2.2.5.1 Particle impact ionization

This ionization is a phenomenon in which particles, predominantly electrons or ions, strike the atoms and make them lose or gain a charge depending on the amount of transmitted energy during collision. In fact, the transferred energy has to surpass the ionization energy (Ei) of the atom. During electron impacts, an atom can absorb an electron and the absorbed electron can excite the outermost electrons of the atom until it becomes ionised if continuously provided with enough energy. Furthermore, this type of ionization probably occurs in regions bounded by strong electric or magnetic field where the particles are usually accelerated. In case the electrons produced during the ionization process have high energy, a secondary ionization can be induced. The author explained further that ions can also be accelerated and interact with atoms and ionize them. Since ions are heavier species, their acceleration requires extreme amount of energy in the presence of strong electric and magnetic field. Nuclear reactions are often used for ions acceleration and ionization of gases. However, this approach is not safe and is not the subject of interest in the present study.

2.2.5.2 Photo or irradiative ionization

As per this type of ionization, Panicker (2003) mentioned that photons of high energy can ionize atoms provided that the amount of energy associated with photon is greater than that of the atom. Gamma rays, X-rays and ultraviolet rays, are often solicited for such process. In correlation with the current work, the UV radiations generated in the present DBD plasma reactor scatter in different direction and are diffused in the bulk solution, and hence, irradiate molecular and ionic species present in the polluted solution.

2.2.5.3 Electric field ionization

Electric field ionization involves the circulation of gas (air in the actual study) between the ionized electrodes (anode and ground electrodes). In this process, depending on the polarity of the electrode, atoms or molecules brought in contact with the surface of the metal electrodes loose or gain charges. In order to initiate ionization, the density of the electric field has to be as high as possible. Another essential parameter necessary for rapid ionization is electrode geometry. Indeed, electric fields around sharp materials and metallic surfaces with low radii of curvature are stronger than around rounded frames. However, when particles such as oxygen approach an electrode highly surrounded by a strong electric field, it gets ionized before reaching it. The degree of ionization drops with the decrease in the electric field intensity. The electric field ionization is easily generated and controlled in the laboratory. Also different electrodes geometries with various conformations can be designed and varied for specific task.

2.2.5.4 Formation of UV light and reactive species in the DBD system

In plasma processes, the high energetic electrons impact with neutral molecules such as O_2 and N_2 in the air gap region (of the present DBD configuration) excites these molecules to higher energy levels (Equations 2.12 & 2.14). The relaxation of the excited molecules (O_2* and N_2*) to their lower energy states (Equations 2.13 & 2.15) according to Jiang et al., (2014) leads to the emission of the UV light that shines around the whole anode electrode and propagated in all directions within the bulk solution.

$N_2 + e^- \rightarrow N_2^* + e^-$ excitation …… (2.12)

$N_2^* \rightarrow N_2 + hv$ relaxation…….. (2.13)

$O_2 + e^- \rightarrow O_2^* + e^-$ excitation……... (2.14)

$O_2^* \rightarrow O_2 + hv$ relaxation…….. (2.15)

This process has been widely observed during the photodecomposition of organic pollutants. This view was expressed by Willberg et al. (1996) and Joshi et al. (2013) who independently observed that when an organic compound (C) is illuminated by UV light, it gets promoted to an excited state (C^*) and instantly falls back to the ground state (C) due to its short lifetime (10^{-9}–10^{-8} s). During relaxation of the compound, the decomposition of the molecules new species becomes evident as shown in Equation (2.16).

$C + hv \rightarrow C^* \rightarrow$ products……. (2.16)

Additionally, Peyton and Glaze (1988) and Anpilov et al. (2001); supported the claims that, besides the photo-degradation of organic molecules, UV light also plays an important role in the dissociation of ozone and hydrogen peroxide and hence enhance the production of OH in plasma treatment process. Furthermore, the generated $OH^{\cdot}$ radicals attack and decompose the target pollutants. Therefore in the present DBD system, the UV light is generated in the discharge gap as a result of the collision between highly energetic electrons and the neutral O_2 and N_2 molecules from the dry air.

2.2.5.5 Ozone formation and properties (Oxygen based species)

Several species of oxygen and nitrogen are formed during plasma process induced by the decomposition of air via electrical discharge (Wilhelmus, 2000**)**. Among the oxygen species, ozone (O_3) is identified as an allotrope of oxygen and remains the principal molecule responsible for the decomposition of the target organic contaminants (Jiang et al. 2014). According to Jiang and co-workers (2014), O_3 is usually produced via the exposure of oxygen to electrical discharge in the air gap zone of a DBD plasma reactor and circulated within the bulk solution with continuous flow of dry air and current both in contact. This strong oxidizing O-based species exhibits crucial chemical properties. Ullmann (1991) and Kirk and Othmer (1996) showed that O_3 is a strong oxidizing agent with an oxidation potential of E^0 = 2.08 V. Also, Glaze (1987) stated that ozone mainly

reacts with chemical compounds through three different routes. The author considered ozone as an electron transfer acceptor that can oxidize metal ions, or an electrophile that induces the oxidation of phenol and other stimulated aromatics. Then ozone can act as a dipole addition reagent when added to carbon–carbon multiple bonds. Gurol and Vatistas (1987) affirmed that the electrophilic characteristic of ozone is due to the presence of the positive charge on oxygen atom leading to resonance structures as shown in Figure 2-12.

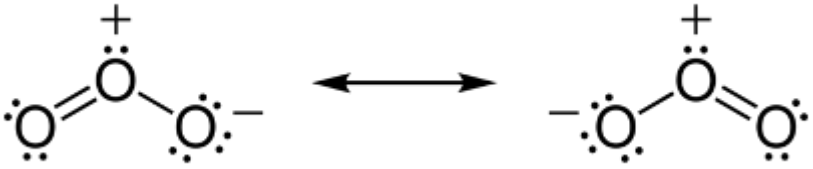

Figure 2-11: Resonance structure of ozone (Vatistas, 1987)

In addition to this, the author concluded that the chemical instability of ozone leads to its decomposition through a various mechanistic reaction chains resulting in the production of $OH^{\cdot}$ radicals as shown in Equations 2.16 and 2.18.

$$O_3 + OH^{\cdot} \rightarrow O_2 + HO_2^{\cdot} \quad \text{(2.17)}$$

$$HO_2^{\cdot} + O_3 \rightarrow OH^{\cdot} + 2O_2^{\cdot} \quad \text{(2.18)}$$

Moreover, Ullmann (1991), Kirk and Othmer (1996), and Lide (1999) proved that at room temperature, ozone is able to oxidize water molecules to hydrogen peroxide. This was supported by Glaze (1987) and presented in Equations 2.19 and 2.20.

$$H_2O_2 \rightarrow H^+ H_2O^- \quad \text{(2.19)}$$

$$O_3 + H_2O^- \rightarrow {}^{\cdot}O_2^- + {}^{\cdot}OH + O_2 \quad \text{(2.20)}$$

As earlier mentioned, the UV light produced in the current DBD system is diffused in the aqueous solution and irradiates the O_3 dissolved in the polluted water. In this regards, Atkinson and Carter (1984) substantiated further that UV radiation with a wavelength of $\lambda \leq 310$ nm can dissociate O_3 into singlet oxygen and oxygen molecule. The singlet oxygen can react with water yielding hydroxyl radicals which eventually recombine to form H_2O_2

(Haugland, 1996). Some dissociative chemical reactions of O_3 are presented in Equations (2.21-2.23).

$O_3 + h\nu \rightarrow O\ (^1D) + O_2\ (1\Delta g)\ \lambda \leq 310$ nm..... (2.21)

$O\ (^1D) + H_2O\ (g) \rightarrow 2OH$ ..... (2.22)

$O\ (^1D) + H_2O\ (l) \rightarrow H_2O_2$..... (2.23)

2.2.5.6 Hydrogen peroxide

Assuming that dry air consists of small traces of hydrogen, therefore the generation of OH radicals in the plasma zone might be possible. However, the diffusion of these powerful reactive species (diffusion distance 6×10^{-9} m) from plasma region to the bulk zone of the target contaminant is very insignificant (Roots and Okada, 1975). Therefore, the formation of long-lived molecular active spices such as hydrogen peroxide in the bulk solution is necessary. Ullmann (1991) and Kirk and Othmer (1996) highlighted that hydrogen peroxide usually considered as the recombination product of hydroxyl radicals has a reduction potential of E^0=1.76 V in acidic medium. However, its presence in water treatment processes is of great importance. Yet, H_2O_2 apart from its oxidizing agent properties substantially contributes to the synthesis via dissociation, photolysis and metal-based catalytic reactions of various other oxidizing reactive species such as $^{\cdot}OH$, HO_2^-, etc. in the polluted solution (Jiang et al., 2014). Lide (1999) also informed that in plasma processes, about 213 KJ/mol (2.2 eV) is required to break the OH-$OH^{\cdot}$ bond during decomposition of H_2O_2 by pyrolysis. The authors submitted that hydrogen peroxide is unstable at high concentration and has the ability to oxidize and reduce itself at room temperature. They affirmed that the decomposition of concentrated hydrogen peroxide is an exothermic process that releases about 98.3 kJ/mol. Furthermore, Moeller (1957) confirmed that hydrogen peroxide is a weak acid with a dissociation constant pKa = 11.75. The chemical reactions based on the formation and decomposition of H_2O_2 are listed in Equations (2.24 – 2.27) (Wilhemus, 2000).

$H_2O \rightarrow H + OH$ ..... (2.24)

$H + O_2 \rightarrow HO_2$…….. (2.25)

$HO_2 + OH^- \rightarrow O_2^- + H_2O$…….. (2.26)

$2HO_2 \rightarrow H_2O_2 + O_2$..... (2.27)

Based on the aforementioned facts from literature, the hydrogen peroxide species is expected to be mostly produced in the bulk MB solution in the current EHD system.

2.2.5.7 Formation of HO· radicals and their reactions

Most advanced oxidation processes (AOPs) reported in literature as water treatment techniques are based on the production of hydroxyl radicals **(**Lukeš, 2001). These powerful free reactive species are highly reactive, nonselective and responsible for the decomposition of various organic and inorganic molecules into harmless compounds.. Indeed, Sangster (1971) and Mark et al. (1998) (recalled that there are three different ways through which OH radicals reacts with organic and inorganic compounds. These include abstraction of a hydrogen atom (Equation 2.28), electrophilic addition to double/triple bonds (Equation 2.29) and electron transfer (Equation 2.30). (Gogate and Pandit, 2004 (a); Gogate and Pandit, 2004)(b).

$OH\cdot + RH \rightarrow R\cdot + H_2O$ ……..... (2.28)

$OH\cdot + R_2C{=}CR_2 \rightarrow R_2\,(OH)\,C\text{-}CR_2\cdot$……..... (2.29)

$OH\cdot + RX \rightarrow XR\cdot{+} + OH^-$ …….. (2.30)

Indeed, the aforementioned theoretical chemical reactions, established for the production of powerful oxidants in EHDs have been summarized by Gupta (2007) and presented in Figure 2-13 below.

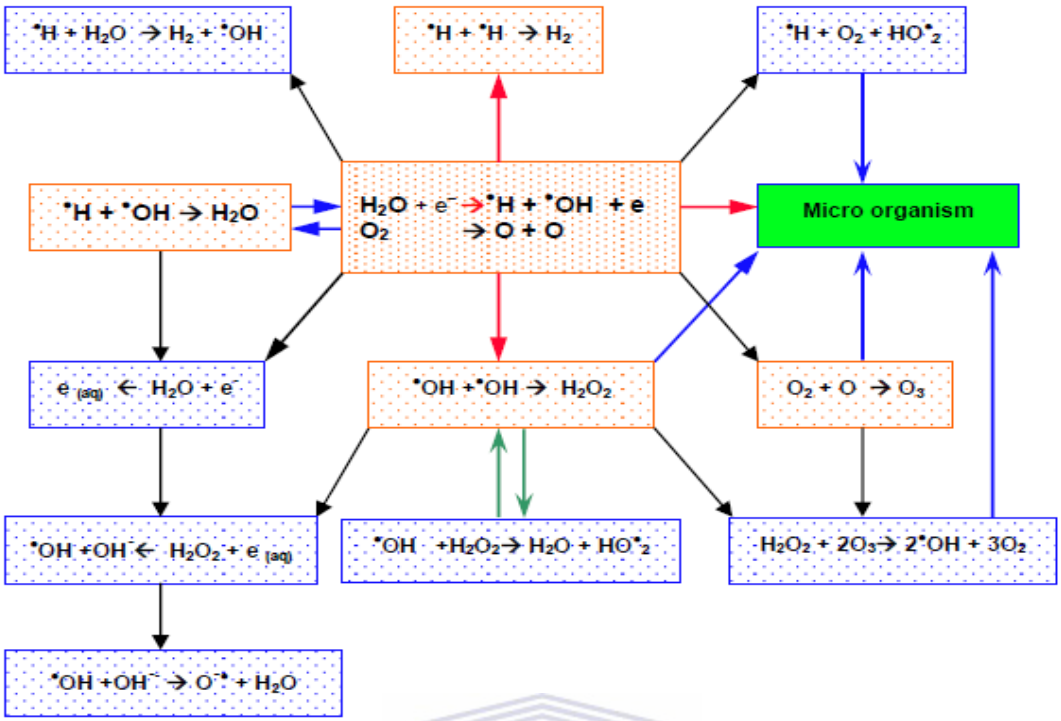

Figure 2-12: Mechanistic summary of possible chemical reactions occurring during plasma process in electrohydraulic discharge system (Gupta, 2007).

2.2.6 Optimisation methodology of DBD reactor

Ibrahim (2012) reported that the traditional one-parameter-at-a-time method has been used to optimise photoreactor systems. In this approach, the optimisation is achieved by varying one factor while the other factors kept constant are. Once the optimum condition based on the decomposition rate of the targeted contaminant has been determined, the rest of the parameters are successively studied till optimization of the whole system is achieved. The one-parameter-at-a-time technique has been extensively recognized and used to boost numerous working systems. Nevertheless the difficulty to assess the interaction of parameters at different levels is a great challenge in this method. In addition, the optimisation procedure is more operational using a multivariable optimisation approach (Chang et al., 2010).

Dielectric barrier discharge (DBD) has already been investigated by various research teams and has been proved to be effective in removing pollutants from contaminated waters. However, optimization of the DBD method does not present concise information in literature. The purpose of this section is to provide information on DBD optimization from

similar previous studies. According to literature, optimization of most of the water treatment approaches has been achieved by varying operational parameters of the process such as dye concentration, pH, solution volume, gas flow rate and the conductivity of the solution. In addition some studies highlight that electrodes and reactor configuration may also play an important role in the removal efficiency of toxins from polluted waters.

From literature, the degradation of MB by electrical discharge has been the subject of various research studies. However, the difference between these works lies on the type of discharges and the electrode or reactor configurations (Magureanu et al., 2007). Most of the studies on MB decolourization have been conducted in pulsed corona electrohydraulic discharge, (Magureanu et al., 2007; Malik et al., 2002; Grabowski et al., 2007). However, the optimization of a DBD using MB as model compound presents little information in literature. Nevertheless, Magureanu et al. (2008) investigated the decomposition of MB in water using a continuous dielectric barrier discharge system. In their study, a coaxial DBD configuration (Figure 2-14) was used to optimize the system by assessing the effect of some of the operating parameters such as the effect of voltage amplitude and polarity, Gas and liquid flow rate were also investigated.

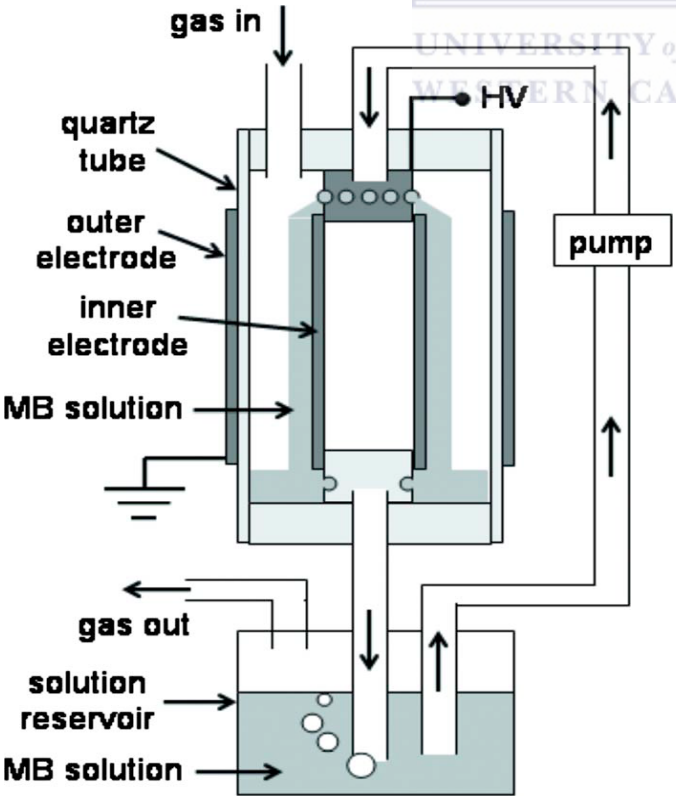

Figure 2-13: Experimental setup of the coaxial DBD system (Magureanu et al. 2008)

The results obtained showed that 95% of MB conversion was achieved after 30 minutes of plasma treatment with a positive polarity of the applied voltage corresponding to a yield of 57 g/kW h. The results also highlighted that gas flow rate did not impact MB removal. Whereas the study showed that the solution flow rate had an effect on MB degradation over a short period of time. In opposition to this authors indicated that for long treatment times, a lower flow rate improved the conversion of MB.

As it can be observed from Figure 2-14, the coaxial DBD reactor used by Magureanu and colleagues is a single dielectric barrier configuration with a quartz tube separating the outer electrode from the MB solution. In comparison with the present configuration, the actual EHD system consists of a double cylindrical DBD reactor whose optimization for decomposition of organic pollutants such as dyes such as MB in air has not yet been mentioned in literature. Nevertheless, the optimization of dielectric barrier discharges for the decomposition of organic compounds other than MB has been attempted in literature.

About a decade ago, Joelle (2006) investigated the optimized operational parameters in a hybrid DBD plasma reactor as shown in Figures 2-15 and 2-16. The optimization process involved was assessing the effect of operational factors such as solution volume (42 – 50 mL), gas flow rate (15-70 cc/min), the treatment time (3-9 minutes) and the gas type (air and oxygen) on the degradation of indigo dyes (blue) using UV-visible absorption spectroscopy**.** The optimization process was carried out by varying one parameter at a time and keeping the rest constant. In Joelle's study, oxygen was used as a feeding gas and optimization of operational parameters was achieved by recording the absorbance of treated and untreated Indigo blue samples at 600 nm (UV-visible). The study showed that decolourization of Indigo blue was more efficient with oxygen used as a feed than air. This was due to the fact that discolouration with air induced to the formation of nitrates and nitrous acid in the bulk solution. As for solution volume, the author reported that the decolourization was found to be optimal at a volume of 45 mL. However, Indigo blue decolourization efficiency decreased with an increase in oxygen flow rate. According to Joelle, this was perhaps due to a smaller residence time of the gas into the reactor.

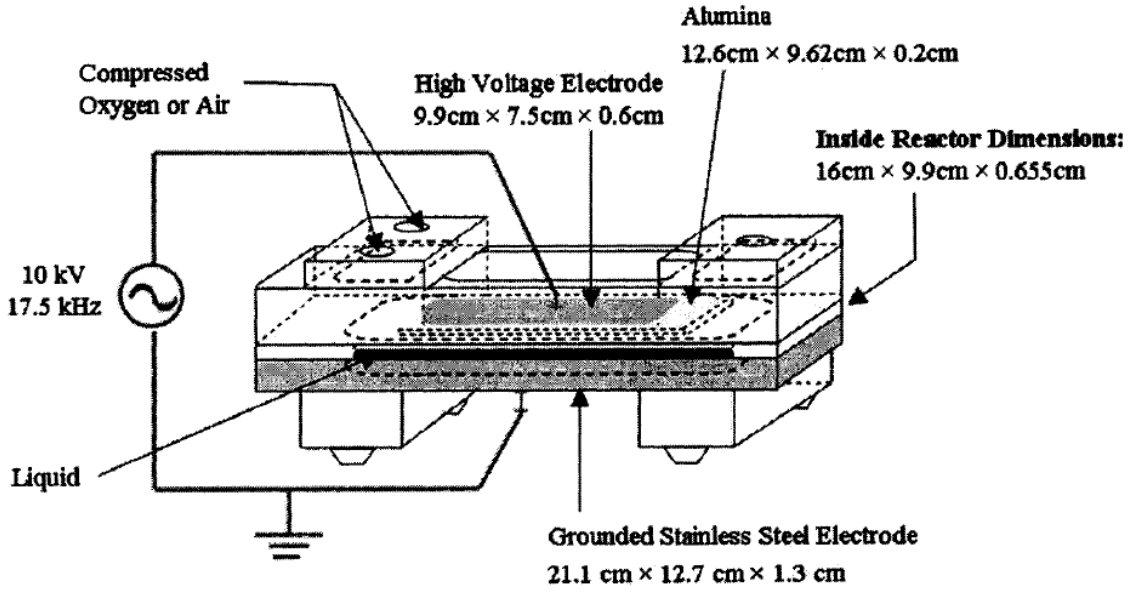

Figure 2-14: Schematic of the parallel hybrid gas-liquid atmospheric pressure dielectric barrier discharge (DBD) reactor (Joelle, 2006)

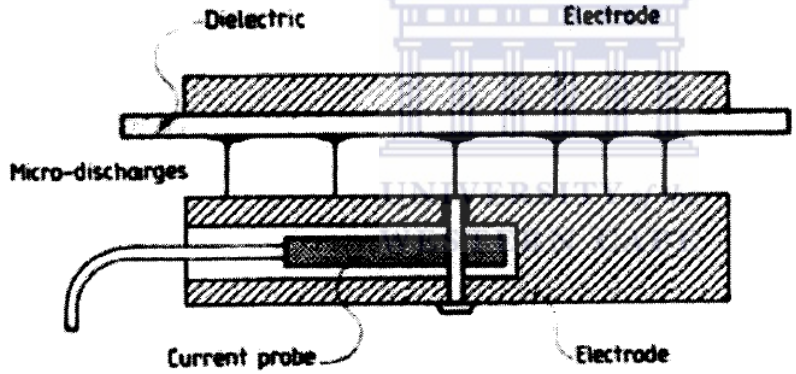

Figure 2-15: Single parallel DBD section of the reactor used to investigate the effect of operational parameters on the degradation of indigo dyes (blue) (Joelle, 2006).

So the optimization methods revised in this subsection have been explored for the optimization of the current DBD plasma system using MB as the model contaminant. The effect of physico-chemical operational parameters such as MB concentration, solution pH, conductivity and volume, etc. electrical parameters and reactor configuration on the decolourization efficiency of MB at ambient conditions. Furthermore, the treated and untreated MB samples were characterized by analytical techniques such as UV-vis and FT-IR. Ecological parameters such as TOC and COD were also assessed. Nitrates and sulphate tests were also performed to investigate the amount of these by-product salts in the bulk

solution before and after treatment. Hence, a corresponding review of these methods has been presented in the following paragraphs.

2.2.7 Model compound: Methylene blue (properties and degradation by DBDs)

Methylene blue (MB) with a chemical structure presented in Figure 2-17 is a heterocyclic aromatic chemical compound with the molecular formula $C_{16}H_{18}N_3SCl$. According to WHO (2008), MB was earlier prepared in 1876 by the German chemist named Heinrich Caro. This two membered ring molecule has been widely used in chemistry and industry especially in photocatalysis and dyeing processes (Hameed et al., 2007). At room temperature, MB is an odourless solid and dark green powder whose dissolution in water leads to a blue solution. In this study, MB was used as simulated targeted organic dye for the optimization of the DBD plasma system.

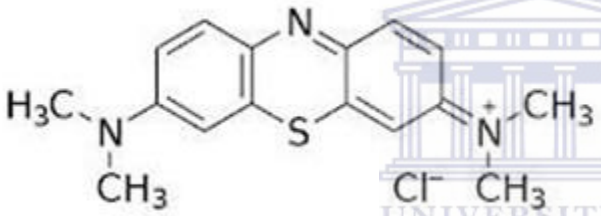

Figure 2-16: Structural formula of methylene blue (Hameed et al., 2007)

Advanced oxidation processes (AOPs) based on DBDs have become quite an interesting research field for the decomposition of dye contaminated wastewaters. This is due to the fact that AOPs have been proved to degrade and mineralize the pollutants whereas physical methods usually transform them from one form to another.

Methylene blue and other dyes such as methylene orange are specific types of organic pollutants that are usually found in effluents from chemistry related industries. Particularly, methylene blue has been the subject of various decontamination studies using traditional and new pollutant removal methods. However its degradation using dielectric barrier discharge (DBD) presents little information.

Few years ago, Huang et al. (2010) investigated the degradation of MB using a single parallel DBD system as shown in Figure 2-18.

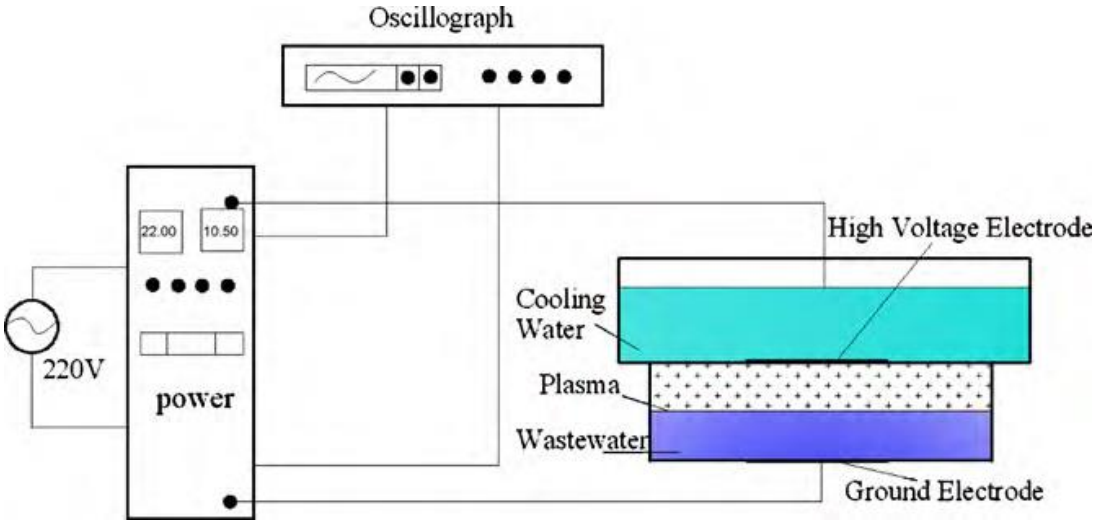

Figure 2-17: Single parallel dielectric barrier discharge experimental set up (Huang et al., 2010)

In their paper, the effect of certain parameters such as pH, dye concentration, etc. affecting the degradation of MB was assessed. The analysis of radical species in the solution was the principle key factor in their DBD method. The results of their study showed that the lowest degradation of MB was obtained at neutral conditions. However, the highest one was achieved in acidic than in basic conditions. Moreover, the authors showed that reactive species such as O_3 and •OH are the driving force in the decomposition process. Hence the authors claimed that the production of OH radicals during the decomposition process was favoured by the presence of OH^-. Furthermore, through ionic chromatogram, Huang and co-workers proved that oxidation of MB in the DBD system leads to the formation of inorganic ions such as NO_3^-, SO_4^{2-}, and Cl^- in the solution. These inorganic species usually lower the pH of the solution during the treatment process.

Additionally, Reddy et al. (2013) conducted a study based on the degradation and mineralization of MB using the same single DBD non-thermal plasma configuration as early shown in Figure 2-9. The effect of the operational parameters like applied voltage, pH, dye concentration, addition of Na_2SO_4 and Fe^{2+} and the formation of H_2O_2 on MB decomposition was evaluated. In their results, it was shown that up to 67 g/kW h of MB degradation yield was achieved. Hydrogen peroxide (H_2O_2) was detected and its formation was confirmed during the reaction. The results also showed that the addition of Fe^{2+}induced photo-Fenton reaction which in turn improved the performance of the reactor.

Even if some researchers might have attempted degrading organic pollutants especially textiles dyes using DBD plasma systems, the full study based on decomposition of MB by a cylindrical double DBD has not been reported yet. So in the present study a complete optimization of a DBD system using a cylindrical double dielectric barrier discharge reactor was conducted. A cross section of the cylindrical double DBD reactor used in this study is presented in Figure 2-19. The performance of the DBD reactor was evaluated by decolourization of simulated synthetic wastewater using MB as a target contaminant.

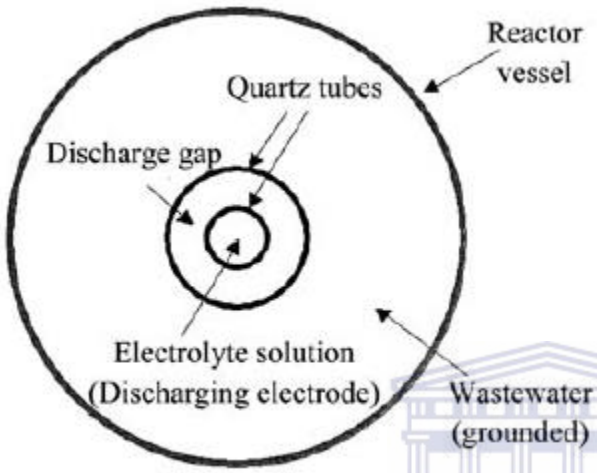

Figure 2-18: Cross –sectional view of the DBD reactor used in this study

2.3 CRITICAL REVIEW OF CHARACTERIZATION TECHNIQUES

In the EHDs literature reviewed in previous sections, decomposition of the targeted contaminants has been investigated by several characterization techniques among which UV/vis, FT-IR, COD, TOC, and nitrate analysis have commonly been explored. So in this subsection a summarized review of these techniques has subsequently been proposed.

2.3.1 Ultraviolet and Visible Spectroscopy (UV/VIS)

Xing (2010) stated that UV/VIS spectroscopic is a useful method usually used to identify unsaturated organic compounds such as aromatics. Pons et al. (2004) confirmed that the absorption of light in these molecules is due to the excitation of the most outer electrons of atoms of these compounds. According to Peuravuori et al. (2002), light absorbing sub units also called chromophores present in dissolved organic carbon (DOC) and humic substances of water sample are responsible for the absorption of both visible (VIS) and

ultraviolet (UV) light. Peuravuori et al. (2002) and Abbt-Braun et al. (2004) highlighted that the chromophores with C=C and C=O, C≡C, N=O double bonds in DOC absorb UV light in the 200 to 400 nm wavelength range. However, UV absorbance is proved to be widely used than VIS not only because the required instrumentation is inexpensive, easy to carry out but mostly because UV light is more absorbed by organic compounds. Moreover, Xing (2010) mentioned that humic substances are the major organic substances that initiate the formation of disinfection by products (DBPs).

Based on the light absorbance measured at the corresponding wavelength, a UV spectrum of absorbance versus wavelength is plotted. Whereas, the few UV absorption spectra obtained from UV analysis are usually broad and practically undistinguished and therefore difficult to interpret. Hence the resulting few and broad peaks are often attributed to the chromophores present in DOC (Peuravuori et al. 2002). Consequently, the practical level of aromatic constituents in the water sample is commonly indicated in the UV spectrum at a wavelength of 54 nm (Allpike et al., 2005; Chen et al., 2003; Chouparova et al., 2004 and Croue et al., 2000).

Moreoverthe concept of specific UV absorbance (SUVA) which represents the ratio between UV absorbance and DOC mass concentration was introduced (Thompson et al., 1997 ; Jame et al., 2003; Liang and Singer, 2003). This was then used to characterize the hydrophobicity of the aromatics of the aquatic DOC. As a result, the high SUVA indicated high molecular size hydrophobic aromatic constituents. In addition, Krasner and Amy (1995) demonstrated that the SUVA can also be used as an indicator of disinfection by-products (DBPs) organic precursors. Apart from this, Kim and Yu (2005) showed that the ratio of UV absorbance at 253 and 203 nm (UV253/UV203) can also be used to illustrate the functional distribution of DOC between the phenolic and carboxylic fractions. In such regard, the higher UV253/UV203 ratio denoted a larger phenolic content and a possibility for the formation of DBP. Furthermore, Martynas et al. (2013) reported that the colour removal of model simulated wastewater represents a preliminary test to assess the decomposition efficacy of organic pollutants used as model compounds in wastewater treatment. In their study, the concentration of dyes was followed by UV/VIS spectroscopy method using UV/VIS spectrophotometer (Genesys™ 8, Thermo Scientific, UK) equipped with a 1 cm quartz cell. Their first step involved scanning dye samples in a complete UV/VIS range by measuring the maximum absorbance at a maximum wavelength. Thereafter the measured absorbance of known concentrations was used to plot a calibration curve which allowed them to estimate the concentration of unknown solutions

sampled during the treatment time. Though UV/vis analysis has extensively been used to investigate the decolourization/degradation of the pollutant, however, additional techniques such as FT-IR is solicited for functional groups identification in treated and untreated solution samples.

2.3.2 Fourier Transform Infrared (FTIR) Spectroscopy

Apart from UV/VIS spectroscopy methods described in the previous section, Bruice (2004) and Xing (2010) reported that, Fourier transform infrared spectroscopy (FTIR) is the most frequently used IR spectroscopic technique due to its sensitivity and short time for analysis. The authors also emphasised that in the traditional IR spectroscopy, an infrared spectrum is produced via a single scan. Whereas the use of an interferometer in the FTIR process leads to various scans. Hence, the Fourier transforms is then used to convert the interferogram into an infrared spectrum. Consequently, the latest studies based on IR spectroscopy constantly refer to FTIR. Therefore several scientists have used FTIR with different procedures to characterize DOC of water samples collected during the treatment processes.

For instance, Kim and Yu (2005) used FTIR to characterize the natural organic matter in conventional water treatment processes for selection of treatment processes focused on disinfection by-products (DBPs) control. In their study, it was shown that the amount of hydrophobic aromatics in the treated water by chlorination decreased while that of aliphatic increased compared to raw water. Thereafter, the amount of aliphatic declined compared to that of aromatics when the treatment process was followed by coagulation and sedimentation.

Martynas et al. (2013) investigated the degradation of various textile dyes as wastewater pollutants under dielectric barrier discharge plasma treatment. In their study, the by-products of the oxidation process were determined by FTIR analysis. As a result, the FTIR examination showed that carboxylic acids, nitrates, amides and amines were mostly present as by-products in the treated wastewater. Moreover, FTIR was also used by Croue et al. (2000) to inspect the nature of organic compounds responsible for the formation of haloacetic acids (HAAs) namely ketones, aromatics, carboxylic acids, amides and amino acids. Their research demonstrated that HAAs mainly derived from the HPOB and HPIB fractions. About a decade ago, Lin et al. (2000) and Drewes et al. (2006) highlighted that the wavenumber resolution of conventional FTIR lies in the 2 to 4 cm^{-1} range. Few years

later, Jones et al. (2006) claimed that the wavenumber resolution of 1/14 μm^{-1} can be achieved with synchrotron light. Based on these facts, Xing (2010) stated that the high sensitivity of FTIR spectroscopy with synchrotron light can be useful to discern the nature of various organic compounds. Therefore, Song et al. (2001), Chouparova et al. (2004) and Jones et al. (2006) supported that numerous studies based on the analysis of water samples (from harbour sediments and refinery effluents for petroleum organic compounds) using FTIR and synchrotron light have been conducted. Furthermore, Martynas et al. (2013) conducted a study on the degradation of various textile dyes as wastewater pollutants under dielectric barrier discharge plasma treatment. In their work, the intermediate decomposition products were qualitatively analysed by FTIR. During the decolourization process, the target toxin might only be changed from one form to another, therefore after identification of the different functional groups, it is also crucial to examine not only the carbon content of the pollutant to assess the degree of degradation using analytical techniques such as total organic carbon (TOC) but knowing the toxicity of compound via the chemical oxygen demand (COD) analysis is of great importance.

2.3.3 Ecological parameters: chemical oxygen demand and total organic carbon

During oxidation of organic pollutants in water/wastewater, the contaminant concentration is usually quantified by spectroscopic techniques such as UV-vis spectroscopy and/or chromatographic methods like high performance liquid chromatography (HPLC). Apart from this, the global organic pollution can also be measured rather than the resulting oxidation intermediate products only. This is often achieved by using two types of analysis including the chemical oxygen demand (COD) and the total organic carbon (TOC) (Mohamed, 2011). Vujevic (2004) reported that ecological parameters such as COD, TOC, etc. quantified before and after corona treatment of wastewater offer possibilities of reusing the treated wastewater as process water or the water could be discharged into the environment. In addition, COD and TOC have also been widely used as viable factors to study the toxicity and the degradation of organic pollutants from water/wastewater. However, the detailed procedures on TOC and COD analysis and their calculation are usually scarce in literature even though various papers have highlighted their use as important ecological parameters in the treatment of water/wastewater (Sharma et al., 1993; Vujevic et al., 2004; Grabowski, 2006; Reddy et al., 2014 and Rong et al., 2014) but details on COD and TOC analysis and their calculations have not been clearly mentioned.

In order to fill up this gap, authors like Soresa (2011) proposed full detailed analytical procedures and calculations of COD and TOC during the treatment of Ayka Addis textile wastewater by the Fenton's reagent. The COD and TOC analysis and the calculations suggested by Soresa have therefore been summarised and presented in subsequent paragraphs. These findings on COD and TOC suggested by Soresa have thus been explored in this study to evaluate not only the toxicity of the simulated wastewater treated by the EHD system, but also to inspect the degradation of the methylene blue used as a model compound

2.3.3.1 TOTAL ORGANIC CARBON

The total organic carbon (TOC) is commonly defined as a measure of the carbon content present in an aqueous solution (Mohamed, 2011). However, the type of instruments used to accomplish such analysis might vary with respect to their affordability. For instance, Mohamed (2011) investigated the removal of organic compounds from water by adsorption and photocatalytic oxidation. In his research, the mineralization of organic compounds was indicated by the TOC analysis performed with a TOC-meter (TC Multi Analyser 2100 N/C) in which the organic molecules were completely oxidized at 850°C in the presence of a platinum catalyst. The amount of CO_2 discharged by the reaction was then quantified by infra-red spectrometry (IR).

On the other hand, Reddy et al. (2014) studied the mineralization of endosulfan in aqueous medium using a catalytic non-thermal plasma reactor. In that study, the decomposition of endosulfan was assessed by the TOC content that was measured by a standard method (5310 A combustion and detection method) using TOCVCPH total carbon analyzer (Shimadzu, Japan). Furthermore, during the dielectric barrier discharge induced degradation of diclofenac in aqueous solution conducted by Rong et al. (2014), the mineralization of diclofenac was determined by total organic carbon (TOC) achieved on a Shimadzu 5000A TOC analyzer. Even though the equipment/machines for TOC analysis differ from one another, the principle used to estimate TOC content of specific samples might commonly be unchanged.

2.3.3.2 TOTAL ORGANIC CARBON ANALYSIS: PRINCIPLE

The measurements of TOC were performed as stated by standard methods for the examination of water and wastewater, high temperature combustion method 5310 B (APHA-AWWA-WPCF, 1989).

The principle of TOC analysis involves the homogenization and dilution of the sample and its injection in micro portion into a heated reaction chamber packed with an oxidative catalyst such as cobalt oxide, platinum group metals or barium chromate. The organic carbon is oxidized to CO_2 and H_2O after the water has been totally evaporated. The resulting CO_2 is transported in the carrier-gas streams and measured by a non-dispersive infrared analyzer or by colorimetric titration **(**Soresa, 2011).

2.3.3.3 TOC CONTENT

In 2014, Reddy and colleagues stated that the TOC content can be calculated by the difference of total carbon content (TC) and total inorganic carbon content (TIC). In such regards, acidification of the sample is prominent as a first step in order to remove the inorganic carbon (IC) for organic carbon (OC) analysis. Secondly, TC was estimated by catalytic oxidation of the sample at 680^{o}C and the CO_2 was quantified using infrared detector (Wilhelmus, 2000). Thereafter, TOC was measured by calibration with potassium hydrogen phthalate standards.

Based on sample acidification, Mohamed (2011) showed that the inorganic carbon present in solution mainly as carbonate (CO_3^{2-}), monohydrogencarbonate (HCO^{3-}) and dihydrogencarbonate (H_2CO_3) could be eliminated by addition of few drops of concentrated phosphoric acid (84%) to the sample, to produce CO_2, which is degassed by a current of nitrogen (Reddy et al., 2014).

2.3.4 Principle of Chemical oxygen demand

According to Soresa (2011), the chemical oxygen demand (COD) measures the quantity of oxygen required to completely and chemically oxidise organic compounds and mineral substances to inorganic end products. Potassium dichromate ($K_2Cr_2O_7$) is commonly used in excess as a strong chemical oxidizing agent in this process**.** The global level of organic pollution of effluents in municipal and industrial laboratories is often determined by this

method. This therefore, makes COD a valuable measure of water quality that is expressed in milligrams of oxygen per litre (Gravosky, 2006). Thus, COD remains an imperative and rapidly quantifiable variable for the determination of the organic substance content of water samples. Most research papers have highlighted the principle of either the use of COD as indicator of toxicity assessment or some of them just mentioned the COD measurements whereas only little detailed experimental procedures for this toxicity factor are found in the literature. A few years ago, Soresa presented coherent methodologies on COD measurement procedures. These COD measurement methods are in line with those recommended by standard methods for the examination of water and wastewater, high temperature combustion method 5310 B (APHA-AWWA-WPCF, 1989).

2.3.4.1 CHEMICAL OXYGEN DEMAND MEASUREMENT/CALCULATIONS

Soresa (2011) suggested a comprehensive methodology on COD measurement including its calculations. In this procedure, the following chemicals $K_2Cr_2O_7$, H_2SO_4, Ag_2SO_4, $FeSO_4{\cdot}7H_2O$ and ferrous ammonium sulphate titrant (FAS) [Fe $(NH4)_2(SO_4)_2{\cdot}$ $6H_2O$] were used to prepare standard solutions employed in the determination of COD. As a result, the chemical oxygen demand (COD) concentration was calculated using the formula shown in Equation (2.13) as follows:

$$COD\ (mg/L) = [(FAS_s - FAS_p) * N * f] / V_s \quad \ldots\ldots (2.31)$$

Where FAS_s is the ferrous ammonium sulphate concentration (mg/L) used for the sample, FAS_p is the ferrous ammonium sulphate concentration (mg/L) used for pure water, f is the dilution factor (8000), while N and Vs are the normality of FAS and the sample volume (mL), respectively. This principle was therefore used to estimate the COD content in raw and treated MB samples used as a model compound in this study. The analytical techniques reviewed above have also been used in the present study to investigate the decomposition of MB dye by the DBD plasma process.

2.4 SUMMARY OF CHAPTER TWO

On the whole, most dielectric barrier discharge studies elaborated in this chapter involved chemical additions as investigated by Nehra et al. (2008); Madhu et al. (2009); Joshi et al. (2011); Heon et al. 2012). The actual EHD system however, does not require addition of any chemical. So without adding any chemical, the present EHD system was investigated

and optimized to improve decomposition of organic contaminants such as dye MB at ambient conditions. Jo and Mok (2009) attempted optimizing the DBD system using similar configuration (double cylindrical DBD reactor). However in their study they used azo dye as a contaminant, with addition of H_2O_2 and O_3 in the system. Apart from this, they only studied the effect of few parameters on the degradation of the dye pollutant. In this current study, dielectric barrier electrohydraulic discharge was used as an advanced oxidation process to investigate the degradation of MB at ambient conditions. Alteration of the following parameters: the initial MB concentration, the applied voltage, solution pH, conductivity and so forth was fully investigated systematically.

From literature review, some authors suggested mechanistic pathways for the formation of reactive species (Prendiville et al., 1986; Tarr, 2003; Hayashi et al., 2000) but break down mechanisms or decomposition pathways of MB were not thoroughly discussed. This gap would be addressed in the current study and could present photo-degradation pathways of MB in an EHD system.

It is known that DBD is widely used to eliminate organic pollutants from water and wastewater, however reactor configurations, electrode material and geometry and the type of pollutant in DBD processes, differ from one study to another (Bian et al., 2009; Magureanu et al., 2012; Iqbal and Ahmad, 2013).

Variation of the dielectric region (air gap) between the outer and the inner tube has not been well explored in literature. Additionally, Magureanu et al. (2012) and Bian et al. (2009) used reactor configurations involving several high voltage electrodes in parallel as well as a catalyst to enhance the degradation efficiency of pollutants. However, the current reactor only consists of one single cell that accommodates one high voltage electrode in order to optimize the configuration of an operational unit that is capable to efficiently decolourize and decompose organic pollutants without any chemical addition.

Apart from this, dielectric barrier electro hydraulic discharge also referred to as liquid electrical discharge is characterised by its physical and chemical parameters such as shock waves, UV- radiations and reactive species including $OH^{\cdot}$, H_2O_2, O_3, $O^{\cdot}$ etc. resulting mainly from dissociation of water molecules and oxygen gas (Iqbal and Ahmad, 2013). Even though Lukes (2002) and Grymonpré et al. (2001) investigated the quantification of these species, determination of the amount of the reactive species remains an on-going challenge in electrohydraulic discharge systems. Hence, the current study investigated methodologies of quantifying reactive species in the treated solution. To recall, decolourization and degradation are two different aspects which are usually highlighted in

treatment of water and wastewater effluents. While decolourisation refers to colour removal of a specific pollutant as a result of the destruction of its chromophoric form, degradation indicates how much organic carbon of the contaminant has been removed. Since literature reviewed above showed that several water/wastewater treatment technologies have been developed, the efficiency of any treatment system could be evaluated by its capability of achieving high percentage of decolourization as well as destruction of the target pollutant simultaneously. Nevertheless, some technologies would reach these two parameters separately. A very few authors in this review have attempted a full optimization of the DBD plasma system and none of them highlighted the use of various reactors for at optimizing of the EHD system using MB as the target pollutant. This study, therefore, aims to optimize the actual double cylindrical DBD plasma system projected to shorten the decolouration time of pollutants and thus enhance their decomposition. This optimization process is intended to improve the efficiency of the current EHD system in which dye decolourization and degradation time would be, consequently, improving dye degradation. The study also aims to determine which radical species are responsible for the destruction of the pollutants as well as determine what intermediate products form at various conditions. Thus, the optimization procedures as well as the quantification and characterization methodologies are provided in the following chapter.

CHAPTER THREE: EXPERIMENTAL AND ANALYTICAL METHODOLOGIES

3. INTRODUCTION

In this chapter, chemical materials, physical equipment and experimental procedures as well as analytical methods used during optimization of the electrohydraulic discharge (EHD) system are set out. In addition, experimental procedures on quantification of the free reactive species are also discussed. The physical equipment and chemical materials used in this work are presented in the following subsections.

3.1 MATERIALS AND SUPPLIERS

In order to optimize the EHD experiments as well as detection and quantification of free reactive species generated during the EHD process, the materials and chemicals listed in Tables 3-1 and 3-2 respectively were used.

Table 3-1: Electrical tools used in EHD system

Equipment	Suppliers
Electrodes [copper, silver and stainless steel (0.5 and 1.5 mm)]	C.J.LABS
Quartz tubes reactors	Glass Chem./Stellenbosch RSA Glass tech / Johannesburg
GW INSTEK programmable power supply PSP- 405 with (U-Const. 40 V, I-const. 5 A, P- cost. 200 W)	E, E & Eng./ Stellenbosch RSA
Apply upper scale transformer (input 0 – 30 V), peak voltage (0 – 10 kV)	E, E & Eng./ Stellenbosch RSA
DARO TWIN Aquarium Air Pump. IPx4: 220 – 240 V; 50 Hz; 3.5 - 4.5 W	E, E & Eng./ Stellenbosch RSA
Air flow meter: Rotameter MFG.CO.LTD., made in England / tube number R868119/H.D. Free liter/minute Nitrogen 25 ºC 20 p.s.i.g. (Maximum flow rate 16 L/ min)	Kimix Chemical & Laboratory Suppliers, SA
Copper wire (Various sizes)	Kimix Chemical & Laboratory Suppliers, SA

Table 3-2: Chemicals used for the detection and quantification of free radicals during EHD process

Chemicals	Purity/ identifier	Suppliers
Sulphuric acid	20%	Kimix, RSA
Di sodium hydrogen orthophosphate, CP	99%	Kimix, RSA
Phosphoric acid	85%	Kimix, RSA
Sodium sulphate decahydrate, CP	99%	Kimix, RSA
Terephtalic Acid	98%	Sigma Aldrich, RSA
2-bromoterphtalic acid	95%	Sigma Aldrich, RSA
Sodium hydroxide flakes CP	97%	Kimix, RSA
Sodium acetate trihydrate CP	99%	Kimix, RSA
Copper powder	99.999%	Sigma Aldrich
Phenolphthalein powder CP	Batch no. A-02/04/13k24/1013	Kimix, RSA
Potassium hydroxide	5%	Kimix, RSA
Di potassium hydrogen orthophosphate, CP	98%	Kimix, RSA
Methylene blue powder	Batch no.1041221k02/0513	Kimix, RSA
Dimethyl sulfoxide	≥ 99.99%	Sigma Aldrich, RSA
Titanium (IV) oxysulfate	≥ 29%	Sigma Aldrich, RSA
Potassium indigo trisulfonate	Pubchem substance ID: 24854018 Reilstein Registry number: 4932187 MDL number: MFCD0013160	Sigma Aldrich, RSA
2,4- dinitrophenylhydrazine	97%	Sigma Aldrich, RSA
Acetonitrile	99.5%	Sigma Aldrich, RSA

3.2 EXPERIMENTAL FLOW DIAGRAM OF THE CURRENT STUDY

Based on various aspects that need to be investigated in this study, a comprehensive experimental flow diagram was required. In the schematic flow diagram shown in Figure 3.1, chapter three is divided into three sections. The first section is based on the full optimization of the EHD system, followed by the detection and quantification of the free reactive species, while the last section focuses on characterization techniques used to analyse the treated and untreated MB samples.

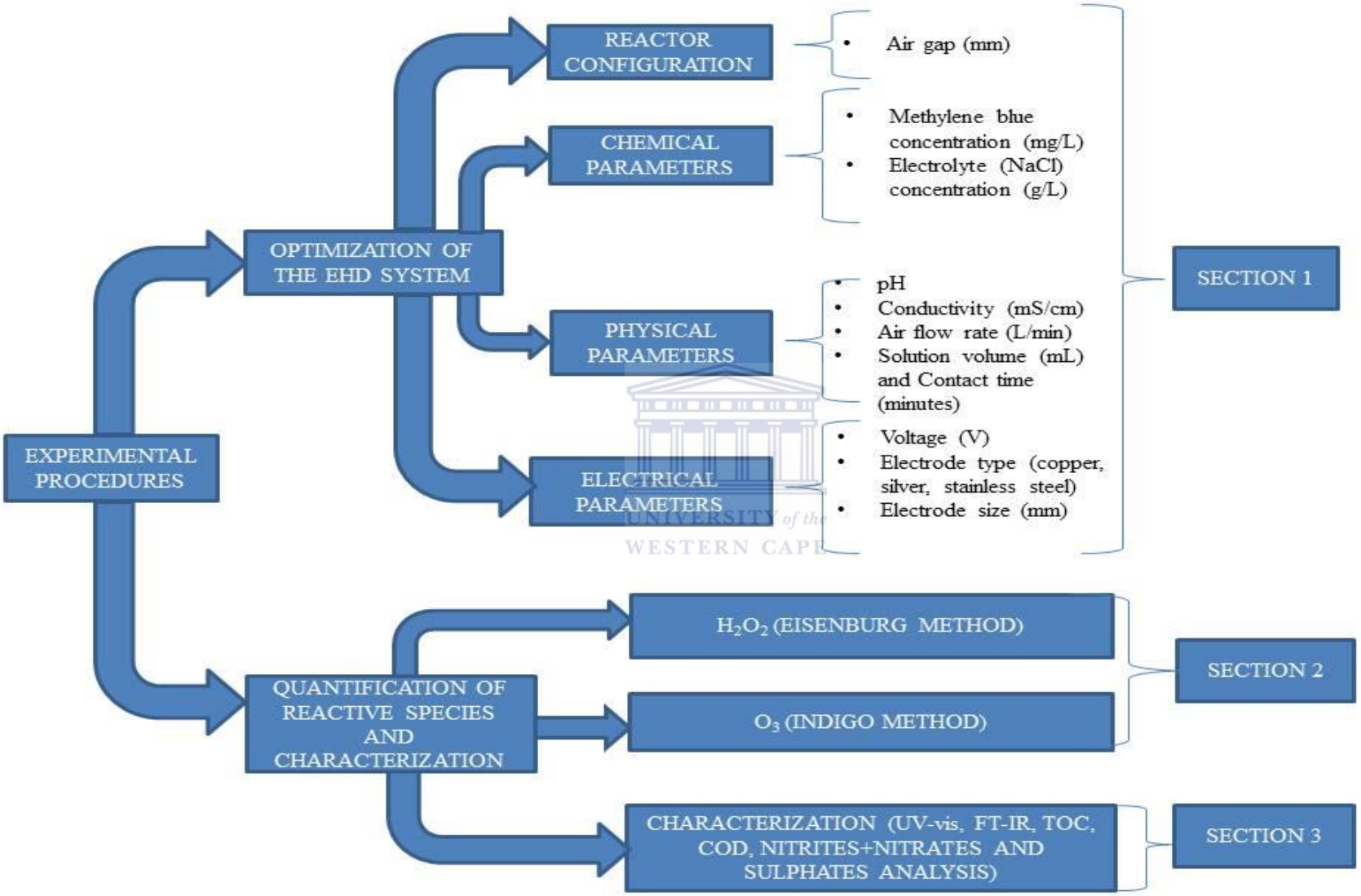

Figure 3-1: Experimental flow diagram of the actual study

3.3 EXPERIMENTAL PROCEDURES

This section describes the various stages of the experiments. The experimental procedures used to optimize the EHD system (section 1) and detection and quantification of free reactive species (section 2) are described below.

3.3.1 Electrohydraulic discharge

This subsection describes the EHD methodology. The EHD process in this study was performed in a number of steps as described in the following paragraphs. At the end of each EHD experiment, UV-vis spectroscopy was used as quick techniques to measure the absorbance of untreated and treated MB samples and calculate the decolourization percentage obtained.

3.3.1.1 PREPARATION OF METHYLENE BLUE STANDARD SOLUTIONS

The initial model solutions of 100 mg/L MB were prepared as follows: About 0.2 g of powdered MB was weighed and quantitatively transferred into a 2 000 mL volumetric flask and made up to the mark with deionised water. Other solutions of different concentrations (0.5, 1, and 1.5 up to 10 mg/L) were prepared by serial dilutions. Each of these solutions was separately used to perform the degradation of MB using electrohydraulic discharge. Based on the EHD experimental procedure explained in the following section, a series of 20 completed EHD experiments at concentrations taken from 0.5 to 10 mg/L with increments of 0.5 were performed.

3.3.1.2 DESCRIPTION OF EHD SYSTEM

The current DBD (Figure 3-2) reactor used in this study is similar to the double dielectric used by Rong et al. (2014). However, in the actual DBD reactor used the inner and outer dielectric tubes are made of quartz while in Rong‘s reactor, the inner insulator tube was made of quartz but the outer dielectric layer was a plexi–glass tube. In addition to the tube material, the configuration used by Rong and colleagues had two air flow distribution tubes. This might be beneficial for even distribution of bubbles in the bulk solution, but the configuration design would be very complex. Contrary to this configuration, the DBD

reactor used in this study has a single air outlet distributing pathway that circulates bubbles into the simulated water. With the aid of a sparging outlet, the generated bubbles are uniformly distributed to achieve a considerable oxidation of the target pollutant. Moreover, the reactor tube in the current DBD configuration can be placed and moved out of the treatment vessel. This means that the double dielectric configuration can be easily scaled up to treat the desired volumes of the pollutants.

In this project, the cylindrical double DBD electrode/reactor configuration was used as one of the advanced oxidation processes to treat wastewater at room temperature and ambient pressure. Methylene blue was particularly used as a model target contaminant in simulated wastewater. The schematic representation of the actual DBD system is presented in Figure 3-2 and its description is given in Table 3-3.

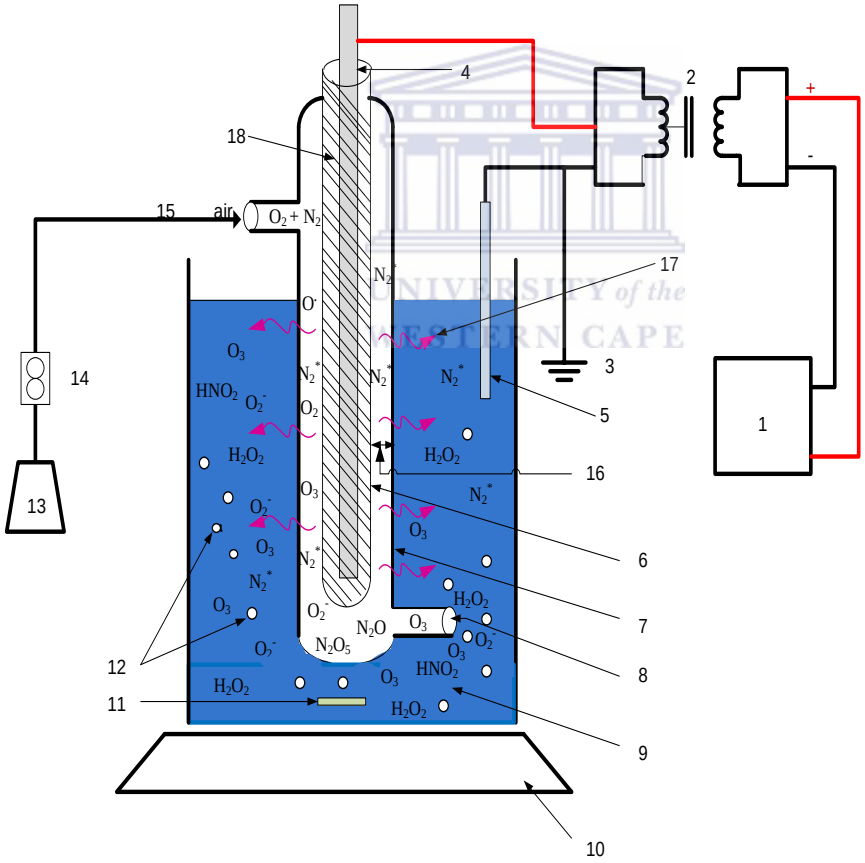

Figure 3-2: Electrode/reactor arrangement of the actual DBD system

Table 3-3: Legends of Figure 3-5

Experimental setup	
Number	Description
1	Power supply
2	Step up transformer
3	Ground (earth)
4	High voltage electrode
5	Copper foil
6	First quartz dielectric tube
7	Second quartz dielectric tube
8	Gas outlet
9	Methylene blue solution
10	Magnetic stirring base
11	Stirring rod
12	Bubbles formed (active species)
13	Air pump
14	Flow meter
15	Air inlet
16	Discharge/air gap
17	UV radiations
18	NaCl electrolyte

A power supply set at 25 V, delivering a current of 3 A and a power of 80 W, was directly connected in series to a transformer that steps the AC voltage up to a DC peak voltage of ~8 kV directly delivered into the system. A 0.5 mm silver electrode directly connected to the high voltage (output of the transformer) was immersed in a 50 g/L (or as specified) of electrolyte solution of sodium chloride placed in the sealed inner tube of a single cell reactor (Figure 3-2). The latter was placed in a 1 800 mL beaker containing 1.5 L of MB solution. An air pump with a high and low flow speed switch was connected to an air flow meter that was directly connected to the single cell reactor tube for air (mostly oxygen) production. The air pump had a maximum flow rate of 4.8 L/min but was varied as further specified. The electrical discharge values mentioned above as well as dye volume and air flow were kept constant or varied as specified in the experiments. The reactor consisted of

an inner and outer tube. The diameter of the inner tube was approximately equal to 1 mm and that of the outer tube was 7 mm. The reactor was 23 cm long with an inlet and outlet for air circulation. The air gap was about 2 mm but was varied as specified. The simulated polluted water placed in the beaker was used as the ground and earthed to complete the circuit (see Figure 3-2).

3.3.1.3 EHD EXPERIMENTAL PROCEDURE

An electrode directly connected to the high voltage (output of the transformer) was immersed in the electrolyte solution of sodium chloride placed in the inner tube of the single cell reactor. This latter was placed in an 1 800 mL beaker containing 1 L of methylene blue dye solution of specified concentrations. An air pump with a high and low switch was connected to an air flow meter that was directly connected to the single cell reactor tube for air (mostly oxygen) production.

Methylene blue solution of specified concentrations was sampled at the time t = 0, 10, 20,30, 40, 50 and 60 minutes, pH and electrical conductivity of methylene blue samples at these time scales were measured. Methylene blue samples, collected at 0, 10, 20, 30, 40, 50 and 60 minutes of each experiment were further analysed using UV-vis in the range of 600-700 nm. Absorbance values of these samples obtained at a fixed wavelength of 665.0 nm were recorded. Therefore, using the initial concentrations of standard solutions and their corresponding absorbance, a calibration curve of absorbance vs. dye concentration was plotted to estimate the unknown concentration of methylene blue samples. Finally having initial and final concentrations of samples, the decolourization efficiency of dye over time was calculated. Thereafter, the effect of various parameters on MB discoloration efficiency was assessed.

3.3.1.4 OPTIMIZATION OF REACTOR CONFIGURATION: EFFECT OF AIR GAP BETWEEN THE OUTER AND INNER TUBES OF THE EHD REACTOR

In this section, the reactor configuration, namely the air gap between the two dielectric quartz tubes of the DBD reactor that was optimized by adopting the air gap variation of 2, 4 and 6 mm while the rest of the parameters were kept constant. The variation of air gap was coded AG as described in Table 3-4 below.

Table 3-4: Varied and fixed parameters during optimization of the air gap of the DBD reactor

Unique number	Varied parameters	Fixed parameters
AG	**Air gap (mm)**	Applied voltage 25 V, peak voltage 7.8 kV, MB concentration 5 mg/L, MB volume 1 500 mL, pH (6.04 – 6.64), MB solution conductivity (0.02 to 0.09 mS/cm), air flow rate 3 L/min, 50 g/L NaCl, air gap 2 mm and 0.5 mm silver electrode
AG1	2	
AG2	4	
AG3	6	

Procedure

Besides the effect of electrode type and diameter, the distance between the outer and the inner tubes is believed to impact on the decolourization/degradation of the pollutant. This was supported by Zhang et al. (2008) and others researchers who highlighted that the air gap in electrical discharge reactors might impede the degradation % removal of organic pollutants. Therefore, three reactor tubes/cells, were designed at different air gaps of 2, 4 and 6 mm, were used in the EHD system to investigate the effect of air gap on MB degradation efficiency at the following experimental conditions: MB concentration 5 mg/L, pH (between 6.04 and 6.64), applied voltage 25 V, peak voltage 7.8 kV, dye volume 1 500 mL, inlet air flow rate 3 L/min, 50 g/L NaCl electrolyte, a 0.5 mm silver electrode and a contact time of 60 minutes at 25ºC. The absorbance of MB solutions treated with each reactor at a specific air gap was measured. The MB solution was sampled every 10 minutes. The unknown concentrations of MB samples and their degradation efficiencies were estimated and presented in order to compare the performance of the three reactor configurations. The UV results of these data were plotted and based on these results, the reactor tube with air gap 2 mm was used for all further experiments**.** The dimensions of reactor configurations and air gap varied in DBD experiment are presented in Table 3-5 and the schematic representations of DBD reactor tubes used in this section are presented in Figures 3-4, 3-5 and 3-6, respectively.

Table 3-5: Inner and outer tube dimensions of reactors 1, 2 and 3

Reactors	Inner tube		Outer tube		Air gap (cm)	Reactor length (23 cm)
	ID (cm)	OD (cm)	ID (cm)	OD (cm)		
Reactor tube 1	0.2	0.3	0.5	0.7	0.2	20
Reactor tube 2	0.2	0.4	0.8	1	0.4	20
Reactor tube 3	0.3	0.5	1.1	1.3	0.6	20

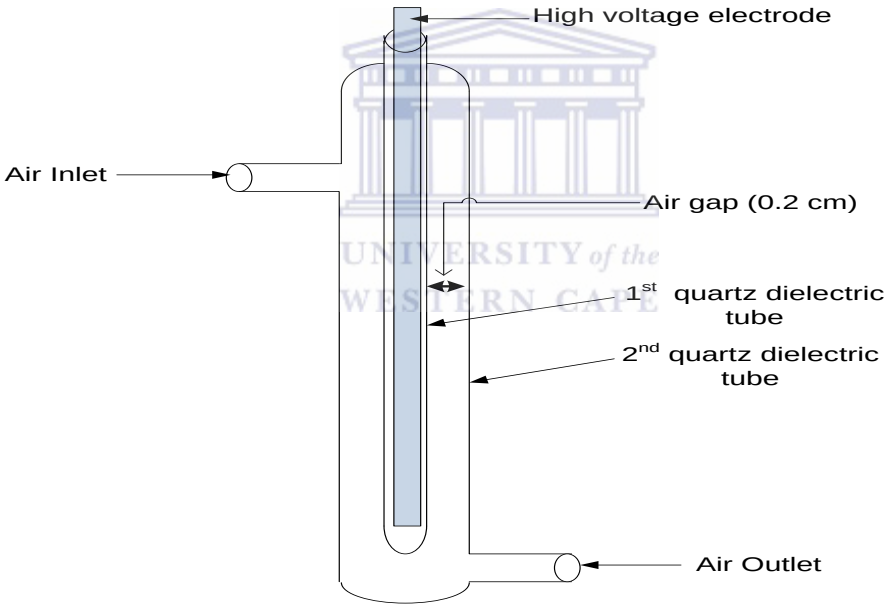

Figure 3-3: Schematic representation of the DBD reactor (tube) 1 (air gap = 0.2 cm)

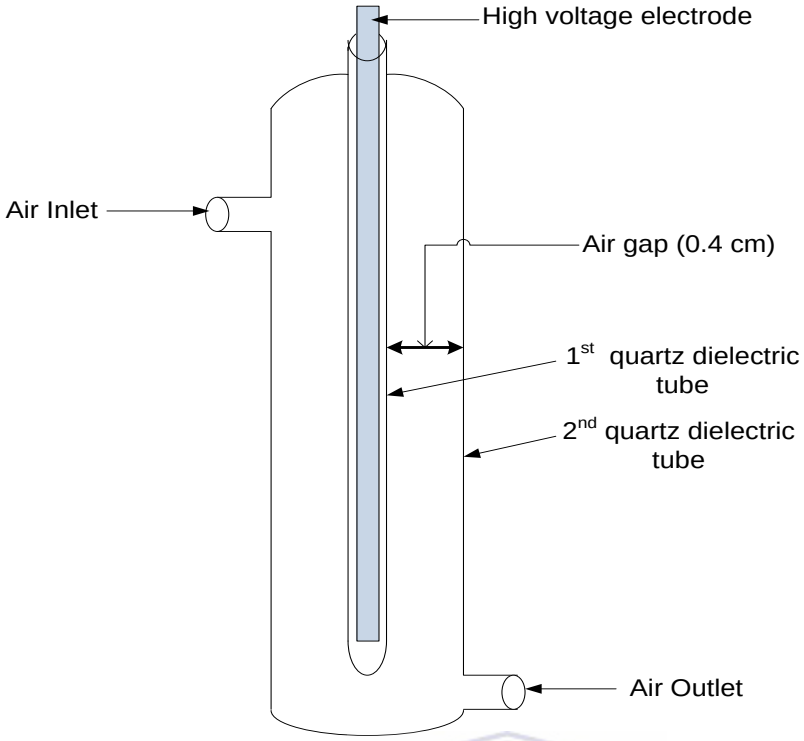

Figure 3-4: Schematic representation of the DBD reactor (tube) 2(air gap = 0.4 cm)

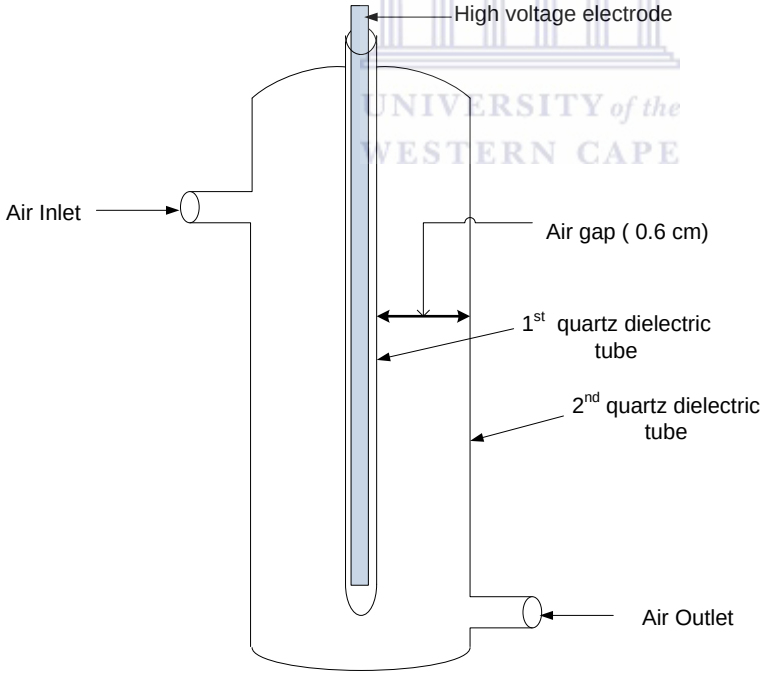

Figure 3-5: Schematic representation of the DBD reactor (tube) 3(air gap = 0.6 cm)

3.3.1.5 OPTIMIZATION OF CHEMICAL PARAMETERS

The chemical parameters studied in the EHD optimization process include: MB initial concentration and the concentration of aqueous sodium chloride electrolyte used in the inner tube of the DBD reactor (also considered as part of the positive electrode). The experimental methods for the optimization of these parameters at specific fixed parameters were discussed in the following paragraphs. The variation of MB concentration and that of NaCl electrolyte concentration were coded MBC and EC, respectively as described in Table 3-6.

Table 3-6: Optimization of the chemical parameters

Unique number	Varied parameters	Fixed parameters
MBC	MB concentration (mg/L)	Applied voltage 25 V, peak voltage 7.8 kV, MB volume 1 500 mL, pH (6.04 – 6.64), solution conductivity (0.02 to 0.09 mS/cm), air flow rate 3 L/min, 50 g/L NaCl, 0.5 mm silver electrode, air gap 2 mm and 0.5 mm silver electrode
Range	0.5 - 10	
EC	NaCl concentration (g/L)	Applied voltage 25 V, peak voltage 7.8 kV MB concentration 5 mg/L, MB volume 1500 mL, pH (6.04 – 6.64), MB solution conductivity (0.02 to 0.09 mS/cm), air flow rate 3 L/min, 50 g/L NaCl, 0.5 mm silver electrode, air gap 2 mm and 0.5 mm silver electrode
EC1	5	
EC2	10	
EC3	30	
EC4	50	

3.3.1.5.1 EFFECT OF MB INITIAL CONCENTRATION ON MB DECOLOURATION (UNIQUE NUMBER: MBC)

In this subsection, different solutions of 0.5, 1, and 1.5 up to 10 mg/L with increments of 0.5 mg/L were prepared by serial dilution of a 100 mg/L initial solution of MB dye as described in section 3.3.1.1. This was done to determine the optimum concentration at which the model MB dye pollutant could decolourize rapidly, that is the MB concentration

at which the current DBD reactor would operate proficiently. The MB solutions of concentrations prepared in the range of (0.5 - 10) mg/L were separately run in the DBD system while the following parameters: applied voltage 25 V, peak voltage 7.8 kV, MB volume 2 L, pH (in between 6.04 and 6.64), air flow rate 3 L/min, 50 g/L NaCl, 0.5 mm silver electrode, air gap 2 mm, 0.5 mm silver electrode and contact time of 60 minutes were kept constant. Also MB solution pH and conductivity behaviour during DBD experiments was recorded particularly at 5 mg/L MB.

3.3.1.5.2 THE EFFECT OF AQUEOUS ELECTROLYTE ON MB DECOLOURATION EFFICIENCY (UNIQUE NUMBER: EC)

In order to evaluate the effect of sodium chloride electrolyte solution on decolourization efficiency of MB dye, the following procedures were followed. Accurately weighted 10 g, 30 g and 50 g of granulated sodium chloride (NaCl) was respectively transferred into three separate 1 000 mL volumetric flasks. The granulated NaCl was then dissolved by continuous shaking and filled up to the mark with deionised water. The obtained solution at different concentrations; 10 g/L, 30 g/L and 50 g/L was used as electrolyte in the central electrode compartment of the electrohydraulic discharge system under the following conditions: applied voltage 25V, peak voltage 7.8 kV, MB concentration 5 ppm, solution pH (in between 6.04 and 6.64), air flow rate 3 L/min, air gap 2 mm, 50 g/L NaCl electrolyte and MB volume 1500 mL using silver electrode. About 8-10 mL of the specified concentration of sodium chloride solution was put into the central electrode compartment of the electrohydraulic discharge reactor as electrolyte. Though sodium chloride solution is a good conductor of electricity, it was mostly used in this system to avoid sparking between the high voltage electrode and reactor tube walls during electrohydraulic discharge reactions.

3.3.1.6 OPTIMIZATION OF PHYSICAL PARAMETERS

The physical parameters that were optimized include: the solution pH and conductivity, air solution volume, flow rate and the contact time. The variation of pH, conductivity and solution volume were coded SP, SC and SV, respectively while the air flow rate and contact time were coded AF and CT, correspondingly. The protocols used were

summarized and presented in Table 3-7. The experimental procedures of these factors were distinctly detailed in the following sections.

Table 3-7: Experimental summary of the optimization of physical parameters

Unique number	Varied parameters	Fixed parameters
SP	**Solution initial pH**	Applied voltage 25 V, peak voltage 7.8 kV, MB concentration 5 mg/L, MB volume 1 500 mL, MB conductivity (20 to 5 mS/cm), air flow rate 3 L/min, 50 g/L NaCl, 0.5 mm air gap 2 mm and silver electrode
SP1	2.5	
SP2	4.5	
SP3	6.5	
SP4	8.5	
SP5	10.5	
SC	**Solution initial conductivity (mS/cm)**	Applied voltage 25 V, peak voltage 7.8 kV, MB concentration 5 mg/L, MB volume 1 500 mL, pH (10 – 2.5), air flow rate 3 L/min, 50 g/L NaCl, air gap 2 mm and 0.5 mm silver electrode
SC1	5	
SC2	10	
SC3	15	
SC4	20	
SV	**Solution volume (mL)**	Applied voltage 25 V, peak voltage 7.8 kV, MB concentration 5 mg/L, pH (6.04 – 6.64), MB solution conductivity (0.02 to 0.09 mS/cm), air flow rate 3 L/min, 50 g/L NaCl, 0.5 mm silver electrode, air gap 2 mm and 0.5 mm silver electrode
SV1	500	
SV2	1000	
SV3	1500	
SV4	2000	
AF	**Air flow rate (L/min)**	Applied voltage 25 V, peak voltage 7.8 kV, MB concentration 5 mg/L, MB volume 1 500 mL, pH (6.04 – 6.64), MB conductivity (0.02 to 0.09 mS/cm), 50 g/L NaCl, air gap 2 mm and 0.5 mm silver electrode
AF1	2	
AF2	3	
AF3	4	
CT	**Contact time(L/min)**	Applied voltage 25 V, peak voltage 7.8 kV, MB concentration 5 mg/L, MB volume 1 500 mL, pH (in between 6.04 and 6.64), MB conductivity (0.02 to 0.09 mS/cm), 50 g/L NaCl, air gap 2 mm and 0.5 mm silver electrode
Range	**0 - 60**	

3.3.1.6.1 THE EFFECT OF pH ON DECOLOURATION EFFICIENCY OF MB

In this subsection, the variation of solution pH coded as (SP) in Table 3-7 was performed as follows:

A few drops of either concentrated H_2SO_4 or NaOH were carefully diluted in separate beakers containing approximately 400 mL of deionised water. About 1 500 mL of 5 mg/L MB solution was placed in a 200 mL beaker in which a pH/conductivity probe was immersed. The pH of MB solution was varied from 2.5 to 10.5 and was adjusted to the desired value by adding a reasonable amount of diluted H_2SO_4 and NaOH drop wise using 10 ml syringes. During this process the solution was continuously swirled with pH/conductivity meter probe to get the pH value needed. The monitored solution was further used in the electrohydraulic discharge experiment at the following experimental conditions: applied voltage 25 V, peak voltage 7.8 kV, air flow rate 3 L/min, air gap 2 mm, 0.5 mm silver electrode and 50 g/L of NaCl for 60 minutes.

3.3.1.6.2 EFFECT OF SOLUTION CONDUCTIVITY ON DECOLOURATION EFFICIENCY OF MB

About 1 500 mL of MB solution was placed in a 2 000 mL beaker. With the aid of a pH/conductivity meter, MB conductivity denoted SC in Table 3-7 was adjusted from 5, 10, 15 to 20 mS/min by drop wise addition of diluted HNO_3/NaOH in the beaker and swirling the solution with the pH/conductivity probe until the desired conductivity value was obtained. Furthermore MB solution at a fixed conductivity value was then used as model sample pollutant to which electrohydraulic discharge was applied for 60 minutes while the following parameters were kept constant: applied voltage 25 V, peak voltage 7.8 kV, air flow rate 3 L/min, air gap 2 mm, MB concentration 5 mg/L, solution pH (in between 6.04 and 6.64), 50 g/L NaCl electrolyte and 0.5 mm silver electrode. The sampled solutions were analysed using a UV-vis spectrophotometer. Absorbance of these samples was used to determine unknown concentrations. These values were used to calculate the decolourization efficiency of methylene blue.

3.3.1.6.3 THE EFFECT OF AIR FLOW RATE ON MB DECOLOURATION EFFICIENCY

Using the EHD system as described in the previous section, most parameters were kept constant (applied voltage 25V, peak voltage 7.8 kV, MB concentration 5 mg/L, solution pH (in between 6.04 and 6.64), 50 g/L NaCl electrolyte and MB volume 1 500 mL, air gap 2 mm) while the air flow rate coded as AF in Table 3-7 was altered from 2, 3 to 4 L/min, respectively. In total 3 experiments were performed in the same way during a period of 60 minutes whilst sampling every 10 minutes. The sampled solutions were analysed using a UV-vis spectrophotometer. Absorbance of these samples was used to determine unknown concentrations. These later were used to calculate the decolourization efficiency of methylene blue.

3.3.1.6.4 THE EFFECT OF MB VOLUME AND TREATMENT TIME ON THE DECOMPOSITION

A 100 mg/L methylene blue stock solution was prepared by dissolving 0.1 g of powder MB in deionised water in a 1 L volumetric flask which was then filled up to the mark with deionised water. Different volumes of 500, 1 000, 1 500 and 2 000 mL of 5 mg/L solution of methylene blue coded SV1, SV2, SV3 and SV4, respectively in Table 3-7 were prepared by serial dilutions. The following parameters were then applied during EHD experiments using these solutions: Voltage 25 V; peak voltage 8 kV; MB concentration 5 mg/L, air flow rate of 3 L/min, air gap 2 mm, , pH (in between 6.04 and 6.64) and 50 g/L NaCl electrolyte were kept constant, using electrohydraulic discharge experimental procedure described in the previous section. For each experiment, a single reactor tube (25 cm long) was immersed in a 2 000 mL beaker. Methylene blue degradation efficiency was evaluated when increasing the dye volume with time. The sampled solutions were analysed using UV-vis spectrophotometer. Absorbance of these samples was used to determine unknown concentrations. These later were used to calculate the decolourization efficiency of Methylene blue.

3.3.1.7 OPTIMIZATION OF ELECTRICAL PARAMETER

The electrical parameters assessed in the EHD system were the applied voltage, electrode type and size. The variation of the applied voltage was coded AV, whereas ET and ES are those of electrode type and size, respectively. A summary of their experimental procedures

is presented in Table 3-8 and details of these procedures are separately given in the following paragraphs.

Table 3-8: Summary of electrical parameters optimization

Unique number	Varied parameters	Fixed parameters
AV	**Voltage (V)**	
AV1	20	MB concentration 5 mg/L, MB solution volume 1 500 mL, pH (6.04 – 6.64), MB solution conductivity (0.02 to 0.09 mS/cm), air flow rate 3 L/min, 50 g/L NaCl, air gap 2 mm and 0.5 mm silver electrode
AV2	22	
AV3	25	
ET	**Electrode type**	
ET1	Copper	Applied voltage 25 V, peak voltage 7.8 kV, MB concentration 5 mg/L, MB solution volume 1 500 mL, pH (6.04-6.64), MB solution conductivity (0.02 to 0.09 mS/cm), air flow rate 3 L/min, 50 g/L NaCl and air gap 2 mm, 0.5 mm electrode
ET2	Silver	
ET3	Stainless steel	
ES	**Electrode size (mm)**	Applied voltage 25 V, peak voltage 7.8 kV, MB concentration 5mg/L, MB solution volume 1 500 mL, pH (6.04 – 6.64), MB solution conductivity (0.02 to 0.09 mS/cm), air flow rate 3 L/min, 50 g/L NaCl electrolyte, air gap 2 mm and silver electrode
ES1	0.5	
ES2	1.5	

3.3.1.7.1 EFFECT OF APPLIED VOLTAGE ON DEGRADATION EFFICIENCY OF MB

In this section the applied voltages were 20 V, 22 V and 25V, corresponding to the peak voltages of 6.4 kV, 6.8 kV and 7.8 kV respectively delivered by the power supply and step up transformer. The following parameters were kept constant: [MB] concentration 5 ppm, solution pH (between 6.04 and 6.64), air flow rate 3L/min, air gap 2 mm, 50 g/L NaCl electrolyte and dye volume 1500 mL and silver electrode. Altogether three electrohydraulic discharges experimental reactions were performed by altering the applied

voltage between 20 V and 25 V as indicated above. The experiment was performed over 60 minutes and MB solution was sampled every 10 minutes.

3.3.1.7.2 THE EFFECT OF ELECTRODE TYPE ON MB PERCENTAGE REMOVAL

Besides various chemical and physical parameters that have been inspected in this study, it was also believed that the type of electrode used would have an effect on MB removal. Several studies on ED have used different types of electrodes such as graphite, stainless steel and copper using different ED reactors. However, different results have been reported. To verify this parameter and select the most suitable electrode for the current EHD reactor tube, three types of electrodes: copper, silver and stainless steel (25 cm long and 1 mm diameter) were selected and used in the ED system. The rest of the parameters including MB concentration 5 ppm, solution pH (between 6.04 and 6.64), applied voltage 25 V, peak voltage 7.8 kV, air flow rate 3 L/min, air gap 2 mm, 50 g/L NaCl electrolyte and dye volume 1 500 ml were maintained constant while varying the electrode type. Using the same EHD procedure as previously described, three ED experiments were carried out. Each experiment was run for 60 minutes. Methylene blue solution was sampled every 10 minutes. The samples were analysed using UV- absorption spectroscopy. The recorded absorbance values were used to calculate unknown concentrations as well as the colour removal of MB.

3.3.1.7.3 EFFECT OF THE ELECTRODE DIAMETER ON MB DECOLOURIZATION

Electrical energy in conductive material may sometimes depend on their length and diameter. That necessitates the investigation of the different diameters of silver electrode on MB colour removal percentage. In this case, ED procedure remained the same. The following parameters were applied: MB concentration mg/L, solution pH (between 6.04 and 6.64), dye volume 1 500 mL, applied voltage 25, peak voltage 7.8 kV, air gap 2 mm and air flow rate of 3 L/min, 50 g/L NaCl electrolyte and silver electrode were retained constant during the experiments while silver electrode diameter was changed from 1 mm to 1.5 mm. Therefore, two experiments were performed over 60 minutes, whilst sampling every 10 minutes.

3.3.1.8 EHD EXPERIMENT PERFORMED AT OPTIMAL CONDITIONS.

In order to test the efficacy of the optimized electrohydraulic discharge (DBD) system, two DBD experiments at normal and optimum conditions were carried out. The experimental normal conditions included: applied voltage 25 V, peak voltage 7.8 kV, [MB] = 5 mg/L, pH (between 6.04 and 6.64), MB volume 1 500 mL, air flow rate 3 L/min, 0.5 mm silver electrode, 50 g/L NaCl electrolyte, air gap 2 mm and running time of 60 minutes. As for the optimum parameters, the following: applied voltage 25 V, peak voltage 7.8 kV, MB concentration 5 mg/L, solution pH 2.5 was adjusted using HNO_3 acid and NaOH solution, MB volume 1500 mL, air flow rate 3 L/min, 1.5 mm silver electrode, 50 g/L NaCl electrolyte, air gap 2 mm and running time of 60 minutes were used.

3.3.2 Experimental procedures for detection and quantification of active species

This section outlines the chemical methods used to detect and quantify hydrogen peroxide (H_2O_2) and ozone (O_3) produced in EHD system. Each method presents in full the details of the sample preparation, the detection and measurement mode of each oxidant.

3.3.2.1 QUANTIFICATION OF H_2O_2

The concentration of the yellow-coloured peroxotitanyl complex was determined by UV absorption spectroscopy at 410 nm (Uher et al., 1991). The absorbance at this wavelength ($\varepsilon = 730\ M^{-1}\ cm^{-1}$) was directly proportional to the initial hydrogen peroxide concentration. OH radicals have a short lifetime of about 2.4 – 10.6 µS (Arakaki and Faust, 1998). Therefore, the titanylsulphate traps the H_2O_2 leading to the yellow-coloured peroxotitanyl complex whose absorbance corresponds to that of H_2O_2 trapped. Approximately 2.4 g of titanylsulfate (hydrate) was weighed and mixed with 100 mL (20%) H_2SO_4 in a volumetric flask. The remaining volume of the flask was made up to 500 mL with Millipore water. After electro hydraulic discharge treatment, 3 mL of the treated water was sampled from the DBD reactor and immediately mixed with 0.3 mL of the prepared titanylsulphate solution in a cuvette (flask). From the absorbance measured with a photo spectrometer the H_2O_2 concentration can be derived.

$$TiOSO_4 + H_2O_2 + H_2SO_4 \rightarrow TiO_2(SO_4)_2^{2-} + H_2O + 2H^+ \quad \text{(3.1)}$$

MnO_4^-+5 H_2O_2 + 6 H^+ → 2 Mn^{2+} + 5O_2 + 8 H_2O…… …….. (3.2)

3.3.2.2 DETECTION OF OZONE IN THE LIQUID PHASE

Ozone, being one of the active species produced in underwater streamer discharges was detected and quantified using the indigo method as described by Bader et al. (1981). Indigo has a strong absorbance at 600 nm (ε = 20 000 L $mol^{-1}cm^{-1}$). One molecule of ozone could decolourise one molecule of the indigo dye. The decolorized products hardly consumed further ozone. The amount of ozone scavenged could be determined from the decolourisation of the reagent measured at 600 nm. During measurement, no interference with OH radicals was expected after pulsing of the reactor. This had been earlier demonstrated by Bader and Hoigne (1981) that the presence of hydrogen peroxide does not interfere with the measurement of $OH^{\cdot}$ radicals. Indigo reagent could be prepared as follows:

Solution-A: About 0.5 mL of phosphoric acid was mixed with 310 mg of indigo trisulfanate in a volumetric flask and filled up to 500 mL with Millipore water.

Solution-B: 14 g of sodium dihydrogen phosphate was mixed with 17.5 g of H_3PO_4 together in a volumetric flask and filled up to 500 mL with Millipore water.

Two mL of each solution (A and B) were mixed together in a volumetric flask and filled up to 25 mL with Millipore water. The absorbance of this solution was measured and recorded as a reference [blank absorbance count]. To determine the ozone concentration dissolved in the water sample, again 2 mL volumes of each reagent were mixed immediately together in a 25 mL volumetric flask and the rest of the volume filled up with treated water sample. Then the absorbance of the solution was measured and recorded as the sample absorbance.

As earlier described, the O_3 concentration was calculated from the differences in absorbance between the initial indigo solution and that of the solution exposed to ozone.

3.3.2.3 ENERGY DENSITY OF MB DEGRADATION

Despite various parameters associated with MB decomposition, the feasibility of the actual DBD reactor was evaluated by determining the amount of MB decomposed per unit of energy (yield). Reddy et al. (2013) estimated the energy yield (Y) of MB decomposition using Equation 3.3 given by:

Y (g/kWh) = [C (g/L) x V (L) x 1/100 x decolourization %] / P (kW) x t (h)..... (3.3)

Where C is the concentration of dye, V is the solution volume, P is the power consumed during MB degradation and t is the experimental running time.

So, the DBD experiment was carried out over 60 minutes while sampling at 10 minutes interval and the experiment was performed at the following experimental conditions: MB concentration 5 mg/L, pH (between 6.04 and 6.64), applied voltage 25 V, peak voltage 7.8 kV, MB volume 1 500 mL, air flow rate 3 L/min, 0.5 mm silver electrode at 25 ºC. During each experiment the change in the following parameter: applied voltage (V), peak voltage (kV), current (A), Power (W) was measured. In addition, the UV absorbance of MB solutions sampled every 10 min, was recorded. The unknown concentration of MB solutions was calculated using the calibration curve presented in Figure 4-8 of chapter four. From the initial and calculated MB concentrations, MB degradation efficiency was determined. Thus having all these data, the energy required to degrade 5 mg/L MB was estimated using Equation 3.3.

3.4 ANALYTICAL TECHNIQUES

The characterization techniques used to analyse treated and untreated MB samples include UV-vis and FT-IR spectroscopy, TOC, COD, nitrates and sulphates tests which are successively explained below.

3.4.1 UV-vis spectroscopy

UV-vis spectroscopy technique was used to record the absorbance and hence to determine unknown concentrations of MB samples in this study.

3.4.1.1 SAMPLE PREPARATION

An initial model solution of 100 ppm methylene blue was prepared as follows: About 0.2 g of powered methylene blue was weighed and quantitatively transferred into a 2 000 mL volumetric flask and made up to the mark with deionised water. Other solutions of different concentrations (0.5; 20; 30; 40 and 50 ppm) were prepared by serial dilutions. Each of these solutions was separately used to perform the degradation of methylene blue using electro hydraulic discharge.

3.4.1.2 EXPERIMENTAL SET UP FOR UV VIS SPECTROSCOPY

In experimental set up, Hellma precision cells made of quartz Suprasil were used to run UV-vis of all samples. The quartz Suprasil had characteristic specifications as follows: cuvettes 2, Type No. 110-QS, light path nm: 10 nm and match.c: 284, as shown in Figures and 3-7 below.

Figure 3-6: Cuvettes pieces used in UV-vis analysis of samples

Figure 3-7: UV/ Vis spectroscopy set up

In addition, Figure 3-8 above shows a GBC UV/VIS 920 spectrometer set up that was used to analyse dye samples as described in UV/vis procedure below

3.4.1.3 UV-VIS PROCEDURE

First, the two quartz Suprasil cuvettes were washed and filled up with deionised water. Then the cuvettes were placed in the UV machine for baseline analysis using deionised

water as a reference solution. After the baseline run, one cuvette was removed from the instrument and the other was left as reference. The removed cuvette was washed with deionized water and filled up with the sample of interest and placed back into the machine. All the samples were run at a fixed wavelength of 665 nm. Wavelength, absorbance and other parameters of these samples could be obtained from UV-vis instrument.

In order to determine the corresponding concentration of each of these absorbance values, absorbance of standards solutions (from 0.5 to 10 mg/L) of methylene blue were obtained from UV-vis spectrometer and presented in Table 3-9 below. Results showed that the absorbance of samples increased linearly with an increase of dye concentration.

Table 3-9: Standard concentrations vs Absorbance

Standard concentrations (mg/L)	**Absorbance**
10	1.28
20	2.4
30	3.498
40	4.54
50	5.75

The obtained absorbance of standard dye solutions were used to plot a calibration curve as shown in Figure 3-9. Likewise absorbance of samples taken in the time scale of 60 minutes at various MB concentrations was extrapolated on the calibration curve to find unknown concentrations of MB samples. The absorbance of MB solutions sampled between 0 and 60 minutes decreased as dye concentration was decreasing during degradation. This trend indicated that MB dye was being degraded as the experimental running time increased. That is, absorbance of the solution sampled after 10 minutes for example was greater than that of the one taken after 20 minutes and so forth.

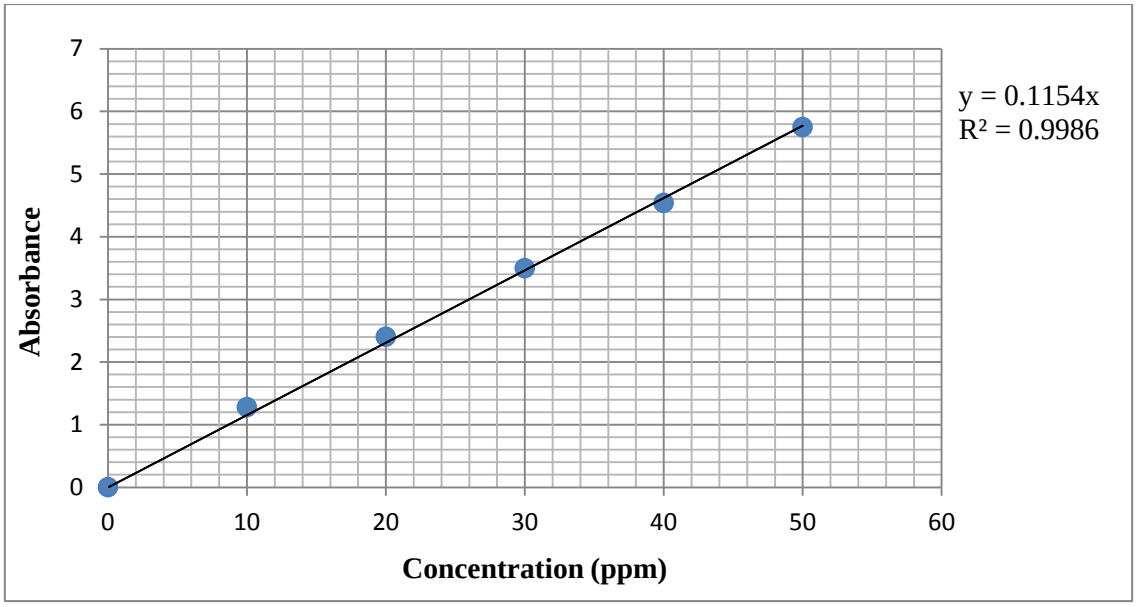

Figure 3-8: Calibration curve of absorbance vs. concentrations of methylene blue at t = 0 minutes.

Since the calibration curve was a straight line passing through the origin, it therefore obeyed the equation: y = mx, where y represents absorbance values, m the slope of the line and x the unknown concentration that needed to be determined. According to the calibration curve above the equation of the line was given by

Y = 0.1154x……. (3.4)

where m = 0.1154 and y any absorbance value on the y-axis.

Therefore, unknown concentrations of methylene blue samples (represented by x in the equation (3.4)) taken after 10, 20, 30, 40, 50 and 60 minutes were estimated using

X = Y/0.1154…….. (3.5)

Alternatively, once the absorbance value is identified on the y-axis, the value can be extrapolated on the straight line to deduce the corresponding value of x, thus measuring the inferred concentration. This procedure could be applied to all solutions of unknown concentrations.

Decolourization efficiency could be referred to as the effectiveness of colour removal of dye methylene blue by electro hydraulic discharge. Recently Reddy et al. (2013), studied the degradation and mineralization of methylene blue by dielectric barrier discharge non-thermal plasma reactor. In that study, methylene blue degradation efficiency also called degradation percentage or decolourization efficiency was calculated using the formula presented in Equation (3.6):

Decolourization percentage (D %) = $[(C_o - C_t) / C_o] \times 100$…… (3.6)
Where C_o and C_t are the initial and the final concentrations of MB solution respectively. So in the current study, the formula highlighted above can also be used to evaluate methylene blue degradation percentage at the given initial and final concentrations.

To evaluate the degree of electrode corrosion that occurred during EHD experiments and to analyse MB treated and untreated samples, the following techniques were used: scanning electron microscopy (SEM), Fourier transformer infra-red spectroscopy (FT-IR) and total organic carbon (TOC), chemical oxygen demand (COD), sulphate and nitrogen (as nitrite + nitrate) content were determined.

3.4.2 Scanning Electron Microscopy: Investigation of electrode corrosion

During optimization of electrode material in the EHD system, it was noticed that the optimized copper, silver and stainless steel electrodes corroded after a certain number of experiments. Therefore, to evaluate the rate of corrosion in a simple fashion, portions of each electrode type before and after each set of experiment were viewed by SEM for surface analysis. Specifically in this case, the surface of the electrode was investigated using SEM. The SEM of the electrode samples was performed using Hitachi X 650 Scanning Electron Microscope at an applied voltage of 5.00 kV, a working distance of 3.5 nm and at various magnifications. The machine resolution depended on the experiment. The procedure adopted for SEM analysis of electrodes samples is detailed as follows.

3.4.2.1 SEM PROCEDURE

A small portion of about 2 mm of each electrode taken from the surface was placed on carbon tape which in turn was placed on top of a specimen holder. After dusting electrode samples with carbon, the holder was positioned in the SEM instrument. In order to get a clear area of electrode samples, various scans were accomplished. The scans executed at different magnifications led to multiple electrode images. However, only those showing clear images of the electrode surface were selected and recorded for corrosion interpretation.

3.4.3 Fourier Transformer Infra-red spectroscopy

As much as UV-vis reveals information about absorption bands related to the colour change of MB when exposed to plasma treatment, FT-IR was used to qualitatively analyze untreated and treated water samples to determine intermediate degradation products. The main objective was to determine the types of degradation products remaining in the solution, hence showing the degree of MB degradation during exposure to electrical discharge. FT-IR of MB samples was performed on a Perkin Elmer spectrum 100 FT-IR spectrometer as described in the following procedure.

3.4.3.1 FT-IR PROCEDURE

Initially, 4 mL of dichloromethane was dropped on a towel paper to clean the ATR sample holder of the Perkin Elmer spectrum 100 FT-IR spectrometer. About 0.5 mL of MB sample was withdrawn from the sample container with a 5 mL dropper and was placed on the attenuated total reflectance (ATR) sample holder of the Perkin Elmer spectrum 100 FT-IR spectrometer. The sample was analyzed in the range of 4 000 - 380 cm^{-1}. After the desired background was selected, the baseline was corrected and the spectra were smoothened. The spectra obtained showed various vibration bands of different functional groups suggesting the presence of several organic and inorganic compounds.

3.4.4 Total organic carbon

The total organic carbon (TOC) is defined as all carbons covalently bonded in organic molecules and in surface and ground water as well as organic carbon which is not purgeable by acidification and gas stripping (Mohamed, 2011; Wilhelmus, 2000). The TOC measurement as stated in section 2.3.3.2 was performed according to standard methods for the examination of water and wastewater, high temperature combustion method 5310 B (APHA-AWWA-WPCF, 1989).

Initially, few µmL of the sample was acidified with 2 N HCl (pH 2) and reasonable amount of the acidified sample was inserted into the analyser. The resulting CO_2 was purged, removing any inorganic carbon present in the sample. Afterwards the remaining carbon from the sample prepared in this manner was determined via combustion. The digestion is performed in the multi N/C 3100 by thermocatalytic high-temperature

oxidation in the presence of a platinum catalyst. This enables the quantitative digestion even for very stable, complex carbon compounds. The sample aliquot was directly dosed into the hot zone of the filled reactor (combustion tube). Here the pyrolysis and oxidation of the sample in the carrier gas flow was performed with the aid of the catalyst (Equations (3.5) - (3.7). The carrier was also used as an oxidation agent.

$R + O_2 \rightarrow CO_2 + H_2O$..... (3.5)

$R - N + O_2 \rightarrow NO + CO_2 + H_2O$..... (3.6)

$R - Cl + O_2 \rightarrow HCl + CO_2 + H_2O$..... (3.7)

Where R is a carbonic substance.

The measuring gas was cooled in the condensation coil and condensed water was separated from the measuring gas in the subsequent total inorganic carbon (TIC) condensate container. After further drying and removal of corrosive gases, the measuring gas CO_2 was added to the NDIR detector. Calculations of TOC were achieved as described in section 2.3.3.3

3.4.5 Chemical oxygen demand

As defined by Gravosky (2006), COD is a measure of water quality that is expressed in millgrams of oxygen per litre. It is the measure of the quantity of oxygen required to totally oxidize and mineralize organic substances to inorganic derivatives. A full review on COD principles is presented in section 2.3.4

The chemical oxygen demand (COD) for the degradation of MB in the EHD system was evaluated using the methodology suggested by Pitwell (1983) and described as follows:

A sample volume of 2 mL was oxidized in a Hach sample vial containing 4.17 mM of potassium dichromate in 5 ml of sulphuric acid and digested at 150^{o}C for 2 h. Samples were determined spectrophotometrically using a Hach DR/2010 spectrophotometer at absorbance of 420 nm described by manufacturer instruction manual method 8000 (Hach, Colorado, USA) (Pitwell, 1983). Calculation of COD in this study was performed

according to the comprehensive methodology suggested by Soresa (2011) and described in section 2.3.4.1

3.4.6 Nitrate and nitrite analysis (US EPA, 1983)

About 10 mL of filtered sample was injected into a LACHAT QuickChem® flow injection analyser (FIA) carrier stream with flow rate of 2.5 µL/cm. The sample was moved through a QuikChem® 10-107-04-1-A cadmium column for reagent preparation. The activated cadmium reduced the entire nitrate in the sample to nitrite. The nitrite was then determined by diazotizing with 58.07 mM of sulphanilamide followed by coupling with 3.85 mM of N-(1-naphthyl) ethylenedaimine dihydrochloride (Merck, Germany). The absorbance of nitrites and the reduced nitrates were measured at 520 nm with colorimeter detector. Nitrite alone was determined in absence of the cadmium column. The data were exported from the omnion software as an excel sheet. Correlation coefficient of > 0.999 was accepted. In house quality control samples as well as external proficiency testing (PT) samples were used for quality control. This analysis was performed by CSIR Company at Stellenbosch

3.4.7 Major cation: sulphate

Filtered liquid samples were injected into the nebulizer of cyclonic spray chamber of QuikChem® 10-107-04-1-A analyser and carried into plasma through an injector tube located at the torch. The sample aerosol was injected directly into the inductively coupled plasma (ICP, Thermo scientific, MA, USA), subjecting the constituent atoms to temperature range of 6 000 to 8 000 K with a constant flowing stream of argon gas ionized by applied radio frequency field typically oscillating at 27.1 MHz. Ionization of a high percentage of the atoms producing ionic emission spectra was then recorded. Ionic emission was detected and quantified by simultaneous ICP with CID detector. A correlation coefficient of > 0.999 was accepted. In house quality control samples as well as external proficiency testing (PT) samples were used for quality control.

CHAPTER FOUR: RESULTS AND DISCUSSION OF SECTION 1

4 INTRODUCTION

This chapter firstly presents the results of the optimization of reactor configuration and the optimization of physico-chemical parameters at normal conditions of temperature and pressure using the EHD system. It also contains results and discussion of the EHD experiment run at optimal conditions.

4.1 OPTIMIZATION OF REACTOR CONFIGURATION: EFFECT OF AIR GAP BETWEEN THE OUTER AND INNER TUBES OF THE EHD REACTOR

Three different reactor configurations were designed and tested for MB decolouration efficiency. The aim was to evaluate the impact of the distance between the inner and the outer quartz tubes (air gap) on MB degradation. The air gap was varied from 2, 4 and 6 mm as presented in section 3.3.1.4 of chapter 3. The EHD experiments on degradation of MB solution were performed using the three configurations. Each experiment was carried out within 60 minutes and sampled every 10 minutes. Absorbance of MB solution sampled over 60 minutes using reactors with air gap 2, 4 or 6 mm, their calculated concentrations as well as their corresponding decolourization efficiencies are shown in Tables 4-1, 4-2 and 4-3, respectively.

Table 4-1: Absorbance of MB solution sampled within 60 minutes using reactor 1 with air gap 2 mm (Experimental conditions: MB concentration 5 mg/L, applied voltage 25 V, Peak voltage 7.8 kV, pH (in between 6.04 and 6.064), MB solution conductivity (0.02 to 0.09 mS/cm), dye volume 1500 mL, inlet air flow rate 3 L/min, 50 g/L NaCl electrolyte, 0.5 mm silver electrode.

TIME (minutes)	Absorbance (nm)	Concentration (mg/L)	Degradation % removal
0	1.023	5	0
10	0.423	3.665	26.7
20	0.200	1.733	65.34
30	0.096	0.832	83.36
40	0.045	0.389	92.22
50	0.016	0.138	97.24
60	0.000	0.000	99.999

Table 4-2: Absorbance of MB solution sampled within 60 minutes using reactor 2 with air gap 4 mm (Experimental conditions: MB concentration 5 mg/L, applied voltage 25 V, Peak voltage 7.8 kV, pH (in between 6.04 and 6.64), MB solution conductivity (0.02 to 0.09 mS/cm), dye volume 1500 mL, inlet air flow rate 3 L/min, 50 g/L NaCl electrolyte, 0.5 mm silver electrode.

Time (minutes)	Absorbance (nm)	Concentration (mg/L)	Degradation % removal
0	1.077	5	0
10	0.553	4.792	4.16
20	0.304	2.634	47.32
30	0.116	1.005	79.9
40	0.062	0.537	89.26
50	0.042	0.364	92.72
60	0.025	0.2166	95.68
70	0.008	0.069	98.62
80	0.000	0.000	99.999

Table 4-3: Absorbance of MB solution sampled within 60 minutes using reactor 3 with air gap 6 mm (Experimental conditions: MB concentration 5 mg/L, applied voltage 25 V, Peak voltage 7.8 kV, pH (in between 6.04 and 6.64), MB solution conductivity (0.02 to 0.09 mS/cm), dye volume 1500 mL, inlet air flow rate 3 L/min, 50 g/L NaCl electrolyte, 0.5 mm silver electrode)

Time (minutes)	Absorbance (nm)	Concentration (mg/L)	Degradation % removal
0	1.059	5	0
10	0.58	5	0
20	0.57	4.94	1.2
30	0.467	4.05	19
40	0.335	2.903	41.94
50	0.224	1.941	61.18
60	0.149	1.291	74.18
70	0.080	0.693	86.14
80	0.049	0.426	91.48
90	0.033	0.286	94.28
100	0.020	0.173	96.54
110	0.008	0.069	98.62
120	0.000	0.000	99.999

Tables 4-1, 4-2 and 4- 3 show that the air gap which is the space between the inner and the outer quartz tubes of the DBD reactor affected the amount of air circulating in the dielectric region which had an effect on dye decolouration. From the calibration curve previously described in chapter 3 of this study and by using the Beer's law, unknown concentrations of samples were calculated from the UV data presented in these Tables. Having the initial and final concentrations of MB samples, decolourization efficiency of this dye with time was estimated and results obtained were plotted in Figure 4-1.

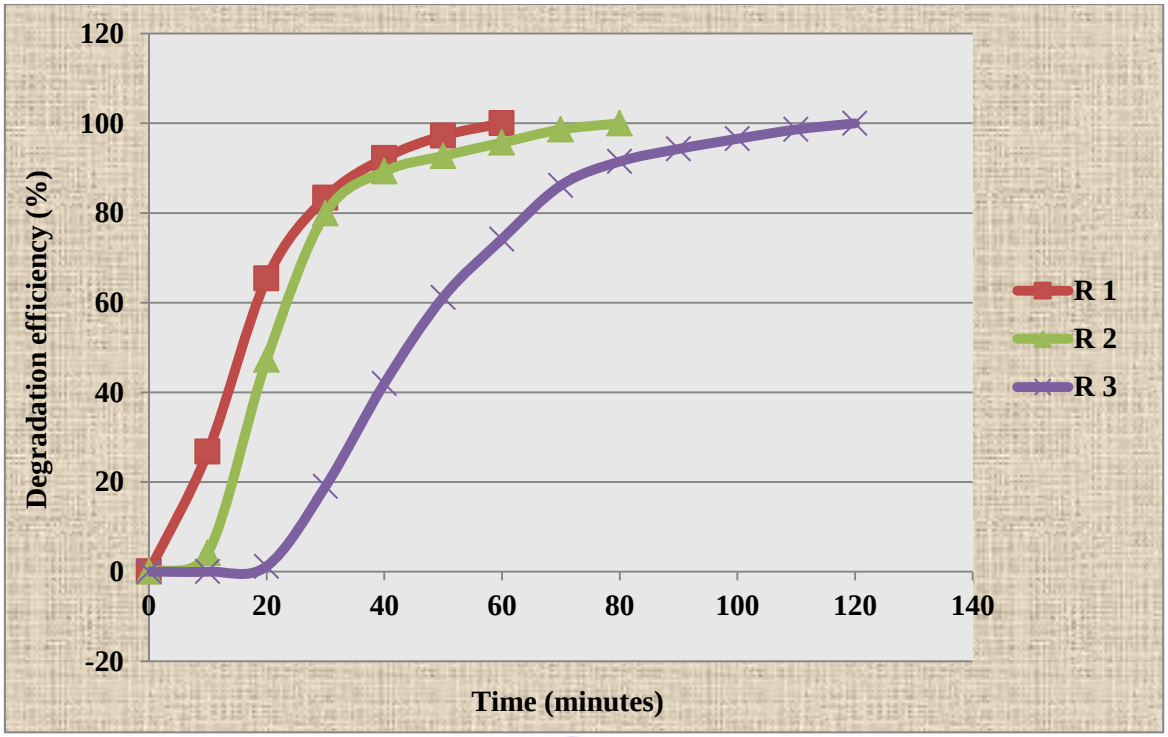

Figure 4-1: Effect of air gap on MB degradation percentage. Varied parameter: air gap, [from 2 mm (R1), 4 mm (R2) and 6 mm (R3)]. Fixed parameters: Applied voltage 25 V, peak voltage 6.7 kV, MB concentration 5 mg/L, solution pH (in between 6.04 and 6.64), MB solution conductivity (0.02 to 0.09 mS/cm), inlet air flow rate 3 L/min, dye volume 1500 mL, 50 g/L NaCl electrolyte, 0.5 mm silver electrode.

Figure 4-1 presents the effect of air gap between the inner and the outer tube of the DBD reactor tube on MB decolourization efficiency. The results presented in Figure 4-1 showed that complete decolouration of MB in reactor 1 with a 2 mm air gap was achieved within 60 minutes. However, with reactor 2, MB was totally decolourized after 80 minutes and 120 minutes in reactor 3. These results clearly demonstrate that the shortest decolouration time of MB was achieved with reactor 1 having an air gap of 2 mm, closely followed by reactor 2 and reactor 3. This showed that the air gap has a direct impact upon the efficiency. At a particular experimental time, for example after 20 minutes of experiment, about 65.34 % of MB was decolourized with reactor 1 compared to 47.32 % with reactor 2 and 1.2 % with reactor 3. This trend was also observed after 10 minutes of experiment whereby 26.7 % of dye decolourisation was achieved with reactor 1, 4.16 % with reactor 2 and 0 % with reactor 3. Based on these air gap dimensions and results presented in Figure 4-1, it could be inferred that degradation efficiency of MB significantly decreased with an increase in air gap. This could primarily be explained by the fact that the inlet air flow rate

might have decreased due to the increase of the air gap size. The decrease of the air flow rate probably reduced the amount of oxygen circulating in the discharge zone, and hence, a small amount of reactive species was produced in the air gap of the DBD reactors tubes 2 and 3 having higher air gap sizes.

On the other hand, the small air gap in reactor 1 for instance, might have induced a strong electric field leading to high electron energy around the inner tube. These electrons might have increased the length and number of micro discharges that dissociated oxygen molecules quickly into singlet atomic oxygen which probably reacted back with oxygen to generate ozone and other active species such as hydrogen peroxide. These active species were then bubbled directly into MB solution. The interaction of these species with dye could have resulted in the formation of other powerful and non-selective oxidants like $^{\cdot}OH$ contributing to the quick decolourization of MB solution. Based on these observations, it was obvious that the increase of air gap in reactors 2 and 3 reduced the length and number of micro discharges as well as electron energy induced around the inner tube of the rector. This eventually resulted in the decrease of oxygen molecules dissociation. Hence the decrease of active species formation that led to the diminution of MB degradation efficiency. Therefore, reactor 1 was the optimum configuration used further for the current EHD system.

Another aspect that might have lowered MB decolouration in reactors 2 and 3 could be the decrease of UV radiation intensity. In fact UV radiations (also called photons) generated in DBD discharge zone have been proved to decompose water molecules into hydroxyl radicals and other species (Prendiville et al., 1986). Since the air gap in reactors 2 and 3 were enlarged, this might have weakened and reduced the intensity of these radiations. However, it was not easy to measure the decrease due to the lack of instrumentation. Therefore, the intensity of photons reaching the bulk solution was weak and could not dissociate water molecules as expected. This reduced the formation of reactive species and thus dramatically contributed to decrease of MB decolouration efficiency.

From the analysis of results presented in Figure 4-1, it was concluded that the dielectric region or air gap had an impact on the MB decolouration efficiency. Precisely, colour removal percentage of MB decreased with an increase of air gap. This finding correlates with Zhang et al. (2008) observations, hence reactor 1 was chosen as the optimum configuration for further experiments varying other parameters for MB decolouration in

this study. In water/wastewater treatment technology, reactor configuration as mentioned in literature remains one of the most critical parameters.

4.2 OPTIMIZATION OF CHEMICAL PARAMETERS

In order to assess the efficiency and effectiveness of the actual EHD reactor, most chemical parameters were taken into account. The chemical parameters studied include, methylene blue (MB) initial concentration and NaCl electrolyte concentration which have been investigated subsequently.

4.2.1 Effect of initial MB concentration on MB decolourization by EHD

In the current study, the effect of initial MB concentration on decolourization of MB and the performance of the DBD reactor were evaluated. The main goal of this section was first to determine the optimum concentration at which the DBD reactor would operate efficiently during 60 min. That is, the behaviour of absorbance of MB samples with respect to their concentrations and the colour of the final MB solution sampled after 60 minutes of contact time were considered. Therefore, the MB concentration giving rise to a clear solution with a reasonable absorbance after 60 minutes of treatment was chosen as optimum and was used in all further DBD experiments. Thus, the effect of the initial MB concentration on MB decolourization efficiency was evaluated by plotting the decolouration percentage of dye against its concentration which was varied from 0.5 to 10 mg/L at the applied conditions.

The absorbance of MB solution was measured within 1 hour at concentrations ranging from 0.5 to 10 mg/L with increment of 0.5 mg/L at the applied conditions as described in section 3.3.1.1. Results obtained are presented in Table 4-4 and the results were plotted in Figure 4-2. The different colour changes of the final MB solution were photographed to confirm the optimum concentration and are shown in Figure 4-3. Furthermore, the UV data and decolouration efficiencies of MB dye were recorded at the applied conditions and are presented in Appendices 1-3. Finally to assess the effect of initial concentration on MB decolouration a higher concentration increment of 10 mg/L starting from 5 mg/L was considered. Therefore, the UV data on the influence of initial concentration on colour percentage removal was recorded in Appendices 30 – 34 and the results were plotted and are exhibited in Figure 4-4.

Table 4-4: Absorbance of samples withdrawn every 10 minutes within 60 minutes at MB concentration ranging from 0.5 to 10 mg/L at the following DBD experimental conditions: applied voltage 25 V, Peak voltage 7.8 kV, pH (in between 6.04 and 6.64), MB solution conductivity (0.02 to 0.09 mS/cm), air gap 2 mm, air flow rate 3 L/min, solution volume 1500 mL, 0.5 mm silver electrode, 50 g/L NaCl electrolyte.

Initial conc (mg/L)	**Absorbance within 60 minutes**						
	0 min	10 min	20 min	30 min	40 min	50 min	60 min
0.5	0.087	0.029	0.002	0.000	0.000	0.000	0.000
1	0.161	0.007	0.000	0.000	0.000	0.000	0.000
1.5	0.323	0.031	0.009	0.002	0.000	0.000	0.000
2	0.415	0.053	0.014	0.002	0.000	0.000	0.000
2.5	0.418	0.084	0.014	0.003	0.000	0.000	0.000
3	0.485	0.060	0.009	0.005	0.000	0.000	0.000
3.5	0.453	0.040	0.009	0.007	0.003	0.000	0.000
4	0.619	0.119	0.025	0.009	0.006	0.002	0.002
4.5	0.701	0.181	0.037	0.014	0.006	0.004	0.003
5	0.742	0.194	0.004	0.020	0.009	0.004	0.004
5.5	0.707	0.167	0.029	0.010	0.005	0.002	0.000
6	0.752	0.156	0.026	0.010	0.005	0.000	0.000
6.5	0.842	0.220	0.053	0.024	0.011	0.005	0.003
7	0.862	0.287	0.077	0.026	0.011	0.006	0.005
7.5	0.896	0.232	0.060	0.023	0.015	0.009	0.006
8	0.914	0.265	0.049	0.013	0.006	0.000	0.000
8.5	0.957	0.279	0.041	0.010	0.001	0.000	0.000
9	0.996	0.198	0.044	0.016	0.010	0.005	0.005
9.5	1.036	0.319	0.113	0.046	0.016	0.009	0.005
10	2.476	1.254	0.589	0.290	0.124	0.073	0.034

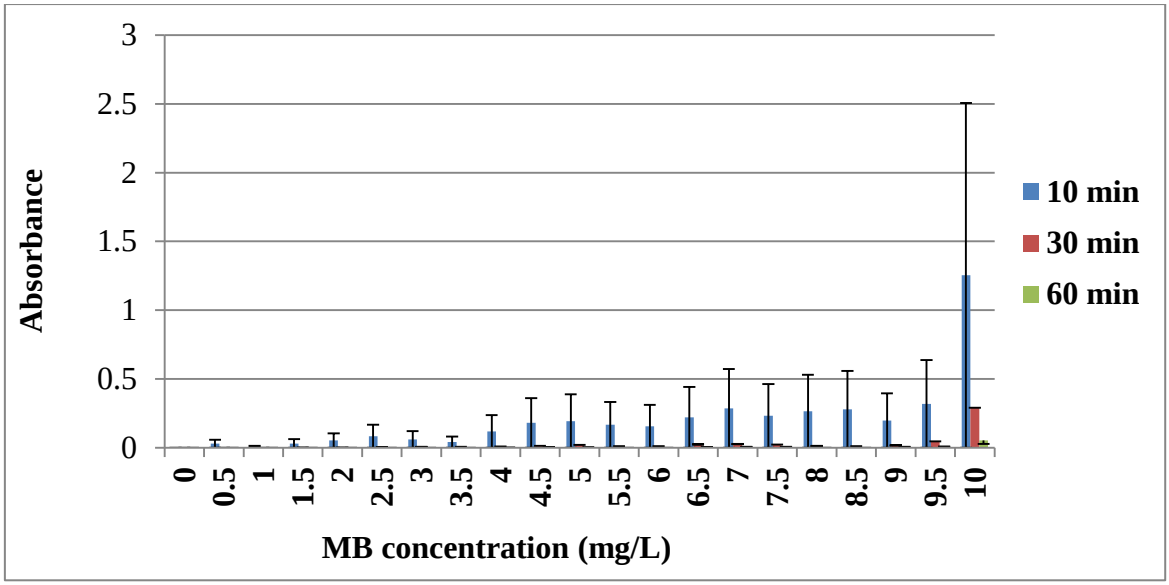

Figure 4-2: Absorbance of various MB concentrations during EHD experiment at the following experimental conditions: Applied voltage (25 V), peak voltage 7.8 kV, MB volume 1500 mL, pH (in between 6.04 and 6.64), MB solution conductivity (0.02 to 0.09 mS/cm), air flow rate 3 L/min, air gap 2 mm, 50 g/L NaCl electrolyte and 0.5 mm silver electrode. (Replication, n = 2).

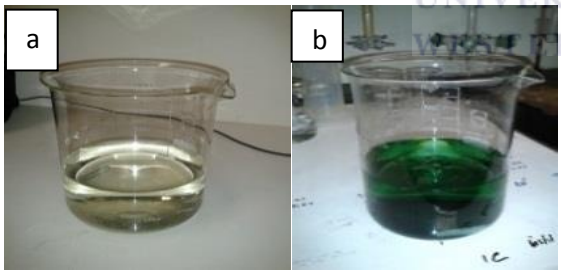

Figure 4-3: MB solutions obtained within 60 minutes at concentrations from: 0.5 to 5 mg/L (a) and above 5 mg/L (b) at the following experimental conditions: solution pH (in between 6.04 to 6.64), MB solution conductivity (0.02 to 0.09 mS/cm), air flow rate 3 L/min, air gap 2 mm, dye volume 1500 mL, 50 g/L NaCl electrolyte and 0.5 mm silver.

Table 4-4 shows the absorbance of MB solution at various MB concentrations in the range of 0.5 to 10 mg/L sampled within 60 minutes at the applied conditions. Figures 4-2 presents the trend between MB concentrations and their absorbance during DBD experiment and colours of the final MB solutions sampled after 60 minutes. On the other

hand, Figure 4-3 shows colour of MB final solutions sampled after 60 minutes of experiment.

The results presented in Table 4-4, demonstrate that, from the absorbance of MB solution sampled within 1 hour of treatment in the EHD reactor, complete decolourization of MB was observed for 0.5 and 1 mg/L MB within 30 minutes. Likewise from 1.5 to 3 mg/L complete discoloration was achieved after 40 minutes. Above 3 mg/L of MB, the absorbance of samples slightly fluctuated at different concentrations and different sampling times. This means that the quantity of active species produced in the DBD system was enough to decompose MB at those concentration ranges. From the results shown in Figure 4-2, the absorbance of samples linearly increased with an increase in the concentration of MB samples. This implies that greater amounts of reactive species are needed to decolourize MB dye solution as its concentration increases.

In addition to this, from 0.5 to 5 mg/L of MB the final solution sampled within 60 minutes was clear whereas a different trend was noticed as MB concentration increased from 6 to 10 mg/L. At concentrations above 5 mg/L, the colour of the solution withdrawn at 60 minutes varied from light yellow to deep green as the concentration of MB increased as shown in Figure 4-3. This implies that 0.5 to 5 mg/L of MB is the optimum concentration range in which the single cell DBD system can operate efficiently thus this concentration was used for further optimization of the system. The slight fluctuation of absorbance and changes in colours of MB samples previously observed, confirm that initial concentration of MB dye had an effect on the decolouration rate by the DBD operated under the given conditions. Based on this, the effect of MB concentration on MB decomposition was assessed at the applied conditions. In this way, having the initial concentrations (C_i) and the final concentrations (C) of MB at specified sampling time intervals, Equations 4.1 and 4.2 was used to calculate the rate constant K (min^{-1}) of MB decomposition.

$$\ln(C/C_i) = - kt \quad \text{(4.1)}$$

$$K = \ln(C/C_i)/t \quad \text{(4.2)}$$

Where t is the sampling time (minutes) and k the rate constant (min^{-1}) of MB decomposition. The K values calculated were tabulated in Appendices 46 – 47 and the results were plotted and are presented in Figure 4-4.

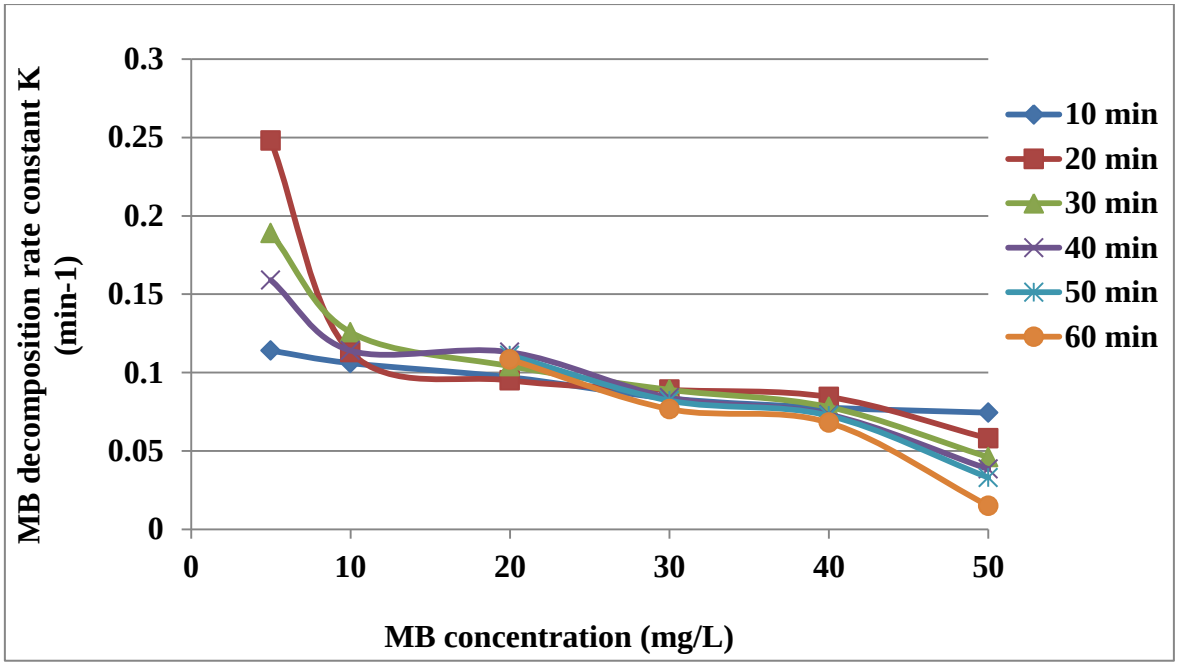

Figure 4-4: Effect of initial concentration (varied from 5 to 50 mg/L) on MB decomposition rate constant. [experimental conditions: applied voltage 25 V, Peak voltage 7.8 kV, pH (in between 6.04 and 6.64), MB solution conductivity (0.02 to 0.09 mS/cm), MB volume 1500 mL, air flow rate 3 L/min, air gap 2 mm, 50 g/L NaCl electrolyte, 0.5 mm silver electrode].

Figure 4-4 illustrates the decomposition rate constant k (min^{-1}) of MB at different concentrations over 60 minutes and sampling at 10 minutes intervals at the applied conditions. The results presented in Figure 4-4 showed that over 60 minutes of treatment time, the rate constant of MB decomposition decreased with an increase in MB concentration. This might be due to the fact that, the intensity of the UV-light produced in the DBD system was weak and therefore could not totally penetrate the bulk solution as dye concentration was increased. In that case, only the water layer surrounding the second or the outer dielectric quartz tube were primarily exposed to the UV light generated and probably got decolourized first while the remaining water layer required a significant stirring and prolonged time to be illuminated and hence dissociated.

In addition to this, the ozone that was produced by the DBD reactor during EHD experiment might also have been responsible for the decrease of MB decolouration percentage at high MB concentration. In fact ozone produced in the air gap was bubbled into the polluted water. Apart from the fact that ozone by its own attacks the pollutant directly, ozone gets dissociated by the UV light and its dissociation products would react

with other active species (see Equations 5-4 to 5-9) which are the source of significant amounts of powerful oxidizing agents mainly OH radicals that are diffused into the bulk and unselectively mineralised the contaminant. Consequently, the decrease of ozone quantity obviously leads to small amounts of free reactive species in the contaminated solution and hence results in the decline of MB decomposition efficiency. Generally, information on decolouration of MB or dyes using double cylindrical DBD plasma reactor is still scarce in literature. However, various researchers have conducted similar studies on dye decolouration using other types of electrical discharges. Authors like Inaloo et al. (2011) and Zhang et al. (2012) reported that dye decolouration decreases with an increase of its initial concentration. In addition, Reddy et al. (2012) studied the degradation and mineralization of aqueous organic pollutants by discharge plasma. It was observed that dye colour removal was beneficial at low concentration because the performance of the technique used decreased with an increase of initial dye concentration.

Since these trends reported in literature are in line with the one observed in Figure 4-4 above, it follows that the degree of decolouration of dye depends on its initial concentration.

To conclude this section, the MB concentration range in which the single cell DBD system operates efficiently was 0.5 - 5 mg/L. In this case 5 mg/L was considered as the optimum concentration and was used in all subsequent DBD experiment runs. Yet, it was noted that at 5 mg/L of MB, the initial pH of untreated MB solution fluctuated from 6.04 to 6.64. So during optimization of other parameters this range of pH was considered instead of a specific pH value. Thus the performance of the DBD plasma reactor during optimization studies was dictated by its ability to clearly decolourize MB at 5 mg/L. The effect of initial concentration showed that decolouration of MB dye decreases with an increase in its initial concentration. Hence, the decomposition of dye depends on its initial concentration.

4.2.1.1 Behaviour of solution pH and conductivity during DBD experiments (pH trends during DBD experiments)

When studying the effect of initial concentration on MB decolouration at the applied conditions as described in section 3.3.1.5.1, the behaviour of pH and solution conductivity at different concentrations was also noted. The increment in MB concentration was from 0.5 to 10 mg/L in order to observe the effect of initial concentration on MB decomposition. So the UV data based on pH and solution conductivity behaviour were recorded and

shown in Appendices 35 and 36, respectively. The UV results were then plotted against time and are presented in Figures 4-5 and 4-6, respectively.

The results in Figure 4-5 show the decreased of pH of MB solutions with time during experiments while the conductivity of solution in Figure 4-6 shows a progressive increase with treatment time. For example in Figure 4-5, at 10 mg/L of MB, the initial pH was 6.09, and after 60 minutes of treatment, its value decreased to 2.57. Meanwhile at the same concentration of MB, solution conductivity in Figure 4-6 increased progressively from 0.04 to 0.8 mS/cm. This implies that more acidic species were being formed in the bulk solution as the treatment time increased. Since the current DBD system does not have any chemical additive, therefore the resulting acidic species might have resulted either from the decomposition of MB molecule or from air that was used as a feeding gas. This trend was observed in all electrohydraulic discharge experiments of MB decolouration at normal conditions of temperature and pressure. Additionally, the abrupt decrease of pH and increase of solution conductivity was also observed by Dang et al. (2008) and Magureanu et al. (2012) who also investigated the decomposition of MB by non-thermal plasma. Magureanu and colleagues discussed that the decrease of pH and increase of solution conductivity during plasma treatment of MB was due to the formation of nitric and nitrous acids as shown in Equations 5.32 -5.34. These acids probably resulted from the interaction of electrical discharge with air consisting of nitrogen and oxygen. These statements were also highlighted and supported by Zhang et al. (2007) and Dojcinovic et al. (2011). Moreover, Brisset et al., (2011) discussed that the acidic effects induced in water by electrical discharge might be caused by the formation and dissolution of nitrogen gases into the liquid leading to nitrite (NO_2^-) and nitrate ions (NO_3^-) and further to nitric acid (HNO_3), nitrous acid (HNO_2) and peroxynitrous acid (ONOOH). This literature is in conformity with the findings obtained in the present study. Indeed, about 16 mg/L of nitrogen content as (nitrites + nitrates) was found in treated MB sample in the actual study as shown in section 5.2.3. Consequently these nitrate salts may have been responsible for both pH decrease and solution conductivity growth during electrohydraulic discharge treatment of MB.

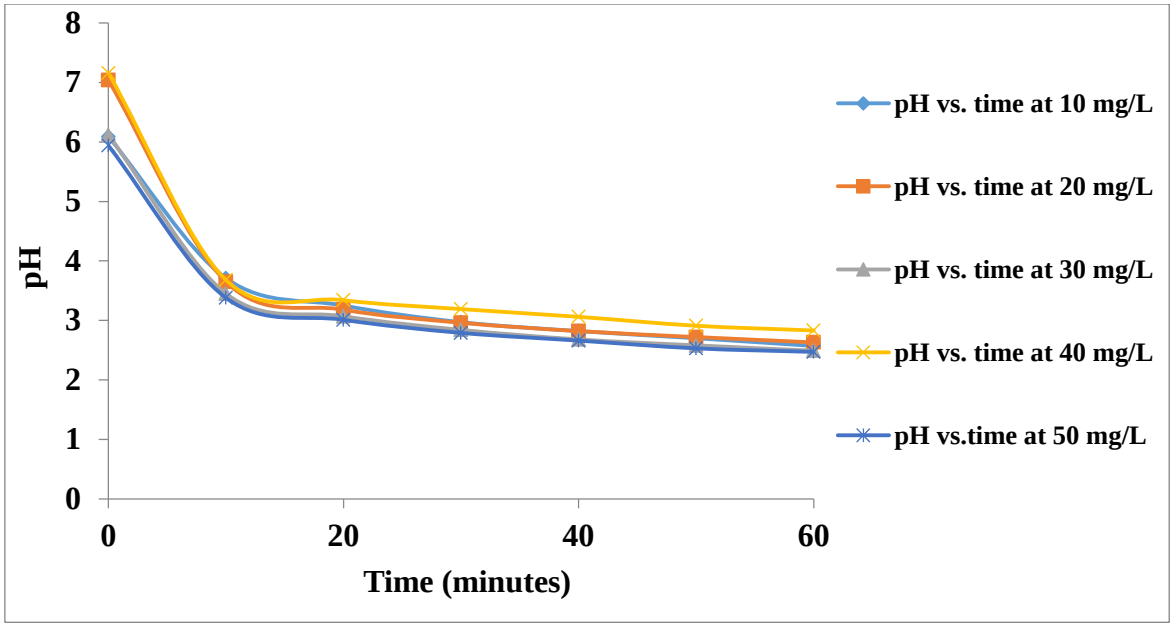

Figure 4-5: pH behaviour with time during decomposition of MB by DBD system. Experimental conditions: MB concentration varied from 5, 10, 20, 30, 40 to 50 mg/L. Fixed parameters: solution pH (in between 6.04 and 6.64), MB solution conductivity (0.02 to 0.09 mS/cm), air flow rate 3 L/min, dye volume 1500 mL, 50 g/L NaCl electrolyte,0.5 mm silver electrode.

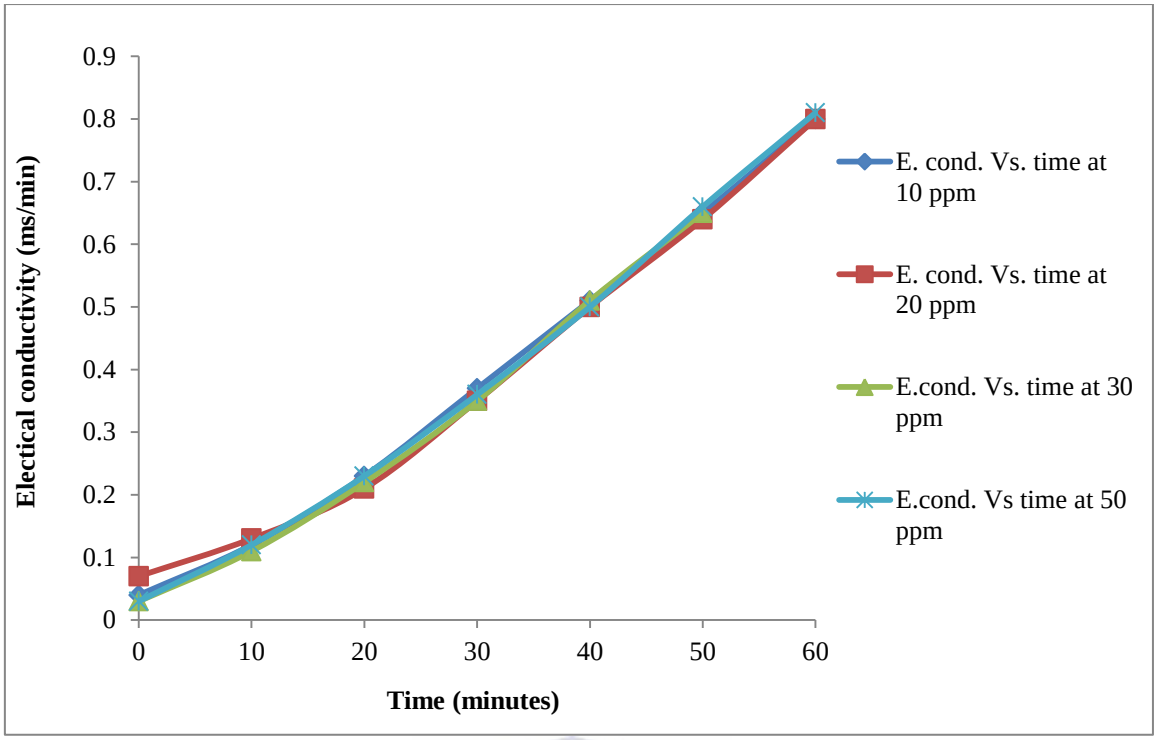

Figure 4-6: Behaviour of solution conductivity with time during MB decomposition by DBD system. Experimental conditions: MB concentration varied from 5, 10, 20, 30, and 40 to 50 mg/L. Fixed parameters: solution pH (in between 6.04 and 6.64), MB solution conductivity (0.02 to 0.09 mS/cm), air flow rate 3 L/min dye volume 1500 mL, 50 g/L NaCl electrolyte, 0.5 mm silver electrode.

On the whole, during electrohydraulic discharge treatment of MB, the pH of solution decreased while its electrical conductivity increased progressively. The gradual decline of pH and the increase in solution conductivity were due to acidic species such as nitrite (NO_2^-), nitrate ions (NO_3^-), nitric acid (HNO_3), nitrous acid (HNO_2) and peroxynitrous acid (ONOOH) formed in solution during plasma decomposition of MB. As pH and solution conductivity showed opposite behaviour during decomposition of MB by the DBD reactor, it was certain that these behaviours might have impacted MB decolourization. Therefore it was necessary to evaluate their effect on MB decolouration efficiency, hence their optimization in the current DBD reactor. The optimization results and discussion of pH and solution conductivity are discussed in section 4.3.

4.2.2 Effect of NaCl electrolyte concentration on MB decolourization efficiency

In this subsection, absorbance, concentrations and decolouration percentage of MB samples obtained within 60 minutes of DBD experiment at different concentrations of NaCl electrolyte are given in Appendices 4-6.

The effect of varying the NaCl electrolyte concentration in the electrode compartment on MB decolourization efficiency is shown in Figure 4-7.

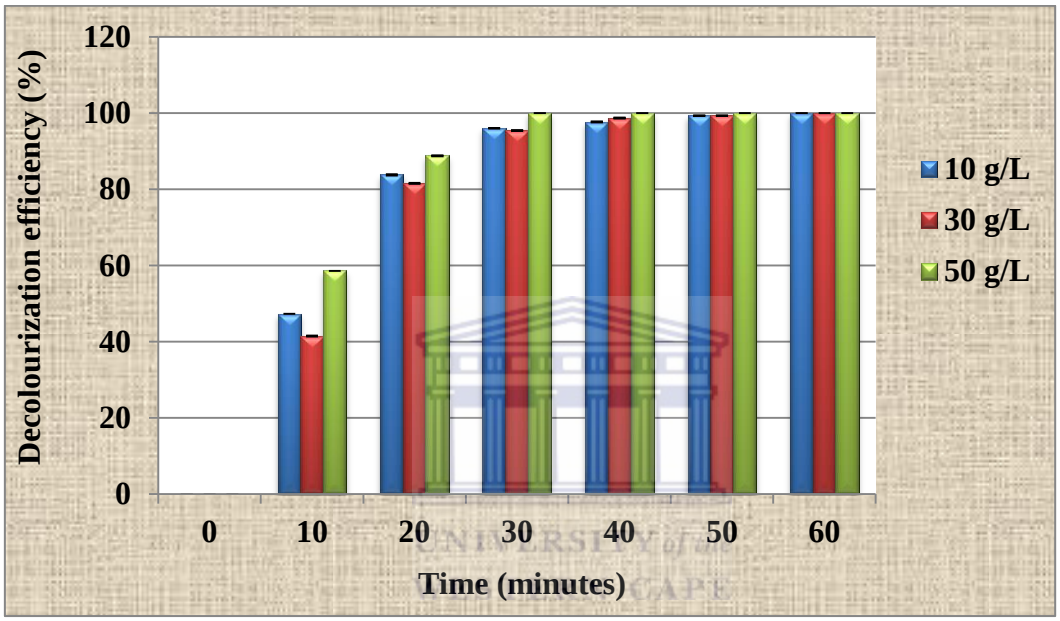

Figure 4-7: Effect of electrolyte on decolourization efficiency. Experimental conditions: applied voltage 25 V, peak voltage 7.8 kV, MB concentration 5 mg/L, solution pH (in between 6.04 and 6.64), MB solution conductivity (0.02 to 0.09 mS/cm), air gap 2 mm, air flow rate 3 L/min, MB volume 1500 mL, 0.5 mm silver electrode.

Figure 4-7 displays UV-vis data of the influence of NaCl electrolyte concentration on MB decolourization efficiency at the applied conditions. The results in Figure 4-7 show that there was no significant difference in methylene blue decolourization at concentrations of 10 g/L and 30 g/L of electrolyte sodium chloride. Whereas better MB colour removal was obtained when 50 g/L of sodium chloride was used as electrolyte as shown in Figure 4-7. This could be explained by the fact that salt solutions such as NaCl conduct electricity at a certain extent based on their saturation. Even if the progressive trend between MB volume and discolouration efficiency was not observed, the high decolourization obtained at 50 g/L of NaCl electrolyte over 10 and 30 g/L perhaps inferred that at 50 g/L the electrolyte

was saturated and therefore conducted electricity better compared to 10 and 30 g/L. This, in other words, means that at 50 g/L, the amount of sodium cations (Na^+) and chlorine anions (Cl^-) were sufficient to conduct current in the inner dielectric quartz tube and hence resulting in an improved distribution of high energetic electrons around the first dielectric quartz tube. This consequently might have led to significant decolouration efficiency.

Additionally, it is important to recall that full optimization of the current DBD plasma reactor has not been fully covered in literature. Only few authors including Jo and Mok (2009) used a similar configuration to generate ozone and UV light for the treatment of wastewater using Azo dye as a model compound. In their configuration (Figure 4-8), authors separately used aqueous NaCl solution and a 9.5 mm copper road as anode electrodes. Results of their research showed that the rate of ozone generation with NaCl electrolyte was higher than that of copper electrode alone. This was justified by the fact that the contact of the aqueous electrolyte solution with the inner dielectric quartz tube was impeccable in minimizing the loss of energetic electrons which were fully delivered through the air gap between the inner and the outer tubes of the reactor. On the contrary, in the actual study a 0.5 or 1.5 mm silver electrode was immersed in aqueous NaCl electrolyte solution and together were used as the powered anode electrode.

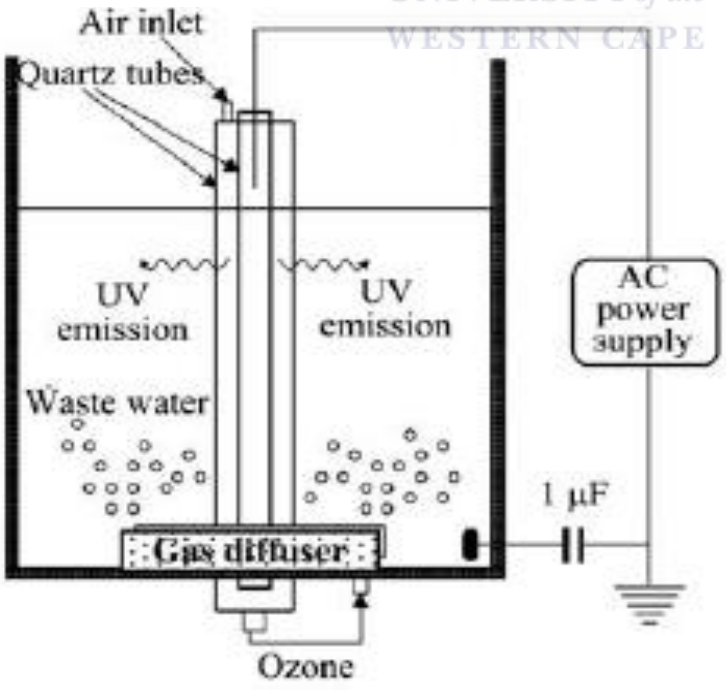

Figure 4-8: Schematic diagram of the experimental apparatus (Jo and Mok, 2009)

Moreover in their study, H_2O_2 was added to the wastewater solution while the present DBD system had no chemical additives. To recall, in both studies the DBD reactor produces UV light, O_3 and other reactive species responsible for the decomposition of the target contaminants. Therefore, in their study, the few parameters including, NaCl concentration, wastewater initial pH, concentration of H_2O_2 added and so on, were evaluated in terms of the rate of O_3 generation. But in the actual work, the assessment of all parameters was based on decolourization efficiency of MB dye. These two situations are hence similar because on the one hand, the ozone generated participates in the decomposition of Azo dye while on the other hand, the decomposition of MB dye in this study is mainly induced by ozone, H_2O_2 and their precursors.

Indeed, ozone in the air gap is produced via contact of air gas with energized electrons distributed all along the inner quartz dielectric tube. So the increase of NaCl electrolyte concentration is believed to decrease its electrical resistance hence declining the transfer of energized electrons onto the inner dielectric tube that could thus diminish the production of ozone in the discharge zone (Jo and Mok, 2009). However, in their research the rise of NaCl concentration from 10, 20, 30, 40 to 50 g/L did not impact the rate of production of O_3. Likewise, the same behaviour was observed in the present study when NaCl concentration was altered from 20, 30 to 50 g/L. This was perhaps due to the high electrical resistance of the discharge gap. In fact, the discharge gap resistance might have been higher than that of the aqueous electrolyte. Thus, the rate of production of ozone in their study and the degradation efficiency of MB dye in the present work were not affected. Apart from the study conducted by Jo and Mok in 2009, the effect of sodium electrolyte on the decomposition of organic contaminants in a double cylindrical DBD reactor has not been investigated elsewhere. With reference to this discussion, it can be remembered that this parameter does not affect the decomposition of organic pollutant but plays a significant role in DBD operations by reducing the loss of highly energized electrons supplied by the electrical discharge.

4.3 OPTIMIZATION OF PHYSICAL PARAMETERS

Apart from the chemical parameters discussed in previous sections of this chapter, physical parameters are also significant aspects that had to be investigated for the optimization of the present DBD system. The physical parameters consist of solution pH and conductivity, air flow rate and solution volume.

4.3.1 The effect of pH on decolourization efficiency of MB

In the present study, MB working solution pH were 2.5, 4.5, 3.5, and 8.5 and 10.5 with HNO_3 and H_2SO_4 acids at the applied conditions as described in experimental Table 3.6.
In order to assess the impact of solution pH on MB degradation efficiency, absorbance, concentrations and MB decolourization percentage were recorded and tabulated in Appendices 7- 9. The effect of the variation of pH on the decolourization efficiency of MB within 60 minutes is shown in Figure 4-9 below.

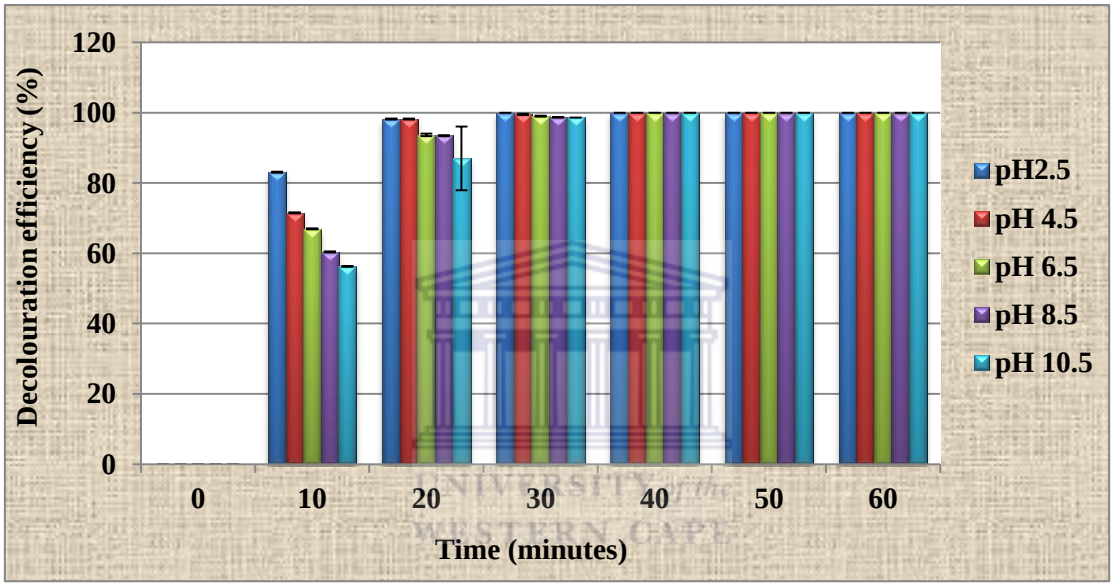

Figure 4-9: Effect of pH on decolourization efficiency of MB, Varied parameter: pH (2.5 - 10.5) at the following experimental conditions: Applied voltage 25 V, Peak voltage 7.8 kV, MB concentration 5 mg/L, MB solution conductivity (20 to 5 mS/cm), air flow rate 3 L/min, air gap 2 mm, 0.5 mm silver electrode, 50 g/L of NaCl and contact time of 60 minutes, n = 2)

Figures 4-9 and 4-10 present the UV data based on the effect of pH variation on MB decolourization efficiency at the applied conditions. The results presented in Figure 4-9 show that, within 30 minutes under the applied conditions about 99.99% of MB colour removal was attained in all cases. In addition, results in Figure 4-10 below shows that within 20 minutes of the start of the experimental run, the colour percentage removal of MB decreased with the increased in solution pH with an optimum removal observed at pH between 2 and 4.

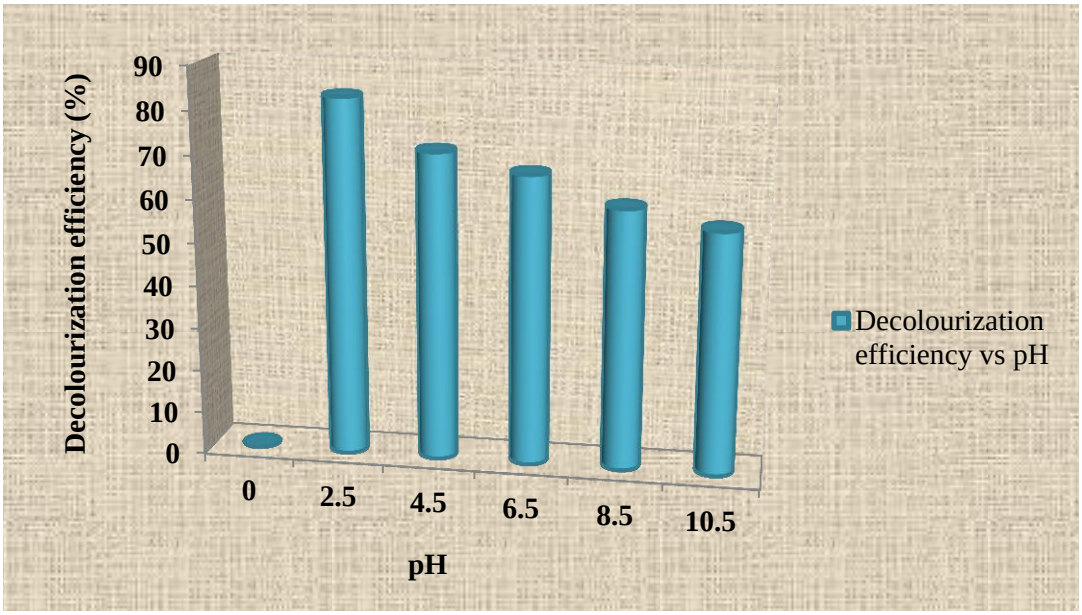

Figure 4-10: Effect of optimum pH on the decolourization efficiency of MB [experimental conditions: Applied voltage 25 V, Peak voltage 7.8 kV, MB concentration 5 mg/L, MB solution conductivity (0.02 to 0.09 mS/cm), MB volume 1500 mL, air flow rate 3 L/min, air gap 2 mm, 0.5 mm silver electrode, 50 g/L of NaCl and running time 20 minutes]

Figure 4-10 also confirmed that the best decolourization was accomplished at pH 2.5. This means that MB dye decolouration happened better in acidic conditions particularly at pH less than 5. During EHD experiments, the decolourization efficiency of MB increased with decrease in solution pH. In other words, MB decolourization efficiency was higher at low pH. This was mostly due to the presence of various nitrate and sulphate by-products resulting from air and the decomposition of MB by the free reactive radicals. The existence of these inorganic acidic species was proven by the nitrate and sulphate tests. Apart from this, other acidic organic residues such as carboxylic acids, etc. might also have evolved from the decomposition of MB dye in the DBD system. This was supported by the decrease in TOC of the pollutant and further confirmed by the FT-IR analysis. Hence, effective decolourization of MB dye using the EHD process is pH dependent. In addition, the few authors who have used the double cylindrical DBD reactor configuration for the decomposition of MB, not only did not use the same configuration as that of the present study but also they did not investigate the effect of pH on MB decolourization efficiency. Nevertheless, the effective discoloration of acidic dyes in EHDs was also reported in several research papers. For example, Sugiarto et al. (2003) investigated the effect of decolourization of several kinds of dyes using the pulsed plasma discharge in water. In

their work, it was found that the discoloration percentage removal increased in acidic conditions. Since the oxidation process is sensitive to solution pH, Ince et al. (1999) confirmed that dyes are more efficiently decolourized at low pH than high pH values. This could be explained by the fact that at a pH higher than 7, hydroxyl radicals are unselective and react easily with scavengers such as carbonate ions, thus reducing the efficiency of the oxidation process considerably. Carbonate ions as reported by Ince et al. (1997) result from the breakdown of the organic materials during the oxidation processes. Joshi et al. (2013) and Jiang et al. (2013), mentioned that the oxidative disconnection of organic substances derives from the action of powerful oxygen-based oxidizers such as $OH^{\bullet}$ and O^{-} (resulting from the conversion of $OH^{\bullet}$) on organic compounds. In this regards, O^{-} acts as a nucleophile and $OH^{\bullet}$ as an electrophile yielding diverse intermediates and thus follow distinct reaction pathways. The pH of the solution is a very crucial factor and its effect needs to be understood when working with wet chemistry. Chemical and physical plasma properties strongly affect solution pH of dyes during their plasma treatment. This idea was also supported by Thagard et al., (2009) who demonstrated that the formation of hydrogen peroxide in either gas phase or liquid phase depends on solution pH. Moreover, acid base equilibriums between various plasma species are also pH-dependent and can significantly obstruct degradation reactions of aqueous pollutants. The general trend depicted in the experimental results reported in literature is in conformity with that noticed in the current study, and shows that decolouration efficiency of organic pollutants such as dyes is mostly achieved in acidic conditions. However different optimal pH could be obtained according to plasma technologies employed. For instance Sugiarto et al. (2003) obtained an optimal pH of 3.5 during the oxidative decolouration of dyes by pulsed discharge plasma in water. They reported that the rate of decolouration at pH 3.5 was more or less three times faster than that at pH 10.3. Conversely, Sato et al. (2007) and Jiang et al. (2013) outlined that better removal efficiency of phenol was reached at pH 10.2 using a gas–liquid phase pulsed discharge plasma reactor. Based on the experimental results highlighted in literature and those of the actual study, the pH of dye solution remains an important parameter in wastewater treatment; hence irrespective of the type of discharge and reactor configuration, the decomposition of dyes in plasma reactors is a pH dependent process.

4.3.2 Effect of solution conductivity on decolourization efficiency of MB

As for solution conductivity (SC), this parameter was varied from 5 to 20 mS/cm using NaOH and HNO_3 solutions at the applied conditions as described in section 3.3.1.6.2 of experimental procedures in chapter 3.The effect of conductivity which was varied from 5 to 20 mS/cm with successive increment of 5 mS/cm on the percentage MB colour removal at the applied conditions was measured. That is, absorbance, concentrations and removal percentage of MB samples were recorded at the applied conditions and the raw UV-vis data are presented in Appendix 9 -12. The UV-vis data was plotted and is presented in Figures 4-11 and 4-12 below.

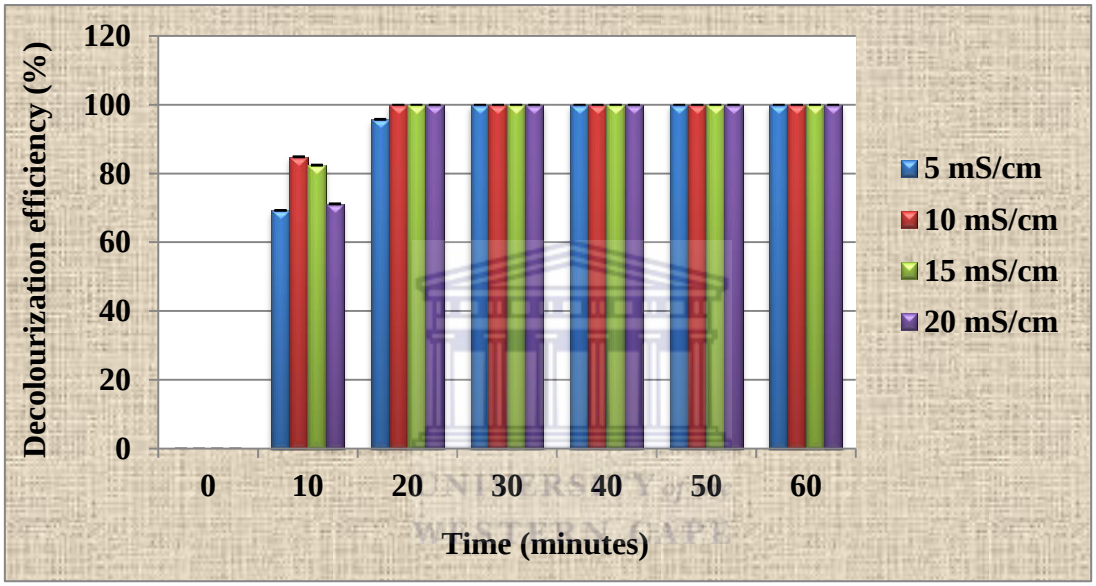

Figure 4-11: Solution conductivity vs. time during degradation of methylene blue using electrohydraulic discharge (experimental conditions: applied voltage 25 V, peak voltage 7.8 kV, MB concentration 5 mg/L, MB volume 1 500 mL, air flow rate 3 L/min, air gap 2 mm, solution, pH (in between 10 and 2), 50 g/L NaCl electrolyte, 0.5 mm silver electrode and contact time of 60 minutes, n = 2).

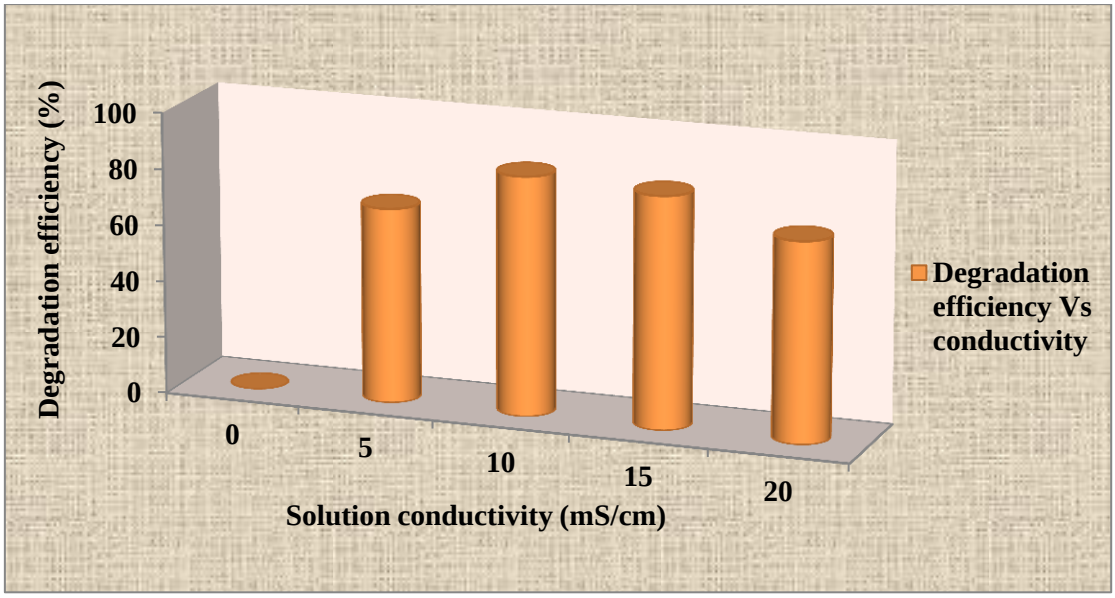

Figure 4-12: Effect of solution conductivity on decolouration of methylene blue using electrohydraulic discharge. Varied parameter: solution conductivity (5- 20 mS/cm) at the following experimental conditions: applied voltage 25 V, peak voltage 7.8 kV, MB concentration 5 mg/L, MB volume 1500 mL, air flow rate 3 L/min, air gap 2 mm, solution, pH (in between 10 and 2), 50 g/L NaCl electrolyte, 0.5 mm silver electrode and contact time of 60 minutes).

Figures 4-11 and 4-12 present the UV-vis results of the effect of solution conductivity on MB decolourization efficiency at the applied conditions. Results presented in Figures 4-11 shows that complete decolouration of MB dye occurred within 30 minutes under the applied conditions. It was then observed that up to 20 minutes of runtime, decolouration of MB increased with an increase of solution conductivity. However, the best decolouration percentage was achieved at an SC of 10 mS/cm. Since pH and electrical conductivity are inversely proportional, this implies that higher conductivity values led to low pH values. This therefore confirmed the trend observed in pH optimization which showed that good percentage removal was reached at low pH, that is an acidic medium. Generally, the concentration of a given solution is directly related to the concentration of hydrogen (pH). For acidic solutions, the lower the pH value, the higher the concentration of hydrogen ions. Based on these findings, it was evident that solution pH and conductivity are strongly related. The high solution conductivity and low pH are plausible due to the presence of inorganic salts by-products such as NO, NO_2, etc. in the solution and whose dissolution

leads to the formation of nitric, nitrous and peroxynitrous acids (Brisset et al., 2011; Magureanu et al., 2013). So these fluctuations between pH and solution conductivity were observed during DBD experiments on decolourization of MB. This was also observed by Reddy et al. (2013) in their study of reaction chains giving rise to the formation of intermediate organic and inorganic acids. The reactions pathway is presented below:

$^{*}e^{-} + O_2 \rightarrow 2\ ^{*}O + e^{-}$ …… (4.2)

$^{*}e^{-} + N_2 \rightarrow 2^{*}N + e^{-}$ …… (4.3)

$^{*}N + {}^{*}O \rightarrow NO$ …… (4.4)

$^{*}O + NO \rightarrow NO_2$ …… (4.5)

$NO_2 + {}^{\cdot}O \rightarrow HNO_3$ …… (4.6)

Nitrous oxides might have originated from air introduced into the system as it was earlier mentioned in literature. However, the rise in electrical conductivity might have been caused by the presence of H^+ and OH^- from the dissociation of water molecules as well as nitrate formation under the applied potential (Porter et al., 2009). Even if the effect of solution conductivity might have been covered with other types of electrical discharges, its influence on dyes decolourization in a double cylindrical DBD plasma reactor remains rare in literature. Yet, solution conductivity is also an important parameter as that of pH and others, that needs to be considered when dealing with plasma treatment of dyes.

4.3.3 The effect of air flow rate on MB decolourization efficiency

Aside from pH, electrical conductivity, and solution volume, the air flow rate is also a critical parameter in dye decolouration. So the effect of air flow rate on decolouration of MB was then studied as described in experimental procedure of section 3.3.1.6.3 and in Table 3-7. The UV-vis data of absorbance, concentration and discoloration efficiency of MB samples were recorded and presented in Appendices 13 -15. The UV-vis results of the effect of flow rate on MB decolouration were plotted and presented in Figure 4-13.

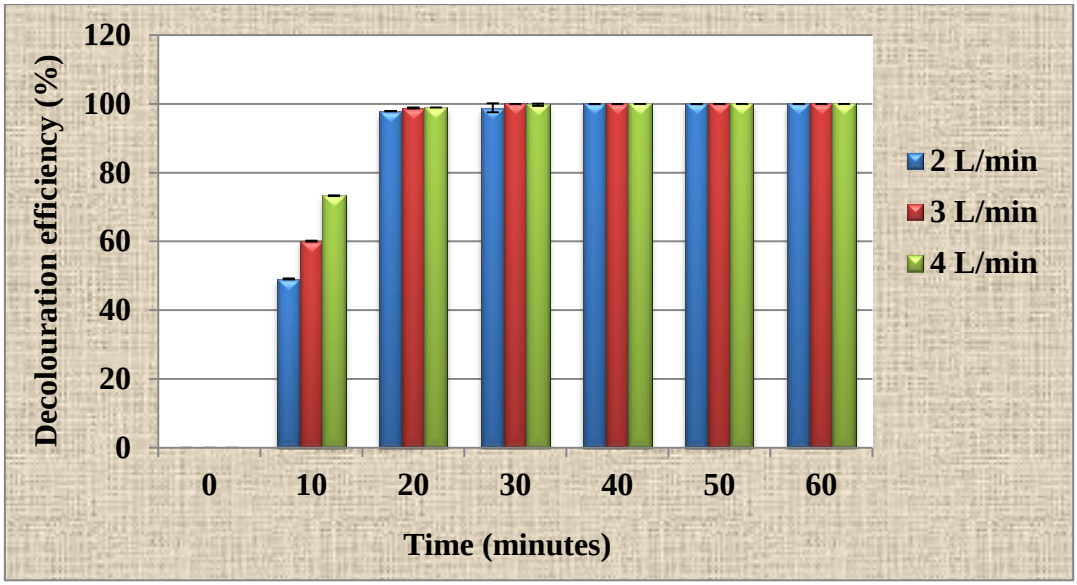

Figure 4-13: Effect of air flow rate on the degradation efficiency (experimental conditions: applied voltage 25V, peak voltage 7.8 kV, MB concentration 5 mg/L, solution pH (in between 6.04 and 6.64), MB solution conductivity (0.02 to 0.09 mS/cm), MB volume 1500 mL, 50 g/L NaCl electrolyte, air gap 2 mm, 0.5 mm silver electrode.

Figure 4-13 presents the UV-vis results of the effect of air flow rate on decolourization efficiency at the indicated conditions. Results presented in Figure 4-13 show that complete decolourization of MB occurred in the first 20 minutes of operation. This means that, perhaps after 10 minutes of experiment, the amount of oxidizing species produced in the DBD system was sufficient to decompose 5 mg/L MB at the applied conditions. Also, as seen in Figure 4-13, the trend between air flow rate and colour removal percentage of MB was well observed after 10 minutes of experiment whereby the rate of dye decolourization increased with an increase in air flow rate. Theoretically, at sea level, air contains approximately 20.95% of oxygen (O_2) and 78.08% of nitrogen (N_2) and small traces of other gases, (Naz et al., 2012). Except for the fact that oxygen has unpaired electrons, it also plays an important biological role as an oxidizing agent. Therefore, as more oxygen is provided, greater amounts of ozone are generated and by various chemical reactions, other active species such as hydroxyl radicals, ozone and hydrogen peroxide that facilitated dye decolourization were also produced.

Consequently, after 10 minutes, 49.2% and 60.14% of MB discolouration were respectively obtained at flow rates of 2 and 3 L/min. However, the maximum of 73.32% of MB colour removal was achieved with air flow rate above 3 L/min. After 20 minutes 100% dye removal was observed in the case of the slower flow rates but the trend was not

consistent, probably due to the residence time of gas bubbles in the liquid effluent. In addition, the trend observed at 10 minutes of experiment in Figure 4-13 was not consistent along the treatment time. For instance, after 30 minutes of EHD experiment, the results displayed above show that 99.999% of colour removal was achieved at 3 L/min compared to 98.78 and 99.96 at 2 L/min and 4 L/min airflow respectively. This was probably due to the fact that nitrogen, excessively present in air, might have been competing with oxygen atoms to form nitrogen based species such as NO, NO_2 N_2O_5, etc. instead of O_3 being generated in the air gap. Based on these results, and because 3 L/min was the air flow rate that fitted the actual DBD reactor vessel, all further experiments were performed using 3 L/min of air which was chosen as the optimum air flow rate value for all experiments. Also it was observed that when air flow rate was increased beyond 3 L/min, a lot of bubbles were formed leading to the solution being spilt and short-circuits occurring during electrohydraulic discharge. Apart from this, a sparking effect was also noticed which ultimately led to circuit shut down. As a consequence of this development, 3 L/min was chosen as an optimum air flow rate for testing the current reactor configuration. The limits of the current reactor configuration will need to be evaluated and improved up on to provide sufficient mixing and circulation of the produced ozone without affecting the electrical circuitry. Even if gas flow rate might be an important parameter in non-thermal plasma electrical discharges, air used as a feed gas in this study did not show a significant impact on MB decolourization because the trend observed after 10 minutes in Figure 4-13 was not uniform at all times during treatment process. Perhaps to overcome this limitation a pure gas like O_2 should be used as a feeding gas to directly generate ozone that is then bubbled into the polluted water.

4.3.4 The effect of MB volume and treatment time on the degradation efficiency

During the optimization of MB volume, the absorbance, concentrations and degradation efficiencies of MB samples were recorded at the applied conditions and the UV data are presented in Appendices 16 -18.

The UV-vis results obtained during the variation of dye volume with time were plotted and are presented in Figure 4-14 below.

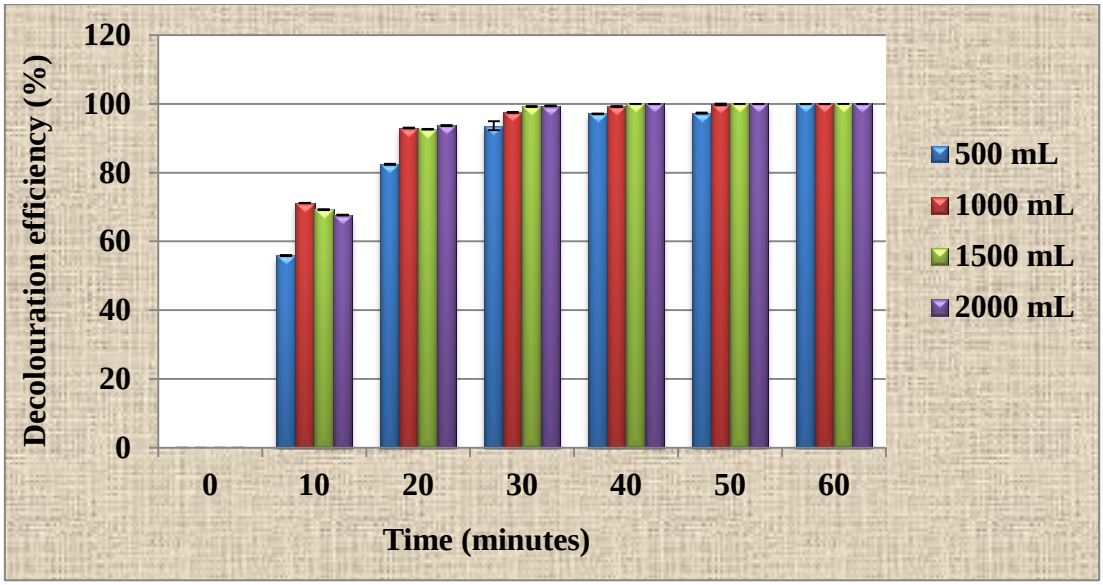

Figure 4-14: Effect of methylene blue volume on the degradation efficiency (experimental conditions: applied voltage 25V, peak voltage 7.8 kV, MB concentration 5 mg/L, solution pH(in between 6.04 and 6.64), MB solution conductivity (0.02 to 0.09 mS/cm), air flow rate 3 L/min, 50 g/L NaCl electrolyte, air gap 2 mm, silver electrode.

Figure 4-14 exhibits the UV-vis results of the effect of solution volume on MB discoloration with time at the applied conditions. The results presented in Figure 4-14 show that complete decolourization of MB was achieved within 40 minutes irrespective of the volume of 5 mg/L solution of methylene blue used. For example at 30 minutes experimental time, 92.7% of MB colour removal was achieved with a volume of 500 mL. A similar trend was observed at 40 and 50 minutes under the applied experimental conditions. 97.58%, 99.3% and 99.48% removal were obtained with 1 000 L, 1 500 L or 2 000 L volumes of 5 mg/L solution, respectively. However, the decomposition percentage varied and the decolourization efficiency of MB increased with an increase in solution volume. The reported trend could be justified by the fact that the 23 cm reactor tube was longer than the beaker, thus the generated UV radiations could not be effectively utilized as they were not completely focused in the solution for the smaller volumes used. Therefore increasing dye volume led to the absorption of more of the UV radiation generated, thus enhancing the MB colour removal percentage. In this experiment, 1 500 mL was chosen as the optimum volume over 2 000 mL because when air was passed through the system, an abundance of bubbles containing the reactive species were produced and had a longer path length in the larger volumes. However, excessive bubbles in the largest volumes used resulted in overloading of the system causing short- circuits.

Even though a slight rise of MB degradation efficiency was noticed, it might be hard to generalize that dye volume has a significant effect on the decolourization achieved except to comment that the system showed no reduction in efficiency for larger volumes of the simulated waste solution. This can also be verified by the small difference between MB colour percentages removals mentioned above. Because the single reactor tube was applied, bubbles containing reactive species escaped the system, and a strong odour of ozone arose around the working system which could not be quantified. It is likely that other reactor configurations that sparge the bubbles more finely into the fluid, and utilize the reactive species more effectively and higher volumes will show an effective maximum removal depending upon the applied conditions. Currently a new reactor system is being implemented at the University of the Western Cape by the Environmental and Nano Science research group that will recirculate the fluid allowing better contact between reactive species in the gaseous phase and the liquid effluent to be treated.

As for the impact of time on decomposition of MB dye, Figure 4-14 shows that at a particular dye volume, the discolouration efficiency of MB increased with increase in treatment time. For instance at 500 mL of MB dye, 55.9, 93.63 and 99.99 % of MB discolouration percentages were consecutively achieved after 10, 30 and 60 minutes. While, 71.15, 97.49 and 99.99 % of MB colour removal were respectively reached at a volume of 1 000 mL of MB. This was possibly due to better disclosure of MB solution to the micro discharges generated in the EHD system with time. This in turn probably led to higher concentrations of reactive species in the bulk solution.

A part from this, at 1 000 mL of MB for example, the progressive decolouration of MB observed after 10 minutes might have also been caused by the following aspects: the agitation of the solution by the magnetic stirrer (50 rpm), the irradiation of the bulk solution by the micro discharges and the dispersion of oxidizing reactive species in the polluted water, correspondingly. This was earlier confirmed by the gradual discolouration change observed in the DBD reactor with time in Figure 4-3.

Furthermore, the change in colour of MB solution during DBD experiment could be explained by the fact that the micro discharges primarily interact with water surface close to outer dielectric quartz tube while the rest of the solution remains blue. With the aid of continuous mixing using magnetic stirrer, the solution gradually turns from light yellow to deep green for concentration beyond 5 mg/L within 60 minutes of treatment time. As early mentioned in this section, regardless of the solution volume used, complete decolourization was achieved within 40 minutes. However, in most of the parameters

optimized in this study, total discolouration was reached within 30 minutes. Therefore 30 minutes was considered as the optimum time for the discoloration of MB in the actual DBD discharge. Even though the effect of solution volume and time on dye decomposition in a double cylindrical DBD plasma reactor presents little information in literature, these trends were at least highlighted by Joelle (2006) who used the single parallel DBD configurations presented in Figures 2-12 and 2-13.

On the whole, dye volume and the treatment time are also considerable parameters in the treatment of wastewater using DBD plasma system. Their impact on decomposition of dye contaminants showed that the volume of dye solution with respect to the trend observed in this study slightly affects MB discolouration percentage and depends on the reactor scale. The optimum volume chosen for the current DBD configuration was 3 L/min and was used in all EHD experiments. On the other hand, the decolourization of dye in DBD plasma reactor is a time dependent process. Therefore, a prolonged treatment time results in great decolourization of the pollutant. The optimum contact time for the DBD system was 30 minutes.

4.4 OPTIMIZATION ELECTRICAL PARAMETER

Electrical parameters assessed in the EHD system involved voltage, current, electrode type and electrode size. Their impacts on MB degradation were evaluated individually at different applied conditions.

4.4.1 Effect of applied voltage on degradation efficiency of MB

The effect of the applied voltage on decolourization efficiency of Methylene blue was obtained by varying the voltage through 20 V, 22 V and 25 V while the rest of the variables were kept constant. The experimental procedure was earlier given in section 3.3.1.3.4 and in Table 3-8 of chapter three. The absorbance and concentrations of MB solutions sampled within 60 minutes as well as their corresponding degradation efficiency were respectively recorded at the applied conditions and the UV-vis raw data of absorbance, concentrations and decolourization efficiency are presented in Appendices 19-21. The effect of the applied voltage on decolourization efficiency of Methylene blue obtained from the UV data is shown in Figure 4-15. The applied voltage (V) is the value read on the power supply whereby the peak voltage (kV) is the corresponding value

delivered by the step up transformer. However, in this study the applied voltage values (V) were chosen and were mostly used in the recorded data and for plotting data.

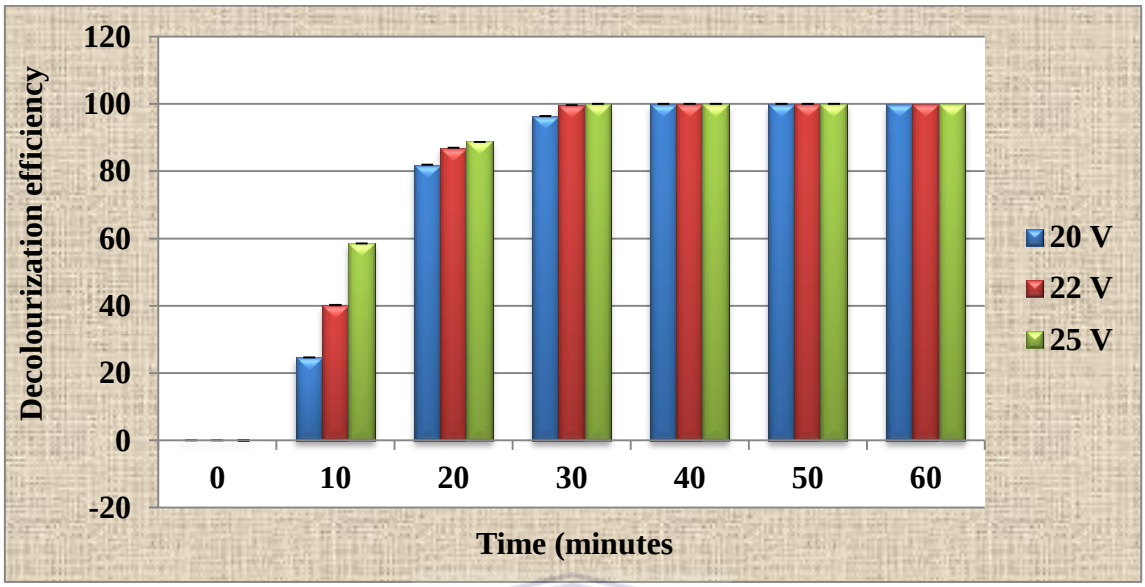

Figure 4-15: Effect of applied voltage on the degradation efficiency (experimental conditions: MB concentration 5 mg/L, solution pH (in between 6.04 and 6.64), MB solution conductivity (0.02 to 0.09 mS/cm), air gap 2 mm, air flow rate 3 L/min, dye volume 1500 mL, 50 g/L NaCl electrolyte, 0.5 mm silver electrode and sampling interval of 60 minutes)

Figure 4-15 exhibits the UV- vis data showing the impact of the applied voltage on MB discolouration efficiency at the indicated conditions. Experimental results shown in Figure 4-15 demonstrate that after 30 minutes under the applied experimental conditions, complete decolourization of MB was achieved at a voltage of 22 V and 25 V. This probably implies that after 30 minutes at voltages of 22 and 25 V, there was already enough oxidizing species such as $OH^{\cdot}$ radicals diffused in the bulk that led to the destruction of MB chromophoric form and hence to its discolouration. In addition, after 10 minutes under the applied experimental conditions, 24.62% of colour removal was reached using 20 V. Likewise 40.22% and 58.58% were achieved at 22 V and 25 V, respectively. This trend clearly shows that at a particular time, rate of decolourization of MB increased with an increase of the applied voltage. The same trend could also be observed after 20 minutes. Perhaps this was due to the fact that at high voltage (25 V), more high energetic particles were discharged into the conductive NaCl electrolyte, which successfully distributed them on the inner dielectric quartz tube. Usually, the highly energized electrons

are dispersed around the first dielectric quartz tube and are often accompanied with a strong electric field. Therefore, their contact with compressed air might have resulted in the generation of significant amounts of micro discharges, UV light and thus considerable quantity of reactive species in the air gap as well as in the contaminated wastewater. Consequently, this might have induced great discoloration percentage achieved at 25 V after 30 minutes. For this reason, 25 V was chosen as the optimum voltage and was used in all EHD experiments. Even if the trend between the applied voltage and discolouration percentage of MB dye in a double cylindrical DBD plasma reactor presents little information in literature, the behaviour of the applied voltage on decolouration efficiency of organic pollutants was observed and confirmed by other researchers using corona type electrical discharge. Gupta (2007) demonstrated that the increase of the anode voltage has two significant effects on the streamer generated in corona electrohydraulic discharge. On one hand, their study proved that streamer length increases with voltage increase. In this scenario, Gupta evaluated the streamer length by increasing the pulse voltage stepwise above the corona onset voltage. It was found that from 20 kV and above, the length of streamer increased with an increase in anode voltage. On the other hand, he confirmed that apart from the streamer length, the increase of the applied voltage might also increase the number of streamers in the discharge channel and hence resulting in high amount of free reactive species in the solution being treated. So based on electrical discharge and the type of configuration used, Gupta (2007) study is quite different from the present one, but the impact of voltage increase on the rate of decolouration of contaminant remains the same: the production of important quantity of free radicals that destroy the pollutant. Thus, from the discussion above, the applied voltage has an impact on dye discoloration percentage. The decolourization percentage of MB dye therefore increases with increase in the applied voltage due to successful transmission of highly energised electrons around the inner dielectric, which then leads to the generation of significant amounts of micro discharges, free active species as well as the UV light in the DBD system. Based on this, the optimum voltage for the actual DBD was 25 V corresponding to a peak voltage of 7.8 kV.

4.4.2 The effect of electrode type on MB percentage removal

In this section, the effect of electrode material on MB decolouration efficiency was investigated by varying the type of the electrode (copper, silver or stainless steel) at a fixed length of 25 cm and diameter of 0.5 mm. The experimental procedure is provided in

section 3.3.1.7.2 and was summarized in Table 3-8. It should be noted that the electrodes were housed in the inner electrode compartment and submerged in a NaCl solution of 50 g/L.

The UV-vis data of absorbance, concentrations and decolouration efficiencies of MB samples obtained during EHD experiments were recorded at the applied conditions and the raw data are presented in Appendices 22-24.

The UV-vis results based on the effect of the metal type used for the electrodes in MB decolouration efficiency were plotted and are presented in Figure 4-16 below.

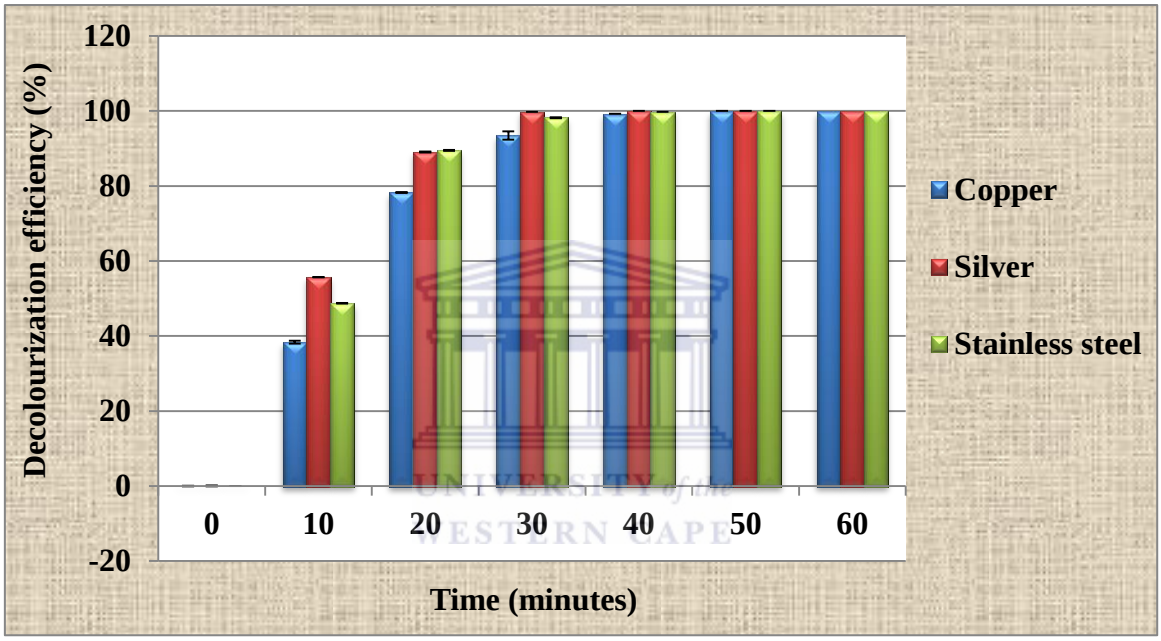

Figure 4-16: Effect of electrode material on MB decolourization efficiency. Varied parameter: copper, silver and stainless steel electrodes. Fixed experimental conditions: MB concentration 5 mg/L, solution pH (in between 6.04 and 6.64), MB solution conductivity (0.02 to 0.09 mS/cm), applied voltage 25 V, peak voltage 7.8 kV, air flow rate 3 L/min, dye volume 1500 ml, air gap 2 mm 50 g/L NaCl electrolyte and sampling at 10 min interval over 60 minutes.

Figure 4-16 displays the UV-vis results on the effect of electrode type immersed in NaCl electrolyte in the inner tube compartment of the DBD reactor on MB decolouration efficiency as earlier indicated in the experimental set up shown in Figure 3-5.

From the results presented in Figure 4-16, it was noted that for all three types of electrodes, decolouration of MB reached 99.84% after 30 minutes, and was complete after

40 minutes of duration of the DBD experiment. However, about 55.8% of colour removal of MB was achieved with the silver electrode, after 10 minutes under the applied conditions compared to 38.3% and 48.8%, obtained with copper and stainless steel electrodes respectively. The most rapid and highest methylene blue decomposition was achieved with the silver electrode. Thus the composition of electrode has an impact on MB colour removal percentage. This may be due to the modification of physical and chemical properties by the electrode materials during DBD experiments.

In addition to this, after a few experimental runs (10 series of DBD experiments), it was observed that copper and stainless steel electrodes corroded while the silver electrode was still in good condition but later corroded after 20 DBD experiments. Therefore, based on the durability and MB colour removal percentage, the silver wire was chosen as the optimum electrode material for the current DBD system.

Since copper, silver and stainless steel electrodes visibly corroded differently during DBD experiments in this study, electrode erosion was examined using Scanning Electron Microscopy (SEM). Both unused and used copper, silver and stainless steel electrodes were used as samples. One specific aspect: the tip (edge) of the electrode was taken into account to visualise the morphology of sample electrodes collected after 20 EHD experiments and images obtained from HRSEM are presented in Figures 4-17, 4-18 and 4-19.

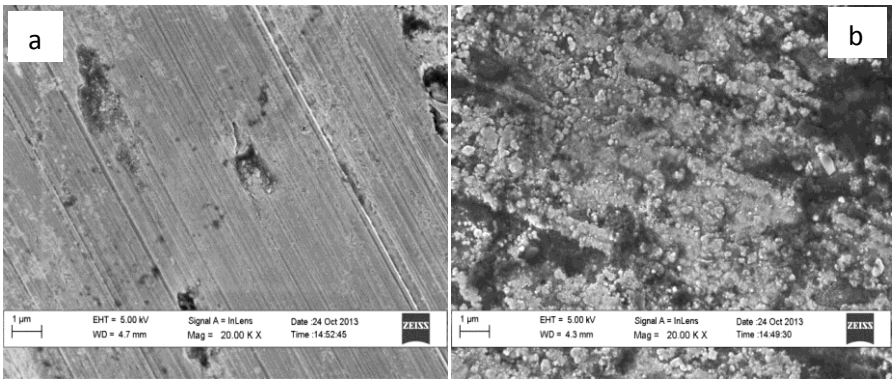

Figure 4-17: SEM images of unused (a) and used (b) copper electrode taken on surface of electrode after 10 cycles of EHD experiments.

.

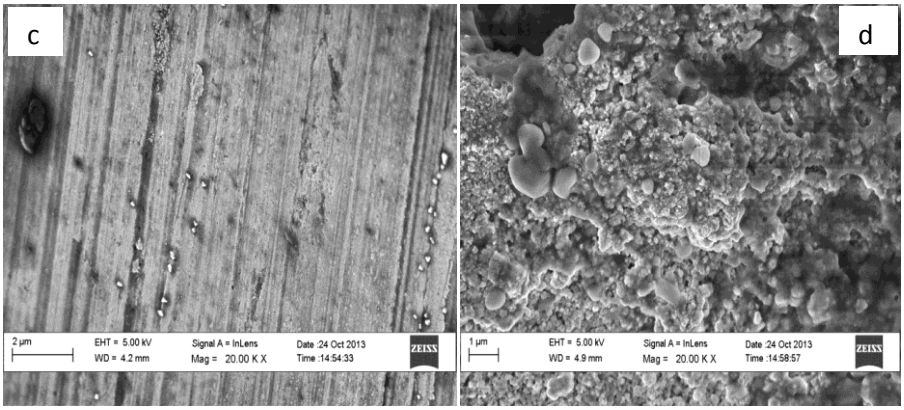

Figure 4-18: Morphology of unused (c) and used (d) silver electrodes taken on surface of electrode after 20 cycles of EHD experiments.

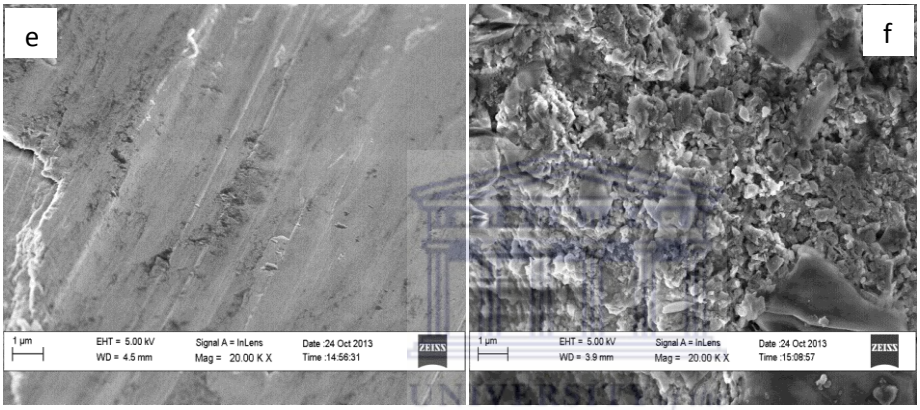

Figure 4-19: Morphology of unused (e) and used (f) stainless steel electrode taken on surface of electrode after 10 cycles of EHD experiments.

Based on results presented in Figures 4-17, 4-18 and 4-19, the physical appearance of electrodes surface showed a significant difference between unused (4-17 a, 4-18 c and 4-19 e) and used (4-17b, 4-18 d and 4-19 f) electrodes. Unused (4-17 a, 4-18 c and 4-19 e) copper, silver and stainless steel electrode which corroded during the electrohydraulic discharge experiment respectively exhibited smooth and uniform morphology before use. Used electrodes showed a corroded and roughened surface. In addition, the morphology of the utilized electrodes showed that the silver electrode corroded the least, followed by stainless steel whereas copper corroded considerably. The corrosion of the different electrodes could be that at the anode, the corrosion of copper was perhaps due to its gradual oxidation (dissolution) in the aqueous NaCl electrolyte solution in the inner tube compartment as shown in Equations 4.7 and 4.8 below.

$Cu\ (s) \rightarrow Cu^{2+}\ (aq) + 2\ e^{-}$ (oxidation)……. (4.7)

$Cu\ (s) + 2\ Cl^{-} \rightarrow CuCl_2\ (s) + 2e^{-}$ …… (4.8)

Not only does the copper become unstable by losing 2 electrons, but also the copper (II) chloride formed ($CuCl_2$) absorbs moisture (impurities) and its accumulation in the aqueous NaCl possibly induced further rapid corrosion of the copper electrode immersed in NaCl electrolyte in the inner tube compartment. These facts eventually might have led to the short life time of the copper electrode during the EHD experiment.

As for stainless steel electrode, it is important to mention that even if stainless steel is used as electrode in a few cases, it is a complicated alloy. Its electrochemical reactions in salt water are not clear. In terms of its chemical composition, stainless steel mainly consists of chromium oxide on the surface of the steel (Asaduzzaman et al., 2011). This layer is probably formed in oxidative conditions. In that case the oxidation of chromium involves the removal of 3 or more electrons from its valance shell, making it more unstable and hence it readily corrodes as shown in Equation (4.9) below:

$Cr\ (s) \rightarrow Cr^{3+}\ (aq) + 3\ e^{-}$ (oxidation)…… (4.9)

In contrast, silver electrode (metal) from its composition is very stable and non-toxic and can be used with saturated saline solutions such as KCl, NaCl, and AgCl etc. So the chemistry of Ag electrode in NaCl electrolyte in the inner quartz tube compartment can be explained in two different ways. First, at the anode, Ag wire is oxidized and therefore donates an electron and becomes ionised according to reaction Equation (4.10).

$Ag \rightarrow Ag^{+} + e^{-}$ (oxidation) ……. (4.10)

Thereafter, the chloride ion resulting from the dissociation of NaCl in water, reacts with silver to form not only stable silver chloride (AgCl) but releases an electron as shown in equation (4.11)

$Ag\ (s) + Cl^{-}\ (aq) \rightarrow AgCl\ (s) + e^{-}$…….. (4.11)

In Equations 4.9 and 4.10 above as can be noted in both cases, the reaction of silver is a source of free energised electrons which freely circulate in NaCl electrolyte solution contained in the inner tube compartment. Since the quartz dielectric tube has been proved to conduct current better, the free energized electrons are then dispersed on the inner tube. Their continuous and random motions result in high electric and magnetic fields on the surface of the inner dielectric quartz tube. The interaction of compressed air with energetic electrons present in strong electric and magnetic fields results in the production of significant amounts of free radicals in the air gap which are further bubbled into the bulk as explained in section 5.1.1.2. This probably induced greater decolouration of MB dye compared to copper and stainless steel. There is a very little piece of information available in literature about the effects of electrode materials on dye removal using double cylindrical DBD plasma reactor as well as their chemical behaviour during DBD experiment. However, some authors mentioned the causes responsible for electrode deterioration in other types of electrical discharges, mainly corona electrohydraulic discharge. Lasagni et al. (2004) supported that the mixture of complex electrode erosion events such as particle ejection, vaporisation and sputtering could be responsible for electrode damage during electrical discharge experiments. In addition, Shiki et al. (2007) highlighted that the performance and lifetime of the electrodes could dramatically be limited by electrode corrosion caused by erosion events resulting from interactions of electrical discharges within the surface of the electrodes. Similarly, this was also confirmed by Hayes et al. (2013) who observed that the generated plasma on the needle electrodes resulted in shortening caused by erosion mechanisms which are in conformity with the short circuits observed in the current EHD system. So in the research conducted by Shiki et al. (2007), it was advised that electrode decomposition in electrical discharge could be avoided by working at low frequency by applying a reasonable voltage and reducing air flow rate into the system and/or rather using pure oxygen as gas than air. Their advice could be used to minimize the electrode corrosion in future.

Even though the cause of electrode corrosion during the electrohydraulic discharge process was attributed to particle ejection, vaporisation and sputtering (Lasagni et al., 2004), the erosion of these wires could also result from their physical properties such as electrical conductivity and its reciprocal, electrical resistivity (Matijasevic and Brandt, 1998). The physical properties of electrode materials such as copper, silver and stainless steel used as anodes electrode in this research were proposed by Matijasevic and Brandt (1998) and are presented in Table 4-5.

Table 4-5: Electrical properties of copper, silver metals and stainless steel conductive alloy

Material	Thermal conductivity [W/m-K]	Resistivity [μΩ-cm] at 20 ^{0}C
Copper	397	1.68
Silver	429	1.587
Stainless steel	304	72

Source: Matijasevic and Brandt (1998).

In fact, electrical conductivity as defined by Brandt and colleague is the product of the number of charge carriers n, the charge e, and the mobility of the charge carrier μ (Equation 4.12).

$K = n.e.\mu$ …… (4.12)

So from the equation above, electrical conductivity of electronic materials can result in the change of their physical properties and thus impacting results obtained during their application. In this case, Table 4-5 shows that the thermal conductivity of silver, 429 W/m-K is superior to that of copper 329 W/m-K 7 and stainless steel 304 W/m-K, respectively. Since electrical conduction is characterised by the circulation or transportation of electric charges (carried by electrons, electron holes and ions) in the presence of an electric field (Matijasevic and Brandt, 1998), therefore a higher thermal conduction implies an important circulation of electrical charges, thus a significant electrical conductivity. Consequently silver has the highest thermal conductivity, therefore the highest electrical conductivity compared to copper and stainless steel respectively, and this explanation correlates with observations in this study during its application compared to copper and stainless steel electrodes. Hence these theoretical results corroborate with those experimentally obtained in the current study. However, the reasons behind electrode performance and their corrosion in the actual study are typically evident as clearly shown in this section by chemical reaction in Equations 4-7 to 4-11.

Conclusively, because silver electrode corroded the least in the present study, after a prolonged use compared to copper and stainless steel, silver was then considered as the optimum electrode type for the actual DBD system and was thus used to optimize the current DBD system. Based on the limitations observed during DBD experiments, the

choice of a suitable electrode would probably depend on the type of electrolyte chemicals and reactor configurations used.

4.4.3 Effect of electrode diameter on MB discolouration percentage

As shown in the previous section, the silver electrode was chosen as the optimum electrode for the actual EHD system. So to examine the effect of electrode diameter on MB discolouration percentage, the silver electrode was varied in size between 0.5 and 1.5 mm using the length of 25 cm (0.5 mm × 25 cm; 1.5 mm × 25 cm) at the applied conditions. The 0.5 and 1.5 mm radius were used because the silver electrode was difficult to obtain in various other sizes in the market. The experimental procedure was earlier presented in section 3.3.1.7.3 and in Table 3.8. Note that the electrode was still in the NaCl solution in the inner compartment of the DBD reactor tube.

Absorbance, concentrations and degradation efficiencies of MB samples were recorded during experiment at the applied conditions and the UV-vis raw data are shown in Appendices 24 - 27. The UV-vis outcomes showing the impact of silver electrode diameter on MB colour removal percentage is presented in Figure 4-20 below.

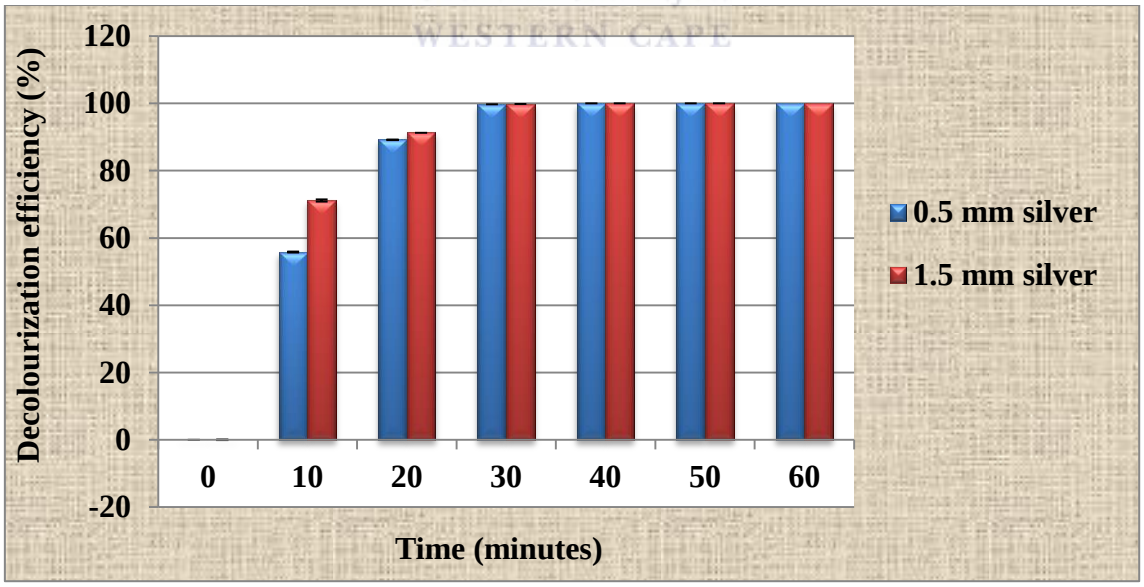

Figure 4-20: Effect of silver electrode diameter (0.5 or 1.5 mm) on the decolouration percentage of MB solution (experimental conditions: applied voltage 25, peak voltage 7.8 kV, MB concentration 5 mg/L, solution pH (in between 6.04 and 6.064), MB solution conductivity (0.02 to 0.09 mS/cm), dye volume 1500 mL, air gap 2 mm, air flow rate of 3 L/min, sampling at 10 minutes time intervals over of 60 minutes.

Figure 4-20 represents the UV-vis results based on the impact of silver electrode size on MB discoloration efficiency at the applied conditions. The results show that the percentage removal of MB increased with increasing anode radius and complete decolouration of MB dye was achieved within 30 minutes. After 10 minutes, 71.24% of colour removal was attained with the 1.5 mm diameter silver electrode whereas only 55.8% was achieved after 10 min with the 0.5 mm diameter silver electrode of the same length. A similar trend was observed after 20 minutes. Based on this observation, it could be inferred that 1.5 mm diameter silver electrode produces satisfactory results. Thus the diameter of electrode positively influenced the dye colour removal and thus 1.5 mm was taken as the optimum electrode radius in this study compared to 0.5 mm. The differences in the performance of the two electrode sizes could be explained in terms of surface area and applied voltage.

The results in Figure 4-20 show that great decolouration of MB was achieved with 1.5 mm silver electrode compared to 0.5 mm. The reasons behind these results are provided step wise in the following paragraphs.

Generally, the surface area (A) of a material is defined as the product of its length (L) and width (l) given as:

$A\ (cm^2 \text{ or } mm^2) = L \times l$…….. …….. (4.13)

This is often affected by the shape and size (thickness) of the electrode on contact and all conditions affect the surface area of the electrode on contact as mentioned in Gasanova (2013) who refers to the amount of current that is being delivered to a specific area (A) of that material.

However, the electrical power (P) flowing in most electric materials is directly proportional to the product of current (I) and voltage (V) as reported by Gasanova (2013) and shown in Equation (4.14).

$P = I \times V$…… ……. (4.14)

Thus, electrical current can be derived as the ratio of power over voltage as shown in Equation 4.15.

$I = \frac{P}{V}$ …….. (4.15)

The current density (I_d) of a specific conductive material is defined as the ratio of the applied current to specific surface area (A) and mathematically represented in Equation (4.16)

$I_d = \frac{I}{A}$ ……. (4.16)

Where, I is the electrical current flowing at specific area of the material.

So from Equation (4.16), it can be noted that current density is inversely proportional to the surface area. Thus, the higher the current density, the lower the surface area and vice versa. This means that the application of a high electrical current would induce a low voltage in Equation (4.15) and an electrode with a small surface area can accommodate high electrical current and a low voltage. In contrast, electrical materials with high surface area can accommodate low electrical current and high voltage. Based on this background, it is obvious that the electrode with high surface area and voltage induces greater decolouration efficiency compared to the one with a small surface area. Subsequently, the decolouration efficiency of MB was higher with 1.5 mm than 0.5 mm silver electrode in the present DBD system.

These results are in agreement with Nian Shi et al. (2009) who varied the screw electrode radius from 5 mm to 12 mm and the optimum screw anode radius was found to be 8 mm. This study has proved that electrode size has an effect on dye MB decolouration percentage. The high surface area of 1.5 mm silver electrode accommodates a small current and high voltage, hence resulting in higher decolourization percentage as compared to 0.5 mm silver electrode. Thus, the 1.5 mm silver electrode was chosen as the optimum anode for the present EHD system.

4.5 DECOLOURATION OF MB AT OPTIMUM CONDITIONS

In order to assess the efficacy of the DBD system after all parameters were optimized, a DBD experiment of MB decolouration was performed at optimum conditions presented in Table 4-6 below.

Table 4-6: Optimum conditions achieved during optimization of the DBD system.

Parameters	Optimum
Applied voltage (V)	25
Peak voltage (kV)	7.8
MB concentration	5
Solution volume (mL)	1 500
Inlet air flow rate	3

(L/min)	
Silver electrode size (mm)	1.5
NaCl concentration (g/L)	50
Air gap (mm)	2

The UV data of MB decomposition recorded at these optimum conditions are shown in Table 4-7. The results of MB decolouration at optimum conditions were plotted versus time and are presented in Figure 4-21.

Table 4-7: DBD experiment performed at optimum conditions (Applied voltage 25 V, peak voltage 7.8 kV, [MB] = 5 mg/L, pH 2.5, solution conductivity 10 mS/cm, V= 1500 mL, air flow rate 3 L/min, 1.5 mm silver electrode, 50 g/L NaCl electrolyte, air gap 2 mm and running time of 60 minutes).

Time (minutes)	Absorbance	Concentration (mg/L)	Decolourization %
0	1.144	5	0
10	0.170	1.473	70.54
20	0.001	0.0086	99.82
30	0.000	0.000	99.999

40	0.000	0.000	99.999
50	0.000	0.000	99.999
60	0.000	0.000	99.999

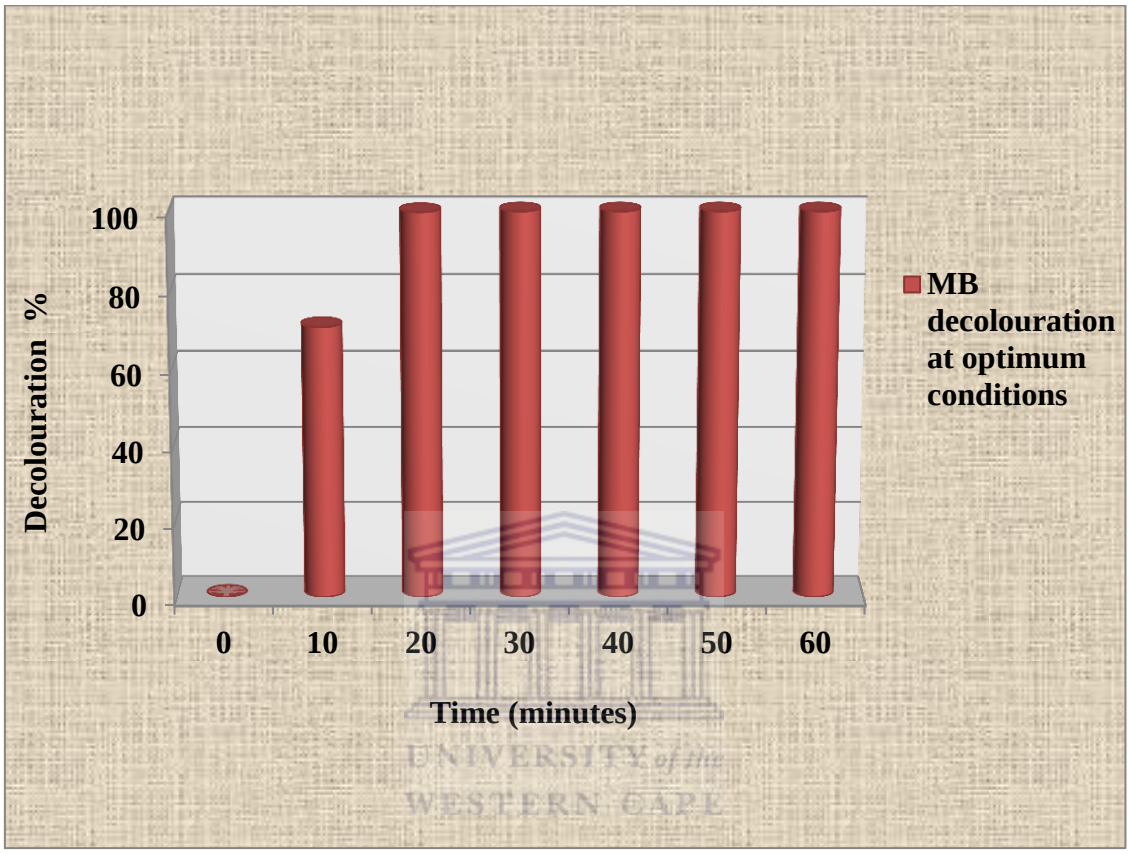

Figure 4-21: Decolourization efficiency of MB at the following optimum conditions: Applied voltage 25 V, peak voltage 7.8 kV, [MB] = 5 mg/L, pH 2.5, solution conductivity, 10 mS/cm, V= 1500 mL, air flow rate 3 L/min, 1.5 mm silver electrode, 50 g/L NaCl electrolyte, air gap 2 mm and running time of 60 minutes.

Figure 4-21 represents the plot of MB decolouration efficiency at optimum conditions. The results presented in Table 4-7 and Figure 4-21 show that at optimum conditions, MB decolourized progressively with increase in treatment time and complete decolourization was almost achieved within 20 minutes. It has been stated that MB dye is a chromophoric molecule as any coloured material contains a form responsible for its intense blue colour. Therefore the progressive decolourization of MB noticed during these experiments could be explained by the destruction of the chromoric form by free reactive species such as O_3, H_2O_2, etc. generated during plasma treatment. The reduction in treatment time from 30 to 20 minutes at which complete MB decolourization was achieved shows that the optimized

DBD system improved MB colour removal. Hence the decrease of treatment times for total decolouration of MB shows the better performance of the optimized DBD system which can further be used for treatment of water/wastewater effluents.

4.6 COMPARISON OF THE OPTIMIZED PARAMETERS

In order to deduce which factors were most effective on MB discoloration efficiency this subsection therefore focuses on comparison of the optimized chemical, physical and electrical parameters.

4.6.1 Chemical parameters

To identify which chemical parameter was the most significant on MB decomposition, the colour percentage removal of MB achieved at optimum NaCl electrolyte concentration and that obtained at optimum MB concentration at their respective applied conditions as shown in Figures 4-3 and 4-7 were plotted vs time and are presented in Figure 4-22 below.

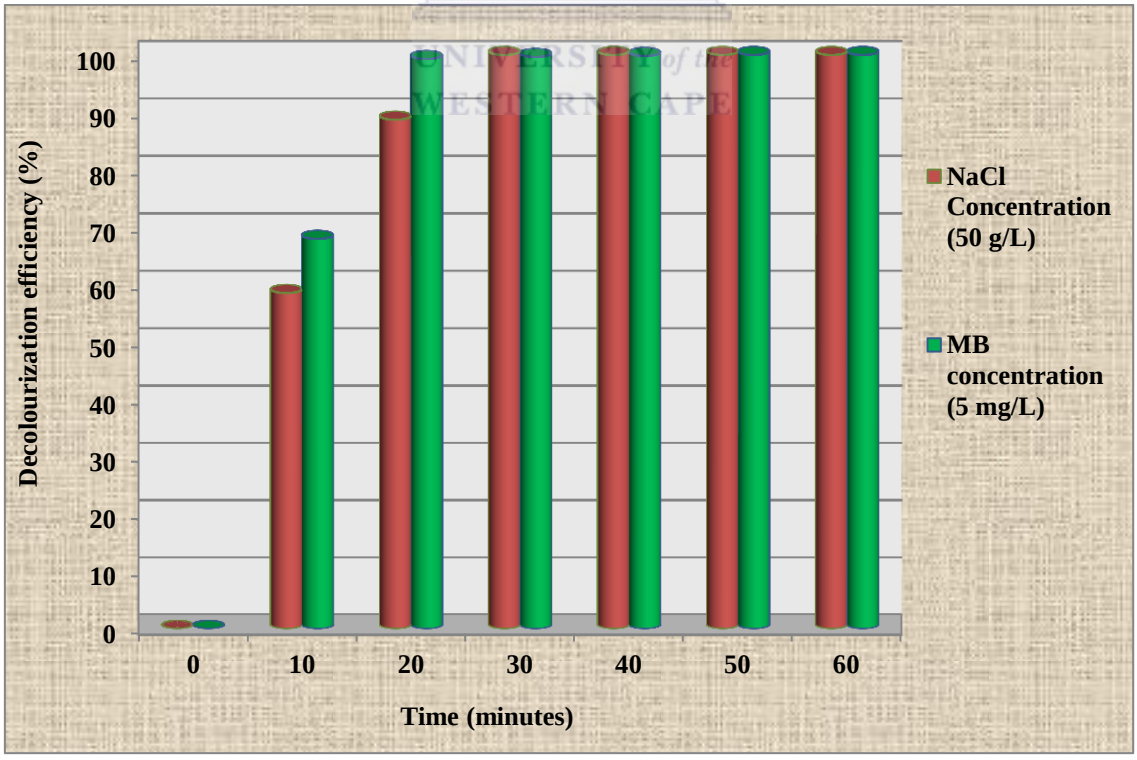

Figure 4-22: Comparison of decolouration achieved by either MB optimum concentration or NaCl electrolyte concentration at the applied conditions (Applied voltage 25 V, peak

voltage 7.8 kV, pH (in between 6.04 and 6.64), MB solution conductivity (0.02 to 0.09 mS/cm), MB volume 1500 mL, air flow rate 3 L/min, air gap 2 mm, 0.5 mm silver electrode and a run time of 60 minutes) as presented in Figure 4-3 and 4-7.

Figure 4-22 above presents the effect of optimum NaCl electrolyte concentration (50 g/L) and that of the optimum MB concentration (5 mg/L) on dye decolouration at the applied conditions. The results presented in Figure 4-22 show that in both cases, complete discolouration of MB was achieved within 30 minutes. However, after 10 minutes of treatment, the colour removal percentage of MB at optimum concentration is higher than the one achieved with optimum NaCl electrolyte concentration. That is 76.91 % of MB decolouration was achieved at 5mg/L MB compared to 58.58 % of MB colour removal obtained at 50 g/L of NaCl electrolyte. The same trend was still observed after 20 minutes. This implies that initial concentration had the greatest impact on MB discoloration compared to NaCl electrolyte concentration. Hence, MB initial concentration was the chemical parameter that significantly affected MB decolouration in the present DBD plasma system. This was previously justified in section 4.2.

4.6.2 Physical parameters

Apart from chemical parameters, the effect of optimum physical parameters on MB decolouration was also compared to verify which physical parameter was the most effective at their different applied conditions.

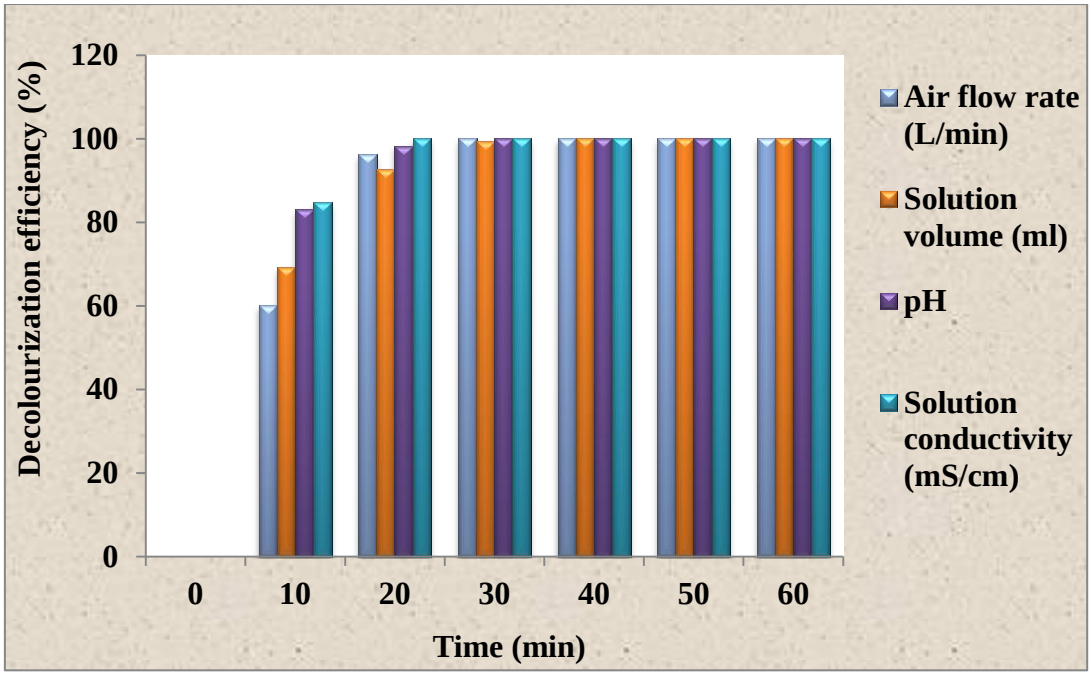

Figure 4-23: comparison of the optimum physical parameters obtained at the following experimental conditions: Applied voltage 25 V, peak voltage 7.8 kV, pH (in between 6.04 and 6.64), MB solution conductivity (0.02 to 0.09 mS/cm), MB volume 1500 mL, air flow rate 3 L/min, air gap 2 mm, 0.5 mm silver electrode)

Figure 4-23 displays the comparison of the optimum physical parameters namely: air flow rate, solution volume, and pH and solution conductivity on MB discoloration percentage achieved at their respective applied conditions. The results show that for all physical parameters, complete decolouration of MB was reached within the first 30 minutes of treatment. Nevertheless, within the first 20 minutes, solution conductivity and pH were more effective than the other parameters even though conductivity values were slightly higher than those of pH. Hence after 10 minutes of experiment, 84.84 % and 83.11 % of MB colour removal were respectively achieved at optimum solution conductivity of 10 mS/cm and optimum pH of 2.5 pH compared to 69.24 % obtained at optimum solution volume and 60.06 % at optimum air flow rate. A similar trend was also observed after 20 minutes. Hence, solution conductivity was the most effective physical parameter followed by solution pH.

4.6.3 Electrical parameters

Beyond physical parameters, the same evaluation was also conducted for optimum electrical parameters taken at in their respective conditions as shown in their optimization experimental procedures in Table 3-8 of chapter 3.

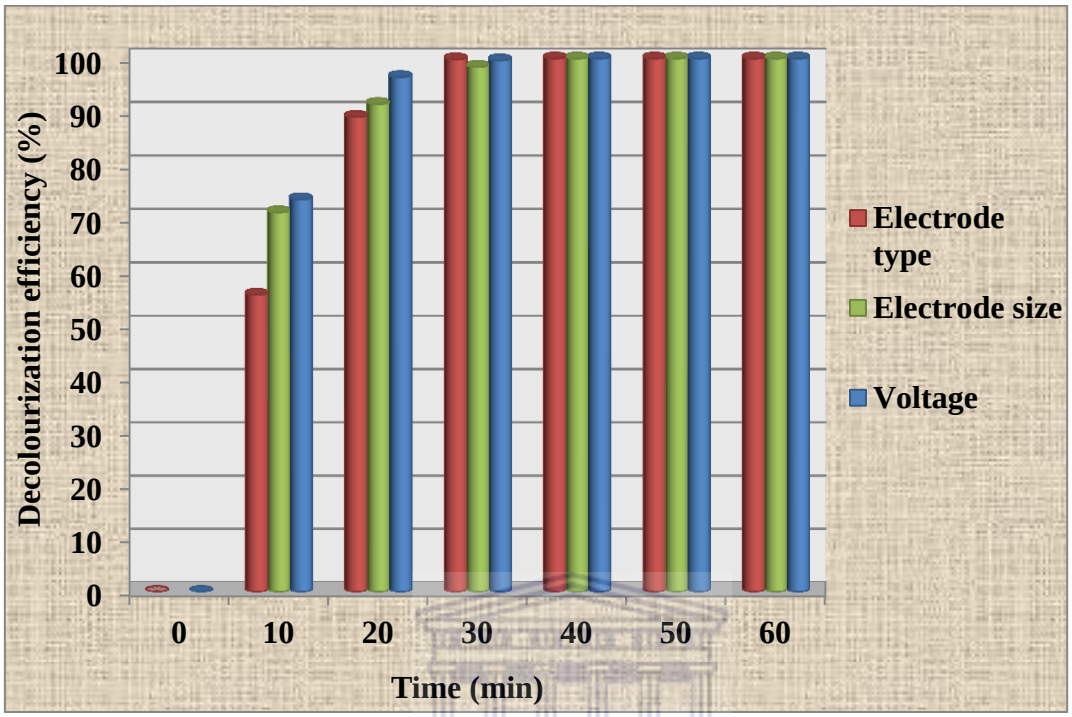

Figure 4-24: Comparison of the optimized electrical parameters recorded at their optimum conditions ((Applied voltage 25 V, peak voltage 7.8 kV, pH (in between 6.04 and 6.64), MB solution conductivity (0.02 to 0.09 mS/cm), MB volume 1500 mL, air flow rate 3 L/min, air gap 2 mm, 0.5 mm silver electrode and a run time of 60 minutes) as shown in experimental Table 3-8 of chapter 3.

Figure 4-24 exhibits the comparison of the optimized electrical parameters at their corresponding conditions as described in section 4.4.2 of this chapter. Results in Figure 4-24 show that the influence of all electrical parameters on MB colour removal was observed in the first 20 minutes of EHD experiments. However, after the first 10 minutes, the applied voltage showed a dominant impact on MB decolouration compared to the electrode size followed by electrode type. Conclusively, the applied voltage was the most influential electrical factor in MB decolouration process. The impact of the applied voltage on MB removal was earlier justified in section 4.4.1.

In total, after all chemical, physical and electrical parameters have been optimized in the present DBD plasma reactor; it was found that MB initial concentration, solution

conductivity proportional to the pH and the applied voltage were the most influencing parameters in the discoloration of MB dye.

4.7 SUMMARY OF CHAPTER FOUR

In this chapter, a full optimization of the DBD system was achieved. The optimized DBD system tested at optimum conditions showed a significant improvement in MB decolouration compared to normal conditions. However, MB initial concentration, solution conductivity and pH and the applied voltage were the most influencing parameters in the decolourization of MB dye at ambient conditions using the DBD plasma system. Hence the decomposition of MB in the present EHD system mostly depended on the initial concentration, solution conductivity and pH and on the applied voltage. The full summary of chapter 4 showing the optimized reactor configuration, chemical, physical and electrical parameters are presented in Tables 4-8, 4-9. The summary of DBD plasma treatment tested at optimum conditions is shown Table 4-10. Likewise, the reactive species responsible for MB decomposition were not identified in this chapter but their quantification and characterization of treated and untreated MB samples are provided in the next chapter.

Table 4-8: Summary of chapter four

Code	Varied parameters	Fixed parameters	Comment
	REACTOR CONFIGURATION:		
AG	Air gap (mm)	Applied voltage 25 V, peak voltage 7.8 kV, MB concentration 5 mg/L, MB volume 1500 mL, pH (in between 6.04 and 6.64), MB conductivity (0.02 to 0.09), air flow rate 3 L/min, 50 g/L NaCl, air gap 2 mm and 0.5 mm silver electrode and fixed time of 60 minutes.	This parameter significantly affected MB decolourization. In fact, MB decolourization increased with a decrease in air gap. Thus the optimum air gap was 2 mm.
AG1	2		
AG2	4		
AG3	6		
	CHEMICAL PARAMETERS:		
MBC	MB initial concentration (mg/L)	Applied voltage 25 V, peak voltage 7.8 kV, MB concentration 5 mg/L, MB volume 1 500 mL, pH (between 6.04 and 6.64), MB conductivity (0.02 to 0.09 mS/cm), air flow rate 3 L/min, 50 g/L NaCl, 0.5 mm silver electrode, air gap 2 mm and 0.5 mm silver electrode and fixed time of 60 minutes.	Between 0.5 and 5 mg/L, the final treated solution obtained after 60 minutes was clear. However, for concentration above 5 /mg/L, the colour of the final solution varied from light yellow to deep green. Thus the optimium concentration was 5 mg/L which was used in all experiments in this study.
Range	0.5 - 10		
EC	Electrolyte (NaCl) concentration (g/L)	Applied voltage 25 V, peak voltage 7.8 kV, MB concentration 5 mg/L, MB volume 1 500 mL, pH (in between 6.04 and 6.64), MB conductivity (0.02 to 0.09 mS/cm), air flow rate 3 L/min, 50 g/L NaCl, 0.5 mm silver electrode, air gap 2 mm and 0.5 mm silver electrode and fixed time of 60 minutes.	There was no increasing or decreasing trend observed during variation of NaCl concentration. Neverthless, the optimum NaCl concentration was 50 g/L. Perhaps the excess of NaCl may have promoted electrode corrosion.
EC1	10		
EC2	30		
EC3	50		
	ELECTRICAL PARAMETERS:		
AV	Applied voltage (V)	Solution volume 1500 mL, MB concentration 5 mg/L, MB pH (in between 6.04 and 6.64), MB conductivity (0.02 to 0.09), MB volume 1 500 mL, air flow rate 3 L/min, 50 g/L NaCl, air gap 2 mm and 0.5 mm silver electrode and fixed time of 60 minutes	At a particular sampling time, MB decolourization efficiency increased with increase in applied / peak voltage. The optimum voltage was 25 V (7.8 kV).
AV1	20		
AV2	22		
AV3	25		
ET	Electrode type	Applied voltage 25 V, peak voltage 7.8 kV, MB concentration 5 mg/L, MB conductivity (0.02 to 0.09 mS/cm), MB volume 1 500 mL, pH (in between 6.04 and 6.64), air flow rate 3 L/min, 50 g/L NaCl and air gap 2 mm, 0.5 mm electrode and fixed time of 60 minutes.	All three types of electrode corroded, However silver corroded after a large number of experiments (20 experiments) compared to copper and stainless steel which corroded after 10 to 15 experiments. Hence, silver was selected as the optimum electrode type for this system.
ET1	Copper		
ET2	Silver		
ET3	Stainless steel		
ES	Electrode size (mm)	Applied voltage 25 V, peak voltage 7.8 kV, MB concentration 5 mg/L, MB volume 1 500 mL, pH (in between 6.04 and 6.64), MB conductivity (0.02 to 0.09), air flow rate 3 L/min, 50 g/L NaCl, air gap 2 mm and silver electrode and fixed time of 60 minutes.	Within 60 minute of treatment time, decolourization of MB increased with increase in electrode diameter. So 1.5 mm silver electrode was recorded as the optimum electrode diameter.

Table 4-9: Summary of chapter four (cont.)

Code	Varied parameters	Fixed parameters	COMMENTS
	PHYSICAL PARAMETERS		
SP	Solution initial pH		
SP1	2.5	Applied voltage 25 V, peak voltage 7.8 kV, MB concentration 5 mg/L, MB solution conductivity (20 to 5 mS/cm), MB volume 1 500 mL, air flow rate 3 L/min, 50 g/L NaCl, 0.5 mm air gap 2 mm and silver electrode and fixed time of 60 minutes.	Complete decolourization of MB occurred within 30 minutes. MB decolourization percentage increased with a decrease in pH. Hence the optimum pH recorded was 2.5
SP2	4.5		
SP3	6.5		
SP4	8.5		
SP5	10.5		
SC	Solution initial conductivity (mS/cm)		
SC1	5	Applied voltage 25 V, peak voltage 7.8 kV, MB concentration 5 mg/L, MB conductivity (0.02 to 0.09 mS/cm), MB volume 1 500 mL, pH (in between 6.04 and 2), air flow rate 3 L/min, 50 g/L NaCl, air gap 2 mm and 0.5 mm silver electrode and fixed time of 60 minutes	A continuous trend was not observed when varying solution conductivity. However, the optimum solution conductivity was 10 mS/cm
SC2	10		
SC3	15		
SC4	20		
SV	Solution volume (mL)	Applied voltage 25 V, peak voltage 7.8 kV, MB concentration 5 mg/L, MB conductivity (0.02 to 0.09 mS/cm), MB volume 1 500 mL, pH (in between 6.04 and 6.64), air flow rate 3 L/min, 50 g/L NaCl, 0.5 mm silver electrode, air gap 2 mm and 0.5 mm silver electrode and fixed time of 60 minutes.	The decolourization of MB increased with increase in solution volume. At low solution volume, most of the UV generated in the EHD system were wasted and hence resulting in low decolourization efficiency. Neverthless, the optimum volume for this actual EHD reactor vessel was 1500 mL which was used for all experiments.
SV1	5		
SV2	10		
SV3	15		
SV4	20		
AF	Air flow rate (L/min)	Applied voltage 25 V, peak voltage 7.8 kV, MB concentration 5 mg/L, MB conductivity (0.02 to 0.09 mS/cm), MB volume 1 500 mL, pH (in between 6.04 and 6.64), 50 g/L NaCl, air gap 2 mm and 0.5 mm silver electrode and fixed time of 60 minutes	The colour removal efficiency of MB increased with increase in air air flow rate. But the optimum air flow corresponding to the capacity of the container used was 3 L/min.
AF1	2		
AF2	3		
AF3	4		
RT	Contact time (min)	Applied voltage 25 V, peak voltage 7.8 kV, MB concentration 5 mg/L, MB conductivity (0.02 to 0.09), MB volume 1 500 mL, pH (in between 6.04 and 6.64), 50 g/L NaCl, air gap 2 mm and 0.5 mm silver electrode and fixed time of 60 minutes.	Complete decolourization of MB mostly occurred wothin 30 minutes of the EHD experimental run. In this time scale, it was noticed that MB decolouration efficiency increased with increase in treatment time. So the optimum time recorded for this system remains 30/60 minutes.

Table 4-10: summary of chapter four (cont.)

DBD experiment performed at optimum conditions	Applied voltage 25 V, peak voltage 7.8 kV, MB volume 1 500 mL, pH 2.5, MB conductivity 20 mS/cm, air flow rate 3 L/min, 50 g/L NaCl and air gap 2 mm, 1.5 mm electrode and fixed time of 60 minutes.	Complete decolourization of MB was achieved within 20 minutes with 1.5 mm silver electrode compared to 0.5 mm when MB dye was totally decolourized within 30 minutes of EHD experiment.

CHAPTER FIVE: QUANTIFICACATION OF FREE REACTIVE SPECIES AND CHARACTERIZATION OF TREATED AND UNTREATED MB SAMPLES

5. INTRODUCTION

Although the current EHD system was proved to completely decolourize MB at 5 mg/L, this does not mean MB was also degraded and mineralized at that concentration. Therefore there was a need in this chapter to detect and quantify the free reactive species responsible for MB decomposition and investigate the degree of MB degradation at normal conditions.

5.1 DETECTION AND QUANTIFICATION OF FREE REACTIVE SPECIES IN THE BULK SOLUTION AT NORMAL EXPERIMENTAL CONDITIONS

This subsection outlines the results of two electrohydraulic discharge experiments that were carried out to quantify molecular free reactive species, mainly H_2O_2 and O_3 using Eisenberg and indigo methods, respectively. These reactive species were quantified every 10 minute of the EHD experiment at the following conditions: applied voltage 25 V, peak voltage 7.6 kV, air flow rate 3 L/min, air gap 2 mm and MB concentration 5 mg/L, MB volume 1 500 mL, 50 g/L NaCl electrolyte and 0.5 mm silver electrode as described in experimental procedures of section 3.4.1 and 3.4.2. In addition, energy density defined as the amount of energy (kWh) required to decompose 1 g of MB was also thought to be a crucial parameter and had to be investigated. In this case, the energy density of the decomposition of MB dye by these active species was calculated at the same experimental conditions as described in experimental section 3.5.

So, the absorbance of H_2O_2 at 405 nm ($\varepsilon = 750\ M^{-1}cm^{-1}$) and that of O_3 at 600 nm ($\varepsilon = 2\ 0000\ M^{-1}cm^{-1}$) measured during electrohydraulic discharge were reported in Appendix 28. By using de Beer's law, the concentrations of these two species were calculated and presented in Table 5-1 and their results were plotted in Figure 5-1. Simultaneously, the energy density and UV-vis data for the decomposition of MB were recorded in Table 5-2 and the results were plotted against time and shown in Figure 5-2.

Table 5-1: Concentrations of H_2O_2 and O_3 estimated using de Beer's law at the following experimental conditions: applied voltage 25 V, Peak voltage 7.8 kV, MB concentration 5 mg/L, solution pH (in between 6.04 and 6.64), MB solution conductivity (0.02 to 0.09 mS/cm), air flow rate 3 L/min, air gap 2 mm, MB volume 1500 mL, 50 g/L NaCl electrolyte, 0.5 mm silver electrode.

Time (minutes)	H_2O_2 concentration ($\times 10^{-7}$ mol/L)	O_3 concentration ($\times 10^{-7}$ mol/L)
0	0.00	0.00
10	6.05	0.00
20	4.76	0.00
30	5.40	0.50
40	4.32	0.00
50	3.67	1.15
60	2.80	0.65

Table 5-2: Absorbance of MB samples recorded during degradation process and energy density for the decomposition of MB at the following experimental conditions: MB concentration 5mg/L, solution pH (in between 6.04 and 6.64), MB solution conductivity (0.02 to 0.09 mS/cm), air flow rate 3 L/min, dye volume 1500 mL, 50 g/L NaCl electrolyte, 0.5 mm silver electrode, (The UV data are presented in Appendix 29).

Time (minutes)	**Absorbance**	**Concentration (mg/L)**	**Degradation efficiency (%)**	**Energy (g/kWh)**
0	0.911	5	0.00	0
10	0.399	3.457	30.86	0.087
20	0.135	1.20	76	0.0375
30	0.033	0.286	94.28	0.00733
40	0.007	0.060	98.8	0.0012
50	0.002	0.0173	99.65	0.000281
60	0.000	0.000	99.999	0.000

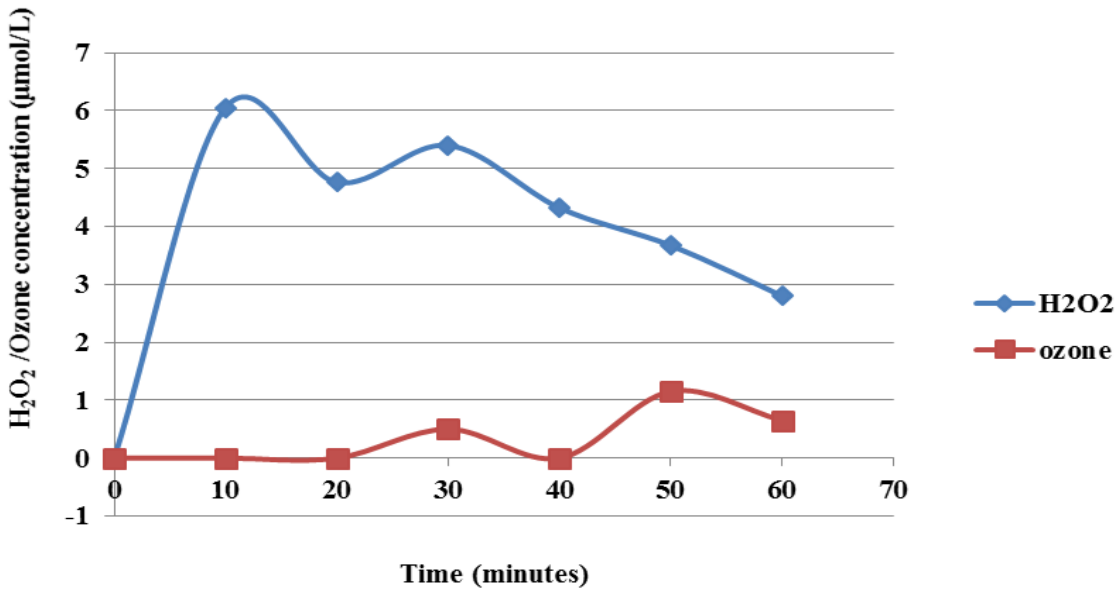

Figure 5-1: Evolution of hydrogen peroxide, ozone concentrations at normal conditions and energy density with time (experimental conditions: MB concentration 5 mg/L, solution pH (between 6.04 and 6.64), MB solution conductivity (0.02 to 0.09 mS/cm), dye volume 1500 mL, applied voltage 25 V, peak voltage 7.8 kV, air flow rate of 3 L/min, air gap 2 mm, 50 g/L NaCl electrolyte, 0.5 mm silver electrode.

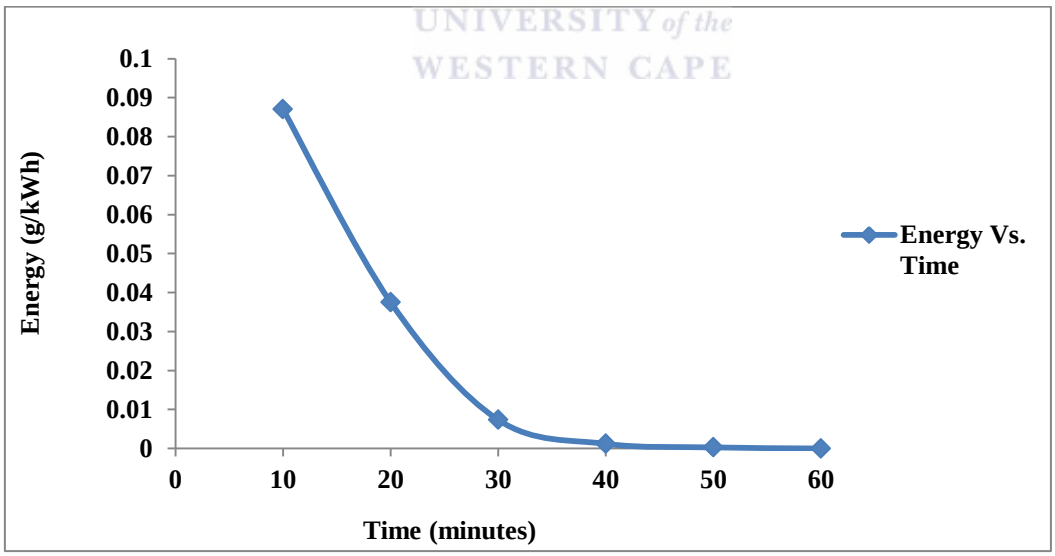

Figure 5-2: Evolution of energy density (g/ kWh) with time at the following experimental conditions: MB concentration 5 mg/L, solution pH (between 6.04 and 6.64), MB solution conductivity (0.02 to 0.09 mS/cm), dye volume 1500 mL, applied voltage 25 V, peak voltage 7.8 kV, air flow rate of 3 L/min, air gap 2 mm, 50 g/L NaCl electrolyte, 0.5 mm silver electrode.

Figure 5-1 presents the evolution of H_2O_2 and O_3 concentration with time at the specified experimental conditions. The results recorded in Table 5-1 and plotted in Figure 5-1 show that within the first twenty minutes, no significant amount of ozone was produced, whereas the concentration of hydrogen peroxide significantly increased and reached 6.05×10^{-7} mol/L after 10 minutes and then decreased to 4.76×10^{-7} mol/L after 20 minutes. This shows that hydrogen peroxide rather than ozone is the first species to be found in the solution.

The detection of H_2O_2 and the absence of O_3 in the first 20 minutes of EHD experiment need to be discussed. In fact, the oxidation potential of O_3 (2.1 V) is higher than that of hydrogen peroxide (1.8 V). This shows that O_3 is a stronger oxidizing agent than hydrogen peroxide. The fact that in the first 20 minutes of EHD experiment, only H_2O_2 was quantified while O_3 was not detected in the solution being treated was probably due to the direct generation H_2O_2 in the bulk solution as a dissolved liquid in the polluted water via various chemical reactions. Ozone, on the other hand, was generated as gas in the air gap and bubbled into the polluted water. So during its circulation in the air gap, ozone might have disappeared due to its shortlife time. In addition, the absence of ozone in the first 20 minutes of DBD experiment could have been due to the decrease of singlet atomic oxygen that was being consumed by nitrogen oxide (NO) in the system as shown in Equation 5.29. Apart from the fact that NO reacted with singlet atomic oxygen, Equation 5.30 shows that NO also reacted with ozone to yield NO_2 and O_2 in the DBD reactor. All these side reactions might have induced the decrease of ozone concentration during the first 20 minutes of DBD experiment. Furthermore, during its diffusion into the water being treated, O_3 might have escaped because the EHD configuration used in this study is an open batch system that is not sealed. Also, the evaporation of ozone was confirmed by an irritating smell during experiment even though the reaction was performed in the fume hood. Based on this fact, it is obvious that the amount of ozone in the solution was very low during the first 20 of the EHD experiment and hence could not be detected.

On the other hand, Figure 5-2 represents the evolution of energy density of the decomposition of MB with time during the DBD experiment at the indicated experimental conditions. The results presented in Figure 5-2 show that energy density of MB decolouration increased rapidly and reached 0.8 g/kWh in the first 10 minutes due to the presence of chromoric groups such as $(=N^{+}(CH_3)_2$ in MB molecular structure that needed to be destroyed. After 10 minutes, the energy density dropped off progressively to zero as the treatment time increased because the functional groups responsible for colour rise in

MB structure were no longer present. So, the high concentration of H_2O_2 (6.05×10^{-7} mol/L) after 10 minutes in the water being treated as observed in Figures 5-1, and the peak energy density (0.8 g/kWh) recorded in Figure 5-2 after 10 minutes were obtained at the experimental conditions and correlate in contact time. This correlation shows that the high concentration of H_2O_2 and the peak energy density were possibly responsible for the decomposition of MB that mostly occurred in the first 30 minutes of the EHD experiments. Indeed, active species such as hydroxyl radicals resulting from water molecule dissociation by UV light (see Equation 5.5) generated in the EHD system recombine to form hydrogen peroxide. Apart from this, hydro peroxide radicals ($HO_2^{\cdot}$) generated in the system via chemical processes induced in water might have reacted with atomic hydrogen ($H^{\cdot}$) to produce hydrogen peroxide. Hydrogen peroxide in turn is irradiated by UV light generated in the EHD system and gets dissociated into OH radicals (Equation 5.6) which unselectively decompose the MB dye. Details on chemical reactions responsible for these dissociation, recombination, ionization, reactions of reactive species in the DBD system are further explained in Equations 5-10 to 5-20.

Even though the observed energy trends was not discussed in previous research papers, it is important to mention that this is one of the critical points of energy behaviour during treatment of organic pollutant by non-thermal plasma that scientists should consider. Moreover, because experimental conditions including plasma reactor, voltage, power, dye concentration, gas flow rate, etc. used in previous research papers are different from those used in the present study, therefore the energy yield as highlighted by Reddy (2012), depends on the type of discharge reactor, initial concentration, and type of compound. So the benefit of non-thermal plasma technologies for wastewater treatment remains the use of a reasonable or small amount of energy, highlighting the cost effective applicability of this technique and its availability compared to other treatment methods.

In addition, the abrupt decay of energy density of MB decomposition is probably related to the decrease of H_2O_2 in the bulk solution. The progressive decline of H_2O_2 over time was perhaps the result of various chemical reactions between ionic species and peroxide in the bulk solution as described in Equations 5-3 to 5-8 of this section.

As for ozone, perhaps its amount formed during the first 20 minutes was not significant because the oxygen dissociated into singlet atomic oxygen which reaction might have taken time to be completed. According to Prendiville et al, (1986) the produced atomic

oxygen reacts with oxygen molecules to yield ozone as shown in the following chemical equations.

O_2 (DBD) → $O^{\cdot}$ + $O^{\cdot}$ ..... (5.1)

$O_2 + O^{\cdot} + \rightarrow O_3$ ..... (5.2)

Moreover, from 20 to 30 minutes in Figure 5-1, both the concentration of hydrogen peroxide and that of ozone fluctuated until these species reached 4.5×10^{-7} mol/L and 0.5×10^{-7} mol/L, respectively. The presence of these species after 30 minutes was followed by a slight decrease for 10 minutes. At 30 minutes, hydrogen peroxide and ozone might have reacted to generate hydroxyl radicals which are considered as powerful oxidants that attacked methylene blue dye and thus led to complete decolourization within 30 minutes. Beyond this time, the concentration of hydrogen peroxide decreased continuously while that of ozone continued to rise in a sinusoidal fashion. This could be explained by the fact that from 30 up to 60 minutes, hydrogen peroxide was being used to generate other active species that certainly contributed to the formation of hydroxyl radicals. Meanwhile the fluctuating production of ozone might be due to the recombination of those species as shown in chemical equations below suggested by Tarr (2003).

$2O_3 + H_2O_2 \rightarrow 2\ OH + 3O_2$ ..... (5.3)

$O_3 + h\nu + H_2O \rightarrow H_2O_2 + O_2$ ..... (5.4)

$H_2O_2 + h\nu \rightarrow 2\ OH$ ..... (5.5)

$O_3 + OH^- \rightarrow O_2^{\cdot -} + HO_2$ ..... (5.6)

$O_3 + HO_2^- \rightarrow HO^{\cdot} + O_2^{\cdot -} + O_2$ ..... (5.7)

$O_3 + O_2^{\cdot -} \rightarrow O_3^{\cdot -} + O_2$ ..... (5.8)

$O_3 + HO^{\cdot} \rightarrow HO_4^{\cdots}$ ..... (5.9)

Thus, during EHD experiment, UV light (as shown in Figure 5-4), H_2O_2 and O_3 are produced in the DBD plasma process. The shining UV-vis light in the DBD reactor is presented in Figure 5-3. However, their formation zones need to be clarified.

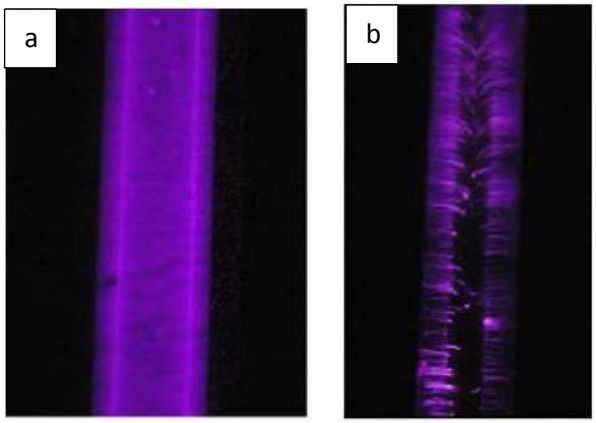

Figure 5-3: Photograph of the UV light produced in double dielectric barrier discharge with the aqueous electrolyte solution ((a) plus 1.5 mm silver rod and (b) silver rod alone in the inner tube compartment, used as the anode electrode) (Jo and Mok, 2009).

In order to understand where the UV light and some of the highlighted species in equations above are formed in the actual EHD system, a schematic double cylindrical DBD plasma reactor was drawn and presented in Figure 5-4 and the possible different reaction zones were subsequently described.

5.1.1 Discussion of the different zones and formation of the free active species

In the current work, the effect of plasma physics and chemistry on pollutant decomposition was examined by the action of the generated free active species on MB decolourization at ambient conditions. In this regards, a comprehensive schematic diagram of the present DBD plasma process was drawn and represented in Figure 5-4. The different reaction zones of the DBD system are indicated. The formation of UV radiations and the most common reactive species formed in this process is also discussed.

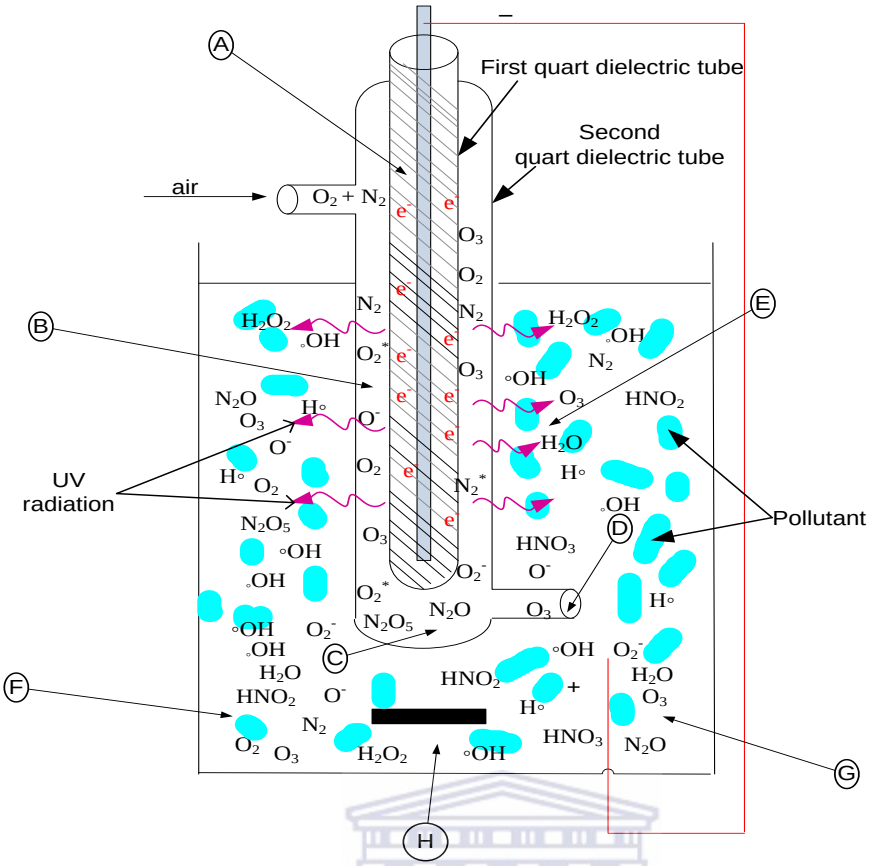

Figure 5-4: Different reaction zones (a-h) encountered in the electrohydraulic discharge (EHD) system.

5.1.1.1 ZONE (A)

In this region, electric discharge is a source of highly energized particles (electrons) whose motion gives rise to electric and magnetic fields. The electric field accelerates the particles while the magnetic field facilitates their deviation along the anode electrode and its curvature. Kogelschatz et al., (2003) reported that the continuous flow of current increases electron density and their motion around the anode rod and sometimes lead to their collision called electron avalanche. This magnifies the intensity of the electric and magnetic fields around the high voltage anode electrode. Lopez, (2008) and Kaunas, (2012) supported the theory that the use of the dielectric material (first quartz dielectric tube) as an insulator of the anode does not only minimize the amount of charges transported by a single micro discharge (micro plasma) but also permits the even distribution of the micro discharges around the anode surface area. So the anode rod and the first dielectric quartz tube together constitute one single and powered electrode that becomes a permanent source of high energy electrons.

5.1.1.2 ZONE (B)

Zone (b) also called discharge/air gap is the space between the two dielectrics (first and second quartz dielectrics tubes). In this region, the feeding gas (dry air from an air pump) is passed through and interacts with the highly powered anode electrode. Since air mostly consists of oxygen (O_2) and nitrogen (N_2), these molecules readily react with high energy electrons, generating not only UV light but also lead to the production of various types of oxygen and nitrogen based species such as atomic oxygen, ozone, peroxide ions, etc. formed via dissociation, ionization, recombination and associative chemical reactions, as shown in Equations (21 – 31), (Wilhelmus, 2000).

$O_2 + e^- \rightarrow 2O + e^-$ dissociation …… (5.10)

$O_2 + e^- \rightarrow O_2^+ + 2e^-$ ionization …….... (5.11)

$O_2 + e^- \rightarrow O_2^-$ attachment ……. (5.12)

$O_2 + e^- \rightarrow O^- + O$ dissociative attachment …… . (5.13)

$O_2 + O \rightarrow O_3$ association …… (5.14)

$N_2 + e^- \rightarrow 2N + e^-$ dissociation …… (5.15)

$N_2 + e^- \rightarrow N_2^+ + 2e^-$ ionization …… (5.16)

$N + O \rightarrow NO$ association …… (5.17)

$NO + O \rightarrow NO_2$ association …… (5.18)

$N_2^+ + O_2^- \rightarrow 2NO$ recombination …… (5.19)

$N_2 + O \rightarrow N_2O$ association ……... (5.20)

5.1.1.3 ZONE (C) AND (D)

Region C is also part of the discharge zone. This is the zone where oxygen, nitrogen and their resulting species produced in the plasma region are circulated through region C until they reach the outlet (zone D) of the double cylindrical DBD plasma reactor. At zone C, molecular and ionic species such as O_3, O_2, O_2^-, N_2, N_2O, etc. generated in regions B and C are bubbled into the bulk solution to induce oxidation of the target pollutant.

5.1.1.4 ZONE (H)

In this region of the bulk solution, a magnetic stirring bar of about 3 cm with stirring speed in the range 50 – 60 rpm was used to evenly disperse the reactive and active species from zone D into the contaminated solution.

5.1.1.5 ZONE (E)

Zone e represents the region next to the outer tube (second dielectric quartz tube). In this area of the EHD system, the UV radiations diffused in the bulk solution dissociate water molecules into OH radicals. The decomposition of H_2O molecules by UV light suggested by Wilhemus, (2003) is presented in Equations (5.32 to 5.34).

$H_2O + e^- \rightarrow OH^{\cdot} + H + e^-$ dissociation …… (5.21)

$H_2O + e^- \rightarrow H_2O^+ + 2e^-$ ionization …….. (5.22)

$H_2O^+ + H_2O \rightarrow H_3O^+ + OH^{\cdot}$ dissociation ……. (5.23)

In addition to this, the dissolved O_3 mostly in region E can also be irradiated by the UV light (Atkinson and Carter, 1984; Haugland, 1996) and consequently decomposed into H_2O_2 (See Equation (5.4). Furthermore, the shining UV also illuminates H_2O_2 and dissociates it into OH radicals (Equation (5.5) which non-selectively attack and mineralize the target contaminant into water and dissolved CO_2 (Jin-Oh and Mok, 2009).

$H_2O_2 + hv \rightarrow OH^{\cdot} + OH^{\cdot}$ ……..... (5.24)

5.1.1.6 ZONES (F) AND (G)

In these regions, the active species such as ozone and OH radicals, diffused in the bulk solution and destroy the pollutant. Moreover, in regions F and G, the free reactive species such as hydroxyl radicals resulting from various dissociation processes by UV light might recombine to form hydrogen peroxide (see Equation (5.25). Additionally, other various species such as nitrogen based species including NOx, formed via several chemical

reaction chains are also found in these DBD zones. The mechanism of formation of NOx species in DBD plasma system had earlier been proposed by Jin-Oh and Mok, (2009) and given in Equations 5.27- 5.36.

$OH^{\cdot} + OH^{\cdot} \rightarrow H_2O_2$…….. (5.25)

$O_2+e \rightarrow 2O$ ……. (5.26)

$N_2+O \rightarrow NO+N$ …….. (5.27)

$N_2+e \rightarrow 2N$…….. (5.28)

$N+O_2 \rightarrow NO+O^{\cdot}$…….. (5.29)

$NO+O^{\cdot} \rightarrow NO_2$…… (5.30)

$NO+O_3 \rightarrow NO_2+O_2$ …… (5.31)

$NO_2 + O_3 \rightarrow NO_3 + O_2$……. (5.32)

$NO_3 + NO_2 \rightarrow N_2O_5$……. (5.33)

Additionally, when the plasma fluid generated in zone B is transferred to the bulk solution, it is probable that the NO_2 coexisting with ozone is dissolved to form nitric acid and nitrous acid as shown in Equations (5.32 – 5.34). This was also supported by Jo and Mok (2009).

$2NO_2 + H_2O \rightarrow HNO_2 + HNO_3$…….. (5.34)

$HNO \rightarrow H^+ + NO^-$…… (5.35)

$HNO \rightarrow H^+ + NO^-$…… (5.36)

These common chemical reaction chains induced by nitrogen based species in plasma processes are summarized and presented in Figure 5-5. These nitrogen based impurities

were certainly responsible for the increase of the acidity of MB solution being treated as described in section 4.2.1.1 of chapter four.

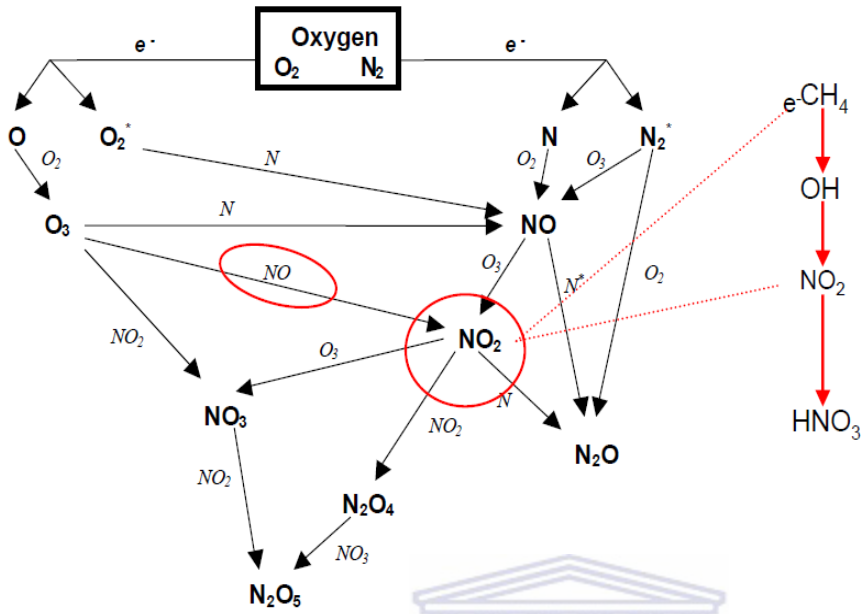

Figure 5-5: Plasma chemistry nitrogen based impurities (Lopez, 2008)

Furthermore, the optimization of a double cylindrical DBD plasma reactor system at ambient conditions using MB as a target compound has not been totally covered in literature. Nevertheless, a few researchers who have attempted to study the decomposition of MB by electrical discharges used different configurations as earlier discussed in literature review. The evolution of H_2O_2 concentration with time was slightly mentioned in previous work, while that of energy density for the decomposition of pollutant remains scarce. Hence, the fluctuation of H_2O_2 with time observed in this study is similar to the findings of the research conducted by Luís et al. (2011) even if the experimental conditions used in their studies are different from those of this investigation. In terms of energy density for the decomposition of MB assessed in this study, the high concentration of H_2O_2 attained after 10 minutes was responsible for the production of powerful OH radicals that attacked MB molecules. Therefore, the energy density peaking at 10 minutes of experiment could be attributed to the breakdown of C-S^+=C bonds by OH radicals and electrophilic reaction of sulphur atom in the central heterocyclic ring of MB molecule into various intermediate products. This argument was also supported by Ibrahim, (2012). Furthermore, during plasma treatment of MB in the present DBD system, MB dye may first be converted into intermediates products of lower molecular weight than the initial

compound whose mineralization required high energy during the first 10 minutes of EHD experiment. Consequently, important quantities of powerful oxidants such as OH radicals, superoxide anions, etc. were required. In the current DBD system, these oxidising agents mainly originate from a variety of chemical reactions including dissociation of water molecules and H_2O_2 by UV light and the dissociation of O_2 molecules by high energetic electrons as shown in Equations 5.21-5.24 and 5.26, respectively. Hence, the formation of these free reactive species by dissociation of water molecules and H_2O_2 and their attack on MB molecule might have required considerable energy in the first 10 minutes of experiment. This correlation between the produced active species and the energy density for their production in a double cylindrical plasma reactor is still an undiscussed concept in literature.

5.2 CHARACTERIZATION OF UNTREATED AND TREATED MB SAMPLES

In this section, the following analytical techniques: UV-vis, FT-IR, TOC, COD, etc. were used to characterise the final solution of MB samples withdrawn every 10 minutes within an hour of EHD experimental run.

5.2.1 Ultraviolet- visible spectroscopy (UV-vis)

The UV-vis spectra obtained for MB samples within 60 minutes of treatment are shown in Figure 5 -6

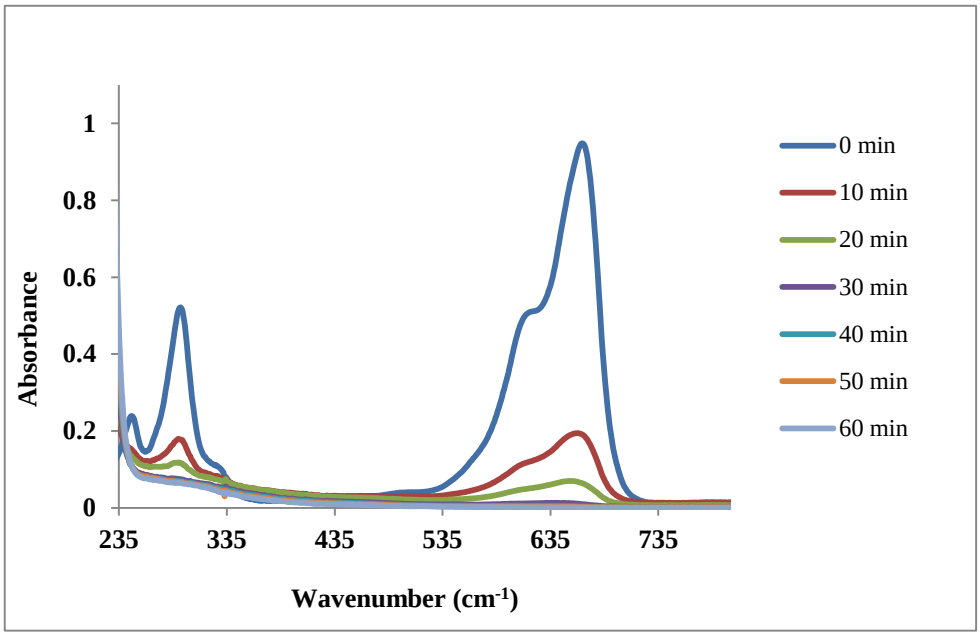

Figure 5-6: Ultra violet- Visible Spectra of MB samples extracted within 60 minutes of EHD experiment at the following experimental conditions: applied voltage 25 V, Peak voltage 7.8 kV, pH (in between 6.04 and 6.64), MB solution conductivity (0.02 to 0.09 mS/cm), air gap 2 mm, air flow rate 3 L/min, MB volume 1500 mL, 50 g/L NaCl electrolyte, 0.5 mm silver electrode and contact time of 60 minutes.

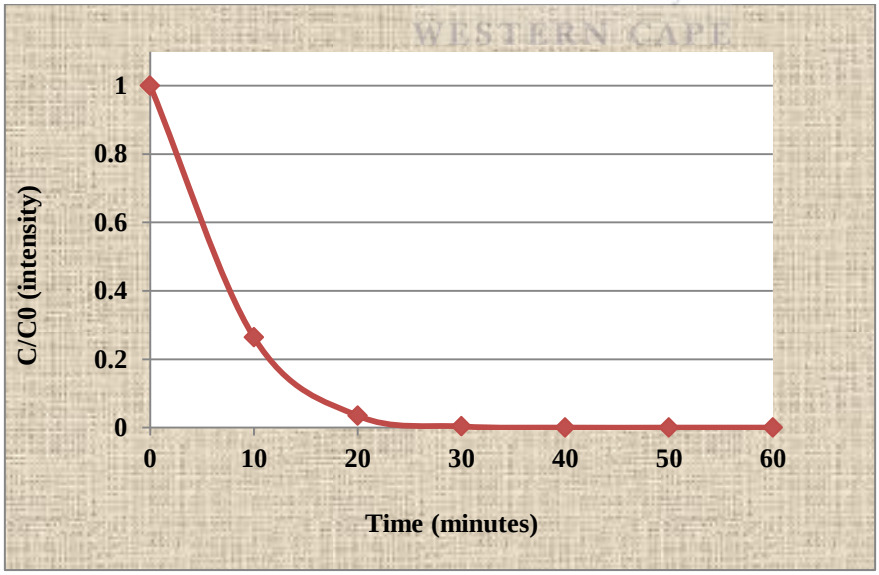

Figure 5-7: Intensity vs time of MB degradation showing progressive degradation of MB (using UV-vis data)

Figure 5-6 shows UV spectra of the degradation of MB carried out within 60 minutes and where the solution was sampled every 10 minutes. The UV-vis spectra in Figure 5-6 show that MB absorption bands occurred within two distinct regions. Higher energy absorption bands occurred between 535 cm^{-1} and 735 cm^{-1} and lower energy absorption bands appeared in the 235 cm^{-1}- 335 cm^{-1} range. However, nothing was observed between the two absorption regions. In addition, the spectra show a progressive decrease of the intensity absorption bands over time, and therefore demonstrate a considerable decrease of MB concentration, hence increasing degradation of MB with an increase of the treatment time. In addition, the spectra show that complete decolourization of MB was achieved within 30 minutes because absorption bands obtained after 40, 50 and 60 minutes overlap one another and lie closely with the x-axis. This implies that after 30 minutes of the experiment, MB was decolourized. This statement is in conformity with the plot of intensity over time results shown in Figure 5-7.

Indeed, some organic molecules and functional groups absorb electromagnetic radiations in the UV/visible region that is, wavelength in the 190-800 nm range. As for electron transition phenomenon in organic molecules, except for alkanes, electrons may undergo several transitions where some are allowed transitions and others are referred to as forbidden transitions. Based on this, the appearance of absorption bands of spectra presented in Figure 5-6 in two different regions could be the result of electron transitions from the highest occupied molecular orbital (HOMO) to the lowest unoccupied molecular orbital (LUMO) of higher energy when MB molecule absorbs energy. Whereas, the region of spectra without absorption bands in Figure 5-1 might result from the forbidden transitions. Generally, organic molecules such as dyes contain a chromophoric part that is responsible for giving rise to the UV or visible spectrum. An example of this is the $=N^{+}(CH_3)_2$ group in Methylene blue structure which was highlighted by Magureanu et al. (2007). So the rapid decolourization of MB observed within 20 minutes was principally due to the destruction of the $=N^{+}(CH_3)_2$ group by hydroxyl radicals. This is because apart from $C\text{-}S^{+}=C$ functional group in methylene blue structure, the nitrogen atom in $=N^{+}(CH_3)_2$ group is also an electrophilic centre that is attacked by powerful OH radicals during plasma exposure. This was also confirmed by Xing et al, (2010). Moreover, substitution of hydrogen by auxochrome groups such as methyl, hydroxyl, alkoxy, halogen and amino groups on a basic chromophoric structure changes the intensity of absorption and possibly the wavelength. Consequently, the appearance of absorption bands in the higher energy range of spectra (535 cm^{-1} - 735 cm^{-1} range) could result from the

substitution of hydrogen by methyl group in basic chromophoric structure ($=N^{+}(CH_3)_2$) of MB. Furthermore, the appearance of absorption bands in the range of 250 cm^{-1} to 310 cm^{-1} observed from these spectra is probably due to aromatic rings that are detectable in this range because of their conjugated pi electron system.

As a whole, the decline of peak intensity in the UV-vis absorption spectra presented in Figure 5-6 and results given in Figure 5-7 show a decrease of MB concentration with time. These were just visible observations; however the theoretical observations behind the nature of ionic and molecular species present in treated and untreated MB sample still remain undefined. Therefore analysis of MB samples using FT-IR spectroscopy could give qualitative information of the samples' organic content to determine if intermediate products still remain in solution.

5.2.2 FT-IR spectrum of deionised water and MB samples

The main goal of this section was to compare the existing stretching vibrations functional groups in the raw and treated MB, hence showing the possible formation of new intermediates during treatment of MB. The FT-IR spectra of deionised water, deionised water + MB and that of treated MB solution are presented in Figure 5-8.

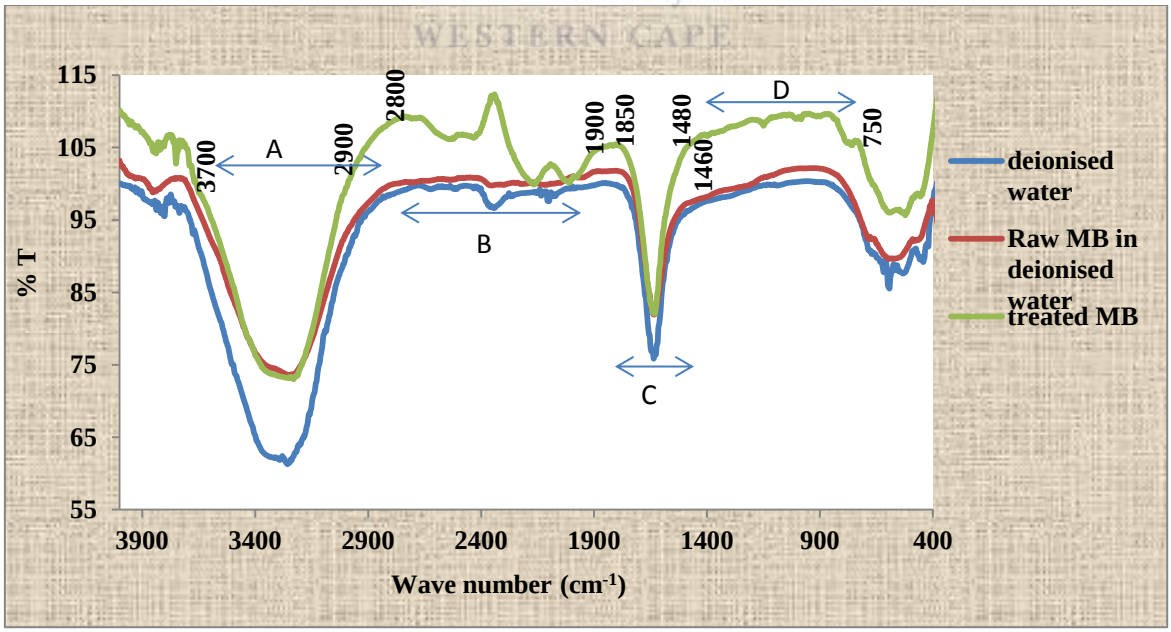

Figure 5-8: FTIR Spectra of deionised water, untreated MB solution and that of treated MB solution at the following conditions: applied voltage 25 V, Peak voltage 7.8 kV, pH (in between 6.04 and 6.64), MB solution conductivity (0.02 to 0.09 mS/cm), air gap 2 mm,

air flow rate 3 L/min, MB volume 1500 mL, 50 g/L NaCl electrolyte, 0.5 mm silver electrode and contact time of 60 minutes.

The FT-IR spectra shown in Figure 5-8 can be divided into the following regions: A (3700 -2700 cm^{-1}), B (2800 - 1900 cm^{-1}), C (1850 - 1480 cm^{-1}), D (1460 - 750 cm^{-1}). In all these absorption bands it can be noticed that spectral bands of raw and treated MB shifted from that of deionised water even though their shapes around certain regions look similar. This is because when dissolving MB in deionised water, some hydroxyl groups might have been replaced by other functional groups leading to the compression of bands in raw and treated MB spectra, hence their shift. Likewise in certain absorption regions, it can also be seen that the spectrum of treated MB is shifted compared to those of raw MB and that of water. This implies that some chemical reactions, mainly oxidation of MB, might have occurred during the plasma treatment.

Moreover, in region A (3700 -2700 cm^{-1}), despite the shift of spectral bands of MB samples from that of water, the wide and broad band mostly between 3600 cm^{-1} and 3040 cm^{-1} is still persistent. This could be due to the overlap of OH and the symmetric N-H stretching vibrations, whereby OH stretching might be due to water and the N-H could result from amines, or amide functional groups present in treated and untreated MB samples. The anti-symmetric NH_2 stretching vibrations usually observed in 3300 -3100 cm^{-1} and 3140-3350 cm^{-1} respectively may appear in this region. As for region B (2800 - 1900 cm^{-1}), apart from the significant shift of peaks in the spectrum of treated samples compared to those of raw MB and deionised water, about four new absorption bands were formed, whereas such bands were almost invisible in raw MB and deionised water. The resulting vibration bands are probably due to stretching vibrations of new functional groups. The first two bands appearing at 2590 cm^{-1} and 2392 cm^{-1} can be attributed to S-H and $N\text{-}H^{+}$ stretching vibrations. The last two bands in region B are related to C ≡ C and C ≡ N appearing at 2167 cm^{-1} and 2000 cm^{-1} and can probably be due to the presence of unsaturated compounds in the treated MB.

In addition, in region C (1850 - 1480 cm^{-1}), for treated and untreated samples, MB spectra show a sharp and intense overlapping peak which is shifted compared to that of deionised water. This peak is probably due to the overlapping of C=N, C=C, N-H and probably C=O stretching vibrations. Thus C=N, C=C, N-H bands are more likely to appear in 1740 -1650 cm^{-1} sub-range. The C=O stretching vibrations appears around 1700 cm^{-1} and characterise

the presence of carboxylic acid by-products in treated MB solution. In region D (1460 - 750 cm^{-1}), although treated MB spectrum is highly shifted compared to that of raw MB and deionised water, a number of small absorption bands appeared. Likewise the band at 1360 and 1430 cm^{-1} can be assigned to in-phase and out of phase CH_3 groups. Aliphatic NO_2 group in 1390-1300 sub-regions can also be visualized. Finally, C-N and C-O stretching vibration can be localised in the 1220-750 sub-range.

From the analysis of these FT-IR results, it can be inferred that oxidation of MB by reactive species (such as OH radicals, H_2O_2, O_3, etc. generated in plasma) during electrical discharge leads to the formation of various intermediate MB by-products. These latter could be further mineralised to CO_2 and H_2O over time.

To conclude this section, despite the fact that FT-IR spectra analysed above showed that some functional groups (such as OH and N-H) in the initial MB solution were still present in the treated solution, the appearance of new stretching vibrations, hence the appearance of new organic compounds in the treated sample implies that MB degraded and therefore decomposed to various different intermediate by-products. Apart from these qualitative analysis performed on MB samples, more evidence on the degradation by-products was needed. Therefore quantitative investigation of MB solutions sampled before and after treatment was of great importance.

5.2.3 Quantitative parameters of MB degradation

The degradability of MB during the EHD experiment was evaluated in terms of parameters such as total organic carbon (TOC), chemical oxygen demand (COD), sulphate content and nitrogen (as nitrate + nitrite) content as explained in chapter three. Results obtained from these methods are presented in Table 5-3.

Table 5-3: Ecological parameters of untreated and treated MB solution at the following conditions: applied voltage 25 V, Peak voltage 7.8 kV, pH (in between 6.04 and 6.64), MB solution conductivity (0.02 to 0.09 mS/cm), air gap 2 mm, air flow rate 3 L/min, MB volume 1500 mL, 50 g/L NaCl electrolyte, 0.5 mm silver electrode and contact time of 60 minutes.

Analysis	**Unit**	**Raw MB**	**Treated MB**
Sulphate as SO_4 Dissolved	mg/L	1.5	1.1
Nitrate + Nitrite as N	mg/L	Not detected	16
Total Organic Carbon (TOC)	mg/L	8.3	3.9
Chemical Oxygen Demand (COD)	mg/L	<5	<5

Table 5-3 shows that, sulphate content in samples decreased from 1.5 mg/L before treatment to 1.1 mg/L after treatment, showing a decrease of sulphur (as sulphate) during the EHD experiment. On the other hand, about 16 mg/L of (nitrate + nitrite) as nitrogen content was found. In addition, the TOC content of untreated MB sample was 8.3 mg/L which decreased to 3.9 after 60 minutes of treatment. This was probably due to the fact that some of the carbon atoms from the degradation of MB may have reacted with oxygen atoms to form small traces of CO_2 gas as expected. Methylene blue chemical oxygen demand (COD) content before and after treatment was less than 5 mg/L which is within permissible limit recommended by the World Health Organization (WHO) (2008) regulations. The decrease of sulphate content during EHD is probably due to the breaking of C-S^+=C bonds in the MB molecule. In fact, the sulphur atom in MB frame work is a strong electrophilic centre. So when the dye was exposed to electrical discharge in air, oxidising species such as O_3, H_2O_2 and probably OH generated in plasma are primarily attracted to electron deficient sites. Therefore, the $OH^{\cdot}$ radicals attack on bonds in C-S^+=C functional group probably leads to the formation of SO_4^{2-} ions and other intermediates that may have been oxidized into volatile gases such as SO_2. This was previously demonstrated by Houas et al. (2001). Or sulphate salts may have reacted with H atoms to form hydrogen sulphide H_2S that was given off during DBD experiment and evidenced by the offensive smell and hence justifying the decrease in SO_4^{2-} content as shown in Table 5-3.

Moreover, the 16 mg/L of nitrogen content in the treated solution might have evolved from the decomposition of MB molecule by reactive species or from the introduced air that was

used as a feeding gas. Even though air was used as oxygen provider for the EHD system, it should be recalled that air largely consists of nitrogen and a small amount of oxygen. Therefore it can be inferred that the identified nitrogen content is mostly derived from air. A similar opinion was also expressed by Magureanu et al. (2013) who demonstrated that nitrogen based compounds detected in plasma treated MB sample mainly evolved from air and not from MB degradation. As for the total organic carbon, its decrease from 8.3 to 3.9 mg/L shows that the long carbon framework of the MB molecule was broken into small carbon chain intermediates. This was also highlighted by Houas et al. (2001). So the TOC efficiency was then calculated according to the formula suggested by Reddy et al. (2014) and given by:

TOC removal percentage = $[(t_o - t)/t_o] \times 100$…….. (5.35)

So for the current study, TOC removal percentage was calculated as follows:

TOC removal percentage = $[(8.3 - 3.9)/8] \times 100$

= 53%

This means that at 5 mg/L MB, about 53% of MB decomposition and mostly in colour removal was achieved over time. The degradation pathway of methylene blue is indicated in Figure 40. This once again shows that decolourization does not mean degradation. Even if 100% of MB decolourization at 5 ppm was achieved within 60 minutes, only 53% of its carbon content was removed by the EHD reactor system.

The above conversion is not in agreement with 98% removal reported by Vujevic et al. (2004) but closely related to the 48% removal obtained by Reddy et al. (2012). In addition, the inconsistence of results reported in literature and those of the current work could be due to experimental conditions used. Therefore implementation of the present EHD system could be significant in achieving higher TOC removal not only for MB but for any other type of pollutants. Furthermore, the large difference between TOC removal percentages reported by Vujevic et al. (2004), Reddy et al. (2012) and 53 % of the present study could be explained by the statement about salts and solution pH raised by Salome and colleagues in 2006. In fact, Salome et al. (2006) highlighted that the presence of salt in treated wastewater by plasma discharge may positively affect the TOC removal and negatively impact the colour removal percentage of organic pollutants. For instance, Table 5-3 of this section shows that during treatment of MB by corona discharge, about 16 mg/L of nitrogen based compounds largely resulting from air used as the feeding gas (Jo and Mok, 2009) were detected in the treated sample. On the other hand, sulphur content (1.5 mg/L) as SO_4 in the untreated MB decreased to 1.1 mg/L. So the reduction and production of these by-

products might have led to the formation of acidic species such as HNO_3, HOON, H_2SO_4, etc. (Magureanu et al. 2013) which eventually decreased solution pH and raised its electrical conductivity. Based on the pH evidence, Salome and co-workers emphasized that organic compounds may be hydrolysed when the pH of the solution is close to 7 after ozonation. Likewise the pollutant is not hydrolysed when the solution pH is around 3.9. This meant that the decrease of solution pH favours colour removal at the expense of dye mineralization, hence a lower TOC removal. In other words in the present research, MB was decomposed to various intermediates by-products, the resulting aliphatic compounds such as carboxylic acids, aldehydes, amines, amides, etc. indicated by the presence of their functional groups in section 5.2.2 were not oxidised into CO_2 and H_2O but remained in the solution. This finding was also reported by Jun et al., (2008) who stated that during treatment of dyes by non-thermal plasma (NTP), both TOC and colour removal percentage cannot be successfully achieved at the same time. Thus optimization of the current EHD system is significant in order to overcome the limitation between TOC and decolourization percentage removal.

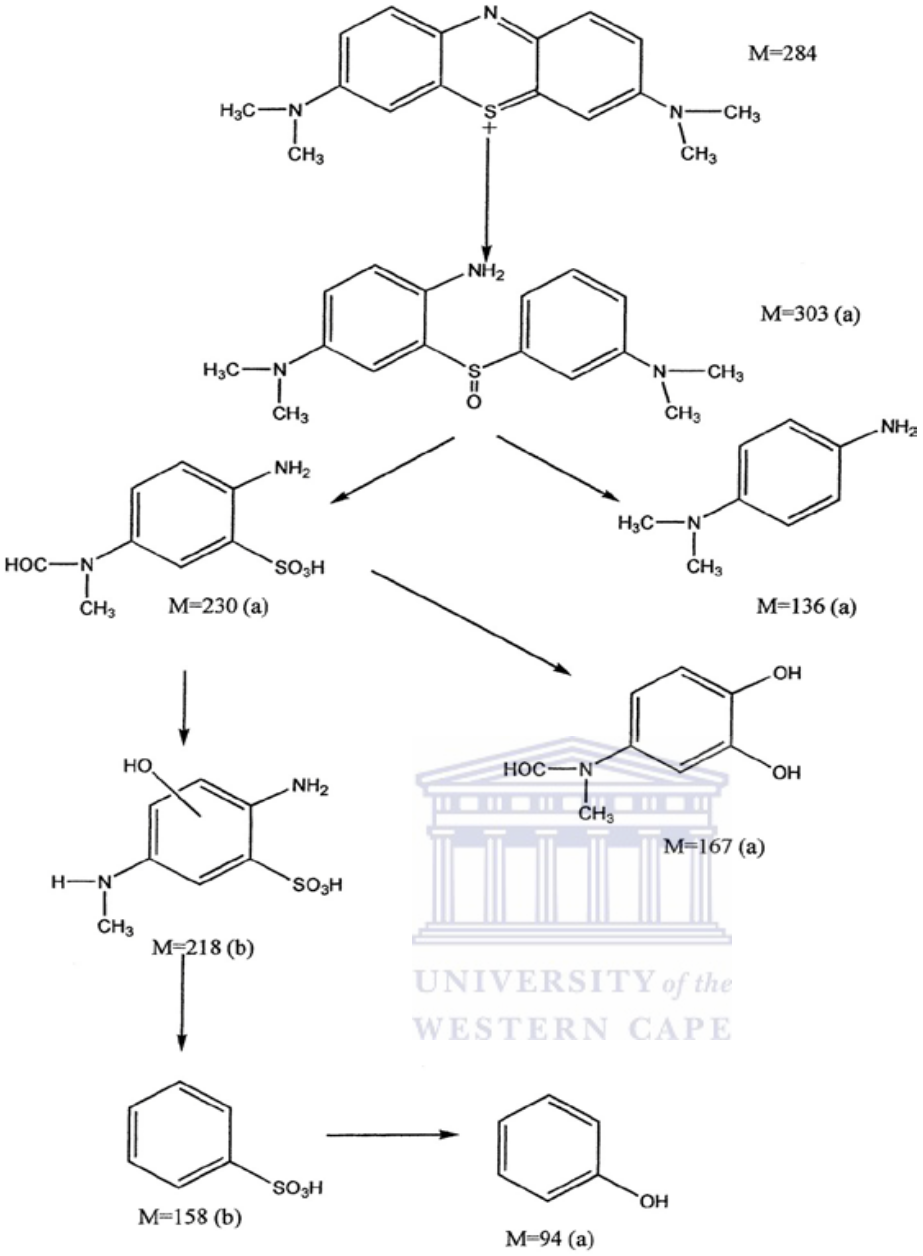

Figure 5-9: Pathway of MB decomposition (Houas et al., 2001).

5.3 SUMMARY OF CHAPTER FIVE.

Based on the description of the current DBD system as elaborated above, the UV light observed in the DBD system are formed in the air gap via the decay of excited oxygen (O^*) and nitrogen (N^*) molecules to their ground energy levels (zone b) as indicated in Equations (2.12 – 2.15). The free reactive species mainly O_3 is also formed in the discharge gap (zone b) via association of oxygen molecules and atomic oxygen radicals (Equation 5.15). As for H_2O_2 quantified in the bulk solution, its formation mostly occurs via recombination of hydroxyl radicals as shown in Equation 5.25 and its decrease was likely due to its decomposition by UV-vs light or side - reactions chains in the system. The absence of ozone in the first 20 minutes was due to its escape during the DBD experiment because of the opened reactor configuration. Or during the first 20 minutes, O_3 may have been consumed by side chain chemical reactions taking place during the DBD process.

The decomposition of MB in this study was also associated with the formation of inorganic salts such as nitrates and sulphates. The reduction of MB toxicity was shown by the decrease in COD value early presented in Table 5-3. So the presence of these decomposition by-products in the actual DBD system was proved in section 5.2.3 and were largely formed in the plasma zone (zones b and c), and to some extent, in the bulk solution. Their production occurring through various reaction chains was earlier summarized in Figure 2-13. Thus, the optimization of a double cylindrical DBD plasma system for water/wastewater treatment and quantification of active species such as H_2O_2 and O_3 naturally produced in such configuration are important aspects that were achieved in this study, but have not been covered in previous literature. Energy density of MB decomposition in the present configuration was successfully evaluated but remains also undefined in previous research papers.

Conclusively, in this chapter, it was proved that the DBD plasma reactor produces UV-vis radiations and free reactive species mainly O_3 and H_2O_2 which were probably responsible for the decomposition of MB, as evidenced by the decrease in TOC, the absorption bands in UV-vis spectroscopy as well as the presence of various functional groups in the FT-IR spectra. Hence, the goals of this chapter were achieved; however some aspects involving the quantification of OH radicals and the identification of MB degradation intermediate products by LC-MS/GC-MS were not covered in this study and their achievements remain the subject of a future study.

CHAPTER SIX

6. INTRODUCTION

This chapter highlights the findings and general conclusions of the study carried out on optimization of the EHD system and quantification of reactive species produced in the EHD reactor. Answers to research questions and objectives achieved in this study as well as recommendations for future work are also outlined.

6.1 OVERVIEW

The aim of this study was to optimize the corona electrohydraulic discharge (CEHD) system using methylene blue (MB) dye as a model synthetic organic pollutant, while the objectives include assessing the progressive decolouration/degradation efficiency of methylene blue. The study investigated the effect of physicochemical and electrical parameters as well as reactor configurations on the decolouration/degradation efficiency of the pollutant, establishing the pathways for the production of active species, and quantifying some of the active species present in the bulk solution. In order to achieve these aims and objectives, several experimental approaches were considered. These included varying the concentration of MB while other parameters were kept constant in order to determine the effect of the concentration on decolourisation/degradation efficiency. The effect of chemical and physical parameters such as the volume of MB and the concentration of NaCl electrolyte concentration, pH, electrical conductivity and air flow rate were investigated sequentially in order to determine their impact on MB degradation efficiency. Apart from these, the effect of voltage, electrode type and diameter of the electrode on decolouration of MB was investigated. The EHD system was then tested at optimum conditions in order to assess the efficiency of the optimized parameters on MB decomposition. Furthermore, the initial and final MB solutions were qualitatively and quantitatively analysed using analytical techniques such as UV- spectroscopy, Fourier Transformer Infrared spectroscopy (FT-IR) and total organic carbon (TOC). The conclusions of this study are given from the results of the experiments and analyses carried out during the study.

6.2 CONCLUSIONS

The effect of reactor configuration, physicochemical and electrical parameters on MB decomposition was evaluated at the following fixed conditions: applied voltage 25 V, peak voltage 7.8 kV, MB volume 1 500 mL, air flow rate 3 L/min, air gap 2 mm, 0.5 mm silver electrode (25 cm long) and contact time of 60 minutes. The reactive species H_2O_2 and O_3 were also detected and quantified at the same conditions. The optimum parameters were obtained by assessing the effect of reactor configuration, physicochemical and electrical factors on MB decolouration efficiency.

6.2.1 Reactor configuration

At the following conditions: applied voltage (25 V), peak voltage (7.8 kV), MB volume (1 500 mL), air flow rate (3 L/min), air gap (2 mm), 0.5 mm silver electrode (25 cm long) and contact time of 60 minutes, the reactor configuration impacted MB decomposition efficiency in such a way that MB removal decreased with an increase of the air gap from 2 to 6 mm. Therefore, after 30 minutes of contact time the optimum removal of 83.36 % was attained with 2 mm air gap while 79.9 % and 19 % were achieved with 4 and 6 mm air gaps, respectively**.** This could be explained by the fact that the small 2 mm air gap might have induced a strong electric field leading to high electron energy around the inner tube and thus, producing a greater amount of reactive species that accelerated MB degradation process. Conclusively, discharge gap is an important factor that needs to be considered in wastewater treatment using double cylindrical dielectric barrier electrohydraulic discharge.

6.2.2 Chemical parameters

The chemical parameters investigated in this study include MB initial concentration and the concentration of NaCl electrolyte used in the inner electrode compartment of the DBD reactor.

The effect of initial concentration on MB decolouration was determined by varying MB concentrations from 0.5 to 10 mg/L at 0.5 mg/L increments. MB decolouration efficiency decreased with an increase in MB concentration due to the power output and the size of the single reactor used. For concentrations ranging from 0.5 to 5 mg/l, the final solution

sampled within 60 minutes was clear indicating complete decolouration. At concentrations above 5 mg/L, the colour of the final solution sampled after 60 minutes changed progressively from yellow to deep green. This study showed that using the DBD single cell complete decolouration of MB could be achieved within 60 minutes with MB concentration ranging from 0.5 to 5 mg/L. Thus, 5 mg/L was further used as the optimum MB concentration for the EHD system being investigated as it worked well within that concentration.

The UV-vis analysis of the treated MB solution showed that complete decolouration of was achieved in the first 30 minutes of contact time due to the breakdown of the chromophoric [=N+(CH_3)$_2$] group in Methylene blue structure. This was proved by FT-IR analysis which showed the trace presence of the following functional groups: C=C, C=O, C=N, NH, NH_3, NO_2, etc. characteristics of carboxylic acids, amines, amides, nitrogen based compounds (salts), aliphatic and unsaturated by-products in the bulk solution. Apart from this, 16 mg/L of nitrates and nitrites and 1.1 mg/L of sulphates mainly originating from air and MB were present in the treated solution. Therefore, during EHD experiment, the organic pollutant MB was degraded into various intermediates saturated and unsaturated by-products as well as salts such as sulphates and nitrogen based species that were formed from air and from the decomposition of MB in the EHD system. This aspect signifies that pure O_2 would be a more suitable feed than air to prevent nitrate and nitrites formation and that times longer than 60 minutes may be needed to remove intermediates completely.

NaCl electrolyte was used in the central electrode compartment of the EHD system to avoid sparking between the 0.50 mm silver electrode and the inner quartz tube of the reactor. The concentration of NaCl was varied from 10 to 50 g/L in 20 g/L increment units using the same experimental conditions. Thus, 58.58 % MB degradation efficiency was achieved with 50 g/L of NaCl while 47.32 % and 41.4 % were reached with 10 and 20 g/L of NaCl, accordingly. Since consistent trend was observed between electrolyte concentration and MB degradation efficiency, therefore NaCl electrolyte concentration of 50 g/L of NaCl was chosen as the optimum electrolyte concentration used for further DBD experiments using a specified reactor configuration.

6.2.3 Physical parameters

The study carried out to determine the effect of physical parameters on MB degradation efficiency showed that when varying the pH from 2.5 to 10.5 at an increment rate of 2, MB decolouration efficiency decreased with an increase in solution pH. In addition to this, it was observed that after 10 minutes of the DBD experiment, 83.02 % of MB removal was achieved at a pH of 2.5 compared to 71.4 %, 67.08 %, 60.32 % and 56.16 % MB removal achieved at pH 4.5, 6.5, 8.5 and 10.5, respectively. Therefore, pH significantly affected MB degradation efficiency. This was probably due to the fact that when the solution pH increased, hydroxyl radicals became unselective and reacted easily with scavengers such as carbonate ions that form during oxidation of organic materials and thus, reduced the efficiency of the oxidation process significantly. In this case, the optimum pH value was 2.5. Consequently, solution pH had a significant effect on MB degradation efficiency.

As for solution conductivity, this factor was adjusted with diluted solutions of NaOH and HNO_3. So, increasing the conductivity values from 5 to 20 mS/cm with increments of 5 mS/cm at the same conditions did not show a significant impact on MB degradation efficiency as a trend between MB removal efficiency and solution conductivity was not observed. However, 84.76 % MB removal was achieved at conductivity of 10 mS/cm followed by 82.32 %, 71.06 % and 69.16 % at conductivities of 15, 20 and 5 mS/cm, correspondingly. Hence, the optimum solution conductivity in this study was selected to be 10 mS/cm.

The air flow rate was varied from 2 to 4 L/min at the following experimental conditions: voltage (25 V), peak voltage (7.8 kV), MB volume (1 500 mL), air gap (2 mm), 0.5 mm silver electrode (25 cm long) and contact time of 60 minutes. After 10 minutes of experiment, the results showed that MB degradation efficiency increased with an increase in the air flow rate. That is, 49.2 %, 60.14 % and 73.32 % MB removal were consecutively obtained at air flow rates of 2, 3 and 4 L/min, respectively at 10 minutes. This could be explained by the fact that the introduction of O_2-containing gas in the DBD system induced the generation of O_3 and other O-based active species that boosted OH• production and together with H_2O_2 and other reactive species significantly augmented MB decomposition. Therefore, 3 L/min was chosen to be the optimum air flow rate for this system because any value above 3 L/min produced an excessive amount of bubbles

resulting in short-circuits in the equipment used. Thus, air flow rate significantly affected MB removal efficiency.

Even though MB removal efficiency slightly increased when the volume of the solution increased from 500 to 2 000 mL at 500 increments at the same experimental conditions, 92%, 97.58%, 99.3% and 99.48% of MB removal was achieved respectively after 30 minutes of experiment. This however does not mean that the solution volume affected MB degradation efficiency. This is because at low volume, some of the UV-vis radiations generated by DBD was wasted due to the fact that the reactor tube was not completely immersed in the polluted water, thereby decreasing MB percentage removal at low volumes. Therefore, 1 500 mL was chosen as the best volume for the EHD reactor because any volume above 1 500 mL would induce overloading of the system. In total, solution volume did not impact the decolouration of MB dye treated in the applied DBD reactor configuration.

The comparison of the optimum physical parameters showed that solution conductivity and pH significantly affected MB dye decolouration compared to air flow rate and solution volume. Hence, the decolouration of dye in the current DBD system is a pH dependent process.

6.2.4 Electrical parameters

In the case of the electrical parameters that were varied, MB decolouration efficiency was affected by the increase of voltage and current under the following conditions: MB volume 1 500 mL, air flow rate 3 L/min, air gap 2 mm, 0.5 mm silver electrode (25 cm long) and contact time of 60 minutes. When voltage was varied from 20 to 22 and 25 V, about 48.02%, 72.46% and 73.66% MB decolouration were respectively achieved after 10 minutes of contact time. The optimum voltage suitable for the EHD system was 25 V corresponding to a peak voltage of 7.8 kV. The increase of MB decolouration efficiency was due to the fact that increasing voltage resulted in an increase of both the number and the length of micro discharges generated in DBD. The strong electric field around the anode electrode therefore accelerated the production of reactive species and hence achieved an increase in MB decolouration.

In the study carried out to optimise the electrode size, the optimum 1.5 mm diameter silver electrode was found to be the most suitable compared to copper and stainless steel. After 10 minutes of experiment, 55.8% of MB decolouration was achieved with silver compared to 38.3% and 48.7% removal that were reached with copper and stainless steel, respectively. Besides the fact that the three types of electrodes (copper, silver and stain less steel) were immersed in NaCl electrolyte in the inner tube of the reactor, the highest percentage removal of MB was achieved with silver wire and its dominance over copper and stainless steel electrodes was also due to the following reasons: The thermal conductivity of silver (429 W/m-K) is superior to that of copper (329 W/m-K) and that of stainless steel (304 W/m-K). The thermal conductivity of copper may have been affected by the mechanical work of NaCl electrolyte used in the inner tube of the reactor. In spite of having a low thermal conductivity, the exposure of stainless steel to moisture (NaCl salt) and heat accelerated corrosion.

When varying the diameter of the electrode, the 1.5 mm diameter silver electrode was considered as optimal compared to 0.5 mm silver electrode. This was ascribed to the fact that the 1.5 mm silver electrode had a greater surface area and closer to the inner dielectric quartz tube which probably favoured the flow and distribution of significant amounts of high-energy electrons around the inner dielectric quart tube. The interaction of these highly energized particles with air yielded considerable amounts of reactive free radicals.

Therefore, 71.24% MB decolouration percentage achieved with 1.5 mm compared to 55.8% of MB colour removal obtained with the 0.5 mm silver electrode. Therefore the type and the size of electrode in the inner electrode compartment influenced MB degradation significantly in the present DBD reactor configuration.

Finally, after the effect of all the parameters on MB removal were assessed, the following optimum values were obtained: Applied voltage 25 V, MB concentration 5 mg/l, solution volume 1 500 mL, pH 2.5, conductivity 10 mS/cm, air flow rate 3 L/min, 50 g/L NaCl electrolyte, 1.5 mm silver electrode. The DBD experiment performed at these optimized conditions showed a reduction in treatment time of MB dye which was shortened from 30 to 20 minutes. Overall, the decolouration of MB dye in the DBD plasma system mostly depended on MB initial concentration, solution pH and conductivity and the applied

voltage as well as electrode type and size which significantly influenced MB decomposition.

The detection and quantification of reactive species performed every 10 minutes during experiment (at a voltage 25 V, peak voltage 7.8 kV, MB volume 1 500 mL, air flow rate 3 L/min, air gap 2 mm, 0.5 mm silver electrode (25 cm long) and contact time of 60 minutes) showed that the concentration of generated H_2O_2 reached 3.73 x 10^{-5} mol/L in the first 10 minutes of the experiment and thereafter decreased to 2.93 x 10^{-5} mol/L after 20 minutes. After 30 minutes of the experiment, H_2O_2 increased from 2.93 x 10^{-5} mol/L to 3.33 x 10^{-5} mol/L while 0.5 x 10^{-5} mol/L of ozone was produced. Beyond 30 minutes, concentration of hydrogen peroxide decreased considerably with time whereas that of ozone fluctuated. These fluctuations were probably due to the escape of ozone from the system. Ozone is not very soluble in water and the sparging of the ozone generated was ineffective and bubbles formed had a low residence time in the solution. It can be expected that a lot of improvement could be achieved if ozone could be recirculated through the water to be treated.

On the other hand, the energy consumption calculated over 60 minutes of the experiment reached 0.087 g/kWh in the first 10 minutes with an applied voltage of 25 V, a peak voltage of 7.8 kV, current of 3.86 A and power of 112 W, as presented in appendices 34 - 36 and progressively decreased to zero with an increase in treatment time.
So the correlation between the increase of H_2O_2 concentration and the rise of energy density after 10 minutes of experiment was certainly due to the production of free reactive species such as OH radicals generated via dissociation of OH-OH bond of H_2O_2 by UV light in the bulk solution. This also justifies why most trends were clearly observed after 10 minutes of EHD experiments. Conclusively, H_2O_2 and O_3 were probably responsible for the decomposition of MB in the first 30 minutes of the EHD experiment.

The current optimized EHD system is feasible, efficient, and environmentally friendly and has proved to decolourize and also fully degrade a model organic pollutant MB at ambient conditions. The reactive species mainly H_2O_2 and O_3 were detected and quantified, and these reactive species influenced MB degradation. The dissociation of H_2O_2 by UV radiation generated in the system probably led to the formation of powerful unselective free radicals such as $^{\cdot}OH$, $O^{\cdot}$, etc. which accelerated the decomposition process. However,

quantification of OH radicals in this DBD system was not covered due to the large number of data generated in this study. The intermediate by-products of MB decomposition were detected by FT-IR but could not be identified because at 5 mg/L MB, the concentration of MB intermediate-products was very low with respect to the sensitivity of the liquid chromatography/mass spectrometry (LC-MS) and gas chromatography/ mass spectrometry (GC/MS) machines used for analysis. Thus the achievements of these two tasks remain the subjects of a future study.

In addition, after all parameters were optimized, a new EHD reactor was constructed. However, because all the optimized conditions were not applied during its construction the new reactor did not generate UV radiation as expected. So the electrode configuration of the new system needs to be revised in future work.

Even though, the concept of electrohydraulic discharge has been widely used as water/wastewater treatment technique, the technology behind this concept has always been challenging. Although trends relating some parameters such as chemical and electrical variables to dye degradation efficiency have been previously reported on different reactor configurations, these same parameters were optimised in the new DBD system (reactor configuration). Hence, this EHD system can further be explored as a powerful technique for water/wastewater treatment.

6.3 RECOMMENDATIONS

Since a clear trend on decolourization efficiency was not noticed when increasing electrolyte concentration, it was difficult to conclude that electrolyte concentration has an important effect on dye decolourization. Changing the type of electrolyte used may have a greater impact upon dye colour removal and should be further investigated.

Since the effect of gas flow rate on dye discoloration has rarely been studied in double cylindrical DBDs. Therefore the influence of this parameter on decomposition of contaminant in DBD still needs great attention.

It would be preferable that for future studies, the EHD system should be sealed completely in order to achieved complete decolourization or degradation of targeted contaminants in a

short period of time, for example after 5 or 10 minutes rather than after 30 minutes as it was the case in this study.

It would be important to consider quantification of hydroxyl radicals produced in the EHD system for better understanding of MB mineralization.

Since the adjustment of MB solution conductivity with HNO_3 also affected dye solution pH, it would be recommended that a suitable buffer or salt solution may be used to regulate the solution conductivity.

Future research should identify the intermediate by-products of the degradation of MB and elucidate the degradation mechanisms of the model pollutant which can be achieved using LC-MS, GC-MS or HPLC-MS, but preconcentration techniques would need to be developed.

To avoid undesirable by-products such as nitrites and nitrates during the treatment of pollutant by EHD system, pure oxygen should be used instead of air.

The future work should also attempt to trap and quantify the CO_2 produced after complete mineralization of the organic pollutant as one of the final end-products even if its presence might be in the order of pico mg/L.

Attempts should be made to measure the UV radiations generated in the EHD system, and quantify its contribution to the production of free radicals in future studies.

REFERENCES

Abbt-Braun G., Lankes, U., and Frimmel, F.H., (2004). Structural Characterization of Aquatic Humic Substances - the Need for a Multiple Method Approach. Aquat. Sci.66 (2): 151-170.

Allpike, B.P., Heitz, A., Joll, C.A., Kagi, R.I., Abbt-Braun, G., Frimmel, F. H., Brinkmann, T., Her, N., and Amy, G., (2005). Size Exclusion Chromatography to Characterize DOC Removal in Drinking Water Treatment. Environmental Science and Technology. 39(7): 2334-2342.

Al-Momani F., E. Touraud, J. R. Degorce-Dumas, J. Roussy, O. Thomas, (2007). Biodegradability enhancement of textile dyes and textile wastewater by VUV photolysis, *Journal of Photochemistry and Photobiology, A: Chemistry* 153 191–197.

Angeloni D.M., S.E. Dickson, M.B. Emelko, J.S. Chang, (2007). Removal of methyl-tert-butyl ether from water by a pulsed arc electrohydraulic discharge system. *J. Journal of Applied. Physics*. 45 8290

Anpilov A.M., E.M. Barkhudarov, Y.B. Bark, Y.V. Zadiraka, M. Christofi, Y.N. Kozlov, I.A. Kossyi, V.A. Kop'ev, V.P. Silakov, M.I. Taktakishvili, S.M. Temchin, (2001). Electric discharge in water as a source of UV radiation, ozone and hydrogen peroxide, *Journal of Physics D: Applied Physics* 34 993-999.

APHA, AWWA, WEF, (1998). *Standard methods for the examination of water and waste water* (20th edn.) Washington, DC: American Public Health Association.

Arakaki T. and Faust Bruce C., (1998). Sources, sinks, and mechanismos f hydroxylr adical ('OH) photoproduction and consumption in authentic acidic continental cloud waters from Whiteface Mountain, New York: The role of the Fe(r) (r = II, III) photochemical cycle. *Journal of Geophysical Research,* VOL. 103, NO. D3, PAGES 3487-3504

Arjunan K. Priya, Gary Friedman, Alexander Fridman and Alisa Morss Clyne, (2012). Non-thermal dielectric barrier discharge plasma induces angiogenesis through reactive oxygen species. *Journal of the Royal Society*. Interface **9**, doi:10.1098/rsif.2011.0220

Atkinson R., Carter W.P.L., (1984). Kinetics and mechanisms of the gas-phase reactions of ozone with organic compounds under atmospheric conditions, Chemistry Review., **84**, 437-470.

Backer, LC, Ashley DL, Bonin MA, Cardinali FL, Kieszak SM, and Wooten JV (2000). Household exposures to drinking water disinfection by-products: whole blood trihalomethanes levels. *Journal of Expo Analytical Environmental Epidemiology*. July-August, 10(4), 321-6.

Bader H., J. Hoigne, (1981). "Determination of ozone in water by the indigo method," *Water Research*. 15, pp. 449-456

Baldrian P., V. Merhautova, J. Gabriel, F. Nerud, P. Stopka, M. Hruby, M.J. Benes, (2006). Decolorization of synthetic dyes by hydrogen peroxide with heterogeneous catalysis by mixed iron oxides. Appl. Catal. B – Environ., 66 pp. 258–264

Bhattacharyya D., T. F. Van Dierdonck, S.D. West, A.R. Freshour, (1995). Two-phase ozonation of chlorinated organics. *Journal of Hazardous Material* 41, 73 – 93

Bian W., Xiangli Ying, Junwen Shi, (2009). Enhanced degradation of *p*-chlorophenol in a novel pulsed high voltage discharge reactor. *Journal of Hazardous Materials* 162 906–912

Brisset J-L, Benstaali B, Moussa D, Fanmoe J, Njoyim-Tamungang E (2011). Acidity control of plasma chemical oxidation: applications to dye removal, urban waste abatement and microbial inactivation. *Plasma Sources Science and Technology* 20:034021

Bruice P., (2004). Organic Chemistry. 4th Ed. Pearson Education, Upper Saddle River, N.J.

Drewes, J.E., Quanrud, D.M., Amy, G.L., and Westerhoff, P.K. (2006). Character of Organic Matter in Soil-Aquifer Treatment Systems. J. Environ. Eng. 132(11): 1447-1458.

Carla C. A. Loures, Marco A. K. Alcântara, Hélcio J. Izário Filho, Antonio C. S. C. Teixeira, Flávio T. Silva, Teresa C. B. Paiva, and Gisella R. L. Samanamud, (2013). Advanced Oxidative Degradation Processes: Fundamentals and Applications. *International Review of Chemical Engineering* (I.RE.CH.E.), Vol. 5, N. 2 ISSN 2035-1755

Chang, J.S., (2008). Physics and chemistry of plasma pollution control technology. *Plasma Sources Sci Tech.* 17 045004Ching W. K., A.J. Colussi, H.J. Sun, K.H. Nealson, M.R.

Chang J.S. O.L. Li, and Y. Guo, (2010). Pulsed Arc Electrohydraulic Discharge Characteristics, Plasma Parameters and optical emission of Sludge-Water IEEE *Electrical Insulation* (EI) Magazine 27 8

Chen, W., Westerhoff, P., Leenheer, J. A., and Booksh, K., (2003). Fluorescence excitation-emission matrix regional integration to quantify spectra for dissolved organic matter. *Environmental Science and Technology*. 37(24): 5701-5710.

Cheng H., Chen S., Wu Y. and Ho D., (2007). Non-thermal plasma technology for degradation of organic compounds in wastewater control: a critical review, *journal of Environment Engineering and management*, 17(6), 427-433

Chiron S., A. Fernandez-Alba, A. Rodriguez, E. Garcia-Calvo, (2000). Pesticides chemical oxidation: state-of-the art. *Water Research*, 34, 366–377.

Chouparova, E., Lanzirotti, A., Feng, H., Jones, K.W., Marinkovic, N., Whitson, C., and Philp, P., (2004). Characterization of petroleum deposits formed in a producing well by synchrotron radiation-based microanalyses energy fuels. 18(4): 1199-1212.

Cooper, P. J. and K. S. Ahluwalia (2000). "Operating results from supercritical water oxidation plants." Industrial and Engineering Chemistry Research 39: 4865-4870.

Crites R., Tchobanoglous G. (1998) Small and decentralized wastewater management systems. McGraw Hill, NY, USA.

Croue, J.P., Korshin, G.V. and Benjamin, M., (2000). Characterization of Natural Organic Matter in Drinking water. AWWA.

Dang TH, Denat A, Lesaint O, Teissedre G, (2008). Degradation of organic molecules by streamer discharges in water: coupled electrical and chemical measurements. *Plasma Sources Science Technology*, 17:024013

Daneshvar N., A. Aleboyeh A.R. Khataee, (2005). The evaluation of electrical energy per order (E_{Eo}) for photooxidative decolorization of four textile dye solutions by the kinetic model. *Chemosphere* 59 761–767

Deng S., Cheng Cheng, Guohua NI, Yuedong Meng, and Hua Chen, (2008). Bacterial inactivation by atmospheric pressure dielectric barrier discharge plasma jet. *Japanese Journal of Applied Physics*, Vol. 47, No. 8, pp. 7009–7012

Dojcinovic B.P, Roglic GM, Obradovic BM, Kuraica MM, Kostic MM, Nesic J, Manojlovic DD (2011). Decolorization of reactive textile dyes using water falling film dielectric barrier discharge. *Journal of Hazardous Materials* 192:763–771

Donghai W., Hong You, Jiaxuan Du, Chuan Chen, Darui Jin, (2011). Effects of UV/Ag-TiO_2/O_3 advanced oxidation on unicellular green alga Dunaliella salina: Implications for removal of invasive species from ballast water. *Journal of Environmental Sciences*, 23(3) 513–519

Drewes, J.E., Quanrud, D.M., Amy, G.L., and Westerhoff, P.K. 2006. Character of Organic Matter in Soil-Aquifer Treatment Systems. *Journal of Environmental Engineering* 132(11): 1447-1458.

Ellis T.G. (2004) Chemistry of wastewater. Encyclopedia of Life Support System (EOLSS), Developed under the Auspices of the UNESCO, Eolss Publishers, Oxford, UK, http://www.eolss.net.

Emsley J., (2011). *Nature's Building Blocks: An A-Z Guide to the Elements*. Oxford University Press. pp. 120–125. ISBN 978-0-19-960563-7.

Farre M.´, Maria Isabel Franch, Sixto Malato, Jose´ Antonio Ayllo´n, Jose´ Peral, Xavier Dome´nech, (2005). Degradation of some biorecalcitrant pesticides by homogeneous and heterogeneous photocatalytic ozonation. *Chemosphere* 58 1127–1133

Galindo C., Jacques P. and Kalt A., (1999).Total mineralization of an Azo Dye (Acid Orange 7) by UV/H_2O_2 oxidation. *J. Adv. Oxid. Technol.*, 4, 400-407

Gasanova S., (2013). Aqueous-phase electrical discharges: generation, investigation and application for organics removal from water. PHD thesis, *Institut für Instrumentelle Analytische Chemie der Universität Duisburg-Essen*

Gatewood B.M., (1995). Evaluation of after treatments for reusing reactive dyes. *Tex. Chem. Colorist* 28, 38-42

Glaze W.H., (1987). Drinking-water treatment with ozone, *Environmental science and technology* 21 224–230.

Gogate P.R. and Pandit A.B., (2004a). A review of imperative technologies for wastewate r treatment I: oxidation technologies at ambient conditions, Adv. Environ. Res.,8, 501-551.

Gogate P.R. and Pandit A.B., (2004b). A review of imperative technologies for wastewate r treatment II: hybrid methods, Adv. Environ. Res., 8, 553-597

Grabowski L. R., van Veldhuizen EM, Pemen AJM, Rutgers WR, (2006). Corona above water reactor for systematic study of aqueous phenol degradation. *Plasma Chemistry and Plasma Processes 26:3–17*

Grabowski L. R., E. M. van Veldhuizen, A. J. M. Pemen, and W. R. Rutgers, (2007) *Plasma Sources Sci. Technol*. 16, 226

Griffith J. W. and D. H. Raymond, (2002). "The first commercial supercritical water oxidation sludge processing plant." Waste Management 22: 453-459.

Grymonpre D. R., (2001). An Experimental and Theoretical Analysis of Phenol Degradation by Pulsed Corona Discharge, Florida State University.

Gupta S. B., (2007). Investigation of a physical disinfection process based on pulsed underwater corona discharges, MSc thesis. *Institutfür Hochleistung simpulsund Mikrowellen technic.*

Gurol M.D., Vatistas R., (1987). Oxidation of phenolic compounds by ozone and ozone and U.V. radiation: a comparative study, *Water Research*, 21 (8), 895-900

Hameed B.H., A.T. Mohd Din, A.L. Ahmad, (2007). Adsorption of methylene blue onto bamboo-based activated Carbon: kinetics and equilibrium studies, J. Hazard. Mater. 141: 819–825.

Harrelkas F., A. Paulo, M.M. Alves, L. El Khadir, O. Zahraa, M.N. Pons, F.P. van der Zee, (2008). Photocatalytic and combined anaerobic–photocatalytic treatment of textile dyes. *Chemosphere* 72 1816–1822

Hayashi D., W. Hoeben, G. Dooms, E.M. van Veldhuizen, W.R. Rutgers, G.M.W. Kroesen, (2000). *Journal of Physics D: Applied Physics* 33 2769–2774

Hayes J., Dominik Kirf, Mary Garvey, Neil Rowan, (2013). Disinfection and toxicological assessments of pulsed UV and pulsed-plasma gas-discharge treated water containing the waterborne protozoan enteroparasite Cryptosporidium parvum. *Journal of Microbiological Methods* 94 325–337

Heon L., Sung H. Park, Byung H. Kim, Sun-Jae Kim, Sang-Chai K., Seong-Gyu S., and Sang-Chul Jung, (2012). Contribution of Dissolved Oxygen to Methylene Blue Decomposition by Hybrid Advanced Oxidation Processes System. *International Journal of Photoenergy*. Volume 2012, Article ID 305989, 6 pages. doi:10.1155/2012/305989

Houas A., Lachheb H., Ksibi M., Elaloui E., Guillard C., Herrmann J.-M. (2001) Photocatalytic degradation pathway of methylene blue in water. *Applied Catalysis B: Environmental* 31(2), 145-157

Huang C.P., Dong C. and Tang Z., (1993). Waste Management, 13: 361-377.

Huang F., L. Chen, H. Wang, Z. Yan, (2010). Analysis of the degradation mechanism of methylene blue by atmospheric pressure dielectric barrier discharge plasma, Chem. Eng. J. 162 250–256.

Ibrahim E. Saliby, (2012). Photoreactive titanate nanomaterials for water purification systems. A thesis submitted in fulfilment of the requirements for the degree of Doctor of Philosophy. *Faculty of Engineering and Information Technology. University of Technology, Sydney Australia*

Igawa K., Y. Kawasaki, K. Tomooka, (2011). Development of Addition-type Ozone Oxidation and its Application. *Chem. Lett*., 40, 233

Inaloo K. Dindarloo, K. Naddafi , A. R. Mesdaghinia , S. Nasseri, R. Nabizadeh Nodehi, A. Rahimi, (2011). Optimization of operational parameters for decolorization and degradation of c. i. reactive blue 29 by ozone. *Iranian Journal of Environmental Health Science & Engineering,* Volume 8, No. 3, pp. 227-234

Ince N. H. and Tezcanli G., (1999). Treatability of textile dye-bath effluents by advanced oxidation: preparation for reuse. *Water Sci. Technol.*, 40, 183-190

Iqbal M. Ijaz Ahmad Bhatti and I. Ahmad, (2013). Photo-degradation of the methyl blue: Optimization through response surface methodology using rotatable center composite design. *International Journal of Basic and Applied Sciences*, 2 (2) 145-152

Jame W.L., Aiken, B.A., Bergamashi, M.S., Fram, R., and Fujii, K., (2003). Evaluation of specific ultraviolet absorbance as an indicator of the chemical composition and reactivity of dissolved organic carbon. *Environmental Science and Technology* 37, 4702 4708.

Jiang B., J. Zheng, X. Lu, Q. Liu, M. Wu, Z. Yan, S. Qiu, Q. Xue, Z. Wei, H. Xiao, M. Liu, (2013). Degradation of organic dye by pulsed discharge non-thermal plasma technology assisted with modified activated carbon fibers, *Chemical Engineering Journal*. 21-216, 969-978.

Jiang B., Jingtang Zheng, Shi Qiu, Mingbo Wu, Qinhui Zhang , Zifeng Yan, Qingzhong Xue, (2014). Review on electrical discharge plasma technology for wastewater remediation. *Chemical Engineering Journal* 236 348–368

Jo J., Y. S. Mok, (2009). In-situ production of ozone and ultraviolet light using a barrier discharge reactor for wastewater treatment. *Journal of Zhejiang University Science A.* 10(9):1359-1366

Jones, K.W., Feng, H., Stern, E.A., Neuhausler, U., Osan, J., Marinkovic, N., and Song, Z. 2006. Properties of New York/New Jersey Harbor Sediments. Acta Physica Polonica A. 109(3): 279-86.

Joelle J., (2006). Design, characterization and optimization of an atmospheric pressure hybrid dielectric barrier discharge reactor and application on a pharmaceutical compound. Thesis for Master of Engineering. Department of Chemical Engineering Mc Gill University, Montréal, Canada.

Joshi K. M., V. S. Shrivastava, (2011). Removal of methylene blue dye aqueous solution using photocatalysis. *International Journal of Nano Dimension* 2(4): 241-252, Spring 2012.

Joshi R.P., S.M. Thagard, (2013). Streamer-like electrical discharges in water: Part II. Environmental applications, *Plasma Chemistry and Plasma Processes* 33 17–49.

Juan L. Acero, Konrad Stemmler, and Urs Von Gunten, (2000). Degradation Kinetics of Atrazine and Its Degradation Products with Ozone and OH Radicals: A Predictive Tool for Drinking Water Treatment. *Environmental Science and technology,* 34, 591-597

Jun Shen Yong, Lei Le Cheng and Zhang XingWang, (2008). Evaluation of energy transfer and utilization efficiency of azo dye removal by different pulsed electrical discharge modes. *Chinese Science Bulletin* vol. 53 | no. 12 | 1824-1834

Kajitvichyanukul P., Ming-Chun Lu, Chih-Hsiang Liao, Wanpen Wirojanagud, Thammarat Koottatep, (2006). Degradation and detoxification of formaline wastewater by advanced oxidation processes. *Journal of Hazardous Materials* B135 337–343

Kaunas, (2012). Report on the different plasma modules for pollution removal MO 03. *Plasma for environment protection.*

Kim, H., and Yu, M., (2005). Characterization of Natural Organic Matter in Conventional Water Treatment Processes for Selection of Treatment Processes Focused on DBPs Control. Water Res. 39(19): 4779-4789.

Kirk R.E., Othmer D.F., Encyclopedia of chemical technology 1996, 4th ed. Vol. 17, London: Wiley-Interscience, ISBN 0-471-52686-X, *Ozone*, 953-994.

Kochany J., R.J. Maguire, (1994). Sunlight photo degradation of metolachlor in water. *Journal of Agriculture and Food Chemistry* 42 406–412.

Kogelschatz U., (2003). Dielectric-barrier Discharges: Their History, Discharge Physics, and Industrial Applications. *Plasma Chemistry and Plasma Processing*, Vol. 23, No. 1.

Konelschatz U., B. Eliasson and W. Egli, (1997). Dielectric-barrier discharges. Principle and applications. *Journal de physique IV. France 7*

Krasner, S.W., and Amy, G., (1995). Jar Test Evaluations of Enhanced Coagulation. JAWW. 87(12): 93-107.

Lasagni, A., Soldera, F., Mücklich, F., (2004). Quantitative investigation of material erosion caused by high pressure discharges in air and nitrogen. Z. Metallkd. 95, 102.

Legrini O., E. Oliveros, A. M. Braun, (1993). Photochemical processes for water treatment, *Chemical Reviews* 93 671–698.

Liang, L., and Singer, P.C., (2003). Factors Influencing the Formation and Relative Distribution of Haloacetic Acids and Trihalomethanes in Drinking Water. *Environmental Science and Technology* 37: 2920-2928

Lide D. R., (1999). Handbook of Chemistry and Physics 1999, 79th edn., Cleveland (OH): Chemical Rubber Co., ISBN 0-8493-9720-0, *Strengths of chemical bonds*,9-51 - 9-73

Lin, Tsair-Fuh and Shih-Wen Hoang (2000). Inhalation exposure to THMs from drinking water in south Taiwan. *The Science of the Total Environment*, 246, 41-49.

Liuming P., Min Ji, Bin Lu, Xiuduo Wang, Lejun Zhao, (2009). Degradation of Humic Acid by TiO_2 Nonutubes/UV/O_3. *International Conference on Environmental Science and Information Application Technology*

Liuming P., JI Min, Xiuduo W., Lejun Z., (2010). Influence of calcination temperature on TiO_2 Nanotubes' Catalysis for TiO_2/UV/O_3 in Landfill Leachate Solution. *Transactions of Tianjin University*, Volume 16, Issue 3, pp 179-186, DOI 10.1007/s12209-010-0033-2.

Locke B. R., M. Sato, P. Sunka, M. R. Hoffmann, J.-S. Chang, (2006). Electrohydraulic Discharge and Nonthermal Plasma for Water Treatment. *Industrial and Engineering Chemistry Research*, 45, 882-905

Lopez J. L., (2008). Dielectric barrier discharge, ozone Generation, and their applications. *Complex Plasmas Summer Institute*

Luís O. de B. Benetoli, Bruno M. Cadorin, Cícero da S. Postiglione, Ivan G. de Souza and Nito A. Debacher, (2011). Effect of temperature on Methylene Blue decolorization in aqueous medium in electrical discharge plasma reactor. *Journal of the Brazilian Chemical Society*, Vol. 22, No. 9, 1669-1678.

Lukeš P., (2001). Water treatment by Pulsed Streamer Corona Discharge, *Ph.D. Thesis*.

Lukes P., Appleton A.T. and Locke B.R., (2002). Hydrogen peroxide and ozone formation in hybrid gas-liquid electrical discharge reactors, *Annual Meeting of the IEEE - Industry Applications Society*, Pittsburgh, PA

Lukes P, Clupek M, Babicky V, Janda V, Sunka P, (2005). Generation of ozone by pulsed corona discharge over water surface in hybrid gas–liquid electrical discharge reactor. *Journal of Physics D Applied Physics* 38:409–416.

Madhu G. M., M.A. Lourdu Antony Raj and K. Vasantha Kumar Pai, (2009). Titamium oxide (TiO_2) assisted photocatalytic degradation of methylene blue. *Journal of Environmental Biology*. 30(2), 259-264.

Magureanu M., N. B. Mandache, and V. I. Parvulescu, (2007) Plasma Chem. Plasma Process. 27, 589

Magureanu M., Piroi D, Mandache NB, Parvulescu V, (2008). Decomposition of methylene blue in water using a dielectric barrier discharge: optimization of the operating parameters. *Journal of Applied Physics.* 104:103-306.

Magureanu M., Corina Bradu, Daniela Piroi, Nicolae Bogdan Mandache, Vasile Parvulescu, (2012). Pulsed corona discharge for degradation of methylene Blue in Water. *Plasma Chemistry and Plasma Processes*. DOI 10.1007/s11090-012-9422-8

Magureanu M., Corina Bradu, Daniela Piroi, Nicolae Bogdan Mandache, Vasile Parvulescu. (2013). Pulsed Corona Discharge for Degradation of Methylene Blue in Water. *Plasma Chemistry and Plasma Processes* 33:51–64 DOI 10.1007/s11090-012-9422-8

Malik M., Ghaffar A, Malik SA, (2001). Water purification by electrical discharges. *Plasma Sources Science and Technology* 10(1):82–91

Malik M. A., U. Rehman, A. Ghaffar, and K. Ahmed, (2002) *Plasma Sources Science and*

*Technol*ogy 11, 236

Mark G., A. Tauber, R. Laupert, H. P. Schuchmann, D. Schulz, A. Mues, C. von Sonntag, (1998). "OH-radical formation by ultrasound in aqueous solution – Part II: Terephthalate and Fricke dosimetry and the influence of various conditions on the sonolytic yield," *Ultrasonics Sonochemistry.* 5, pp. 41-52

Mark P. Cal and Martin Schluep, (2001). Destruction of benzene with non–thermal plasma in dielectric barrier discharge reactors. *Environmental Progress* Vol.20, No.3

Marc M., Huber, Anke Gobel, Adrianojoss, Nadinehermann, Dirk Loffler, Christa S., Mcarde L, Achimried, Hansruedisiegrist, Thomasa Ternes, Andursvongunte N., (2005). Oxidation of Pharmaceuticals during Ozonation of Municipal Wastewater Effluents: A Pilot Study. *Environmental Science and Technology*, 39, 4290 – 4299

Martynas T., Edvinas Krugly, Viktoras Racys, Rainer Hippler, Violeta Kauneliene, Inga Stasiulaitiene, Dainius Martuzevicius, (2013). Degradation of various textile dyes as wastewater pollutants under dielectric barrier discharge plasma treatment. *Chemical Engineering Journal* 229 9–19

Mastanaiah N., Judith A. Johnson, Subrata Roy, (2013). Effect of dielectric and liquid on plasma sterilization using dielectric barrier discharge plasma. *Los one* 8(8): e70840. doi:10.1371/journal.pone.0070840

Matijasevic G. and Brandt L., (1998). Conductive materials, wires, and cables. *Electrical Engineering – Vol. II - Conductive Materials, Wires, and Cables - Goran Matijasevic, Lutz Brandt*

Moeller T., *Inorganic chemistry* 1957, 6th edn. New York: Wiley, LCCC Nr. 52-7487, 484; 505

Mohamed E. Farouk, (2011). Removal of organic compounds from water by adsorption and photocatalytic oxidation. PhD thesis, University of Toulouse

Movahedyan H., A.M. Seid Mohammadi, A. Assadi, (2009). Comparison of different Advanced Oxidation Processes degrading p-chlorophenol in aqueous solution. *Iranian Journal of Environmental and Health Science Engineering, Volume 6, No. 3, pp. 153-160*

Mulbry W., S. Kondrad, C. Pizarro, E. Kebede -Westhead, *(*2008). Treatment of dairy manure effluent using freshwater algae: Algal productivity and recovery of manure nutrients using pilot-scale algal turf scrubbers, *Bioresource Technology* 99 8137- 8142

Naz M. Y., A. Ghaffar, N. U. Rehman, S. Shukrullah, and M. A. Ali, (2012). Optical characterization of 50 Hz atmospheric pressure single dielectric barrier discharge plasma. *Progress In Electromagnetics Research M,* Vol. 24, 193 -207

Nehra V, Kumar A, Dwivedi HK, (2008). Atmospheric non-thermal plasma sources. *International Journal of Engineering 2*(*1*): 53–68

Oi Lun Li H., Jun Kang, Kuniko Urashima and Nagahiro Saito, (2013). Comparison between the Mechanism of Liquid Plasma Discharge Process in Water and Organic Solution. *J. Inst. Electrostat. Jpn*. 37, 1 22-27

Okolongo G., W. Perold, U. Bettner, A Nechaev, R. Akinyeye and L. Petrik, (2012). Advanced oxidative water treatment process using an electrohydraulic discharge reactor and nano TiO_2 immobilized on nanofibers. *PhD thesis*, *University of the Western Cape*.

Pagga U, Taeger K., (1994). Development of a method for adsorption of dyestuffs on activated sludge. *Water Research*; 28:1051- 7

Peuravuori, J., Koivikko, R., and Pihlaja, K., (2002). Characterization, Differentiation and Classification of Aquatic Humic Matter Separated with Different Sorbents: Synchronous Scanning Fluorescence Spectroscopy. Water Res. 36: 4552-4562.

Peyton G.R., Glaze W.H., (1988). Destruction of pollutants in water with ozone in combination with ultraviolet radiation. 3. Photolysis of aqueous ozone, *Environmental Science and technology* 22 761–767.

Pons, M., Bonte, S.L., and Potier, O., (2004). Spectral Analysis and Fingerprinting for Biomedia Characterisation. Proc., Highlights from the ECB11: Building Bridges between Bioscience. Elsevier, Amsterdam, 1000 AE, Netherlands: 211-230.

Panicker P. K., (2003). Ionization of air by corona discharge, Master of Science in aerospace engineering. University of Texas at Arlington.

Pickering, A., D., Sumpter, J. P. (2003). Comprehending endocrine disrupters in aquatic environments. *Environmental Science and Technology*. 37, 331A-336A.

Pitwell L.R., (1983). Standard COD. *Chemistry British* 19:907.

Prendiville P. W., (1986). Ozone. *Science and Engineering*.8, 77-93.

Reddy P. Manoj Kumar and Ch. Subrahmanyam, (2012). Green Approach for Wastewater Treatment- Degradation and Mineralization of Aqueous Organic Pollutants by Discharge Plasma. dx.doi.org/10.1021/ie301122p *Industrial & Engineering Chemistry Research*, 51, 11097−11103

Reddy P. Manoj Kumar, B. Rama Raju, J. Karuppiah, E. Linga Reddy, Ch. Subrahmanyam, (2013). Degradation and mineralization of methylene blue by dielectric barrier discharge non-thermal plasma reactor, *Chemical Engineering Journal* 217 41–47

Reddy P. Manoj Kumar, Sk. Mahammadunnisa, Ch. Subrahmanyam, (2014). Catalytic non-thermal plasma reactor for mineralization of endosulfan in aqueous medium: A green approach for the treatment of pesticide contaminated water. *Chemical Engineering Journal* 238 157–163

Rey A., M. Faraldos, J. A. Casas, J. A. Zazo, A. Bahamonde, J. J. Rodryguez,(2009). Catalytic wet peroxide oxidation of phenol over Fe/AC catalysts: Influence of iron precursor and activated carbon surface, *Applied Catalysis B: Environmental* 86 69-77.

Rice R. G., (1985). In Safe Drinking Water: The Impact of Chemical on a limited Resource. *Lewis Publishers*, pp. 123-59.

Rong S., Yabing Sun, Zehua Zhao and Huiying Wang, (2014). Dielectric barrier discharge induced degradation of diclofenac in aqueous solution. *Water Science & Technology* 69.1

Roots R., S. Okada, (1975). Estimation of life times and diffusion distances of radicals involved in X-ray-induced DNA strand breaks or killing of mammalian cells, Radiat. *Res.* 64 306–320.

Sahni M., (2006). "Analysis of chemical reactions in pulsed streamer discharges: an experimental study," *PhD thesis*, Florida state university

Salome G.P. Olivia Soares, Jose´ J.M. Orfao, Dionısia Portela, Antonio Vieira, Manuel Fernando R. Pereira, (2006). Ozonation of textile effluents and dye solutions under continuous operation: Influence of operating parameters. *Journal of Hazardous Materials* B137 1664–1673

Sangster D.F. (1971). Free radical and electrophilic hydroxylation, in: The Chemistry of the Hydroxyl Group, ed. Patai S., Part 1, *Interscience, London*, 133-191

Sato M., Yamda Y. and Suriarto A.T., (2000). Decoloration of dyes in aqueous solution by pulsed discharge plasma in water through pinhole. *Trans. Inst. Fluid Flow Machin.*, 107, 95-98.

Sato M., J. Li, T. Ohshima, (2007). Degradation of phenol in water using a gas–liquid phase pulsed discharge plasma reactor, *Thin Solid Films* 515 4283– 4288.

Savage, P. E. and C. H. Oh, (2001). Supercritical Water Oxidation. Hazardous and Radioactive Waste Treatment Technologies Handbook. H. O. Chang. Boca Raton, Fl, CRC Press: Section 4.5.

Selma M., (2007). Chemical processes in aqueous phase pulsed electrical discharges: fundamental mechanisms and applications to organic compound degradation. PhD thesis

Sharma A.K., B.R. Locke, P. Arce, W.C. Finney, (1993). A preliminary-study of pulsed streamer corona discharge for the degradation of phenol in aqueous-solutions, Hazard. Waste Hazard. Mater. 10 209-219.

Shiki, H., Motoki, J., Takikawa, H., Sakakibara, T., Nishimura, Y., Hishida, S., Okawa, T., Ootsuka, T., (2007). Electrode erosion in pulsed arc for generating air meso-plasma jet under atmospheric pressure. *IEEJ Trans. Fund. Material* 127, 567–573.

Smirnov, B. M., (1977). *Introduction to Plasma Physics*, Mir Publishers, Moscow.

Soresa M., (2011). Ayka Addis Textile Wastewater Treatment by the Fenton's Reagent. MSc thesis in Chemical Engineering (Process Engineering). *Addis Ababa University, institute of technology, school of graduate studies*.

Song, Z., Chouparove, E., Jones, K.W., Feng, H., and Marinkovic, N.S., (2001). FTIR Investigation of Sediments from NY/NJ Harbor, San Diego Bay, and the Venetian Lagoon. NSLS Activity Report. **2**: 112–116.

Stasinakis A.S., (2008). Use of selected advanced oxidation processes (AOPs) for wastewater treatment – a mini review, *Global Nest Journal*, Vol 10, No 3, pp 376-385

Sturrock A., (1994). Plasma Physics: An Introduction to the Theory of Astrophysical, Geophysical & Laboratory Plasmas, *Cambridge University Press*.

Sugiarto A. Tri, Shunsuke Ito, Takayuki Ohshima, Masayuki Sato, Jan D. Skalny, (2003). Oxidative decoloration of dyes by pulsed discharge plasma in water. *Journal of Electrostatics* 58 135–145

Sun B., Sato M. and Clements J.S., (2000). Oxidative processes occurring when pulsed high voltage discharges degrade phenol in aqueous solution, Environ. *Sci. Technol.*, 34, 509-513

Sunka P, (2001). Pulse electrical discharges in water and their applications. *Physics and Plasmas* 8(5): 2587–2594

Tarr M., (2003). Chemical Degradation Methods for Wastes and Pollutants, Marcel Dekker Inc., New York, NY.

Thagard S.M., Takashima K., Mizuno A., (2009). Chemistry of the positive and negative electrical discharges formed in liquid water and above a gas–liquid surface, *Plasma Chemistry and Plasma Processes* 29 455–473.

Thompson, J.D., White, M.C., Harrington, G.W., and Singer, P.C., (1997). Enchanced Softening: Factors Influencing DBP Precursor Removal. JAWWA. 89(6): 94-105

Thorpe, K. L., Cummings, R. I., Huchtinson, T. H., Scholze, M., Brighty, G., Sumpter, J. P.; Tyler, C. R., (2003). Relative potencies and combination effects of steroidal estrogens in fish. *Environmental Science and Technology. 37*, 1142-1149.

Uher G., E. Gilbert, U. Siegfried, H. Eberle, (1991). "Determination of hydrogen peroxide in presence of organic peroxides" Vom Wasser, 76, pp. 225 – 234

Ullmann, (1991). Encyclopedia of Industrial Chemistry 5th edn. Vol. A18, Weinheim: Verlag Chemie, ISBN 3-527-20118-1, *Ozone*, 349-357.

Villaverde V., S., (2005). Combined anaerobic–aerobic treatment of azo dyes – a short review of bioreactor studies. *Water Research*, 39 pp. 1425–1440

Vujevic D., N. Koprivanac, A. Loncaric Bozic & B.R. Locke, (2004). The Removal of Direct Orange 39 by Pulsed Corona Discharge from Model Wastewater, *Environmental Technology*, 25:7, 791-800, DOI: 10.1080/09593330.2004.9619370

Walid K. Lafi, Z. Al-Qodah, (2006). Combined advanced oxidation and biological treatment processes for the removal of pesticides from aqueous solutions. *Journal of Hazardous Materials* B137 489–497

Washington, D.C., (1995). Fundamental research to technological applications, national academy press. *The national research council, plasma Science*.

WHO Guidelines for Drinking-Water Quality [electronic resource]: incorporating 1st And 2nd addenda Recommendations. 3rd ed. Geneva, Switzerland, World Health Organization; (2008).

Wilhelemus F. Laurens Maria H., (2000). Pulsed corona-induced degradation of organic materials in water. *Ph.D thesis*, ISBN 90-386-1549-3

Willberg D. M., P. S. Lang, R. H. Hochemer, A. Kratel, and M. R. Hoffmann, (1996). Degradation of 4-Chlorophenol, 3, 4-Dichloroaniline, and 2, 4, 6-Trinitrotoluene in an Electrohydraulic Discharge Reactor. *Environmental science & technology* / Vol. 30, NO. 8

Wu C. and Chern J., (2006). Kinetics of Photocatalytic Decomposition of Methylene Blue. *Industrial Engineering and Chemistry Research*, 45, 6450-6457

Xing Y., (2010). Characterization of dissolved organic carbon in prairie surface waters using Fourier transform infrared spectroscopy, A Thesis for Degree of Master of Science

Yamatake A., D.N. Angeloni, S. Dickson, M.B. Emelko, K. Yasuoke and J.S. Chang, (2007). UV and optical emissions generated by the pulsed arc electrohydraulic discharge. J. Journal of App. Phys. 45 8298

Yijun D., Muqing Q., (2013). Comparative study of advanced oxidation for textile wastewater, *Desalination and Water Treatment*, DOI: 10.1080/19443994.2012.763051

Zhang R., C. Zhang, X. Cheng, L. Wang, Y. Wu, Z. Guan, (2007). Kinetics of decolourization of azo dye by bipolar pulsed barrier discharge in a three phase discharge plasma reactor, *Journal of Hazardous Materials* 142 105–110.

Zhang Y., Zheng J., Qu X., Chen H., (2008). Design of a novel non-equilibrium plasma-based water treatment reactor, *Chemosphere* 70 1518–1524

Zhang J., Deqi Liu, Wenjuan Bian, Xihua Chen, (2012). Degradation of 2,4-dichorophenol by pulsed high voltage discharge in water. *Desalination* 304 49–56

Zou L., Bo Zhu, (2008). The synergistic effect of ozonation and photo catalysis on colour removal from reused water. *Journal of Photochemistry and Photobiology A: Chemistry* 196 24–32

APPENDICES

Appendix 1: Absorbance of MB samples within 60 minutes of DBD experiment at MB concentration (0.5 to 10 mg/L), (n = 2).

MB initial concentration (mg/L)	Absorbance (A)													
	0 min		10 min		20 min		30 min		40 min		50 min		60 min	
	A_1	A_2	A_1	A_2	A_1	A_2	A_1	A_2	A_1	A_2	A_1	A_2	A_1	A_2
0.5	0.087	0.086	0.029	0.028	0.002	0.003	0.000	0.000	0.000	0.000	0.000	0.000	0.000	0.000
1	0.161	0.162	0.007	0.006	0.000	0.000	0.000	0.000	0.000	0.000	0.000	0.000	0.000	0.000
1.5	0.323	0.322	0.031	0.030	0.009	0.008	0.002	0.001	0.000	0.000	0.000	0.000	0.000	0.000
2	0.415	0.414	0.053	0.052	0.014	0.013	0.002	0.001	0.000	0.000	0.000	0.000	0.000	0.000
2.5	0.418	0.417	0.084	0.083	0.014	0.013	0.003	0.002	0.001	0.000	0.000	0.000	0.000	0.000
3	0.485	0.483	0.060	0.061	0.009	0.008	0.005	0.004	0.000	0.000	0.000	0.000	0.000	0.000
3.5	0.453	0.452	0.040	0.041	0.009	0.008	0.007	0.006	0.003	0.002	0.000	0.000	0.000	0.000
4	0.619	0.617	0.119	0.118	0.025	0.024	0.009	0.008	0.006	0.005	0.002	0.001	0.002	0.001
4.5	0.701	0.700	0.181	0.180	0.037	0.036	0.014	0.013	0.006	0.005	0.004	0.003	0.003	0.002
5	0.742	0.741	0.194	0.193	0.004	0.003	0.020	0.021	0.009	0.008	0.004	0.004	0.004	0.003
5.5	0.707	0.706	0.167	0.166	0.029	0.028	0.010	0.011	0.005	0.004	0.002	0.002	0.000	0.000
6	0.752	0.751	0.156	0.155	0.026	0.025	0.010	0.011	0.005	0.006	0.000	0.000	0.000	0.000
6.5	0.842	0.841	0.220	0.221	0.053	0.052	0.024	0.023	0.011	0.010	0.005	0.004	0.003	0.002
7	0.862	0.861	0.287	0.286	0.077	0.076	0.026	0.025	0.011	0.011	0.006	0.007	0.005	0.004
7.5	0.896	0.895	0.232	0.231	0.060	0.061	0.023	0.022	0.015	0.014	0.009	0.008	0.006	0.005
8	0.914	0.913	0.265	0.264	0.049	0.048	0.013	0.012	0.006	0.006	0.000	0.000	0.000	0.000
8.5	0.957	0.956	0.279	0.278	0.041	0.040	0.010	0.010	0.001	0.001	0.000	0.000	0.000	0.000
9	0.996	0.995	0.198	0.197	0.044	0.043	0.016	0.017	0.010	0.011	0.005	0.004	0.005	0.003
9.5	1.036	1.035	0.319	0.318	0.113	0.317	0.046	0.046	0.016	0.015	0.009	0.008	0.005	0.007
10	2.476	2.475	1.254	1.253	0.589	1.252	0.290	0.291	0.124	0.123	0.073	0.072	0.034	0.071

Appendix 2: Average absorbance and standard deviation of MB samples withdrawn at every 10 minutes within 60 minutes of DBD experiment at MB concentration ranging from 0.5 to 10 mg/L with at the same experimental conditions as indicated in section 3.3.1.3.2, (n = 2).

	Average absorbance and standard deviation (replication n=2)													
Conc (mg/L)	0 min		10 min		20 min		30 min		40 min		50 min		60 min	
	Aver. Abs	Sdev.	Aver. Abs	Sdev.	Aver. Abs	Sdev.	Aver. Abs	Sdev.	Aver. Abs	Sdev.	Aver. Abs	Sdev.	Aver. Abs	Sdev.
0.5	0.0865	0.0007	0.0285	0.0007	0.0025	0.0007	0	0	0	0	0	0	0	0
1	0.1615	0.0007	0.0065	0.0007	0	0	0	0	0	0	0	0	0	0
1.5	0.3225	0.0007	0.0305	0.0007	0.0085	0.0007	0.0015	0.0007	0	0	0	0	0	0
2	0.4145	0.0007	0.0525	0.0007	0.0135	0.0007	0.0015	0.0007	0	0	0	0	0	0
2.5	0.4175	0.0007	0.0835	0.0007	0.0135	0.0007	0.0025	0.0007	0.0005	0.0007	0	0	0	0
3	0.484	0.0014	0.0605	0.0007	0.0085	0.0007	0.0045	0.0007	0	0	0	0	0	0
3.5	0.4525	0.0007	0.0405	0.0007	0.0085	0.0007	0.0065	0.0007	0.0025	0.0007	0	0	0	0
4	0.618	0.0014	0.1185	0.0007	0.0245	0.0007	0.0085	0.0007	0.0055	0.0007	0.0015	0.0007	0.0015	0.0007
4.5	0.7005	0.0007	0.1805	0.0007	0.0365	0.0007	0.0135	0.0007	0.0055	0.0007	0.0035	0.0007	0.0025	0.0007
5	0.7415	0.0007	0.1935	0.0007	0.0035	0.0007	0.0205	0.0007	0.0085	0.0007	0.004	0	0.0035	0.0007
5.5	0.7065	0.0007	0.1665	0.0007	0.0285	0.0007	0.0105	0.0007	0.0045	0.0007	0.002	0	0	0
6	0.7515	0.0007	0.1555	0.0007	0.0255	0.0007	0.0105	0.0007	0.0055	0.0007	0	0	0	0
6.5	0.8415	0.0007	0.2205	0.0007	0.0525	0.0007	0.0235	0.0007	0.0105	0.0007	0.0045	0.0007	0.0025	0.0007
7	0.8615	0.0007	0.2865	0.0007	0.0765	0.0007	0.0255	0.0007	0.011	0	0.0065	0.0007	0.0045	0.0007
7.5	0.8955	0.0007	0.2315	0.000707	0.0605	0.000707	0.0225	0.0007	0.0145	0.0007	0.0085	0.0007	0.0055	0.0007
8	0.9135	0.0007	0.2645	0.0007	0.0485	0.000707	0.0125	0.0007	0.006	0	0	0	0	0
8.5	0.9565	0.0007	0.2785	0.0007	0.0405	0.0007	0.01	0	0.001	0	0	0	0	0
9	0.9955	0.0007	0.1975	0.0007	0.0435	0.0007	0.0165	0.0007	0.0105	0.0007	0.0045	0.000707	0.004	0.001
9.5	1.0355	0.0007	0.3185	0.0007	0.215	0.1442	0.046	0	0.0155	0.0007	0.0085	0.000707	0.006	0.0014
10	2.4755	0.0007	1.2535	0.0007	0.9205	0.4688	0.2905	0.0007	0.1235	0.0007	0.0725	0.0007	0.0525	0.0261

Appendix 3: MB decolouration efficiency obtained within 60 minutes of DBD at MB concentration ranging from 0.5 to 10 mg/L with at the following EHD experimental conditions: applied voltage 25 V, Peak voltage 7.8 kV, pH (in between 6.04 and 6.64), air flow rate 3 L/min, MB volume 1500 mL, air gap 2 mm 50 g/L NaCl electrolyte, 0.5 mm silver electrode and contact time of 60 minutes (n = 2).

MB initial concentration (mg/L)	MB decolouration efficiency (D %)											
	10 min				30 min				60 min			
	$D\%_1$	$D\%_2$	A_{verage}	Stdev	$D\%_1$	$D\%_2$	A_{verage}	Stdev	$D\%_1$	$D\%_2$	A_{verage}	Stdev
0.5	66.66	67.816	67.238	0.8174	99.999	99.999	99.999	0	99.999	99.999	99.999	0
1	95.65	96.273	95.961	0.4405	99.999	99.999	99.999	0	99.999	99.999	99.999	0
1.5	90.4.	90.712	90.556	0.2206	99.38	99.69	99.535	0.2192	99.999	99.999	99.999	0
2	87.22	87.469	87.344	0.1760	99.52	99.69	99.605	0.1202	99.999	99.999	99.999	0
2.5	79.90	79.904	79.902	0.0028	99.28	99.521	99.400	0.1704	99.999	99.999	99.999	0
3	87.63	87.423	87.526	0.14637	98.97	99.175	99.072	0.1449	99.999	99.999	99.999	0
3.5	91.2	91.2	91.200	0	98.45	98.675	98.562	0.1590	99.999	99.999	99.999	0
4	80.77	80.94	80.855	0.1202	98.4	98.707	98.553	0.2170	99.670	99.838	99.754	0.1187
4.5	74.2	74.322	74.261	0.0862	98.00	98.145	98.072	0.1025	99.570	99.714	99.642	0.1018
5	73.85	79.989	76.919	4.3409	97.30	97.2	97.250	0.0707	99.460	99.595	99.5275	0.0954
5.5	76.37	76.52	76.445	0.1060	98.58	98.444	98.512	0.0961	99.999	99.999	99.999	0
6	79.25	79.388	79.319	0.0975	98.67	98.537	98.603	0.0940	99.999	99.999	99.999	0
6.5	73.87	73.753	73.811	0.0827	97.14	97.268	97.204	0.0905	99.640	99.762	99.701	0.0862
7	66.70	66.821	66.760	0.0855	96.98	97.1	97.040	0.0848	99.410	99.535	99.4725	0.0883
7.5	74.10	74.22	74.160	0.0848	97.43	97.544	97.487	0.0806	99.330	99.441	99.3855	0.0784
8	71.0	71.12	71.060	0.0848	98.6	98.687	98.643	0.0615	99.340	99.999	99.6695	0.4659
8.5	70.84	70.951	70.895	0.0784	98.95	98.955	98.952	0.0035	99.999	99.999	99.999	0
9	80.12	80.221	80.170	0.0714	98.39	98.293	98.341	0.0685	99.50	99.698	99.599	0.1400
9.5	69.21	69.305	69.257	0.0671	95.55	95.559	95.554	0.0063	99.520	99.324	99.422	0.1385
10	49.35	49.394	49.372	0.0311	88.28	88.247	88.263	0.02333	98.620	97.132	97.876	1.0521

Appendix 4: Absorbance of methylene blue solutions sampled within 60 minutes. Varied parameter: NaCl electrolyte from 10, 30 to 50 g/L. Fixed parameters: MB concentration 5 mg/L, pH (in between 6.04 and 6.64), dye volume 1500 mL, applied voltage 25, peak voltage 7.8 kV, air flow rate of 3 L/min, air gap 2 mm, 50 g/L NaCl electrolyte, 0.5 mm silver electrode and contact time of 60 minutes (n = 2).

	Absorbance (A)													
Time (minutes)	0 min		10 min		20 min		30 min		40 min		50 min		60 min	
NaCl concentration (g/L)	A_1	A_2	A_1	A_2	A_1	A_2	A_1	A_2	A_1	A_2	A_1	A_2	A_1	A_2
10	1.236	1.235	0.304	0.303	0.094	0.093	0.023	0.022	0.014	0.013	0.004	0.003	0.000	0.000
30	1.195	1.194	0.338	0.337	0.107	0.106	0.027	0.026	0.008	0.007	0.004	0.003	0.000	0.000
50	1.159	1.158	0.239	0.239	0.065	0.064	0.000	0.000	0.000	0.000	0.000	0.000	0.000	0.000

Appendix 5: Concentrations of Methylene blue samples recorded within 60 minutes. Varied parameter: NaCl electrolyte concentration from 10, 30 to 50 g/L. Fixed parameters: MB concentration 5 mg/L, pH (in between 6.04 and 6.64), dye volume 1500 mL, applied voltage 25, peak voltage 7.8 kV, air flow rate of 3 L/min, air gap 2 mm, 0.5 mm silver electrode and contact time of 60 minutes (n = 2).

NaCl concentration (g/L)	MB concentration (C) in mg/L within 60 minutes													
	0 min		10 min		20 min		30 min		40 min		50 min		60 min	
	C_1	C_2	C_1	C_2	C_1	C_2	C_1	C_2	C_1	C_2	C_1	C_2	C_1	C_2
10	5	5	2.634	2.625	0.815	0.806	0.199	0.196	0.121	0.112	0.035	0.029	0.000	0.000
30	5	5	2.930	2.920	0.927	0.918	0.234	0.225	0.069	0.060	0.035	0.029	0.000	0.000
50	5	5	2.071	2.071	0.563	0.554	0.000	0.000	0.000	0.000	0.000	0.000	0.000	0.000

Appendix 6: Decolouration efficiencies of MB at different voltages. Varied parameter: NaCl electrolyte concentration from 10, 30 to 50 g/L. Fixed parameters: MB concentration 5 mg/L, pH (in between 6.04 and 6.64), dye volume 1500 mL, applied voltage 25, peak voltage 7.8 kV, air flow rate of 3 L/min, air gap 2 mm, 0.5 mm silver electrode and contact time of 60 minutes (n = 2).

	MB decolouration efficiency (D %)											
NaCl concentration (mg/L)	10 mg/L				30 mg/L				50 mg/L			
Time (minutes)	$D\%_1$	$D\%_2$	A_{verage}	Stdev	$D\%_1$	$D\%_2$	A_{verage}	Stdev	$D\%_1$	$D\%_2$	A_{verage}	Stdev
10	47.320	47.300	47.310	0.0141	41.400	41.600	41.500	0.1414	58.580	58.580	58.580	0
20	83.700	83.880	83.790	0.1272	81.460	81.640	81.550	0.1272	88.740	88.920	88.830	0.1272
30	96.020	96.080	96.050	0.0424	95.320	95.500	95.410	0.1272	99.999	99.999	99.999	0
40	97.580	97.760	97.670	0.1272	98.620	98.800	98.710	0.1272	99.999	99.999	99.999	0
50	99.300	99.420	99.360	0.0848	99.300	99.420	99.360	0.0848	99.999	99.999	99.999	0
60	99.999	99.999	99.999	0	99.999	99.999	99.999	0	99.999	99.999	99.999	0

Appendix 7: Absorbance of methylene blue solutions sampled within 60 minutes. Varied parameter: solution pH from 2.5, 4.5, 6.5, 8.5 to 10.5. Fixed parameters: MB concentration 5 mg/L, dye volume 1500 mL, applied voltage 25, peak voltage 7.8 kV, air flow rate of 3 L/min, air gap 2 mm, 50 g/L NaCl electrolyte , 0.5 mm silver electrode and contact time of 60 minutes (n = 2).

pH	Absorbance (A)													
	0 min		10 min		20 min		30 min		40 min		50 min		60 min	
	A_1	A_2	A_1	A_2	A_1	A_2	A_1	A_2	A_1	A_2	A_1	A_2	A_1	A_2
2.5	1.019	1.018	0.098	0.097	0.010	0.011	0.000	0.000	0.000	0.000	0.000	0.000	0.000	0.000
4.5	0.927	0.926	0.165	0.164	0.032	0.031	0.003	0.002	0.000	0.000	0.000	0.000	0.000	0.000
6.5	0.934	0.933	0.190	0.191	0.036	0.035	0.005	0.006	0.000	0.000	0.000	0.000	0.000	0.000
8.5	0.936	0.935	0.229	0.228	0.038	0.037	0.008	0.007	0.000	0.000	0.000	0.000	0.000	0.000
10.5	0.920	0.919	0.253	0.252	0.111	0.112	0.044	0.045	0.002	0.000	0.000	0.000	0.000	0.000

Appendix 8: Concentrations of methylene blue solutions sampled within 60 minutes. Varied parameter: solution pH from 2.5, 4.5, 6.5, 8.5 to 10.5. Fixed parameters: MB concentration 5 mg/L, dye volume 1500 mL, applied voltage 25, peak voltage 7.8 kV, air flow rate of 3 L/min, air gap 2 mm, 50 g/L NaCl electrolyte , 0.5 mm silver electrode and contact time of 60 minutes.

pH	MB Concentrations (C) in mg/L within 60 minutes											
	10 min		20 min		30 min		40 min		50 min		60 min	
	C_1	C_2	C_1	C_2	C_1	C_2	C_1	C_2	C_1	C_2	C_1	C_2
2.5	0.849	0.840	0.086	0.095	0.000	0.000	0.000	0.000	0.000	0.000	0.000	0.000
4.5	1.430	1.421	0.277	0.268	0.030	0.017	0.000	0.000	0.000	0.000	0.000	0.000
6.5	1.646	1.655	0.312	0.303	0.043	0.052	0.000	0.000	0.000	0.000	0.000	0.000
8.5	1.984	1.976	0.329	0.321	0.069	0.061	0.000	0.000	0.000	0.000	0.000	0.000
10.5	2.192	2.184	0.329	0.970	0.069	0.070	0.000	0.000	0.000	0.000	0.000	0.000

Appendix 9 a: Decolouration efficiency of methylene blue solutions sampled within 60 minutes. Varied parameter: solution pH from 2.5, 4.5, 6.5, 8.5 to 10.5. Fixed parameters: MB concentration 5 mg/L, dye volume 1500 mL, applied voltage 25, peak voltage 7.8 kV, air flow rate of 3 L/min, air gap 2 mm, 50 g/L NaCl electrolyte , 0.5 mm silver electrode and contact time of 60 minutes (n = 2).

pH	Decolouration efficiency (D%) within 60 minutes											
	10 min		20 min		30 min		40 min		50 min		60 min	
	$D\%_1$	$D\%_2$	$D\%_1$	$D\%_2$	$D\%_1$	$D\%_2$	$D\%_1$	$D\%_2$	$D\%_1$	$D\%_2$	$D\%_1$	$D\%_2$
2.5	83.02	83.2	98.28	98.1	99.999	99.999	99.999	99.999	99.999	99.999	99.999	99.999
4.5	71.4	71.58	94.46	94.64	99.4	99.66	99.999	99.999	99.999	99.999	99.999	99.999
6.5	67.08	66.9	93.42	93.94	99.14	98.96	99.999	99.999	99.999	99.999	99.999	99.999
8.5	60.32	60.48	93.42	93.58	98.62	98.78	99.999	99.999	99.999	99.999	99.999	99.999
10.5	56.16	56.32	93.42	80.6	98.62	98.6	99.999	99.999	99.999	99.999	99.999	99.999

Appendix 9 b: Decolouration efficiency of methylene blue solutions sampled within 60 minutes. Varied parameter: solution pH from 2.5, 4.5, 6.5, 8.5 to 10.5. Fixed parameters: MB concentration 5 mg/L, dye volume 1500 mL, applied voltage 25, peak voltage 7.8 kV, air flow rate of 3 L/min, air gap 2 mm, 50 g/L NaCl electrolyte , 0.5 mm silver electrode and contact time of 60 minutes (n = 2).

pH	Decolouration efficiency (D%) within 60 minutes											
	10 min		20 min		30 min		40 min		50 min		60 min	
	Average	Sdev	Average	Stdev	Average	Sdev	Average	Sdev	Average	Sdev	Average	Sdev
2.5	83.110	0.1272	98.190	0.1272	99.999	0	99.999	0	99.999	0	99.999	0
4.5	71.490	0.1272	94.550	0.1272	99.530	0.1838	99.999	0	99.999	0	99.999	0
6.5	66.990	0.1272	93.680	0.3676	99.050	0.1272	99.999	0	99.999	0	99.999	0
8.5	60.400	0.1131	93.500	0.1131	98.700	0.1131	99.999	0	99.999	0	99.999	0
10.5	56.240	0.1131	87.010	9.0651	98.610	0.0141	99.999	0	99.999	0	99.999	0

Appendix 10: Absorbance of methylene blue solutions sampled within 60 minutes. Varied parameter: solution conductivity from 5, 10, 15 to 20 mS/cm. Fixed parameters: MB concentration 5 mg/L, pH (in between 6.04 and 6.64), dye volume 1500 mL, applied voltage 25, peak voltage 7.8 kV, air flow rate of 3 L/min, air gap 2 mm, 50 g/L NaCl electrolyte, 0.5 mm silver electrode and contact time of 60 minutes (n = 2).

Solution Conductivity (mS/cm)	Absorbance (A)													
	0 min		10 min		20 min		30 min		40 min		50 min		60 min	
	A_1	A_2	A_1	A_2	A_1	A_2	A_1	A_2	A_1	A_2	A_1	A_2	A_1	A_2
5	0.912	0.913	0.178	0.177	0.025	0.024	0.000	0.000	0.000	0.000	0.000	0.000	0.000	0.000
10	0.854	0.853	0.088	0.087	0.000	0.000	0.000	0.000	0.000	0.000	0.000	0.000	0.000	0.000
15	0.848	0.847	0.102	0.101	0.000	0.000	0.000	0.000	0.000	0.000	0.000	0.000	0.000	0.000
20	0.855	0.854	0.167	0.166	0.000	0.000	0.000	0.000	0.000	0.000	0.000	0.000	0.000	0.000

Appendix 11: Concentrations of methylene blue solutions sampled within 60 minutes. Varied parameter: solution conductivity from 5, 10, 15 to 20 mS/cm. Fixed parameters: MB concentration 5 mg/L, pH (in between 6.04 and 6.64), dye volume 1500 mL, applied voltage 25, peak voltage 7.8 kV, air flow rate of 3 L/min, air gap 2 mm, 50 g/L NaCl electrolyte, 0.5 mm silver electrode and contact time of 60 minutes (n = 2).

Solution Conductivity (mS/cm)	Concentration (C) in mg/L within 60 minutes											
	10 min		20 min		30 min		40 min		50 min		60 min	
	C_1	C_2	C_1	C_2	C_1	C_2	C_1	C_2	C_1	C_2	C_1	C_2
5	1.542	1.534	0.216	0.208	0.000	0.000	0.000	0.000	0.000	0.000	0.000	0.000
10	0.762	0.754	0.000	0.000	0.000	0.000	0.000	0.000	0.000	0.000	0.000	0.000
15	0.884	0.875	0.000	0.000	0.000	0.000	0.000	0.000	0.000	0.000	0.000	0.000
20	1.447	1.438	0.000	0.000	0.000	0.000	0.000	0.000	0.000	0.000	0.000	0.000

Appendix 12 a: Decolouration efficiency of methylene blue solutions sampled within 60 minutes. Varied parameter: solution conductivity from 5, 10, 15 to 20 mS/cm. Fixed parameters: MB concentration 5 mg/L, pH (in between 6.04 and 6.64), dye volume 1500 mL, applied voltage 25, peak voltage 7.8 kV, air flow rate of 3 L/min, air gap 2 mm, 50 g/L NaCl electrolyte, 0.5 mm silver electrode and contact time of 60 minutes (n = 2).

Solution Conductivity (mS/cm)	Decolouration efficiency (D%) within 60 minutes											
	10 min		20 min		30 min		40 min		50 min		60 min	
	$D\%_1$	$D\%_2$	$D\%_1$	$D\%_2$	$D\%_1$	$D\%_2$	$D\%_1$	$D\%_2$	$D\%_1$	$D\%_2$	$D\%_1$	$D\%_2$
5	69.16	69.32	95.68	95.84	99.999	99.999	99.999	99.999	99.999	99.999	99.999	99.999
10	84.76	84.92	99.999	99.999	99.999	99.999	99.999	99.999	99.999	99.999	99.999	99.999
15	82.32	82.5	99.999	99.999	99.999	99.999	99.999	99.999	99.999	99.999	99.999	99.999
20	71.06	71.24	99.999	99.999	99.999	99.999	99.999	99.999	99.999	99.999	99.999	99.999

Appendix 12 b: Concentrations of methylene blue solutions sampled within 60 minutes. Varied parameter: solution conductivity from 5, 10, 15 to 20 mS/cm. Fixed parameters: MB concentration 5 mg/L, pH (in between 6.04 and 6.64), dye volume 1500 mL, applied voltage 25, peak voltage 7.8 kV, air flow rate of 3 L/min, air gap 2 mm, 50 g/L NaCl electrolyte, 0.5 mm silver electrode and contact time of 60 minutes (n = 2).

Solution Conductivity (mS/cm)	Decolouration efficiency (D%) within 60 minutes											
	10 min		20 min		30 min		40 min		50 min		60 min	
	Average	Sdev	Average	Stdev	Average	Sdev	Average	Sdev	Average	Sdev	Average	Sdev
5	69.240	0.1131	95.760	0.1131	99.999	0	99.999	0	99.999	0	99.999	0
10	84.840	0.1131	99.999	0	99.999	0	99.999	0	99.999	0	99.999	0
15	82.410	0.1272	99.999	0	99.999	0	99.999	0	99.999	0	99.999	0
20	71.150	0.1272	99.999	0	99.999	0	99.999	0	99.999	0	99.999	0

Appendix 13: absorbance of methylene blue solutions sampled within 60 minutes. (Varied parameter: air flow rate (from 2, 3, 4 to 5 L/min) Fixed parameters: MB concentration 5 mg/L, pH (in between 6.04 and 6.64), dye volume 1500 mL, applied voltage 25, peak voltage 7.8 kV, air gap 2 mm, 50 g/L NaCl electrolyte, 0.5 mm silver electrode and contact time of 60 minutes (n = 2).

Air flow rate (L/min)	Absorbance (A)													
	0 min		10 min		20 min		30 min		40 min		50 min		60 min	
	A_1	A_2	A_1	A_2	A_1	A_2	A_1	A_2	A_1	A_2	A_1	A_2	A_1	A_2
2	0.952	0.951	0.293	0.294	0.056	0.057	0.011	0.012	0.000	0.000	0.000	0.000	0.000	0.000
3	0.952	0.951	0.230	0.231	0.022	0.023	0.000	0.000	0.000	0.000	0.000	0.000	0.000	0.000
4	0.952	0.951	0.173	0.174	0.035	0.036	0.002	0.003	0.000	0.000	0.000	0.000	0.000	0.000
5	0.952	0.951	0.154	0.155	0.018	0.019	0.000	0.000	0.000	0.000	0.000	0.000	0.000	0.000

Appendix 14: Concentration of methylene blue solutions sampled within 60 minutes. (Varied parameter: air flow rate (from 2, 3, 4 to 5 L/min) Fixed parameters: MB concentration 5 mg/L, pH (in between 6.04 and 6.64), dye volume 1500 mL, applied voltage 25, peak voltage 7.8 kV, air gap 2 mm, 50 g/L NaCl electrolyte, 0.5 mm silver electrode and contact time of 60 minutes (n = 2).

Air flow rate (L/min)	Concentrations (C) in mg/L within 60 minutes											
	10 min		20 min		30 min		40 min		50 min		60 min	
	C_1	C_2	C_1	C_2	C_1	C_2	C_1	C_2	C_1	C_2	C_1	C_2
2	2.540	2.55	0.485	0.494	0.095	0.104	0.000	0.000	0.000	0.000	0.000	0.000
3	1.993	2.001	0.190	0.199	0.000	0.000	0.000	0.000	0.000	0.000	0.000	0.000
4	1.334	1.335	0.303	0.302	0.017	0.026	0.000	0.000	0.000	0.000	0.000	0.000
5	1.334	1.343	0.156	0.165	0.000	0.000	0.000	0.000	0.000	0.000	0.000	0.000

Appendix 15 a: Decolouration of methylene blue solutions sampled within 60 minutes. (Varied parameter: air flow rate (from 2, 3, 4 to 5 L/min) Fixed parameters: MB concentration 5 mg/L, pH (in between 6.04 and 6.64), dye volume 1500 mL, applied voltage 25, peak voltage 7.8 kV, air gap 2 mm, 50 g/L NaCl electrolyte, 0.5 mm silver electrode and contact time of 60 minutes (n = 2).

Air flow rate(L/min)	Decolouration efficiency (%) within 60 minutes											
	10 min		20 min		30 min		40 min		50 min		60 min	
	D% $_1$	D% $_2$	D% $_1$	D% $_2$	D% $_1$	D% $_2$	D% $_1$	D% $_2$	D% $_1$	D% $_2$	D%$_1$	D% $_2$
2	49.200	4900	98.880	98.890	99.780	97.920	99.999	99.999	99.999	99.999	99.999	99.999
3	60.140	59.980	96.200	96.020	99.999	99.9990	99.999	99.999	99.999	99.999	99.999	99.999
4	73.320	73.300	93.940	93.960	99.960	99.480	99.999	99.999	99.999	99.999	99.999	99.999
5	73.320	73.140	96.880	96.700	99.999	99.999	99.999	99.999	99.999	99.999	99.999	99.999

Appendix 15 b: Decolouration of methylene blue solutions sampled within 60 minutes. (Varied parameter: air flow rate (from 2, 3, 4 to 5 L/min) Fixed parameters: MB concentration 5 mg/L, pH (in between 6.04 and 6.64), dye volume 1500 mL, applied voltage 25, peak voltage 7.8 kV, air gap 2 mm, 50 g/L NaCl electrolyte, 0.5 mm silver electrode and contact time of 60 minutes (n = 2).

Air flow rate (L/min)	Decolouration efficiency (D%) within 60 minutes											
	10 min		20 min		30 min		40 min		50 min		60 min	
	Average	Sdev	Average	Stdev	Average	Sdev	Average	Sdev	Average	Sdev	Average	Sdev
2	49.1	0.1414	98.885	0.0070	98.85	1.3152	99.999	0	99.999	0	99.999	0
3	60.06	0.1131	96.110	0.1272	99.999	0	99.999	0	99.999	0	99.999	0
4	73.31	0.0141	93.950	0.0141	99.72	0.3394	99.999	0	99.999	0	99.999	0
5	73.23	0.1272	96.790	0.1272	99.999	0	99.999	0	99.999	0	99.999	0

Appendix 16: absorbance of methylene blue solutions sampled within 60 minutes. Varied parameter: Solution volume from 500, 1000and 1500 to 2000 mL. Fixed parameters: MB concentration 5 mg/L, pH (in between 6.04 and 6.64), applied voltage 25, peak voltage 7.8 kV, air flow rate of 3 L/min, air gap 2 mm, 50 g/L NaCl electrolyte, 0.5 mm silver electrode and contact time of 60 minutes (n = 2).

Solution Volume (mL)	Absorbance (A)													
	0 min		10 min		20 min		30 min		40 min		50 min		60 min	
	A_1	A_2	A_1	A_2	A_1	A_2	A_1	A_2	A_1	A_2	A_1	A_2	A_1	A_2
500	0.933	0.932	0.255	0.254	0.101	0.102	0.042	0.043	0.017	0.016	0.015	0.016	0.000	0.000
1000	0.933	0.932	0.167	0.166	0.040	0.041	0.014	0.015	0.004	0.005	0.001	0.002	0.000	0.000
1500	0.933	0.932	0.178	0.177	0.042	0.043	0.004	0.005	0.000	0.000	0.000	0.000	0.000	0.000
2000	0.933	0.932	0.187	0.186	0.036	0.037	0.003	0.004	0.000	0.000	0.000	0.000	0.000	0.000

Appendix 17: Concentrations of methylene blue solutions sampled within 60 minutes. Varied parameter: Solution volume from 500, 1000and 1500 to 2000 mL. Fixed parameters: MB concentration 5 mg/L, pH (in between 6.04 and 6.64), applied voltage 25, peak voltage 7.8 kV, air flow rate of 3 L/min, 50 g/L NaCl electrolyte, air gap 2 mm, 0.5 mm silver electrode and contact time of 60 mm (n = 2).

Solution Volume (mL)	Concentrations (C) in mg/L within 60 minutes											
	10 min		20 min		30 min		40 min		50 min		60 min	
	C_1	C_2	C_1	C_2	C_1	C_2	C_1	C_2	C_1	C_2	C_1	C_2
500	2.209	2.201	0.875	0.883	0.364	0.372	0.147	0.140	0.13	0.140	0.000	0.000
1000	1.447	1.440	0.346	0.355	0.121	0.130	0.035	0.043	0.000	0.017	0.000	0.000
1500	1.542	1.534	0.364	0.372	0.035	0.043	0.000	0.000	0.000	0.000	0.000	0.000
2000	1.620	1.612	0.312	0.321	0.026	0.034	0.000	0.000	0.000	0.000	0.000	0.000

Appendix 18 a: Decolouration efficiency of methylene blue solutions sampled within 60 minutes. Varied parameter: Solution volume from 500, 1000and 1500 to 2000 mL. Fixed parameters: MB concentration 5 mg/L, pH (in between 6.04 and 6.64), applied voltage 25, peak voltage 7.8 kV, air flow rate of 3 L/min, 50 g/L NaCl electrolyte, air gap 2 mm, 0.5 mm silver electrode and contact time of 60 mm (n = 2).

Solution Volume (mL)	Decolouration efficiency (D%) within 60 minutes											
	10 min		20 min		30 min		40 min		50 min		60 min	
	$D\%_1$	$D\%_2$	$D\%_1$	$D\%_2$	$D\%_1$	$D\%_2$	$D\%_1$	$D\%_2$	$D\%_1$	$D\%_2$	$D\%_1$	$D\%_2$
500	55.82	55.980	82.50	82.340	92.700	94.560	97.060	97.20	97.400	97.200	99.999	99.999
1000	71.1	71.200	93.080	92.90	97.580	97.40	99.300	99.140	99.999	99.660	99.999	99.999
1500	69.16	69.320	92.720	92.560	99.30	99.140	99.999	99.999	99.999	99.999	99.999	99.999
2000	67.6	67.760	93.760	93.580	99.480	99.320	99.999	99.999	99.999	99.999	99.999	99.999

Appendix 18 b: Decolouration efficiency of methylene blue solutions sampled within 60 minutes. Varied parameter: Solution volume from 500, 1000and 1500 to 2000 mL. Fixed parameters: MB concentration 5 mg/L, pH (in between 6.04 and 6.64), applied voltage 25, peak voltage 7.8 kV, air flow rate of 3 L/min, 50 g/L NaCl electrolyte, air gap 2 mm, 0.5 mm silver electrode and contact time of 60 minutes (n = 2).

Solution Volume (mL)	Decolouration efficiency (D%) within 60 minutes											
	10 min		20 min		30 min		40 min		50 min		60 min	
	Average	Sdev	Average	Stdev	Average	Sdev	Average	Sdev	Average	Sdev	Average	Sdev
500	55.9	0.1131	82.42	0.1131	93.63	1.3152	97.13	0.0989	97.3	0.1414	99.999	0
1000	71.15	0.0707	92.99	0.1272	97.49	0.1272	99.22	0.1131	99.8295	0.2397	99.999	0
1500	69.24	0.1131	92.64	0.1131	99.22	0.1131	99.999	0	99.999	0	99.999	0
2000	67.68	0.1131	93.67	0.1272	99.4	0.1131	99.999	0	99.999	0	99.999	0

Appendix 19: Absorbance of methylene blue solutions sampled within 60 minutes. Varied parameter: voltage from 20, 22 to 25 V. Fixed parameters: MB concentration 5 mg/L, solution volume 1500 mL, pH (in between 6.04 and 6.64), air flow rate 3 L/min, 50 g/L NaCl electrolyte, air gap 2 mm, 0.5 mm silver electrode and contact time of 60 minutes (n = 2).

Applied voltage (V)	Absorbance (A)													
	0 min		10 min		20 min		30 min		40 min		50 min		60 min	
	A_1	A_2	A_1	A_2	A_1	A_2	A_1	A_2	A_1	A_2	A_1	A_2	A_1	A_2
20	0.952	0.951	0.300	0.310	0.104	0.105	0.018	0.019	0.003	0.004	0.000	0.000	0.000	0.000
22	0.952	0.951	0.159	0.16	0.026	0.027	0.002	0.003	0.000	0.000	0.000	0.000	0.000	0.000
25	0.952	0.951	0.152	0.153	0.020	0.021	0.002	0.003	0.000	0.000	0.000	0.000	0.000	0.000

Appendix 20: Concentration of methylene blue solutions sampled within 60 minutes. Varied parameter: voltage from 20, 22 to 25 V. Fixed parameters: MB concentration 5 mg/L, solution volume 1500 mL, pH (in between 6.04 and 6.64), air flow rate 3 L/min, 50 g/L NaCl electrolyte, air gap 2 mm, 0.5 mm silver electrode and contact time of 60 minutes (n = 2).

Applied voltage (V)	Concentration (C) in mg/L within 60 minutes											
	10 min		20 min		30 min		40 min		50 min		60 min	
	C_1	C_2	C_1	C_2	C_1	C_2	C_1	C_2	C_1	C_2	C_1	C_2
20	2.599	2.600	0.901	0.910	0.156	0.164	0.026	0.034	0.000	0.000	0.000	0.000
22	1.377	1.386	0.225	0.234	0.017	0.026	0.000	0.000	0.000	0.000	0.000	0.000
25	1.317	1.325	0.173	0.182	0.017	0.026	0.000	0.000	0.000	0.000	0.000	0.000

Appendix 21: Decolouration efficiency of methylene blue solutions sampled within 60 minutes. Varied parameter: voltage from 20, 22 to 25 V. Fixed parameters: MB concentration 5 mg/L, solution volume 1500 mL, pH (in between 6.04 and 6.64), air flow rate 3 L/min, 50 g/L NaCl electrolyte, air gap 2 mm, 0.5 mm silver electrode and contact time of 60 minutes (n = 2).

	Decolouration efficiency (D %)											
Applied voltage (V)	20 V				22 V				25 V			
Time (minutes)	$D\%_1$	$D\%_2$	A_{verage}	Sdev	$D\%_1$	$D\%_2$	A_{verage}	Stdev	$D\%_1$	$D\%_2$	A_{verage}	Sdev
10	48.020	48.00	24.63	0.0141	72.46	72.28	40.225	0.0070	73.66	73.50	58.54	0.0565
20	81.980	81.80	81.97	0.0141	95.5	95.32	87.010	0.0148	96.54	96.36	88.745	0.0070
30	96.880	96.720	96.37	0.0141	99.66	99.48	99.67	0.0141	99.66	99.48	99.999	0
40	99.480	99.320	99.999	0	99.999	99.999	99.999	0	99.999	99.999	99.999	0
50	99.999	99.999	99.999	0	99.999	99.999	99.999	0	99.999	99.999	99.999	0
60	99.999	99.999	99.999	0	99.999	99.999	99.999	0	99.999	99.999	99.999	0

Appendix 22: Absorbance of Methylene blue samples recorded within 60 minutes when different electrodes were used. (Varied parameter: electrode type (copper, silver and stainless steel electrode). Fixed parameters: MB concentration 5 mg/L, solution volume 1500 mL, pH (in between 6.04 and 6.64), air flow rate 3 L/min, 50 g/L NaCl electrolyte, air gap 2 mm, and contact time of 60 minutes (n = 2).

Electrode type	Absorbance (A)													
	0 min		10 min		20 min		30 min		40 min		50 min		60 min	
Copper	A_1	A_2	A_1	A_2	A_1	A_2	A_1	A_2	A_1	A_2	A_1	A_2	A_1	A_2
Silver	1.034	1.035	0.282	0.283	0.069	0.069	0.014	0.015	0.000	0.000	0.000	0.000	0.000	0.000
Stainless steel	0.978	0.979	0.255	0.256	0.063	0.064	0.001	0.002	0.000	0.000	0.000	0.000	0.000	0.000
	0.976	0.977	0.296	0.297	0.061	0.062	0.010	0.011	0.001	0.002	0.000	0.000	0.000	0.000

Appendix 23: Concentrations of Methylene blue samples recorded within 60 minutes when different electrodes were used. (Varied parameter: electrode type (copper, silver and stainless steel electrode). Fixed parameters: MB concentration 5 mg/L, solution volume 1500 mL, pH (in between 6.04 and 6.64), air flow rate 3 L/min, 50 g/L NaCl electrolyte, air gap 2 mm, and contact time of 60 minutes (n = 2).

Electrode type	Concentration (C) in mg/L within 60 minutes											
	10 min		20 min		30 min		40 min		50 min		60 min	
	C_1	C_2	C_1	C_2	C_1	C_2	C_1	C_2	C_1	C_2	C_1	C_2
Copper	2.444	2.452	0.598	0.597	0.121	0.130	0.000	0.000	0.000	0.000	0.000	0.000
Silver	2.210	2.220	0.546	0.544	0.008	0.017	0.000	0.000	0.000	0.000	0.000	0.000
Stainless steel	2.565	2.535	0.528	0.526	0.086	0.095	0.008	0.017	0.000	0.000	0.000	0.000

Appendix 24: Decolouration efficiency of Methylene blue samples recorded within 60 minutes when different electrodes were used. (Varied parameter: electrode type (copper, silver and stainless steel electrode). Fixed parameters: MB concentration 5 mg/L, solution volume 1500 mL, pH (in between 6.04 and 6.64), air flow rate 3 L/min, 50 g/L NaCl electrolyte, air gap 2 mm, and contact time of 60 minutes (n = 2).

	Decolouration efficiency (D %)											
Electrode type	Copper				Silver				Stainless steel			
Time (minutes)	$D\%_1$	$D\%_2$	Average	Stdev	$D\%_1$	$D\%_2$	Average	Stdev	$D\%_1$	$D\%_2$	Average	Stdev
10	38.300	38.45	38.375	0.1060	55.80	55.60	55.70	0.1414	48.70	48.69	48.695	0.0070
20	78.00	78.56	78.28	0.3959	89.080	89.120	89.10	0.0282	89.440	89.560	89.5	0.0848
30	93.42	93.56	93.49	0.0989	99.840	99.660	99.705	0.1272	98.280	98.120	98.2	0.1131
40	98.44	99.999	99.2195	1.1023	99.999	99.999	99.999	0	99.840	99.690	99.765	0.1060
50	99.999	99.999	99.999	0	99.999	99.999	99.999	0	99.999	99.999	99.999	0
60	99.999	99.999	99.999	0	99.999	99.999	99.999	0	99.999	99.999	99.999	0

Appendix 25: absorbance of methylene blue solutions sampled within 60 minutes. (Varied parameter: silver electrode size (from 0.5 to 1.5 mm) Fixed parameters: MB concentration 5 mg/L, solution volume 1500 mL, pH (in between 6.04 and 6.64), air flow rate 3 L/min, 50 g/L NaCl electrolyte, air gap 2 mm, silver electrode, and contact time of 60 minutes (n =2).

Electrode size (mm)	Absorbance (A)													
	0 min		10 min		20 min		30 min		40 min		50 min		60 min	
	A_1	A_2	A_1	A_2	A_1	A_2	A_1	A_2	A_1	A_2	A_1	A_2	A_1	A_2
0.5	0.978	0.977	0.255	0.254	0.063	0.062	0.001	0.002	0.000	0.000	0.000	0.000	0.000	0.000
1.5	0.978	0.977	0.166	0.167	0.051	0.052	0.009	0.010	0.000	0.000	0.000	0.000	0.000	0.000

Appendix 26: Concentration of methylene blue solutions sampled within 60 minutes. (Varied parameter: silver electrode size (from 0.5 to 1.5 mm) Fixed parameters: MB concentration 5 mg/L, solution volume 1500 mL, pH (in between 6.04 and 6.64), air flow rate 3 L/min, 50 g/L NaCl electrolyte, air gap 2 mm, silver electrode, and contact time of 60 minutes (n = 2).

Electrode size (mm)	Concentrations (C) in mg/L within 60 minutes											
	10 min		20 min		30 min		40 min		50 min		60 min	
	C_1	C_2	C_1	C_2	C_1	C_2	C_1	C_2	C_1	C_2	C_1	C_2
0.5	2.210	2.201	0.546	0.537	0.008	0.017	0.000	0.000	0.000	0.000	0.000	0.000
1.5	1.428	1.447	0.425	0.450	0.078	0.086	0.000	0.000	0.000	0.000	0.000	0.000

Appendix 27 a: Decolouration efficiency of methylene blue solutions sampled within 60 minutes. (Varied parameter: silver electrode size (from 0.5 to 1.5 mm) Fixed parameters: MB concentration 5 mg/L, solution volume 1500 mL, pH (in between 6.04 and 6.64), air flow rate 3 L/min, 50 g/L NaCl electrolyte, air gap 2 mm, silver electrode, and contact time of 60 minutes (n = 2).

Electrode size (mm)	Decolouration efficiency (%) within 60 minutes											
	10 min		20 min		30 min		40 min		50 min		60 min	
	D% $_1$	D% $_2$	D% $_1$	D% $_2$	D% $_1$	D% $_2$	D% $_1$	D% $_2$	D% $_1$	D% $_2$	D%$_1$	D% $_2$
0.5	55.8	55.800	89.080	89.260	99.84	99.66	99.999	99.999	99.999	99.999	99.99	99.999
1.5	71.24	71.060	91.500	91.000	98.44	98.28	99.999	99.999	99.999	99.999	99.999	99.999

Appendix 27 b: Decolouration efficiency of methylene blue solutions sampled within 60 minutes. (Varied parameter: silver electrode size (from 0.5 to 1.5 mm) Fixed parameters: MB concentration 5 mg/L, solution volume 1500 mL, pH (in between 6.04 and 6.64), air flow rate 3 L/min, 50 g/L NaCl electrolyte, air gap 2 mm, silver electrode, and contact time of 60 minutes (n = 2)

	Decolouration percentage (D %)							
Electrode size (mm)	0.5				1.5			
Time (minutes)	$D\%_1$	$D\%_2$	Average	Stdev	$D\%_1$	$D\%_2$	Average	Stdev
10	55.8	55.800	55.8	0	71.24	71.060	71.15	0.1272
20	89.080	89.260	89.17	0.1272	91.500	91.000	91.25	0.3535
30	99.84	99.66	99.75	0.1272	98.44	98.28	99.875	0.0070
40	99.999	99.999	99.999	0	99.999	99.999	99.999	0
50	99.999	99.999	99.999	0	99.999	99.999	99.999	0
60	99.999	99.999	99.999	0	99.999	99.999	99.999	0

Appendix 28: Absorbance of H_2O_2 and O_3 measured at 405 nm (750 M-1cm -1) and 600 nm (ε = 20000 M-1cm-1), respectively. (Experimental conditions: MB concentration 5 mg/L, applied voltage 25 V, Peak voltage 7.8 kV, air flow rate 3 L/min, MB volume 1500 mL, 50 g/L NaCl electrolyte and 0.5 mm silver electrode)

Time (minutes)	Absorbance	
	H_2O_2	O_3
0	0	0
10	0.028	0.00
20	0.022	0.00
30	0.025	0.01
40	0.020	0.00
50	0.017	0.023
60	0.013	0.013

Appendix 29: Electrical parameters recorded during degradation of 5 mg/L MB at the following fixed experimental conditions: solution pH (in between 6.04 and 6.64), air flow rate 3 L/min, dye volume 1500 mL, 50 g/L NaCl electrolyte, silver electrode and running time 60 minutes.

Time (minutes)	Parameters			
	Applied voltage (V)	Peak voltage (kV)	Current (A)	Power (W)
0	0	0	0	0
10	25	7.8	3.86	112.4
20	22.01	6.20	5.00	110.0
30	21.91	6.20	5.00	109.6
40	21.87	6.20	5.00	109.2
50	21.70	6.20	5.00	108.9
60	21.69	6.20	5.00	108.5

Appendix 30: Absorbance of samples withdrawn every 10 minutes at the following experimental conditions: MB concentration varied (from 5, 10, 20, 30, 40 to 50 mg/L). Fixed parameters: solution pH (various), air flow rate 3 L/min, dye volume 1500 mL, 50 g/L NaCl electrolyte, silver electrode and running time 60 minutes.

Initial concentrations (mg/L)	Absorbance within 60 minutes						
	0 min	10 min	20 min	30 min	40 min	50 min	60 min
5	0.742	0.184	0.004	0.002	0.001	0.000	0.000
10	1.28	0.399	0.120	0.0265	0.012	0	0
20	2.4	0.874	0.35	0.102	0.025	0.009	0.003
30	3.498	1.50	0.5816	0.235	0.12	0.057	0.031
40	4.54	2.124	0.854	0.438	0.246	0.123	0.077
50	5.75	2.74	1.795	1.448	1.243	1.11	0.085

Appendix 31: Initial and final estimated concentrations of MB. Varied parameter: MB concentration (5, 10, 20, 30, 40, 50 mg/L). Fixed parameters: Applied voltage 25 V, peak voltage 7.8 kV, MB concentration 5 mg/L, solution pH (in between 6.04 and 6.64), air flow rate 3 L/min, dye volume 1500 mL, 50 g/L NaCl electrolyte, air gap 2 mm, 0.5 mm silver electrode and contact time of 60 minutes.

Initial MB concentration (mg/L)	concentration (mg/L) within 60 minutes					
	10 min	20 min	30 min	40 min	50 min	60 min
5	1.6	0.035	0.017	0.0085	0.00	0.00
10	3.46	1.04	0.23	0.104	0.00	0.00
20	7.58	3.004	0.88	0.217	0.078	0.03
30	13.01	5.04	2.04	1.04	0.494	0.3
40	18.41	7.4	3.8	2.132	1.066	0.66
50	23.74	15.555	12.55	10.775	9.6	0.736

Appendix 32: Rate constant of MB decomposition obtained at concentrations varied from 5 to 50 mg/L at the following applied conditions: Applied voltage 25 V, peak voltage 7.8 kV, MB concentration 5 mg/L, solution pH (in between 6.04 and 6.64), air flow rate 3 L/min, dye volume 1500 mL, 50 g/L NaCl electrolyte, air gap 2 mm, 0.5 mm silver electrode and contact time of 60 minutes.

Parameters	MB concentration (mg/L) with time (minutes)					
	10 min	20 min	30 min	40 min	50 min	60 min
C_i = 5 (mg/L)	1.6	0.035	0.017	0.0085	0.00	0.00
K = ln(C/C_i)/t	0.114	0.248	0.189	0.159	0.00	0.00
C_i = 10 (mg/L)	3.46	1.04	0.23	0.104	0.00	0.00
K = ln(C/C_i)/t	0.106	0.113	0.1257	0.114	0.00	0.00
C_i = 20 (mg/L)	7.58	3.004	0.88	0.217	0.078	0.03
K = ln(C/C_i)/t	0.097	0.095	0.1041	0.113	0.111	0.10837
C_i = 30 (mg/L)	13.01	5.04	2.04	1.04	0.494	0.3
K = ln(C/C_i)/t	0.0835	0.089	0.089	0.0.084	0.0821	0.0767

Appendix 33: Rate constant of MB decomposition obtained at concentrations varied from 5 to 50 mg/L at the following applied conditions: Applied voltage 25 V, peak voltage 7.8 kV, MB concentration 5 mg/L, solution pH (in between 6.04 and 6.64), air flow rate 3 L/min, dye volume 1500 mL, 50 g/L NaCl electrolyte, air gap 2 mm, 0.5 mm silver electrode and contact time of 60 minutes.

Parameters	MB concentration (mg/L) with time (minutes)					
	10 min	20 min	30 min	40 min	50 min	60 min
C_i = 40 (mg/L)	18.41	7.4	3.8	2.132	1.066	0.66
K= ln(C/C_i)/t	0.0776	0.0844	0.078	0.0732	0.0725	0.068
C_i = 50 (mg/L)	23.74	15.555	12.55	10.775	9.6	0.96
K = ln(C/C_i)/t	0.074	0.058	0.046	0.0384	0.033	0.070

Appendix 34: Rate constant of MB decomposition obtained at concentrations varied from 5 to 50 mg/L at the following applied conditions: Applied voltage 25 V, peak voltage 7.8 kV, MB concentration 5 mg/L, solution pH (in between 6.04 and 6.64), air flow rate 3 L/min, dye volume 1500 mL, 50 g/L NaCl electrolyte, air gap 2 mm, 0.5 mm silver electrode and contact time of 60 minutes.

Initial concentrations (mg/L)	Rate constant (min^{-1}) of MB decomposition with time					
	10 min	20 min	30 min	40 min	50 min	60 min
5	0.114	0.248	0.189	0.159	0.00	0.00
10	0.106	0.113	0.1257	0.114	0.00	0.00
20	0.097	0.095	0.1041	0.113	0.111	0.10837
30	0.0835	0.089	0.089	0.084	0.0821	0.0767
40	0.0776	0.0844	0.078	0.0732	0.0725	0.068
50	0.0744	0.058	0.046	0.0384	0.033	0.070

Appendix 35: pH values of solutions sampled within 60 minutes during degradation of MB using EHD system. Varied parameter: MB concentration from 5, 10, 20, 30, 40 to 50 mg/L. Fixed parameters: solution pH (various), air flow rate 3 L/min, dye volume 1500 mL, 50 g NaCl electrolyte, silver electrode and running time 60 minutes.

Initial MB concentration (mg/L)	pH values recorded within 60 min.						
	0 min	10 min	20 min	30 min	40 min	50 min	60 min
5	6.62	3.49	3.03	2.79	2.61	2.56	2.44
10	6.09	3.71	3.25	2.97	2.82	2.7	2.57
20	7.04	3.65	3.18	2.96	2.82	2.72	2.63
30	6.12	3.45	3.07	2.84	2.68	2.58	2.49
40	7.16	3.68	3.34	3.19	3.06	2.91	2.83
50	5.94	3.38	3.01	2.79	2.66	2.53	2.47

Appendix 36: Conductivity values of solutions sampled within 60 minutes during 8degradation of MB by EHD system. Experimental conditions: MB concentration varied from 5, 10, 20, 30, 40 to 50 mg/L. Fixed parameters: solution pH (various), air flow rate 3 L/min, dye volume 1500 mL, 50 g/L NaCl electrolyte, silver electrode and running time 60 minutes.

Initial MB concentration (mg/L)	Electrical conductivity (mS / cm) within 60 minutes						
	0 min	10 min	20 min	30 min	40 min	50 min	60 min
5	0.02	0.09	0.22	0.37	0.54	0.66	0.83
10	0.04	0.12	0.23	0.37	0.51	0.65	0.8
20	0.07	0.13	0.21	0.35	0.5	0.64	0.8
30	0.03	0.11	0.22	0.35	0.51	0.65	0.8
40	0.09	0.21	0.25	0.34	0.46	0.65	0.79
50	0.03	0.12	0.23	0.36	0.5	0.66	0.81

Appendix 37: Decomposition of MB (mg/L.min) at different concentrations at the following applied conditions: applied voltage 25 V, Peak voltage 7.8 kV, pH (in between 6.04 and 6.64), MB volume 1500 mL, air flow rate 3 L/min, air gap 2 mm, 50 g/L NaCl electrolyte, 0.5 mm silver electrode and contact time of 60 minutes], (replication, n =2).

	MB decomposition (mg/L.min) at different concentrations											
Time (minutes)	5 mg/L		10 mg/L		20 mg/L		30 mg/L		40 mg/L		50 mg/L	
	$D\%_1$	$D\%_2$	$D\%_1$	$D\%_2$	$D\%_1$	$D\%_2$	$D\%_1$	$D\%_2$	$D\%_1$	$D\%_2$	$D\%_1$	$D\%_2$
10	0.3319	0.3328	0.627	0.625	1.242	1.243	1.698	1.696	2.517	2.516	3.234	3.232
20	0.0693	0.0682	0.392	0.391	0.892	0.891	1.199	1.197	1.663	1.662	2.12	2.13
30	0.0754	0.0749	0.312	0.313	0.645	0.643	0.92	0.91	1.243	1.241	1.522	1.521
40	0.0024	0.0023	0.247	0.245	0.495	0.494	0.724	0.722	0.95	0.94	1.195	1.195
50	0.00086	0.00084	0.2	0.25	0.398	0.396	0.59	0.58	0.778	0.776	0.977	0.975
60	0	0	0.17	0.16	0.333	0.331	0.495	0.494	0.655	0.654	0.821	0.82

Appendix 38: Average decomposition of MB (mg/L.min) and their standard deviations at different concentrations at the following applied conditions: applied voltage 25 V, Peak voltage 7.8 kV, pH (in between 6.04 and 6.64), MB volume 1500 mL, air flow rate 3 L/min, air gap 2 mm, 50 g/L NaCl electrolyte, 0.5 mm silver electrode and contact time of 60 minutes], (replication, n =2)

	MB decomposition (mg/L.min) at different concentrations											
Time (minutes)	5 mg/L		10 mg/L		20 mg/L		30 mg/L		40 mg/L		50 mg/L	
	Ave.D%	Sdev	Aev. D%	Sdev	Ave.D%	Sdev	Ave.D%	Sdev.	Ave. D%	Sdev	Ave. D%	Sdev
10	0.33235	0.00063	0.626	0.00141	1.2425	0.00070	1.697	0.00141	2.5165	0.00070	3.233	0.00141
20	0.06875	0.00077	0.3915	0.00070	0.8915	0.00070	1.198	0.00141	1.6625	0.00070	2.125	0.00707
30	0.07515	0.00035	0.3125	0.00070	0.644	0.00141	0.915	0.00707	1.242	0.00141	1.5215	0.00070
40	0.00235	7.07E-05	0.246	0.00141	0.4945	0.00070	0.723	0.00141	0.945	0.00707	1.195	0
50	0.00085	1.41E-05	0.225	0.03535	0.397	0.00141	0.585	0.00707	0.777	0.00141	0.976	0.00141
60	0	0	0.165	0.00707	0.332	0.00141	0.4945	0.00070	0.6545	0.00070	0.8205	0.00070